

**Inaugural Dissertation**  
for  
obtaining the Doctoral degree  
of the  
Combined Faculty of Mathematics, Engineering and Natural Sciences  
of the  
Ruprecht – Karls – University  
Heidelberg

Presented by

**Apurva Gopisetty, M.Sc.**

Born in: Mumbai, India, 5<sup>th</sup> September 1994

Oral examination: 8<sup>th</sup> December 2023



**ITCC-P4: Molecular characterization and multi-omics analysis  
of pediatric patient tumor and  
Patient-Derived Xenograft (PDX) models for preclinical  
model selection**

Referees:

Prof. Dr. Benedikt Brors

Prof. Dr. Stefan M. Pfister



## Declaration

The work and results of this dissertation were performed and obtained from April 2019 to October 2023 under the supervision of Dr. Natalie Jäger and Prof. Dr. Stefan Pfister at the Division of Pediatric Neurooncology at the German Cancer Research Center (DKFZ) and the Hopp Children's Cancer Center (KiTZ), Heidelberg, Germany.

The first study, "ITCC-P4: Molecular characterization and multi-omics analysis of Patient-Derived Xenograft (PDX) models from high-risk pediatric cancer" is an on-going collaborative project, together with my co-shared first author, Dr. Aniello Federico (postdoc supervised by Prof. Dr. Marcel Kool, Division of Pediatric Neurooncology, DKFZ, Heidelberg). Parts of the methods, results and discussion of this study have been adapted from our manuscript in preparation – Federico\*, Gopisetty\*, Surdez\* *et al.* Contributions of authors other than myself are indicated within the Methods and Material, and Results section of the thesis or within figure legends.

The second study "Target Actionability Review (TAR): a systematic evaluation of replication stress as a therapeutic target for pediatric solid malignancies" has been a collaborative effort between me and my shared first co-authors, Kaylee M. Keller (Princess Máxima Center for Pediatric Oncology, Utrecht, Netherlands) and Sonja Krausert (KiTZ, DKFZ, Heidelberg). This work has been published in the "European Journal of Cancer" (Keller\*, Krausert\*, Gopisetty\* *et al.*, 2022). Parts of the methods and results of this study have been adapted and modified based on our collaborative findings.

I hereby declare that I have written and submitted this dissertation myself, and in the process have not used any other sources or materials other than those indicated. I declare that I have not applied to be examined at any other institution, nor used the dissertation in this or any other form at any other institution as an examination paper or submitted it to any other faculty as a dissertation.

---

Apurva Gopisetty



## Abstract

Cancer persists as one of the prevailing causes of death in children and adolescents aged 0 to 19 years. There remains to be an unmet need for identification of therapeutic biomarkers and better treatment interventions for these patients.

Advancements in state-of-the-art molecular profiling techniques have resulted in better understanding of pediatric cancers and their driver events. It has become apparent that pediatric malignancies are significantly more heterogeneous than previously thought as evidenced by the number of novel entities and subtypes that have been identified with distinct molecular and clinical characteristics. For most of these newly recognized entities there are currently extremely limited treatment options available. Unfortunately, there is also a lack of compiled and consistently analysed molecular data available, along with limited data of characterization and documentation of patient-derived models and/or genetic mouse models from high-risk pediatric tumors.

Both my studies fall under the “Innovative Therapies for Children with Cancer Pediatric Preclinical Proof-of-concept Platform” ([ITCC-P4](#)) consortium which is an international collaboration between different European academic institutes, several partnering pharmaceutical companies and three contract research organizations. The two studies aim to shed light on identification of potential promising treatment options that specifically match the patient’s specific molecular tumour characteristics and the patient’s genetic data. Genetic information at the molecular level from pediatric tumors in relapsed patients has contributed to advancing our understanding of disease progression and treatment resistance.

The first study overall aims to establish a sustainable platform of >400 molecularly well-characterized PDX models of high-risk pediatric cancers, including the analysis of their original tumors and matching controls. This will enable the selection of PDX models for *in vivo* testing of novel mechanism-of-action based treatments. Hence, facilitating the prioritization of pediatric drug development and clinical stratification of patients across entities.

In a first batch, 251 models were fully characterized, including 180 brain and 71 non-brain PDX models, representing 112 primary models, 93 relapse, 42 metastasis and 4 progressions under treatment models. Using low-coverage whole-genome and deep whole exome sequencing, complemented with total RNA sequencing and methylation analysis, the aim was to define genetic features in the ITCC-P4 PDX cohort and assess the molecular fidelity of PDX models compared to the original tumor. Based on DNA methylation profiling 43 different tumor subgroups within 18 cancer entities were included.

Mutational landscape analysis identified key somatic and germline oncogenic drivers where Ependymoma PDX models displayed the *C11orf95-RELA* fusion event, *YAP1*, *C11orf95* and *RELA* structural variants. Medulloblastoma models were driven by *MYCN*, *TP53*, *GLI2*, *SUFU* and *PTEN*. High-grade glioma samples showed *TP53*, *ATRX*, *MYCN* and *PIK3CA* somatic SNVs, along with focal deletions in *CDKN2A* in chromosome 9.

Neuroblastoma models were enriched for *ALK* SNVs and/or *MYCN* focal amplification, *ATRX* SNVs and *CDKN2A/B* deletions. Sarcoma models displayed characteristic alterations with *PAX3-FOXO1* fusions detected in embryonal rhabdomyosarcoma, along with *TP53*, *CDKN2A*, *NRAS* SNVs, *NCOA1* gains, *NF1* and *CDK4* SVs. Ewing sarcoma PDX models displayed the defining *EWSR1-FLI1* gene fusion in most cases, along with two rarer cases of *EWSR1-ERG* and *EWSR1-FEV* observed in the cohort. Osteosarcomas were defined by highly unstable genomes with large chromosomal alterations, *TP53* and *RB1* tumor suppressor genes were frequently altered and *ATRX* loss and *MYC* gains were observed. Additional sarcomas such as clear cell sarcoma of the kidney showed *CDKN2A* loss, *MYC* gain, *NF1* loss, *TP53* mutations, while Synovial sarcoma models were driven by *SSX* gene fusions and alterations. Large chromosomal aberrations (deletions, duplications) detected in the PDX models were concurrent with molecular alterations frequently observed in each tumor type –isochromosome 17 was detected in five medulloblastoma models, while deletion of chromosome arm 1p or gain of parts of 17q in neuroblastomas which correlate with tumor progression.

Tumor mutational burden across entities and copy number analysis was performed to identify allele-specific copy number events in tumor-normal pairs. Clonal evolution of somatic variants was not only found in certain PDX-tumor pairs but also between disease states. Across the 16 serial model cases, discordance in targetable SNV, SV and CNV, alterations were observed in later disease progressed states compared to the primary models. The multi-omics approach in this study provides insight into the mutational landscape and patterns of the PDX models thus providing an overview of molecular mechanisms facilitating the identification and prioritization of oncogenic drivers and potential biomarkers for optimal treatment.

The second study was a Target Actionability Review on replication stress. Detrimental long-term side effects due to chemotherapy drastically affect the lives of patients under treatment, hence there is an urgent need to identify novel target driven therapies. Decades of published data provide evidence for targeting replication stress therapeutically. Hence, in this study, we evaluated specific targets within the replication stress response (RSR) pathway. A comprehensive, well-structured, and critically evaluated overview of literature related to replication stress across 16 pediatric solid malignancies was generated. The methodology focuses on the systemic extraction and structured evaluation of replication stress as a target. This aims to align targeted anti-cancer therapeutic interventions with specific cancer subtypes based on clinical studies. *ATR*, *ATM*, *PARP*, *WEE1* were observed to represent the most promising targets either using single agents or in combination with chemotherapy or radiotherapy. Evidence on *CHK1* and *DNA-PK* although limited, showed potential to further investigate these promising targets over broader tumor types.

The collective data and results from both studies, the “ITCC-P4: Molecular characterization and multi-omics analysis of Patient-Derived Xenograft (PDX) models from high-risk pediatric cancer” and the “Target actionability review on replication stress”, can be explored further on the interactively designed R2 platform, once users create an account to gain access to the cohort data. (<https://r2-itcc-p4.amc.nl/>).

## Zusammenfassung

Krebs ist nach wie vor eine der häufigsten Todesursachen bei Kindern im Alter von 0 bis 19 Jahren. Es besteht jedoch nach wie vor ein ungedeckter Bedarf an der Identifizierung von therapeutischen Biomarkern und besseren Behandlungsmöglichkeiten für diese Patienten.

Die Fortschritte bei den modernen molekularen Analysemethoden haben zu einem besseren Verständnis der pädiatrischen Krebserkrankungen und der auslösenden Faktoren geführt. Es hat sich gezeigt, dass pädiatrische Krebserkrankungen wesentlich heterogener sind als bisher angenommen, was durch die Anzahl neuer Entitäten und Subtypen mit unterschiedlichen molekularen und klinischen Merkmalen belegt wird. Für die meisten dieser neu erkannten Entitäten gibt es nur äußerst begrenzte Behandlungsmöglichkeiten.

Meine beiden Studien sind Teil des Konsortiums „Innovative Therapies for Children with Cancer - Pediatric Preclinical Proof-of-Concept Platform ([ITCC-P4](#))“, einer internationalen Zusammenarbeit zwischen verschiedenen europäischen akademischen Instituten, mehreren Partner-Pharmaunternehmen und drei Auftragsforschungsinstituten. Die beiden Studien sollen Aufschluss über die Identifizierung potenziell vielversprechender Behandlungsoptionen geben, die speziell auf die spezifischen molekularen Tumoreigenschaften und die genetischen Daten des Patienten abgestimmt sind. Genetische Informationen auf molekularer Ebene von pädiatrischen Tumoren bei Rückfallpatienten haben dazu beigetragen, unser Verständnis des Krankheitsverlaufs und der Behandlungsresistenz zu verbessern.

Die erste Studie im Rahmen des ITCC-P4 hat das übergeordnete Ziel, eine nachhaltige Plattform mit mehr als 400 molekular gut charakterisierten PDX-Modellen pädiatrischer Hochrisikokrebsarten, ihren Tumoren und entsprechenden Kontrollen zu etablieren. Dies würde die Auswahl von PDX-Modellen für In-vivo-Tests neuartiger Behandlungen auf der Grundlage von Wirkmechanismen ermöglichen. Es würde zudem die Prioritätensetzung bei der Entwicklung von Arzneimitteln sowie die klinische Stratifizierung von Patienten über verschiedene Entitäten hinweg erleichtern.

Derzeit sind 251 Modelle vollständig charakterisiert, darunter 180 Hirn- und 71 Nicht-Hirn-PDX-Modelle, die 112 Primärmodelle-, 92 Rezidiv-, 42 Metastasen- und 4 unter Behandlung stehender Progressionsmodelle repräsentieren. Mit Hilfe der sogenannten Whole-Genome und Whole-Exome Sequenzierung, somatischen Mutationsanalyse, und der Analyse von DNA Kopienanzahl sowie Methylierungsdaten sollen genetische Merkmale in der ITCC-P4 PDX-Kohorte definiert und die molekulare Übereinstimmung der PDX-Modelle im Vergleich zu ihrem Patiententumor abgeschätzt werden. Auf der Grundlage von DNA-Methylierungsprofilen wurden 43 verschiedene Tumoruntergruppen innerhalb von 18 Krebsentitäten identifiziert.

Die Analyse der Mutationslandschaft identifizierte die wichtigsten somatischen und Keimbahn-Alterationen, wobei Ependymom-PDX-Modelle das *C11orf95-RELA*-Fusionsereignis, *YAP1*, *C11orf95* und *RELA* SV aufwiesen. Medulloblastom-Modelle

wurden durch *MYCN*, *TP53*, *GLI2*, *SUFU* und *PTEN* angetrieben. Hochgradige Gliom-Proben wiesen somatische SNVs von *TP53*, *ATRX*, *MYCN* und *PIK3CA* sowie fokale Deletionen von *CDKN2A* auf Chromosom 9 auf. Neuroblastom-Modelle waren angereichert mit *ALK*-SNVs und/oder fokaler *MYCN*-Amplifikation, *ATRX*-SNVs und *CDKN2A/B*-Deletionen. Sarkom-Modelle wiesen charakteristische Alterationen wie *PAX3-FOXO1*-Fusionen auf, die bei embryonalen Rhabdomyosarkomen nachgewiesen wurden, zusammen mit *TP53*, *CDKN2A*, *NRAS* SNVs, *NCOA1*, *NF1* und *CDK4* SVs. Ewing-Sarkom-PDX-Modelle wiesen die bekannte und definierende *EWSR1-FLI1*-Genfusion sowie in Einzelfällen *EWSR1*-Fusionen mit *ERG* und *FEV* auf. Osteosarkome zeichneten sich durch hochgradig instabile Genome mit großen chromosomalen Veränderungen aus. Die Tumorsuppressorgene *TP53* und *RB1* waren häufig verändert, und es wurden *ATRX*-Verluste und *MYC*-Amplifikationen beobachtet. Weitere Sarkome wie das klarzellige Sarkom der Niere wiesen einen *CDKN2A*-Verlust, einen *MYC*-Zuwachs, einen *NF1*-Verlust und *TP53*-Mutationen auf, während Synovialsarkom-Modelle durch *SSX*-Genfusionen und -Veränderungen gekennzeichnet waren. Große Chromosomenaberrationen (Deletionen, Duplikationen), die in den PDX-Modellen nachgewiesen wurden, gingen mit molekularen Veränderungen einher, die bei den einzelnen Tumorarten häufig beobachtet wurden: Isochromosom 17 wurde in fünf Medulloblastom-Modellen nachgewiesen, während die Deletion des Chromosomenarms 1p oder die Zunahme von Teilen von 17q in Neuroblastomen mit der Tumorprogression korrelieren.

Die Tumor-Mutationslast zwischen den Entitäten und die Kopienzahlanalyse wurden durchgeführt, um allelspezifische Kopienzahlereignisse in Tumor-Normal-Paaren zu identifizieren. Eine klonale Evolution somatischer Varianten wurde nicht nur bei bestimmten PDX-Tumor-Paaren festgestellt, sondern auch zwischen verschiedenen Krankheitsstadien. Der Multi-omics-Ansatz in dieser Studie bietet einen Einblick in die Mutationslandschaft und -muster der PDX-Modelle und liefert so einen Überblick über die molekularen Mechanismen, die die Identifizierung und Priorisierung von onkogenen Treibern und potenziellen Biomarkern für eine optimale Behandlung erleichtern.

Die zweite Studie, ebenfalls im Rahmen des ITCC-P4-Konsortiums, umfasst ein „Target Actionability Review“ zum Replikationsstress. Zahlreiche veröffentlichte Daten belegen, dass der Replikationsstress ein therapeutisches Ziel darstellt. Allerdings beeinträchtigen die schädlichen Langzeitnebenwirkungen der Chemotherapie das Leben der behandelten Patienten drastisch. In der Studie werden spezifische Zielmoleküle der Replikationsstressreaktion bewertet, verglichen und hervorgehoben. Die Methodik zielt darauf ab, gezielte therapeutische Maßnahmen zur Krebsbekämpfung auf der Grundlage klinischer Studien auf bestimmte Subtypen abzustimmen. Es wurde ein umfassender, gut strukturierter und kritisch bewerteter Review über die Literatur zum Thema Replikationsstress bei 16 pädiatrischen soliden Malignomen erstellt. Es wurde festgestellt, dass *ATR*, *ATM*, *PARP* und *WEE1* die vielversprechendsten Angriffspunkte darstellen, entweder als Einzelwirkstoffe oder in Kombination mit Chemo- oder Strahlentherapie. Die Nachweise zu *CHK1* und *DNA-PK* sind zwar begrenzt, zeigen

aber das Potenzial, diese vielversprechenden Ziele bei einer größeren Anzahl von Tumorarten weiter zu untersuchen.

Die kollektiven Daten und Ergebnisse beider Studien, der „ITCC-P4: Molecular characterization and multi-omics analysis of Patient-Derived Xenograft (PDX) models from high-risk pediatric cancers“ und der "Target actionability review on replication stress", können auf der interaktiv gestalteten R2-Plattform weiter erforscht werden, sobald die Nutzer ein Konto erstellt haben, um Zugang zu den Kohortendaten zu erhalten (<https://r2-itcc-p4.amc.nl/>).

## Acknowledgements

Over the past 4 years, the guidance and encouragement I received to keep moving forward has been immense. It's because of this support network that I was able to complete my PhD journey successfully at the German Cancer Research Center (DKFZ).

First and foremost, I would sincerely like to thank my PhD advisor, **Prof. Dr. Stefan Pfister** for giving me the opportunity to pursue my PhD at the Division of Pediatric Neurooncology (B062) and Hopp Children's Cancer Center Heidelberg (KITZ). Stefan, your dedication and passion for science and oncology research is incredibly inspiring. As my supervisor and TAC member, your extensive knowledge, and innovative ideas on all my projects has been super helpful. Thank you for all the encouragement and the opportunity to work on the ITCC-P4 consortium project. I've had the chance to network and collaborate with some extraordinary scientists in the field of pediatric oncology, not only in academia but also the industry. For this, I am extremely grateful. You've created an amazing work environment at B062 with a diverse group of inspiring scientists who I've learned so much from over the last few years.

To my direct supervisor, **Dr. Natalie Jäger**, thank you for your mentorship and support from day one. Natalie, you've been such an incredible group leader and I really lucked out being able to work under your supervision. You're such an intelligent, empathetic, kind and contagiously humorous human-being and an inspiring woman in science. Thank you on all the talks, bioinformatics feedback, constant support, and especially your pragmatic thinking on getting things done. I really appreciate all the motivation and guidance you've given me, not only on my projects but also my personal development. You're truly one of a kind!

A huge thank you to my other TAC members, **Prof. Dr. Benedikt Brors** and **Dr. Jan Korbelt** for providing excellent inputs, having productive discussions and the all the scientific advice throughout my TAC meetings.

I would also like to thank **Prof. Dr. Marcel Kool**, for all your valuable insight and scientific advice on the ITCC-P4 project. Your support and guidance on various research ideas we had throughout the ITCC-P4 consortium projects was extremely helpful.

Many thanks to my newest supervisor, **Dr. Robert Autry**. The past 10 months of having you as my supervisor have been great. You've been super supportive, enthusiastic, easy to have scientific discussions with. Your friendly and charming Southern American personality is always a joy to be around leading to some hilarious conversations.

I would like to thank my colleague and ITCC-P4 collaborator **Dr. Aniello Federico**. Working so closely on the consortium project, managing collaborators, having brainstorming sessions and several weekly meetings has been a pleasure. Thank you for being so patient with all my doubts and discussions. Your continuous support and trouble-shooting code errors has been incredibly valuable. From the ITCC-P4 general assembly in Zug, Switzerland to the AACR 2023 conference in Florida, you've been

great to work with and such an inspiration. We still have a long way to go, but I'm sure we can wrap up and publish this paper soon!

I would also like to thank all my other ITCC-P4 collaborators, specifically, **Dr. Jan Koster** for all your fruitful discussions, brainstorming ideas, R2 assistance, guidance, and overall positive energy. It's been a pleasure collaborating and learning from you. **Sonja Krausert** and **Kaylee Keller**, working together on the TAR over never-ending Zoom calls during the pandemic was an interesting time to push the project forward. Being able to successfully complete and publish the review during the strangest time of the world, was a truly memorable experience!

To my Clinical Bioinformatics current and former colleagues and friends, **Venu Thatikonda**, you've been such an awesome mentor and most importantly a great friend. Thanks for all the fantastic advice, support, tips-and tricks, coding assistance, uplifting, motivational chats. Your positive vibes have shown me that there's so much more in life and it only gets better! **Pengbo Beck**, thanks for spreading your happy positive energy and all your support and guidance. You've been a wonderful colleague and made our ClinBio group so much livelier and more social even through the pandemic. **Dr. Gnana Prakash Balasubramanian**, my desk buddy, thanks for all the motivational talks, the random Telugu songs, Indian sweets, Chai and samosas. Your words of wisdom will stay with me forever and I will always remember to "*Keep my head down, drink the Kashayam and keep moving forward*". **Dr. Christopher Previti**. Thank you for all the assistance with CNVkit and pre-processing samples and for being flexible with all my "final samples" E-mails and requests. **Dina El Harouni**, continue being a brilliant scientist and spread your joy all over Boston. I will forever be cheering you on, for shooting your shot again at the Olympics! Thanks for all the support and advice! **Rolf**, thank you for teaching me that "*The Only Stupid Question is the One You Don't Ask*". You've been so patient and kind with all the technical and IT assistance, thanks for helping debug code, solving cluster issues, installing all my various R-packages. **Dr. Matrin Sill** and **Dr. Konstantin Okonechnikov** I much appreciate all the advice and guidance on various bioinformatics analysis. Thanks **Lukas Madenach** and **Enrique Blanco** for the entertaining chats, coffee breaks and social gatherings! **Maximilian Deng**, thanks for the spontaneous coffee catchups, laughter, and lunch sessions!

Most importantly, my forever friends, **Felix Schmitt-Hoffner** and **Jasper van der Horst**, one of the best parts of this PhD was our friendship and for that I am eternally grateful. Thank you barely covers what I need to say. You've both made the last 4 years so much more enjoyable and happier! Through all the ups and downs and mental stress, you've added so much laughter, joy, support with all our "*DKFZ Coffee Social Club*", BBQ evenings, cocktail nights, drinks at Café Regie, swimming in the lake evenings and countless core memories. I will always be grateful to have made two lifelong friends on this PhD adventure, no matter where we are or where we end up, someday that Faroe Island trip together is happening! I'm so glad I started talking to you guys in the climbing gym at the PhD initial course! Looking forward new memories we will continue to make in the future. #KamchatkaGirls.

**Michael Persicke**, my DKFZ Dossenheim neighbour and Fika partner, thank you for all the dinners, tears of laughter and conversations reminding me that there's so much more to life. From biking back to Dossenheim post DKFZ PhD parties and Schriesheim vineyard walks, to now, ice-cream and walks around Weststadt. Your everlasting smile and kind heart makes you one of the best people I know.

I also owe a huge thanks to my friends over the world. **Sindhu Vangeti**, thanks for being a massive inspiration. The day you bought me that "København" magnet and said you were starting your PhD at Karolinska Institutet, Sweden, changed my life. You inspire me with all your hard-work and never-endingly wild social battery! The sisterly advice, pep-talks, PhD guidance, being so understanding on professional challenges and relatable on similar struggles of life, made this journey so much easier.

To some of my longest standing supporters, having been through the chapters that aren't in this thesis, **Kunal**, thanks for always listening and being there no matter the time difference. From wake-up calls early in the morning, Office memes, mental health check-ins, motivation, and hype sessions, you've been through it all. Thank you for all the love and support! **Mitali**, one of my oldest friends and we've grown up together seeing and supporting each other through difference seasons of life, thanks for always making me laugh, the amazing Harry Styles conversations and the never-ending motivation and check-in calls! Miss you! **Srishti**, thanks for being my go-to person for all the ranting sessions, laughter, giggles, and support. **Nina**, I'm so glad we started chatting at the doctor's office that day. Thanks for all the coffee chats, mentorship, summer swimming sessions when I needed a writing break. **Nathalie**, my first friend in Heidelberg, thank you for all your positive energy and brunch/coffee chats and laughter since 2019! To all my other friends who I haven't mentioned explicitly, you know who you are. Thank you for coming into my life for a reason, season, or a lifetime. You're all appreciated!

Last but not the least, my family, **Amma** and **Dada**, thank you for teaching me to chase my dreams and doing what makes me happy. Without your unconditional love, encouragement, and never-ending support since the very beginning, I would never be where I am today. Your continuous cheerleading and motivating pep-talks through all the challenging times, made it possible to reach the end of this adventure and for that I am forever grateful. My brother, **Akash**, thank you for being my biggest inspiration and supporter since 1994. We might not always see eye-to-eye but without your infinite advice, calm and rational mindset, and endless love, this would not have been possible. I will always remember you saying, "*Keep your wits about you*". Thank you for all the vacations planned and long road trips, it's my turn to finally take some load off your plate. Brace yourself!

Finally, to my grandparents. My grandmother, **Ammamma** and in the loving memory of my grandfather, **Thathayya**. Your unconditional love, kindness, and wisdom has made me what I am today. You've always believed in me since day one. Thank you for being an incredible source of inspiration in my life and for showing me what true love and happiness is.

## List of abbreviations

450k arrays	Illumina Infinium 450k Methylation BeadChip Arrays
AT/RT	Atypical teratoid/rhabdoid tumors
bp	Base pairs
CBTRUS	Central Brain Tumor Registry of the United States
CCSK	Clear cell sarcoma of the kidney
CNA/CNV	Copy number alteration/Copy number variation
CNS	Central nervous system
DKFZ	Deutsches Krebsforschungszentrum
DNA	Deoxyribonucleic acid
EPN	Ependymoma
ETMR	Embryonal tumour with multilayered rosettes
EWS	Ewing sarcoma
FFPE	Formalin-Fixed Paraffin-Embedded
GEMM	Genetically engineered mouse models
HB	Hepatoblastoma
HGG	High-grade glioma
HGNET	High Grade Neuroepithelial Tumor
IGV	Integrative Genomics Viewer
IMI	Innovative Medicines Initiative
indels	Insertions and Deletions
ITCC-P4	Innovative Therapies for Children with Cancer Pediatric Preclinical Proof-of-concept Platform
KiTZ	Hopp Children's Cancer Center
lcWGS	Low-coverage Whole exome sequencing
LL	Large-cell lymphoma
MB	Medulloblastoma
MPNST	Malignant Peripheral Nerve Sheath Tumor

NB	Neuroblastoma
NGS	Next-generation sequencing
NSG	NOD-SCID Gamma mice
OS	Osteosarcoma
PDX	Patient-Derived Xenograft (s)
PLEX	Plexus tumor
PLGG	Pediatric low-grade glioma
PoC	Proof-of-concept
RNA	Ribonucleic acid
RNA-seq	RNA Sequencing
RMS_ALV	Alveolar rhabdomyosarcoma
RMS_EMB	Embryonal rhabdomyosarcoma
RSR	Replication stress response
RT	Rhabdoid tumors
SARC	Sarcoma
SNVs	Single nucleotide variants
SS	Synovial sarcoma
SV	Structural variants
TAR	Target actionability review
TCF	Tumor cell fraction
t-SNE	t-distributed stochastic neighbor embedding
VAF	Variant allele frequency
WES	Whole exome sequencing
WGS	Whole genome sequencing
WHO	World Health Organisation

# Contents

DECLARATION .....	5
ABSTRACT .....	I
ZUSAMMENFASSUNG .....	III
ACKNOWLEDGEMENTS .....	VI
LIST OF ABBREVIATIONS .....	IX
CONTENTS .....	XI
LIST OF FIGURES .....	XV
LIST OF TABLES .....	XVII
<b>1 INTRODUCTION .....</b>	<b>1</b>
<b>1.1 An introduction to Cancer .....</b>	<b>1</b>
1.1.1 Cancer – a worldwide health crisis .....	1
1.1.2 Hallmarks of cancer.....	2
1.1.3 Cancer genome and epigenome .....	3
1.1.4 Replication stress response (RSR) .....	5
1.1.5 Current treatment strategies & personalized oncology.....	6
<b>1.2 Omics revolution in cancer.....</b>	<b>6</b>
1.2.1 Next-generation sequencing methods .....	6
1.2.2 DNA Methylation .....	7
1.2.3 Gene expression arrays.....	7
1.2.4 Multi-omics integration for genomic profiling.....	8
<b>1.3 Pediatric cancers .....</b>	<b>8</b>
1.3.1 Childhood vs adult cancers.....	8
1.3.2 Pediatric Brain and Central Nervous System tumors.....	11
1.3.3 Neuroblastoma .....	20
1.3.4 Sarcomas .....	20
1.3.5 Other tumors .....	24
<b>1.4 Patient derived xenograft models for preclinical modeling of cancer.....</b>	<b>25</b>
<b>1.5 Precision medicine for pediatric tumors .....</b>	<b>28</b>
<b>1.6 AIMS .....</b>	<b>29</b>
1.6.1 ITCC-P4: Molecular characterization and multi-omic analysis of Patient-Derived Xenograft (PDX) models from high-risk pediatric cancer.....	29
1.6.2 Target Actionability Review (TAR): a systematic evaluation of replication stress as a therapeutic target for pediatric solid malignancies.....	30

<b>2</b>	<b>MATERIALS AND METHODS .....</b>	<b>31</b>
<b>2.1</b>	<b><i>Materials based on ITCC-P4 Genomic profiling .....</i></b>	<b>31</b>
2.1.1	Human tumor samples .....	31
2.1.2	PDX model establishment .....	33
2.1.3	ITCC-P4 Cohort.....	34
<b>2.2</b>	<b><i>Methods based on ITCC-P4 Genomic profiling .....</i></b>	<b>37</b>
2.2.1	Whole Exome Sequencing and Whole Genome sequencing workflow... 37	
2.2.2	"No-control workflow": Analysis of samples without patient-matched germline data .....	38
2.2.3	DNA-Methylation profiling and subgroup classification .....	39
2.2.4	Copy number variant (CNV) workflow .....	39
2.2.5	RNA sequencing workflow and gene fusion calling.....	40
2.2.6	Driver gene annotation of somatic and germline mutations.....	41
2.2.7	Tumor mutational burden (TMB) analysis.....	41
2.2.8	Variant allele frequency (VAF) calculation .....	41
2.2.9	Tumor cell fraction (TCF) – ESTIMATE, Sequenza and CNVkit .....	42
2.2.10	Variant allele frequency using estimated tumor cell fraction .....	42
2.2.11	PDX-Tumor correlation: Pearson scores, delta-VAF and VAF-ratio .....	42
<b>2.3</b>	<b><i>Methods based on the ITCC-P4 Target Actionability Review - Replication Stress .....</i></b>	<b>43</b>
2.3.1	Step 1: Literature search .....	44
2.3.2	Step 2: Critical review and scoring .....	45
2.3.3	Step 3: Adjudication by reviewer .....	51
2.3.4	Step 4: Data visualisation .....	51
<b>3</b>	<b>RESULTS.....</b>	<b>52</b>
<b>3.1</b>	<b><i>Results based on the molecular characterization and multi-omic analysis of Patient-Derived Xenograft (PDX) models from high-risk pediatric cancer .....</i></b>	<b>52</b>
3.1.1	ITCC-P4 PDX model cohort generation and characterization .....	52
3.1.2	Molecular subgrouping of pediatric solid tumors based on DNA methylation and transcriptomic analysis .....	56
3.1.3	Genomic landscape of pediatric solid tumors.....	61
3.1.4	Copy number landscape of ITCC-P4 PDX models .....	73
3.1.5	PDX model fidelity compared to matching patient tumor .....	75
3.1.6	Modeling of tumor progression: "Serial" PDX comparisons .....	88
3.1.7	ITCC-P4 data scope portal: R2 platform .....	92

3.2	<b><i>Results from the ITCC-P4 Target Actionability Review (TAR): Replication stress.....</i></b>	<b>93</b>
3.2.1	Systematic evaluation of replication stress literature.....	93
3.2.2	Druggable targets of replication stress and biomarker scoring.....	94
4	<b>DISCUSSION .....</b>	<b>99</b>
4.1	<b><i>Discussion based on ITCC-P4 genomic profiling .....</i></b>	<b>100</b>
4.1.1	PDX models in pediatric cancer.....	100
4.1.2	PDX models compared to their corresponding patient tumor .....	102
4.1.3	PDX models as a tool for preclinical drug testing .....	104
4.2	<b><i>Discussion based on TAR Replication stress.....</i></b>	<b>105</b>
4.2.1	Targeting Replication stress as a therapeutic approach.....	105
4.3	<b><i>Limitations .....</i></b>	<b>107</b>
4.4	<b><i>Future directions .....</i></b>	<b>109</b>
5	<b>BIBLIOGRAPHY.....</b>	<b>110</b>



# List of Figures

Figure 1: The hallmarks of cancer.....	2
Figure 2: Genomic alterations in cancer .....	4
Figure 3: Replication stress response targets.....	5
Figure 4: Global cancer incidence and mortality.....	9
Figure 5: European centric cancer incidence and mortality.....	9
Figure 6: Molecular classification of Medulloblastoma subgroups.....	15
Figure 7: PDX models for preclinical drug testing is the new era of cancer research .....	26
Figure 8: Established Pediatric precision oncology programs .....	28
Figure 9: PDX model establishment process.....	34
Figure 10: Overview of Replication Stress TAR methodology.....	43
Figure 11: Schematic illustration of ITCC-P4 PDX model establishment .....	52
Figure 12: ITCC-P4 PDX model generation and subgroup classification .....	53
Figure 13: ITCC-P4 PDX model characterization.....	55
Figure 14: DNA Methylation analysis .....	57
Figure 15: Epigenomic correlation assessment of each subgroup .....	59
Figure 16: Analysis of PDX cohort transcriptomic profile.....	60
Figure 17: Tumor mutational burden across PDX and tumor.....	62
Figure 18: Tumor mutational burden across cancer types and subtypes.....	63
Figure 19: Mutational landscape of Ependymoma and Medulloblastoma.....	65
Figure 20: Mutational landscape of High-grade glioma, HGNET-PLEX and AT/RT .....	66
Figure 21: Mutational landscape of Neuroblastoma.....	68
Figure 22: Mutational landscape of Rhabdomyosarcoma.....	70
Figure 23: Mutational landscape of Ewing sarcoma.....	70
Figure 24: Mutational landscape of Osteosarcoma .....	71
Figure 25: Mutational landscape of additional SARC tumors.....	72
Figure 26: Mutational landscape of other tumors .....	72
Figure 27: Copy number landscape of ITCC-P4 PDX cohort .....	74
Figure 28: Tumor cell purity between PDX and tumors.....	75
Figure 29: Tumor cell fraction comparisons .....	76
Figure 30: Change in PDX and tumor variant allele frequency (delta-VAF) .....	79
Figure 31: VAF plot for high-grade glioma samples .....	81
Figure 32: VAF plot for Ewing sarcoma samples.....	81
Figure 33: VAF plot for Neuroblastoma samples.....	82
Figure 34: VAF plot for Rhabdomyosarcoma samples.....	83
Figure 35: VAF plot for Osteosarcoma samples .....	84
Figure 36: Chromosomal landscape and VAF plot concordance in PDX tumor pairs .....	85
Figure 37: ichorCNA CNV profiles and Circos plots for SV comparison .....	86
Figure 38: Serial cases comparisons .....	88

Figure 39: DNA methylation based tSNE for Serial cases .....	89
Figure 40: Serial cases - VAF and copy number profile comparison .....	90
Figure 41: Coverage plots of Serial cases highlighting driver gene events .....	91
Figure 42: ITCC-P4 data scope on the R2 platform .....	92
Figure 43: The TAR workflow process .....	93
Figure 44: Overview of replication stress targets .....	94
Figure 45: Evidence and therapeutic combination reported for TAR .....	95
Figure 46: Summary of TAR appraisal scores .....	97
Figure 47: Overview of specific therapeutic targets .....	98

## List of Tables

Table 1: ITCC-P4 European partnering institutes and their ITCC-P4 barcodes .....	32
Table 2: ITCC-P4 standardised barcode system .....	36
Table 3: WES library prep kits and sequencing platforms used in ITCC-P4 .....	37
Table 4: lcWGS sequencing platforms used in the ITCC-P4 .....	37
Table 5: Replication stress keywords and cancer entities for PubMed queries.....	44
Table 6: Proof of concept (PoC) modules for the TAR.....	47
Table 7: Experimental quality scoring.....	49
Table 8: Experimental outcome scoring .....	50



# 1 INTRODUCTION

## 1.1 An introduction to Cancer

### 1.1.1 Cancer – a worldwide health crisis

Cancer is a disease characterized by the unrestrained proliferation of cells originating from different cell types and organs of the body. These cells can invade normal tissue boundaries and can metastasize in different organ sites. The tumors that stay in the primary origin site are known as benign tumors and have a slower growth. Those cells that grow uncontrollably and spread to distant sites via the bloodstream or lymphatic system are known as metastatic tumors. This extensive growth of metastatic cancer cells can inevitably lead to death. Cancer comprises of over hundred distinct diseases with complex genetic and epigenetic alterations, accounting for 18% of deaths, making it the second leading cause of death by disease in the world. Globally 10 million cancer deaths have been reported according to the 2020 GLOBOCAN from The International Agency for Research on Cancer (IARC) with a prediction of 28 million new cancers cases by 2040 [1], [2].

The diverse rates of cancer incidence, progression and mortality can be accounted for by the difference in biological sex, race, age, geographical locations, and also socio-economic backgrounds. The most common causes of cancer deaths in men aged 60–79 years were reported to be prostate, lung and bronchus and colorectal cancer, while women aged 40–79 years were affected by lung and bronchus, breast, and colon cancer. Tumors affecting the brain and central nervous system are the primary cause of cancer related deaths among children and adolescents younger than 20 years [3]. The largest incidence and mortality difference based on geography were reported for lung, cervical cancer and melanoma of the skin. This could be due to variations in lifestyles and risk factors such as smoking, obesity, alcohol, exposure to UV rays[1]. Predominance of cancer was also reported where more developing countries displayed infection-based cancer deaths potentially caused due to lower access to preventative care, screening and early detection practices, while more developed socio-economically progressive regions displayed higher cancer mortality due to lifestyle [2], [3].

The development of modern medicine and advances in prevention and early detection of cancer have led to a significant decline in cancer mortality by 33% since 1991[3]. There has been an increased 5-year survival rate for all cancers from 49% for diagnoses (mid-1970s) to 68% for diagnoses (between 2012 – 2018)[3]. Although there have been revolutionary therapeutic advances over the past decade, there is still a crucial need to further understand the molecular characterization and biological functioning of cancer based on modern next generation sequencing methods.

### 1.1.2 Hallmarks of cancer

Tumorigenesis is a multi-step process involving distinct characteristics, initially proposed by Douglas Hanahan and Robert Weinberg in 2000 [4] as requirements needed to be fulfilled for cancer cells to form and survive. This seminal paper described six acquired capabilities of cancer cells: evasion of growth suppressors, acquiring resistance to programmed cell death (apoptosis), sustaining proliferating growth signals, enabling replicative immortality, the induction of angiogenesis and activating invasion and metastasis. These core hallmarks provide a framework for distinguishing cancer cells from normal healthy cells. They were further expanded upon in 2011 to include emerging biological hallmarks: ability to avoid immune destruction and deregulation or reprogramming of energy metabolism[5]. Additionally, two consequential enabling characteristics were later highlighted namely: genome instability and mutation, causing genetic variability and tumor promoted inflammation. As cancer is a heavily researched area, new observations shed light on the complexities of a tumor. A tumor is not merely a uniform cluster of dividing cells, but a complex heterogenous “organ” comprising of fibroblasts, immune cells, endothelial cells and mesenchymal cells among others. The heterotypic interactions of these constitutions with the surrounding stromal cells and tumor microenvironment were better understood by the advent of powerful experimental tools and advances in computational technologies over the last decade. This led to the expansion of the hallmarks of cancer in 2022 (Figure 1), to encompass additionally proposed emerging hallmarks: unlocking phenotypic cellular plasticity, cellular senescence and enabling characteristics, non-mutational epigenetic reprogramming, and polymorphic microbiomes[6]. These hallmarks of cancer are necessary for normal cells to transform into cancerous cells.

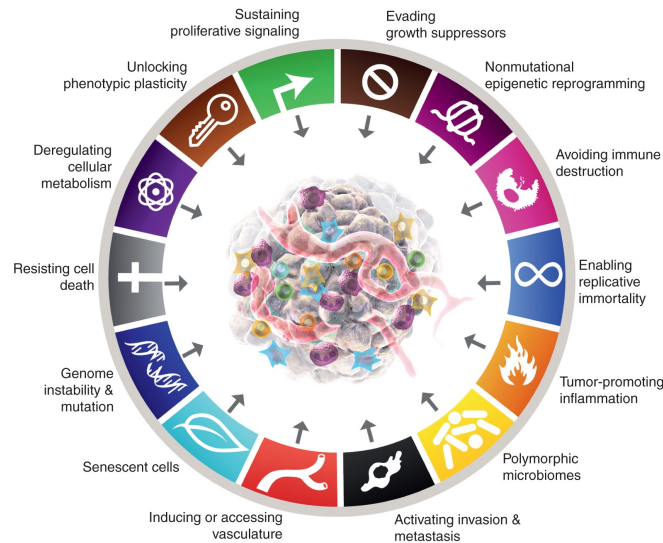


**Figure 1: The hallmarks of cancer**

*The eight core hallmarks of cancer defining the characteristics acquired during tumor growth. It provides a solid foundation for the understanding of cancer biology and development of targeted therapies. (Adapted from Hanahan, 2022[6])*

### 1.1.3 Cancer genome and epigenome

Across billions of mitotic cycles in cell division, throughout the lifespan of a human embryo, the normal physiology, structural integrity, and functions of the DNA need to be preserved. Although the process of copying genetic information from one mitotic cycle to new cells is highly efficient and accurate, sporadic errors and lesions in DNA replication and the repair mechanisms can lead to subtle changes in the DNA sequence. Defects in the normal DNA replication pathways that govern genetic stability, amplifies tumorigenesis, by mutations, clonal selection and evolution and ultimately drive cancer formation [7]–[9].

Mutations that occur within the human genome are either germline or somatic. Germline mutations are inherited from the parent and occur in the gamete (egg or sperm) or cells that produce the gamete, progenitor cells[10], [11]. The resulting embryo and baby will carry this variation in every cell of the body that contains a copy of the gene. The most common example of a pathogenic germline variant is *BRCA1* or *BRCA2*, carried by 1-5% of breast cancer patients. *BRCA1* and *BRCA2* genes play a significant role in DNA homologous recombination repair during stalling of replication fork or DNA strand breaks during replication. The biallelic loss of germline *BRCA1* and *BRCA2* causes less effective or inability to perform homologous repair of double stranded break, leading to a higher rate of DNA mutations and high likelihood of breast and ovarian cancer[12]. Somatic mutations are those that occur in other cells of the body and are not present in every cell of the body, hence are not inherited or passed on from one generation to the other[11], [13].

With technological advances in next-generation sequencing there are two main categories of genomic alterations in cancer [14], [15]. First are small variations that include single nucleotide variants (SNVs) and small insertions and deletions (INDELS). These alterations are caused by substitution of one or more nucleotide bases with different nucleotides. SNVs occur due to a single base change of <1 base pair, while INDELS are <50 base pair regions of the DNA that are inserted or deleted. Second, are large variations also known as structural variants (SVs) or chromosomal rearrangements. SVs span >50 base pairs and are rearrangements of the DNA segment occurring due to deletions, inversions (orientational), tandem duplications(quantitative), insertions (positional), translocation (positional) and copy number changes (quantitative) [14]–[20] (Figure 2). These copy-number alterations (CNAs) occur due to increased (gains) or decreased (losses) number of copies of the chromosomal region of the DNA segment, compared to their corresponding reference or control [18], [21], [22]. Gene fusions or chromosomal rearrangements are an important type of genomic alterations that play a significant role in tumorigenesis. In 1960 the first cancer associated translocation of chromosome 9 and 22, termed as Philadelphia chromosome was identified in patients with chronic myeloid leukemia (CML). This translocation resulted in the formation of fusion proteins as a result of the *BCR* and *ABL* gene fusion[23]–[27].

Most mutations in cancer are assumed to be neutral, termed as “passenger mutations”, that do not stimulate carcinogenesis. Mutations that enhance the progression of tumor

cells are termed as “driver mutations”. These oncogenic mutations drive abnormal proliferation of cancer cells and represent single-nucleotide substitutions or point mutations [28], [29].

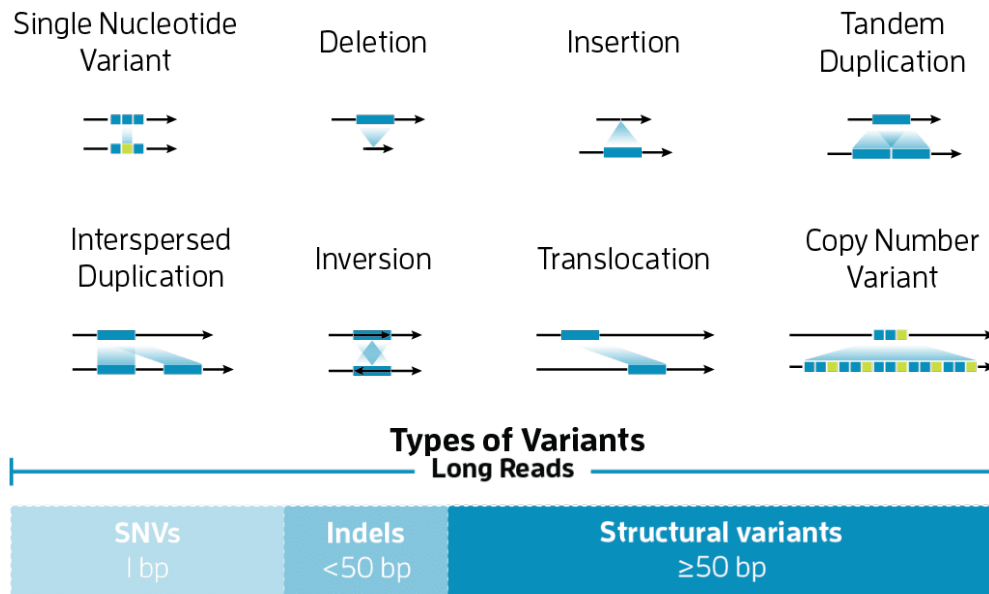


**Figure 2: Genomic alterations in cancer**

Advancements in next-generation sequencing enabled further understanding of genomic variations that can result in tumorigenesis. (Adapted from Logsdon GA et al. 2020 [15] PacBio review[30])

Three main types of genes that play a major role in cancer development, can be affected by somatic mutations. Oncogenes, resulting from “gain-of-function”, in their proto-oncogenic state drive cell cycle forward resulting in the uncontrolled growth of cancer cells. On the other hand, tumor suppressor genes are affected by “loss-of-function” mutations and restrict cell cycle progression. A well-known example of this is the protein product of tumor suppressor gene *CDKN2A* and interacts directly to inhibit the protein product of the *CDK4* oncogene[31], [32]. In many tumors, these genes are lost or inactivated, hence removing the negative feedback of cell proliferation, thus causing rapid cell proliferation and cancer growth[33]–[38]. Furthermore, DNA repair genes are involved in recognition and removal of errors made during DNA replication, nucleotide excision repair, mis-match repair, non-homologous end joining and homologous repair[39]–[42]. Additionally, these genes, affect DNA repair by cell cycle regulation and maintaining genomic stability. Dysregulation (loss or gain) of these DNA repair genes leads to the accumulation of genomic errors, genomic instability, and replication stress, ultimately leading to cancer formation[39], [42].

### 1.1.4 Replication stress response (RSR)

DNA replication stress is a broad term that includes obstruction of DNA replication by stalling or collapse of the DNA replication fork. Stalling causes the overall ribosomal structure to remain intact, but the mechanism of DNA replication is hindered until the issue is fixed. The exhaustion of nucleotides could be a factor causing stalling of the DNA fork. However, disruption of the replisome integrity causes collapse of the DNA fork, due to dissociation of some or all proteins from the DNA template, or the template itself may be processed to generate abnormal DNA structures[31]. The delay in DNA repair can result in the accumulation of further DNA damage. This in turn causes genomic instability and cell death. The replication stress response (RSR) pathway is a multi-faceted signalling pathway that is activated to maintain genomic stability and ensure survival, but in cases of irreparable DNA damage, apoptosis or programmed cell death is then initiated[43], [44]. Molecular errors can occur in two main components of replication stress response pathways – DNA damage repair pathways and cell cycle repair pathways can lead to DNA damage, genomic instability and finally cell death (Figure 3). Hence targeting proteins involved in replication stress as a vulnerability is an attractive therapeutic approach in cancer [43], [44].

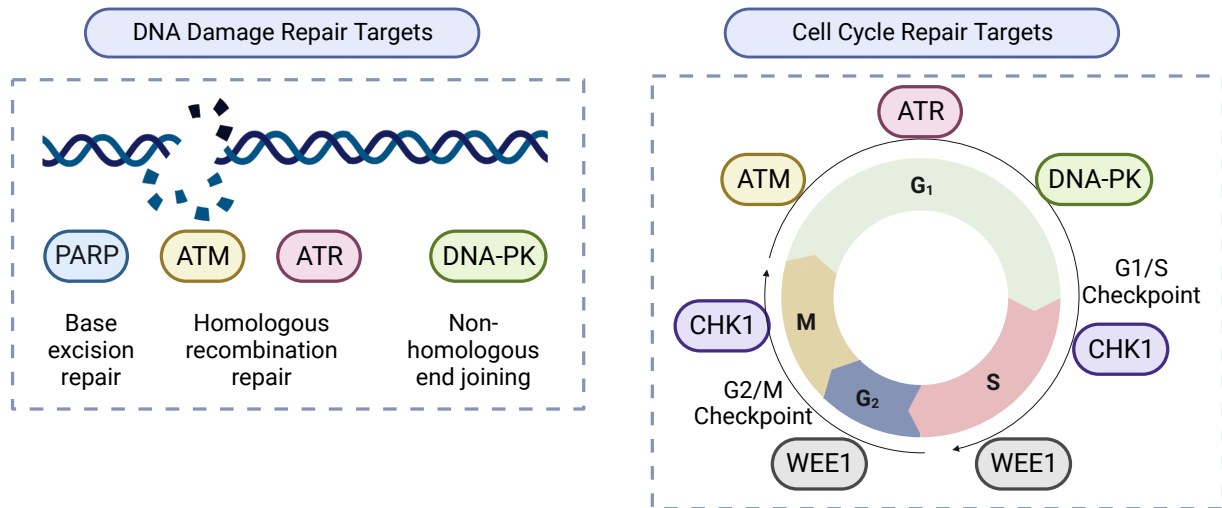


**Figure 3: Replication stress response targets**

*Dissociation of proteins involved in replication stress leads to genomic instability and cell death. Targeted treatment to focus on two main pathways DNA damage repair genes and cell cycle repair genes is widely being used in precision oncology.*

### **1.1.5 Current treatment strategies & personalized oncology**

Cancer is a complex, highly adaptable sequence of disease conditions progressing gradually and leading to the loss of cell growth control. Conventional therapeutic approaches such as surgery, chemotherapy, radiotherapy, and hormonal therapy have fallen short as there is no “one-size” fits all in cancer treatment. Each cancer patient is different from every other patient in clinical presentation, prognosis, tumor response to treatment and tolerance to treatment in addition to variations in risk of occurrence, secondary malignancies, and treatment tolerance[45]. Classical treatments are being administered along with combination treatments and by better molecularly tailored approaches for individual patients [46], [47]. Over the past few decades, two major revolutions in therapeutic strategies have changed cancer treatment: targeting actionable oncogenic drivers and immuno-oncology[46]. Hence, conventional interventions such as chemotherapy and now targeted therapy have significantly improved patient survival and quality of life for patients, with higher rates in complete tumor remission[48], [49].

Personalized oncology or precision medicine is the approach of tailoring medical treatment to personal characteristics of the patient's tumor and the host. By using evidence based statistical approaches to evaluate relationships between patient profile (e.g., genomic, proteomic, or transcriptomic) and the clinical output (e.g, degree of response to treatment)[50], [51]. The main essence of personalized cancer treatment relies on biomarkers, which can be diagnostic, prognostic, predictive and pharmacogenomic[45], [48], [51], [52]. The advances of molecular profiling beyond genomics such as transcriptomics, epigenomics, immunophenotyping and evaluation of combination drug treatments beyond monotherapy approaches has rapidly increased the scope of precision medicine in cancer research.

## **1.2 Omics revolution in cancer**

### **1.2.1 Next-generation sequencing methods**

DNA sequencing formerly suggested by Sanger et al. was based on the interpolation of changed nucleotides for chain elongation by DNA polymerase. However, this method was highly laborious, error-prone and time consuming. In 2005 “next-generation sequencing” (NGS) revolutionized the original “first-generation” Sanger sequencing, by employing synthetic DNA fragments (adapters) specifically designed for every sequencing platform to amplify the DNA library followed by cyclic sequencing. A distinct advantage of NGS over classical sequencing was the ability to implement the multiple stages of sequence and trace the signal concurrently, known as parallel sequencing. Initial NGS methodologies used single-end sequencing to cause difficulties with short-read which affects the quality of genome alignment. Now, paired-end sequencing procedures can significantly identify not only point mutations, but also detect genomic rearrangements such as deletions, amplifications, translocations, inversions, and gene-fusions[53], [54]. NGS can now be separated into “second-

generation sequencing” and “third-generation sequencing”. The former refers to strategies involved in short-read alignment, while the latter entails single DNA molecule-based sequencing, that accounts for the emerging, highly researched single-cell sequencing[55]. Whole-exome sequencing (WES) refers to the targeted sequencing of a subset of the human genome, that is protein-coded. This has become the most utilized sequencing technique in translational research to interpret parts of the human genome at relatively low costs [56], [57]. Whole-genome sequencing accounts for the entire genome sequencing including promotor and regulatory areas. Although oncology research is relying more on WGS characterization for identifying clinically relevant biomarkers, the substantially high cost makes it less favourable than WES. However, with the onset, advancement, and improvement of next generation sequencing (NGS) technologies and bioinformatics, a new era of cancer genomics research has been expanded to fill the gaps in cancer biology[58]. NGS has many advantages in identification of targetable biomarkers by fully sequencing the patient genome and the tumor to identify all types of mutations for hundreds to thousands of genes with increased sensitivity, speed, high-throughput and low-cost [59], [60].

### **1.2.2 DNA Methylation**

DNA-methylation is an epigenetic mechanism involving the transfer of a methyl-group to the C5-position of cytosine to form 5-methylcytosine. Most DNA methylation primarily takes place on cytosines located before a guanine nucleotide, commonly known as CpG sites. It is responsible for regulation of gene expression by recruiting gene repression proteins or by inhibiting transcription factor binding to the DNA[61]. During tumorigenesis, the pattern of DNA methylation constantly changes due to *de novo* methylation and demethylation. This leads to differentiated cells to develop a unique DNA methylation pattern that regulates tissue-specific gene transcription [61], [62]. Microarrays are used to read fractions of DNA that are enriched using a series of treatments with methylation sensitive restriction enzymes [63], [64]. Research has demonstrated that tumor methylation patterns remain consistent and faithfully represent the cell of origin, maintaining their stability throughout the disease's progression. Consequently, this makes it a reliable biomarker for categorizing tumors. DNA methylation has effectively been utilized to further classify significant tumor types, such as medulloblastomas, ependymomas, and supratentorial PNETs, which cannot be differentiated by histological analysis alone [61], [65]. This makes DNA methylation cancer biomarkers well suited for early detection and treatment of cancer.

### **1.2.3 Gene expression arrays**

Advancements in microarray technologies enables the further investigation of large numbers of DNA/RNA fragments in parallel to expand genomic research. Reverse transcribed messenger RNA, which has been labelled with a fluorescent dye, originating from an experimental sample is co-hybridized onto the microarray platform[66]. After the exclusion of non-selectively adhered fluorescent dye, the microarray is scanned under high-resolution to precisely determine the fluorescence intensity on the surface. Given the predetermined positions of the gene probes, it is possible to compute the

relative or absolute quantities of RNA associated with each gene featured on the array. Due to its capacity to include thousands of gene fragments, a microarray offers a comprehensive, genome wide perspective of gene expression aiding the field of cancer research[66], [67].

### **1.2.4 Multi-omics integration for genomic profiling**

A multi-omics investigation is a data-driven scientific analysis that utilizes diverse sets of high-dimensional data encompassing multiple omics levels, that can include the genome, proteome, transcriptome, epigenome, and metabolome. The main objective is to unveil the intricacies inherent to cells and their surrounding environments [68]. An extensive range of emerging omics techniques and multi-view clustering algorithms currently provide unparalleled prospects for further classification of cancer into their different subtypes. This enables the possibility to refine survival prediction and therapeutic efficacy within various subtypes and allows deeper understanding into key pathophysiological processes across different molecular layers in each patient[68], [69].

Genomic profiling of cancer allows refinement of tumor type and subtype classification, identifies which patient is more likely to benefit from systemic therapies and facilitates the recognition of germline variants that influence the predisposing risk to cancer. Integration of multi-omics characterization using large-scale research collaborations and computational advances creates a paradigm shift by identification of novel and targetable biomarkers and improving clinical assessment in cancer research[70]–[72].

## **1.3 Pediatric cancers**

### **1.3.1 Childhood vs adult cancers**

Pediatric cancer is the leading cause of death by disease- approximately 5% of children below the age of 14 years across the world are affected by cancer and about 1% of these cases lead to death in children[73]. Childhood cancer (0-14 years) and adolescent cancer (age 15-19) diagnoses account for 1% of overall global cancer diagnoses[74], indicating that pediatric cancers are far more rare than adult cancers[75], [76]. Reports by the World Health Organization (WHO) showed the leading cause of childhood deaths in 2020 were leukemia, central nervous system, non-Hodgkin lymphoma, kidney tumors, Hodgkin lymphoma, ovary, testis, liver, thyroid and nasopharynx tumors[1](Figure 4). Based on the European Commission, European Cancer Information System (ECIS) reports, the top four estimated cancer types in patients aged 1-19 are leukemia (26.1%), CNS tumors (13.9%), Hodgkin lymphoma (8.5%) and non-Hodgkin lymphoma (6.2%). On the other hand, CNS (29.6%), leukemia (27.9%), non-Hodgkin's lymphoma (5.0%) and kidney tumors (2%) (Figure 5) were the leading causes of childhood cancer death[77]. From a 2019 report, it has been observed that 43% of all pediatric cases [78] end up being insufficiently diagnosed across the world due to lack of early screening and diagnostic tools and insufficient healthcare access across the globe. This under-representation of data causes a significant bias in global health reports

and emphasizes the need for better and more accessible diagnostic tools and treatment options worldwide.

Estimated age-standardized incidence and mortality rates (World) in 2020, World, both sexes, ages 0-14 (excl. NMSC)

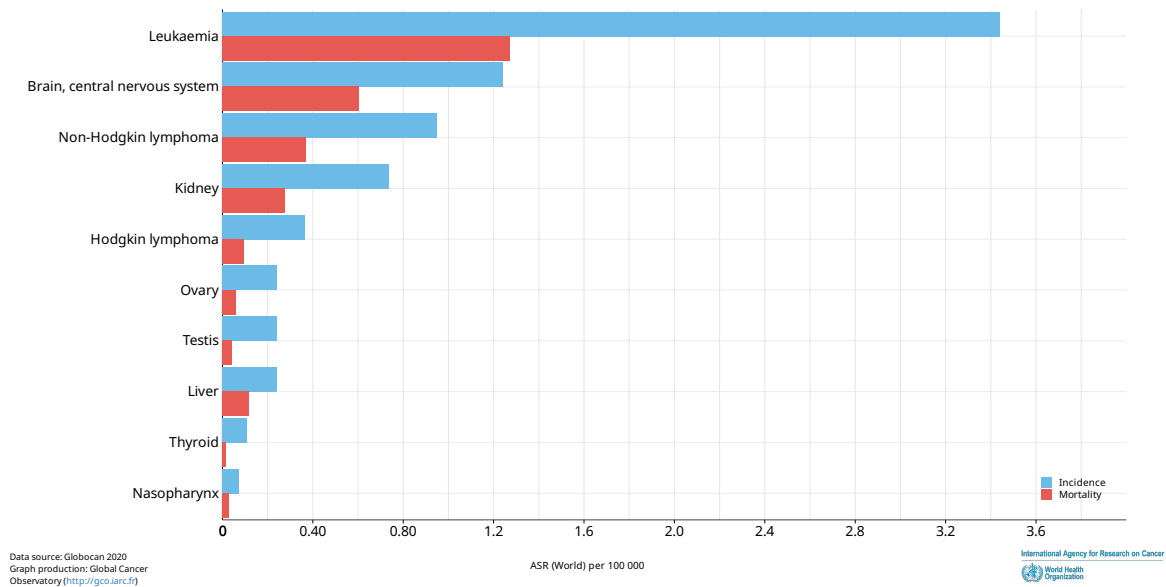


**Figure 4: Global cancer incidence and mortality**

According to WHO statistic, leukemia and Brain CNS tumors are the highest detected and death causing pediatric cancers in the world in 2020. (Figure adapted from GLOBCAN statistics, 2020.[1])

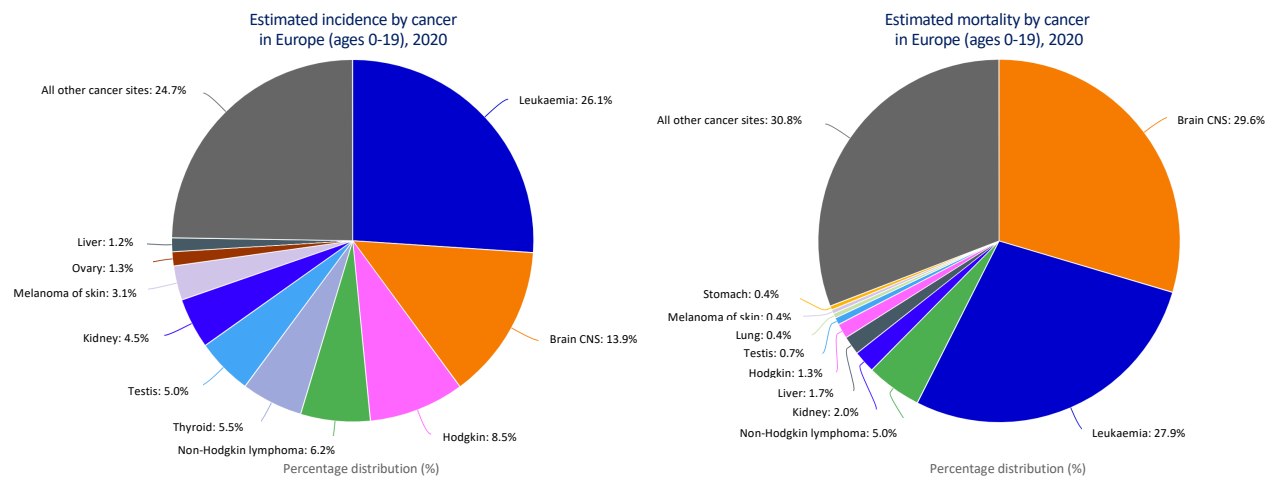


**Figure 5: European centric cancer incidence and mortality**

According to WHO statistic pediatric and adolescent cancer incidence (left) and mortality (right) cause in European childhood population (age 0-19) in 2020. (Adapted from European Commission, ECIS - European Cancer Information System reports [77])

However, due to progress in cancer research, the rapid development of precision medicine, and a rise in involvement in clinical trials, the survival rates for childhood cancer have significantly risen over the last half-century. More than 85% of children diagnosed with cancer now achieve a 5-year survival milestone in the first world. This marks a substantial improvement from the mid-1970s when the 5-year survival rate stood at approximately 58% [74], [79]. Nonetheless, around 60% of these patients who have survived childhood cancer experience long-term (at least 1-year long) complications resulting from the disease itself or the various treatments employed such as surgery, radiotherapy, cytotoxic chemotherapy that substantially impact patient quality of life and increases the risk of succumbing to secondary malignancies [80]–[82].

Pediatric malignancies in contrast to adult cancers, exhibit fundamental distinctions in cancer types and subtypes, their driver genes, driver mutation rates. Overall lower tumor mutational burden, cells-of-origins, molecular characteristics, genetic complexity, and differences in underlying mutational processes [83]. Consistent with findings from earlier research, it's been observed that the overall somatic mutational burden tends to increase with patient age. In contrast to adult cancers, pediatric cancers exhibit markedly lower genomic mutation rates, approximately 14 times lower on average, as previously reported [84], [85]. Moreover, it's worth noting that the mutational load in relapsed pediatric tumors surpasses that of primary pediatric tumors, which is likely linked to mutations induced by radiotherapy or chemotherapy [84], [86], [87].

Germline predisposition is the only known etiological factor for pediatric cancer, due to the high risk and likelihood of cancer inheritance [86]–[90]. Hereditary cancers account for about 10% of all cancers diagnosed [89]. Inherited mutations can operate through dominant or recessive mechanisms, can convey varying levels of penetrance, and can result in cancer manifesting at an early or later stage. This contributes to marked variations in the disease within the population of cancer patients [89] [91]. However, tumor suppressor and DNA repair genes undergoing mutations that are predisposed towards gain-of-function mutations manifest in families more often than would be expected by chance, usually as an exceedingly young age. These serve as indicators of the presence of a genetic mutation that increases the risk of cancer [89]. The most common and well researched example of predisposition in children is that of heterozygous germline mutations in the *TP53* tumor suppressor gene causing autosomal dominant Li-Fraumeni syndrome [89], [92]. Another prominent instance of germline mutation contributing to cancer is a single allele of the germline retinoblastoma protein (*RB1*), which, when coupled with the somatic inactivation of the second allele, leads to the development of retinoblastoma [92]. The presence of a germline mutation in *RB1* also predisposes children to additional malignancies such as sarcomas and melanomas [92], [93]. Germline mutations in genes like *ATM* and *SH2D1A* heighten the susceptibility to lymphomas and leukemias, while mutations in *PTCH1* and *SUFU* amplify the risk of SHH medulloblastoma, as seen in notable instances within pediatric cancer predisposition [89], [92], [94].

### 1.3.2 Pediatric Brain and Central Nervous System tumors

Pediatric brain tumors are the most common type of solid childhood cancer and only second to leukemia as a cause of pediatric malignancies[95]. The 5-year survival rate for individuals with brain tumors exhibits significant variability depending on the specific regions of the brain affected [96]. Advances in the treatment of pediatric brain tumors have come in the form of imaging, biopsy, surgical techniques, and molecular profiling. A statistical report published in 2019, by the Central Brain Tumor Registry of the United States (CBTRUS) statistical report a survey in the United States (between 2012-2016) using population-based data on available primary brain tumors. All rates were age-adjusted using the 2000 US standard population and were presented per 100,000 population. In children and adolescents aged 0-19 years, low-grade gliomas were reported as the most common of all malignant CNS tumors: mainly pilocytic astrocytoma (15.0%), followed by high-grade glioma (11.6%), embryonal tumors (10.5%) that encompassed Medulloblastoma (64%), AT/RT (14%), PNET(10.8%), all other (9.6%), followed by other astrocytoma (7.6%), nerve-sheath tumors (5.3%) and ependymomal tumors (4.7%) [97].

According to the 2021 WHO classification of central nervous tumors[98], pediatric gliomas are a heterogeneous group of tumors that can be classified into 6 different families namely: (1) Adult-type diffuse gliomas (the majority of primary brain tumors in neuro-oncology practice of adults, e.g., glioblastoma, IDH-wildtype); (2) Pediatric-type diffuse low-grade gliomas (expected to have good prognoses); (3) Pediatric-type diffuse high-grade gliomas (expected to behave aggressively); (4) Circumscribed astrocytic gliomas; (5) Glioneuronal and neuronal tumors; (6) Ependymoma[98].

#### Adult-type diffuse gliomas

These represent a category of central nervous system tumors characterized by extensive infiltration, and the prognosis that significantly varies depending on the specific subtype and histological grade[99], [100] and have 5-year survival rate under 5%. However, are not predominantly found in childhood cancer cases.

#### Pediatric type diffuse low-grade gliomas (pLGGs)

Low-grade gliomas together with glioneuronal tumors (classified as WHO grade I or II) represent approximately 25% to 30% of all CNS tumors diagnosed in children. There are four distinct subtypes (1) diffuse astrocytoma, *MYB*- or *MYBL1*-altered; (2) angiocentric glioma; (3) polymorphous low-grade neuroepithelial tumor of the young and (4) diffuse low-grade glioma with *MAPK* pathway alterations, often diagnosed as an exclusionary measure[98], [100]. For instance, a morphological diagnosis like diffuse astrocytoma can be combined with a specific genetic alteration such as *FGFR1* mutation, illustrating a versatile approach of mixing and matching. Accurate classification requires the molecular characterization and the incorporation of both histopathological and molecular data, structured within a tiered diagnostic framework for these tumors and for

most other gliomas. In contrast to adult patients with low-grade gliomas, children with LGGs rarely exhibit *IDH* mutations, instead being mainly *MAPK*-driven. Within this group, several novel entities, largely characterized by molecular factors, have been introduced. The occurrence of malignant progression in pediatric LGGs is exceedingly rare. Typically, patients experience favourable outcomes, with an estimated 5-year overall survival rate of approximately 95% [101]. While certain prognostic markers have been reported, current understanding of the mechanisms underlying the recurrence or advancement of these tumors remains limited [98].

Astrocytic tumors originate from astrocytes and represent the most prevalent group of glial-origin tumors. Among these, pilocytic astrocytoma (PA) stands out as the most commonly occurring brain tumor in childhood with good prognosis and an incidence rate of 0.8 cases per 100,000 individuals. PA constitutes 15% of all brain tumors diagnosed in children and constitutes a substantial portion, ranging from 27% to 40% of pediatric posterior fossa tumors. The most frequently observed genetic anomaly, occurring in approximately 70% to 75% of pilocytic astrocytoma's (PCAs), involves alterations in the *BRAF* gene. Additionally, more than 80% of PCA cases display modifications in the *MAPK* signalling pathway. Furthermore, a notable correlation has been established between *NF1* and the occurrence of PA [98], [102].

Low-grade gangliogliomas/gangliocytomas (GG) is a rare brain tumor with greater than 90% five-year survival rate. Typically, these tumors are characterized by being well-differentiated and slow-growing, thus complete surgical resection has the potential to provide a curative outcome for the majority of these patients. These tumors are often driven by *BRAF V600E* mutations [98], [103].

### **Pediatric type diffuse high-grade gliomas (pHGGs)**

The updated 2021 WHO brain tumor classification made a clear distinction to four different subtypes of pediatric diffuse high-grade gliomas namely, (1) diffuse midline glioma; H3 K27-altered, (2) diffuse hemispheric glioma, H3 G34-mutant; (3) diffuse pediatric-type high-grade glioma, H3-wildtype and IDH-wildtype and (4) infant-type hemispheric glioma[98]. It is necessary to acknowledge that HGGs also occur in adults, but at a molecular level, childhood and adult HGGs are very different. A significant revelation underscoring the distinctiveness of pediatric high-grade gliomas lies in the identification of specific histone mutations. These exclusive mutations occur in the histone genes H3.3 (*H3F3A*) and H3.1 (*HIST1H3B*, *HIST1H3C*).

Diffuse midline glioma (DMGs) occurs in midline regions and encompass those tumors formerly known as diffuse intrinsic pontine gliomas (DIPG)[98]. This classification was based on the presence of the *K27M* mutation identified in the histone H3 gene (*H3F3A*), as well as in the associated *HIST1H3B* or *HIST1H3C* genes. The incidence of the *H3 K27M* mutation is approximately 80% in pediatric patients and 15–60% in adult patients [104]. The defining trait of DMGs is the *H3 K27M* mutation, specifically situated within the coding gene *H3F3A*. *H3F3A* is responsible for encoding the H3.3 histone variant, accounting for mutations in approximately 70% of H3 K27-mutant DMGs. The

remaining 30% of cases are attributed to mutations in *HIST1H3B* and *HIST1H3C*. The *H3 K27M* mutation involves a substitution of lysine with methionine at codon 27 [105]. Those DMGs harbouring wild-type H3 can be seen in up to 15% of cases and can be distinguished by the overexpression of “Enhancer of Zest Homologs Inhibitory Protein” (*EZH1P*) [106], [107]. *TP53* loss, among the most commonly occurring genetic alterations, triggers neural stem cell self-renewal, confers tumor immortality via epigenetic mis-regulation, and has been associated with increased resistance to radiotherapy[108]–[110]. Dysregulation of *PDGFRA* also serves as a driver mutation, exerting influence on cell migration, proliferation, and survival, thus reducing tumor growth, and enhancing cell invasion[110], [111]. Mutations in the *ACVR1* gene, which encodes the activin A receptor type 1 transmembrane protein, lead to the constitutive activation of the *BMP-TGF- $\beta$*  signaling pathway, fostering tumor initiation and gliomagenesis while hindering differentiation[109], [110]. The presence of somatic alterations in the *RTK-PI3K-mTOR* pathway also acts as a driving force in gliomagenesis. Conversely, the occurrence of *RAS-MAPK* pathway alterations, such as *FGFR1*, has been associated with a more favorable prognosis among gliomas featuring H3 mutations[112]. *ATRX* mutations, which typically code for a regulator of chromatin remodeling and transcription, directly interact with the histone H3.3 variant and have also been identified as driver mutations closely linked to H3 mutations[105], [113]. Additionally, other noteworthy genomic alterations include the well-known *MYC* proto-oncogene transcription factor family, *CCND2*, and *PPM1D* [104], [105], [109], [110].

Diffuse hemispheric glioma, H3 G34-mutant is a recently acknowledged, distinct form of high-grade glioma characterized by a bleak prognosis. Alongside the H3 G34 missense mutation, numerous genetic drivers have been detected in these aggressive tumors, including alterations in *ATRX*, *TP53*, and *BRAF* genes[114]. H3 G34-mutant gliomas typically manifest as sizable lesions, accompanied by relatively mild peritumoral edema and variable, often subtle enhancement. These tumors may exhibit calcification, potentially resembling *IDH*-mutant, chromosome 1p/19q-codeleted oligodendrogliomas [115].

Diffuse pediatric-type high-grade glioma, H3-wildtype and *IDH*-wildtype (pHGG) is a rare and aggressive brain tumor distinguished by its distinct DNA methylation profile[116]. This malignancy falls under the category of highly malignant brain tumors (WHO grade 4) and is predominantly found in children and adolescents. Histologically, it presents as a diffusely infiltrating glioma with heightened mitotic activity. Notably, it does not exhibit mutations in *IDH1*, *IDH2*, or *H3* genes. Additionally, the tumor can be further characterized by its DNA methylation profile, aligning with subgroups pHGG *RTK1*, pHGG *RTK2*, or pHGG *MYCN*, or by displaying molecular features such as *PDGFRA* alteration, *EGFR* alteration, or *MYCN* amplification[98], [116], [117].

Finally, infant-type hemispheric glioma, previously referred to as glioblastoma (GBM), is a rare and rapidly proliferating congenital tumor. Studies have reported the involvement of *NTRK* family genes, namely *NTRK1*, *NTRK2*, and *NTRK3*, in infant-type hemispheric gliomas, which tend to exhibit high-grade histology[118], [119].

Additionally, these tumors frequently display other genetic alterations in receptor tyrosine kinases such as *ALK*, *ROS1*, and *MET* [120][98].

### **Ependymoma (EPN)**

Ependymomas (EPN) represent a highly diverse group of CNS tumors that can originate in various regions, including the supratentorial brain (ST-EPN), hindbrain or posterior fossa (PF-EPN), and throughout the spinal cord (SP-EPN), affecting both children and adults. These tumors are known for their aggressive nature and often carry a grim prognosis, especially in pediatric cases, with an overall 10-year survival rate of 63.8% for children[121]. Recent advancements in the identification of biological markers and classification systems, particularly through global DNA methylation profiling, have led to the delineation of ten distinct types of ependymal tumors[98], [122], [123]. This classification system has enhanced the ability to predict patient outcomes more accurately and only four out of the ten were relevant for pediatric patients: *YAP1* (ST), *RELA* (ST), *PF A* (PFA), and *PF B* (PFB)[122]. Supratentorial ependymomas are comprised of two subgroups -one with *ZFTA* (the new designation for *C11orf95*, which is considered more representative of the tumor type than *RELA* because it may be fused with partners more than *RELA*) fusion and another with *YAP1* fusion. These tumors can harbor *YAP1-MAMLD1* fusions, but *YAP1-FAM118B* fusions have also been observed[124]. Clinical characteristics of *ZFTA*- and *YAP1*- altered EPN exhibit variations in terms of the age of onset and prognosis[122].

The posterior fossa ependymomas are comprised of two subgroups- A (PFA) and subgroup B (PFB)[98]. Additionally, a fraction of infratentorial ependymal tumors has been found to harbor mutations in *H3*, *EZH1P*, or *TERT*. Furthermore, *MYCN* amplifications have recently been identified in spinal ependymomas, alongside the previously recognized mutations in *NF2*[98]. For PFA, the most frequently observed copy number aberration is gain of chromosome 1q (60 of 240; 25%) and was also observed in PFB (9 of 51; 18%), and *ST-RELA* tumors (21 of 88; 24%)[122]. The presence of a chromosome 1q gain has been demonstrated as an independent marker of an unfavourable prognosis of PFA[125]. PFA is predominantly observed in young children, with a median age of 3 years, and shows a slightly higher incidence among males. These tumors are associated with extremely poor prognosis, characterized by a 10-year overall survival (OS) rate of 56% and a progression free survival (PFS) rate of 24%[122].

## Medulloblastoma (MB)

Medulloblastoma is one of the most common malignant CNS tumors in children, that arises from the cerebellum and has a median age of diagnosis of 6 years [126], [127].

The genomic, epigenomic, transcriptomic, and proteomic landscapes have now been characterized for several bulk medulloblastoma patient samples, and more recently, also for single medulloblastoma cells - allowing deeper understanding of the molecular mechanisms involved in tumor initiation, progression, and recurrence of various MB subgroups [126]. Initially, a consensus was reached to categorize MB tumors into four primary molecular groups: WNT-activated, sonic hedgehog (SHH)-activated, MB Group 3, and MB Group 4 - each category by distinct omics, clinical and biological features [128].

Subgroup	WNT	SHH						
		$\alpha$	$\beta$	$\gamma$	$\delta$			
Subtype								
Demographics								
Frequency	100%	29%	16%	34%	21%			
Age								
Gender	45 ♂ 55 ♀	63 ♂ 37 ♀	47 ♂ 53 ♀	55 ♂ 45 ♀	69 ♂ 31 ♀			
Clinical features								
Histology	Classic	Classic > Desmoplastic > LCA	Desmoplastic > Classic	Desmoplastic > MBEN > Classic	Classic > Desmoplastic			
Metastasis	12%	20%	33%	9%	9%			
5-year OS	98%	70%	67%	88%	89%			
Molecular features								
Cytogenetics								
Driver events	CTNNB1, DDX3X, SMARCA4 mutation	MYCN, GLI2 amplification TP53 mutation PTCH1 mutation (less)	PTCH1, KMT2D mutation SUFU mutation/deletion PTEN deletion	PTCH1, SMO, BCOR mutation PTEN deletion	PTCH1 mutation TERT promoter mutation			
Subgroup	Group 3/4							
Subtype	I	II	III	IV	V	VI	VII	VIII
Demographics								
Frequency	4%	13%	9%	10%	8%	9%	22%	25%
Age								
Gender	60 ♂ 40 ♀	77 ♂ 23 ♀	78 ♂ 22 ♀	68 ♂ 32 ♀	71 ♂ 29 ♀	67 ♂ 33 ♀	66 ♂ 34 ♀	75 ♂ 25 ♀
Clinical features								
Histology	Classic > Desmoplastic	LCA, Classic	Classic > LCA	Classic	Classic	Classic	Classic	Classic
Metastasis	35%	57%	56%	58%	62%	45%	45%	50%
5-year OS	77%	50%	43%	80%	59%	81%	85%	81%
Molecular features								
Cytogenetics								
Driver events	GF11/GF11B activation OTX2 amplification	MYC amplification GF11/GF11B activation KBTBD4, SMARCA4, CTDNEP1, KMT2D mutation	MYC amplification (less)	no common driver events	MYC, MYCN amplification	PRDM6 activation MYCN ampl. (less)	KBTBD4 mutation	PRDM6 activation KDM6A, ZMYM3, KMT2C mutation

**Figure 6: Molecular classification of Medulloblastoma subgroups**

Overview of the demographics, clinical feature, genetic alterations and RNA expression of the different subgroups of Medulloblastoma (taken from Hovestadt et. al. 2020 [126]).

However, with extensive and more advanced methylation and transcriptomic analysis of data, the 2021 WHO brain tumor classification elaborates on subgroups that have become evident beyond the original four principal groups. These include four subgroups within the SHH category and eight subgroups within non-WNT/non-SHH medulloblastomas (Figure 6).

WNT Medulloblastoma (WNT-MB), although accounting for only approximately 10% of MB diagnoses, is observed to have the best prognosis, with over 95% of children surviving this disease after 5 years[129]. WNT-MB primarily occurs in children after 4 years of age to early adulthood (median age ~11 years)[126]. The defining genetic event in this subgroup, affecting approximately 85% of patients, is the presence of somatic mutations in *CTNNB1*. These mutations serve to stabilize the product of the *CTNNB1* gene,  $\beta$ -catenin, preventing its degradation by a cytoplasmic destruction complex (which includes *APC*) and allowing it to freely relocate to the nucleus, where it functions as a transcriptional co-activator for transcription factors. In cases where tumors lack somatic *CTNNB1* mutations, most patients carry pathogenic germline *APC* variants[130].

Other frequently observed driver genes include *DDX3X*, *SMARCA4*, *TP53*, *CSNK2B*, *PIK3CA*, and *EPHA7*. Notably, *SMARCA4*, *PIK3CA*, and *TP53* are genes that are commonly mutated in various types of human cancers. *DDX3X* encodes an RNA helicase that contributes to the development of WNT tumors. In WNT tumors, *SMARCA4* and other members of the SWI-SNF chromatin remodelling complexes represent specific dependencies that are associated with this subgroup[98], [129], [131], [132]. In terms of tumor genomes, MB-WNT mostly devoid of somatic copy-number alterations, except for the common occurrence of chromosome 6 loss (monosomy 6) in most patients[126].

SHH Medulloblastoma (SHH-MB) displays an interesting age distribution pattern, being the predominant molecular subgroup among infants (<3 years of age) and adults (>17 years of age), while fewer cases are diagnosed during childhood and adolescence. In terms of demographics, SHH-MB is more frequently observed in males than in females, with a male-to-female ratio of approximately 2:1.

In contrast to the relatively uniform characteristics of WNT-MBs, SHH-MBs are characterized by significant biological, pathological, and clinical diversity[127]. Age-related molecular distinctions between infant and adult SHH-MB have been identified through gene expression and DNA methylation array profiling[126], [128]. The most frequently observed alterations include the loss-of-function mutations or deletions affecting *PTCH1* and *SUFU*, as well as activating mutations in *SMO* and amplifications involving *GLI1*, *GLI2*, and/or *MYCN*[133]. In the canonical SHH signalling pathway, the soluble SHH ligand binds to *PTCH1* on the cell surface, releasing the repression of *SMO*. Once activated, *SMO* transmits the SHH signal intracellularly by releasing *SUFU*-mediated inhibition of *GLI1/2*. This enables these transcription factors to move into the nucleus and trigger the expression of target genes, including proto-oncogenes from the *MYC* family, cell cycle-promoting cyclins, and *PTCH1* itself, which serves as a part of

pathway feedback inhibition [134], [135]. Furthermore, the occurrence of loss-of-function mutations, germline or somatic/mosaic, in *TP53* can lead to deficiencies in DNA repair and potentially contribute to clustered chromosomal rearrangements, known as chromothripsis, observed in tumors featuring coincident oncogene amplifications[136]. The age-dependent distribution of genetic abnormalities is also evident, as seen in the prevalence of somatic *TERT* promoter mutations in nearly all adults with SHH MBs, while only 10%–20% of tumors in pediatric patients exhibit such mutations[137]. Alterations in *PTEN*, which functions as a suppressor of the pro-proliferative *PI3K/AKT* pathway, are observed in approximately 7% of SHH-MB cases. These mutations could potentially result in inherent or acquired resistance to targeted therapies aimed at inhibiting the SHH pathway[138]. The most frequent chromosomal alterations include loss of chromosomes 9q, 10q, 14q, and 17p, and gains of chromosomes 2 and 9p[128], [129], [139], [140]. Four distinct subtypes, termed  $\alpha$ ,  $\beta$ ,  $\gamma$  and  $\delta$ , with various demographic compositions and molecular landscapes have been identified with 5-year progression-free survivals[127], [128]. Although the precise molecular mechanisms of the epigenetic or signalling cascades remain unclear, it is apparent that the consecutive activation of SHH collaborates with the disruption of chromatin and canonical signal transduction pathways to drive tumorigenesis[98], [129], [141], [142].

Group 3 Medulloblastoma (MB G3), occurs in infancy and childhood and is rarely observed in patients over 18 years old. This subgroup displays distinctive genomic characteristics, including *MYC* amplification, which is indicative of extremely high-risk disease and is identified in nearly 20% of Group 3 MBs tumors[133], [143]. Additionally, gene amplifications involving *MYCN* and *OTX2* are noteworthy and may collaborate in promoting Group 3 tumorigenesis through mutual transcriptional regulation. *MYCN* plays a well-recognized role in the fundamental biology of MB tumors, contributing to tumor initiation, maintenance, and progression[129], [144], [145]. Another significant observation is that *GF11* and *GF11B* are upregulated in approximately 15% of Group 3 MBs, and these alterations tend to be mutually exclusive[133]. Regarding somatic genetic events, Group 3 MBs exhibit relatively limited alterations. Only a few genes, including *SMARCA4*, *KBTBD4*, *CTDNEP1*, and *KMT2D*, are recurrently mutated in more than 5% of these tumors[133], [146]. Group 3 MBs display somatic in-frame insertions in *KBTBD4* can potentially disrupt substrate recognition[133]. The molecular mechanisms underlying *CTDNEP1* mutations, often occurring as hotspot frameshifts in the phosphatase domain, remain poorly understood[146][147]. The roles of *SMARCA4* and *KMT2D* mutations in Group 3 MB tumors are distinct from their roles in WNT and SHH MBs, respectively, and require further investigation[129]. Aneuploidy, involving isochromosome 17q, gains of chromosomes 1q and 7, as well as losses of chromosomes 8, 10q, and 16q, are all common chromosomal alteration displayed in Group 3 MB tumors [147].

Group 4 Medulloblastoma (MB G4) are the most prevalent molecular subgroup of MB and make up approximately 40% of all MB cases and are typically diagnosed in older children[128]. Roughly 33% of cancer patients progress to metastatic cancer, and Group

4 MB tumors exhibit a longer time to relapse compared to other MB subtypes[127], [148]. *KDM6A*, *ZMYM3*, and *KMT2C* are observed to represent the most commonly mutated genes in Group 4 MB[126]. The most prevalent putative driver event in Group 4 MBs involves the overexpression of *PRDM6*, achieved through enhancer hijacking. *PRDM6* is described as a chromatin modifier and transcriptional regulator in the developing cardiovascular system, although its specific role in MB remains unvalidated. *CDK6*, exclusively amplified in Group 4 tumors, encodes a critical cell cycle regulator involved in the G1-S transition. Like their Group 3 counterparts, Group 4 MBs exhibit gene-level amplifications of *MYCN* and somatic mutations in *KBTBD4* [133], [147], [149]. The presence of *OTX2* amplifications in Group 4 MB tumors suggests an overlapping spectrum of altered genes between Group 3 MB and Group 4 MBs, hinting at similar and continuing in terms of tumor biology[127], [128]. Group 4 MB tumors are characterized by high rates of isochromosome 17q, along with losses of chromosomes 8 and 11, and gains of chromosome 7[133], [147]. Notably, specific cytogenetic events such as chromosome 11 loss and chromosome 17 gain have been associated with a more favorable prognosis in Group 4 MB patients [126], [129], [139].

Medulloblastoma can be linked to rare hereditary tumor predisposition syndrome genes such as *APC*, *BRCA2*, *PALB2*, *PTCH1*, *SUFU* and *TP53*, accounting for 6% of MBs. *SUFU* or *PTCH1*, has been associated with increased risk of MB[137]. Studies also show *APC* germline mutations predisposes to WNT MB[150]. Elevated risk of medulloblastoma can be linked to germline abnormalities in DNA damage response and repair mechanisms. Examples include Li–Fraumeni syndrome (involving *TP53* mutations) and constitutional mismatch repair syndrome (involving mutations in *MLH1*, *MSH2*, *MSH6*, or *PMS2*)[150]–[152].

### **Embryonal tumor with multilayered rosettes (ETMR)**

Embryonal tumor with Multilayered Rosettes (ETMR) is a rare but typically aggressive brain tumor that affects mainly infants with a dismal prognosis [153]. The defining molecular characteristic of ETMRs, involves the amplification of the microRNA cluster (*C19MC*) on chromosome 19 (19q13.42) region, which is detected in approximately 90% of ETMR cases. [154], [155]. In cases where the *C19MC* amplification is absent, it is common to find tumors that carry bi-allelic *DICER1* mutations, which is an inherited germline alteration[155]. According to the 2016 WHO brain tumor classification, a tumor with the absence of *C19MC* amplification is classified as ETANTR/ETMR and should be diagnosed as embryonal tumor with multilayered rosettes, NOS. Despite their histological diversity, all ETMRs are characterized by the upregulation of RNA binding protein *LIN28A*, which is therefore frequently used as a diagnostic marker[154]. Despite their histological diversity, all ETMRs share a common feature: they exhibit significant upregulation of the RNA-binding protein *LIN28A*. As a result, *LIN28A* is frequently employed as a diagnostic indicator for these tumors. Research of the downstream pathways influenced by the disrupted miRNA machinery has given rise to numerous potential therapeutic vulnerabilities such as targeting the WNT, SHH, or *mTOR*

pathways, *MYCN* or targeting chromosomal instability [154]. A significant number of patients do not surpass a year following their diagnosis, and the overall 5-year survival rate remains below 30%.

### **Atypical teratoid/rhabdoid tumor (AT/RT)**

Atypical teratoid/rhabdoid tumors (ATRTs) represent a rare, but aggressive pediatric brain tumor that account for approximately 2% of all brain tumors in pediatric cases. But their prevalence increases to 10-20% of all brain tumors specifically in children under the age of three[156]. AT/RTs are characterized by their rapid growth, and large size upon presentation, leading to brain compression and intracranial hypertension requiring urgent intervention. Across the four AT/RT classified subgroups, the mutations and epigenetic differences across subgroups have been shown to be striking, including different gene expression, methylation profiles and enhancer activities. In the *MYC* group of AT/RT, *MYC* is prominently expressed. Conversely, the sonic hedgehog (SHH) group is identified by active SHH signalling, and the term "TYR" in the TYR group originates from "tyrosinase," one of several highly expressed melanosomal markers within this subgroup[157]. The three major subgroups (AT/RT-SHH, AT/RT-TYR, and AT/RT-MYC) all carry mutations in *SMARCB1*. The distinctive genetic alteration is the presence of bi-allelic mutations in the *SWI/SNF* chromatin remodelling complex member *SMARCB1* (also recognized as *hSNF5/INI1*), which results in the loss of nuclear *SMARCB1* protein expression[157], [158]. The fourth subtype (AT/RT-SMARCA4) is a quantitatively smaller group often characterized by *SMARCA4* mutations [159]. In this subtype, studies have also showed, the reduction in mRNA expression levels of three essential SHH signature genes- *GLI1*, *PTCH1*, and—whose gene products are primarily found in the primary cilium[157]. Genome-wide copy number analysis studies show AT/RTs displaying novel gains on chromosome 1q or losses of chromosome 10 as more frequently recurring alterations[159].

Other embryonal tumors such as “CNS tumor with *BCOR* internal tandem duplication (ITD)” are also classified in the 2021 WHO brain classification[98]. This is a recently identified rare tumor type which is still being researched. The morphological characteristics, genetic alteration, classification, clinical outcomes, and optimal treatment for this tumor entity have not been fully distinctly clarified. Histologically this tumor predominantly displays a solid growth pattern with consistently oval or spindle-shaped cells, a dense network of capillaries and an internal tandem duplication (ITD) occurring in exon 15 of the *BCOR* gene. Exon 15 *BCOR* ITDs have been reported in several morphologically similar sarcomas[98], [160].

### 1.3.3 Neuroblastoma

Neuroblastoma (NB) is a pediatric malignancy of the peripheral sympathetic nervous system (PSNS) that originates from neuroblasts of the migratory neural crest. A unique feature of NB tumors is the combination of early age of onset, high frequency of metastatic disease at diagnosis and the tendency for spontaneous regression of tumors in infancy, hence, leading to heterogeneous clinical outcomes. In 40% of pediatric cases, it manifests as a high-risk disease, and among these patients, half do not attain a sustained response to currently available treatments [161]. Over the past decade the 5-year survival rates of patients with metastatic neuroblastoma have increased from less than 20% to over 50%. This is the result of clinical trials that incorporate high-dose chemotherapy along with autologous stem cell transplantation, differentiation-inducing agents, and immunotherapy with anti-GD2 monoclonal antibodies. [162]. In 40% of the patients, there is the presence of at least one recurrent driver gene alteration. The most frequent aberrations presented include, *MYCN*, *ATRX*, and *TERT* alterations, varying based on the age group. Specifically, *MYCN* alterations typically occur at a median age of 2.3 years, *TERT* alterations at 3.8 years, and *ATRX* alterations at 5.6 years. [163]. Driver point mutations of *ALK* is the most significantly occurring mutation in NB. *ALK* is a receptor tyrosine kinase expressed in tissues of a neural lineage, and its activation results in mitogenic signalling via the *RAS*–*MAPK* and *PI3K*–*AKT* pathways. These *ALK* mutations can exist as clonal or subclonal alterations, although the interpretation of mutant allele frequency (MAF) may be influenced by the tumor cell content of the sample. It is worth noting that both *ALK* mutations and amplifications frequently co-occur with *MYCN* amplifications [164]. Amplifications of *MYCN*, located on chromosome 2p24, is a transcriptional regulator of growth, metabolism, and cellular differentiation. *MYCN* is also a well-established driver of high-risk neuroblastoma and a significant determinant of prognosis. Overexpression of proto-oncogenes, such as *CDK4* and *MDM2*, due to genomic amplifications of other segmental regions are associated with extremely poor outcomes [165]. High risk neuroblastoma exhibits chromosomal alterations – deletion of chromosome 1p, gain of parts of chromosomes 17q, chromosome 2p-gain and chromosome 11q-deletion [166], [167]. Recent studies also show distal loss of chromosome 6q along with *MYCN* amplifications could serve as a novel marker for high-risk neuroblastoma [165][98].

### 1.3.4 Sarcomas

Sarcomas are an extremely heterogeneous group of genetically distinct tumors that represent 12–15% of all pediatric tumors, although rare among adult cancers [168]. With recent advancements in molecular profiling, more than 100 different histological subtypes have been characterized and many more are being discovered. Sarcomas are often prone to metastasis and relapse, typically accompanied by dismal prognosis. Sarcomas have been classified in two large subgroups, according to the anatomical site of occurrence—sarcomas of the skeleton and sarcomas of the soft tissues, referred to as “bone sarcomas” or “soft tissue sarcomas” respectively [168]–[170].

## Rhabdomyosarcoma

Rhabdomyosarcomas (RMS) are the most common soft tissue sarcoma in children that arise from a variety of anatomical sites, not limited to skeletal muscle, and show correspondingly diverse clinical presentations. Presence of metastasis, site of origin, age of the patients and histological and genetic properties of the tumor serves to stratify rhabdomyosarcomas into low, intermediate, and high-risk groups. The variable prognosis and tumor presentation makes the prediction of rhabdomyosarcoma outcome more complicated. According to the 2020 WHO Soft Tissue Tumor classification[169], these tumors can be classified into four major subgroups – embryonal rhabdomyosarcoma and alveolar rhabdomyosarcoma of which 60–70% of sarcoma RMS are embryonal and 20–30% are alveolar; pleomorphic rhabdomyosarcoma (PRMS) and Spindle cell / sclerosing rhabdomyosarcoma, two other less common subtypes[171], [172].

In the Embryonal rhabdomyosarcoma (RMS\_EMB) subgroup, the commonly observed genetic alterations include *SMO*, *PTCH1*, *FGFR4*, *PIK3CA*, *CTNNB1*, *KRAS*, *HRAS*, *BRAF* and *PTPN11*. Point mutations appear to be significantly more frequent in embryonal RMS than in alveolar RMS tumors[173]. *SUFU* mutations causes the inhibition of *GLI1*, and effectively promote sarcomagenesis. Inactivation of *CDKN2A* and *RB1* especially in the presence of a *TP53* mutation is observed in RMS\_EMB. Tumors exhibit *MDM2* and *P53* amplification with cancer associated *P53* missense mutations. *KRAS* and *TP53* inactivation also cause chromosomal gains affecting *YAP1* and *MET*. It is also observed that RMS driven by *YAP1* emerges in cases where both *TP53* and *RB1* are inactivated. Common gene fusions such as *MDM2-ALT1* and *EWSR1-DUX4* have been identified in RMS\_EMB. Additionally, rearrangements involving the *NCOA2* gene on the chr 8q11–13 region have been observed in these tumors [171], [172], [174].

Alveolar rhabdomyosarcoma (RMS\_ALV), constitute the second most common RMS subtype in children and adolescent patients. A specific molecular alteration either a *PAX3-FOXO1* or a *PAX7-FOXO1* gene fusion are detected in most RMS\_ALV cases. The genes on chromosome 2 and chromosome 1 are *PAX3* and *PAX7*, respectively, which encode highly related members of the paired box family of transcription factors. The fusion partner on chromosome 13 is *FOXO1* (FKHR), which encodes for transcription factors. Translocations give rise to fusion genes, which are subsequently transcribed into fusion transcripts and translated into fusion proteins and can generate reciprocal fusions, *PAX3-FOXO1* and *FOXO1-PAX3* (or *PAX7-FOXO1* and *FOXO1-PAX7*), the *PAX3-FOXO1* and *PAX7-FOXO1* genes. Notably, fusions of *FOXO1-FGFR1* and *PAX3* to *NCOA1* or *NCOA2* genes, that encode two similar transcription factors are also observed. While these other variant fusions may account for the absence of a *PAX3-FOXO1* or *PAX7-FOXO1* fusion in a few instances, the vast majority of "fusion-negative" cases lack any rearrangements involving *PAX3*, *PAX7*, or *FOXO1*. Therefore, these cases seem to lack fusions related to these loci[174], [175]. Spindle cell/sclerosing rhabdomyosarcoma (ssRMS) is a rare variant of rhabdomyosarcoma. These tumors are commonly associated with recurring fusions involving *VGLL2* or *NCOA2* and have a favourable prognosis are observed. *MYOD1* mutations are also commonly observed[174], [175].

## Ewing sarcoma

Ewing sarcoma (EWS) is a rare, aggressive, small round cell sarcoma most commonly arising in the bone of adolescents and young adults. With better treatment advancements the 5-year survival rate for patients with localized Ewing sarcoma has improved to 78%. However, approximately 25% of patients with localized tumors and 60-80% of those with metastatic tumors experience disease relapse and do not survive. These tumors are identified by balanced chromosomal translocations where one of the *FET* gene family members combines with an *ETS* transcription factor. The tumor's defining molecular feature is the distinctive *FET-ETS* fusion, with the most common being *EWSR1-FLI1* (70–80%), followed by *EWSR1/FUS-ERG* fusions (15%), *EWSR1/FUS-FEV* (5%), and *EWSR1-ETV1/4* (1%)[176]. The Ewing sarcoma breakpoint region 1 protein (EWSR1)–Friend leukemia integration 1 transcription factor (*FLI1*) is a tumor-specific chimeric transcription factor (*EWSR1-FLI1*) with neomorphic effects that extensively alters the transcriptome[177]. The expression of developmental *EWSR1-FLI1* results in embryonic lethality, whereas conditional expression during later stages can cause developmental defects, including muscle degeneration[174]. Studies have also observed rare cases of *EWSR1/FUS-FEV* fusions showing a prevalence in extra-skeletal sites and aggressive behaviour [178]. Additionally, mutations detected at the time of diagnosis that are infrequent, primarily include *STAG2*, *TP53*, and *CDKN2A* deletions. Frequently recurring chromosomal aberrations observed are chromosome 8 gains (50%), chromosome 2 gains (25%), chromosome 1q gains (25%), and chromosome 20 gains (10–20%). The most common is *CDKN2A* deletion and affects chromosome 9p. Due to imbalanced rearrangement chromosome 1q gains are often linked to 16q losses. Some studies have proposed prognostic implications for chromosome 8 gains, encompassing both whole chromosomes and segment 8q, as well as *MYC* (8q24) and *RAD2* which may be more prevalent in relapsed tumors[176], [177].

## Osteosarcoma

Osteosarcoma (OS), also known as osteogenic sarcoma, represents the most common form of bone neoplasia, accounting for 20% of all benign and malignant bone tumors and around 2% of pediatric cancers. OS is a bone sarcoma characterized by a complex karyotype with highly unstable genomes, and these tumors often harbor far more point mutations than other pediatric solid tumors and leukemias. The majority of OS cases involve mutations or deletions in tumor suppressor genes *TP53* and/or *RB1* genes. Hence the development of OS is higher in patients with genetic predisposition, notably Li-Fraumeni and hereditary retinoblastoma syndromes[174]. Genetic alterations and expression of *TERT* and *ATRX* have also been observed. The main driver genes *TP53*, *RB1*, *BRCA2*, *CDK4*, *BAP1*, *RET*, *MDM2*, *ATM*, *PTEN*, *WRN*, *RECQL4*, *ATRX*, *FANCA*, *NUMA1*, *MDC1*, *NOTCH1*, *MYC*, *FOS*, *NF2*, *APC* and *PTCH1* have been reported [179]. Most of the driver genes are components of the *ERBB*, *PI3K-AKT-mTOR* and *MAPK* signaling pathways. However, the main hallmark of OS is the tumoral heterogeneity, aneuploidy and genome instability caused due to loss of G1/S cell cycle control[179], [180].

“Chromothripsis” is the process by which massive genomic rearrangements and localization of hypermutations (kataegis) are acquired by a single catastrophic event. In contrast to the gradual, stepwise acquisition of driver gene mutations seen in most tumor cells, in chromothripsis, driver genes can emerge through various mechanisms. These include decrease in copy number (resulting to the deletion of tumor suppressor genes), increase in copy number (resulting in the amplification of oncogenes), the fusion of coding sequences from two genes (resulting in the creation of a fusion onco-protein), or the joining of an intact gene with the promoter of a different gene (leading to the dysregulation of its gene expression) [179]–[181]. Kataegis, a phenomenon often accompanying chromothripsis, causes dysregulation of apolipoprotein B mRNA-editing enzyme catalytic polypeptide-like (*APOBEC*) protein families [179], [180], [182], [183]. The extent of somatic vulnerabilities and complexity of the osteosarcoma genome are observed to be similar to that of common forms of adult cancer [179].

### **Synovial sarcoma**

Synovial sarcoma (SS) accounts for 7%–10% of all soft-tissue sarcomas affecting adolescents and young adults. Metastasis is frequently observed and usually targeted to lungs, lymph nodes, and bone marrow. Synovial sarcoma is defined by a signature genetic event, the t(X;18) translocation-mediated fusion of the *SYT* gene on chromosome 18q11 to either *SSX1*, *SSX2*, or, very rarely, the *SSX4* gene located on chromosome Xp11. Another distinctive gene fusion is the pathognomonic chromosomal translocation t(X,18; p11, q11) that creates an in-frame fusion of *SS18* to *SSX1*, *SSX2*, or *SSX4* and is linked to the development of primary synovial sarcoma. Studies report multiple missense mutations of *ADAM17*, have been identified solely in metastatic SS [174], [184]–[186].

### **Malignant peripheral nerve sheath tumor (MPNST)**

Malignant peripheral nerve sheath tumor (MPNST) is rare but is one of the most frequent non-rhabdomyosarcoma soft-tissue sarcomas in the pediatric population. Mutations inactivating or causing a deletion of the tumor suppressor *NF1*, acting inhibitory to *RAS*-signalling are among the most frequent driver genes in MPNST. Additionally genetic alterations in *TP53* and *CDKN2A* inactivation, leads to malignant progression of neurofibromas [174].

### **Clear Cell Sarcoma of Soft Tissue**

Clear Cell Sarcoma of Soft Tissue (CCS) is an aggressive cancer that usually arises in the deep soft tissue of young adults, it is characterized with very low incidence and poor prognosis. The genetic hallmark of CCS is t(12;22)(q13;q12) that leads to a *EWSR1-ATF1* gene fusion [174].

### 1.3.5 Other tumors

Malignant Rhabdoid tumors (RT) are poorly differentiated pediatric tumors that can arise in the soft-tissue or in the kidney and less commonly in the central nervous system (referred to as atypical teratoid rhabdoid tumor; AT/RT). Malignant rhabdoid tumors are characterized by the presence of germline or somatic biallelic inactivating mutations or *SMARCB1* deletions and homozygous or heterozygous deletion of *TP53* [174].

Hepatoblastoma (HB) is the most common primary liver tumor in children that is diagnosed during the first 3 years of life. Studies have reported hypermethylation of the *HNF4A/CEBPA* -binding regions, upregulation of the cell cycle pathway, and overexpression of *NQO1* and *ODC1* genes[187].

Childhood and early adolescent melanoma (ML) are rare. However, pediatric melanoma cases are sporadic and related to ultraviolet (UV) DNA damage and reported to be more pronounced in older children (15-19 years). Inactivating germline mutations of the gene *CDKN2A* and *CDK4* are associated with early-onset melanoma[188].

## 1.4 Patient derived xenograft models for preclinical modeling of cancer

Currently adult cancer is far more heavily researched and investigated for therapeutic and diagnostic options, such as targeted treatments, as compared to childhood cancer. The primary obstacles in the development of effective treatments for pediatric cancer can be associated with the market for pediatric drugs is typically smaller than that for adults drug development hence making large investments in pediatric drug is less of a financially appealing business model. Pharmaceutical companies often prioritize large randomized controlled trials, involving hundreds of patients, as mandated by the licensing process to approve new drugs. However, certain drugs, while clinically significant for specific patient groups, may have a very limited market. A change in the approach to such drugs and patient populations is likely necessary. This could involve making regulatory requirements more adaptable, offering financial incentives to pharmaceutical companies to support essential research, and centralizing such studies in specialized pediatric drug research centers. Important clinical questions regarding efficacy and safety can still be addressed through clinical trials that involve smaller patient cohorts [189].

In 2017, the Research to Accelerate Cures and Equity (RACE) for Children Act came into effect, granting the US Food and Drug Administration (FDA) the authority to mandate pediatric drug testing in children and preclinical models for new cancer drugs that target molecular factors relevant to the development or advancement of pediatric cancers [190]. The act also notably extends pediatric study requirements to drugs intended for the treatment of rare cancers. Before this legislation, pharmaceutical companies were not obligated to conduct clinical trials involving pediatric populations if their product was designed for adult cancer treatment. If sponsors fail to adhere to the stipulated requirements, the FDA has the authority to classify a drug as "misbranded" [191].

Therefore, the current limited availability of preclinical models that can precisely validate therapeutic response and guide pediatric clinical trials needs to be overcome. The requirement to molecularly classify multiple distinct tumors and their subgroups to stratify and identify novel therapeutic biomarkers is extremely necessary. In this era of big data, booming technological advancements and precision oncology, preclinical data classification is exceedingly imperative to explore and determine new therapeutic targets and biomarkers, and to validate known targets across various cancer types and subtypes.

The first Patient derived xenograft (PDX) models to be defined and generated can be dated back to the 1960's when Rygaard and Povlsen extracted colon adenocarcinoma from a patient to implant the tumor fragments into nude mice[192]. However, the unsatisfying transplantation rate of PDX models limited their application back then. Hence more cancer types had *in vitro* cultured human cancer cell line derived xenografts, which also accounted for better consistency, cost-effectiveness, and accessibility. Over the last decade, with optimization of PDX engraftment procedures

and the improvement in deep-learning technologies and the popularization of sequencing technologies have boosted the resurgence of PDX models (Figure 7).

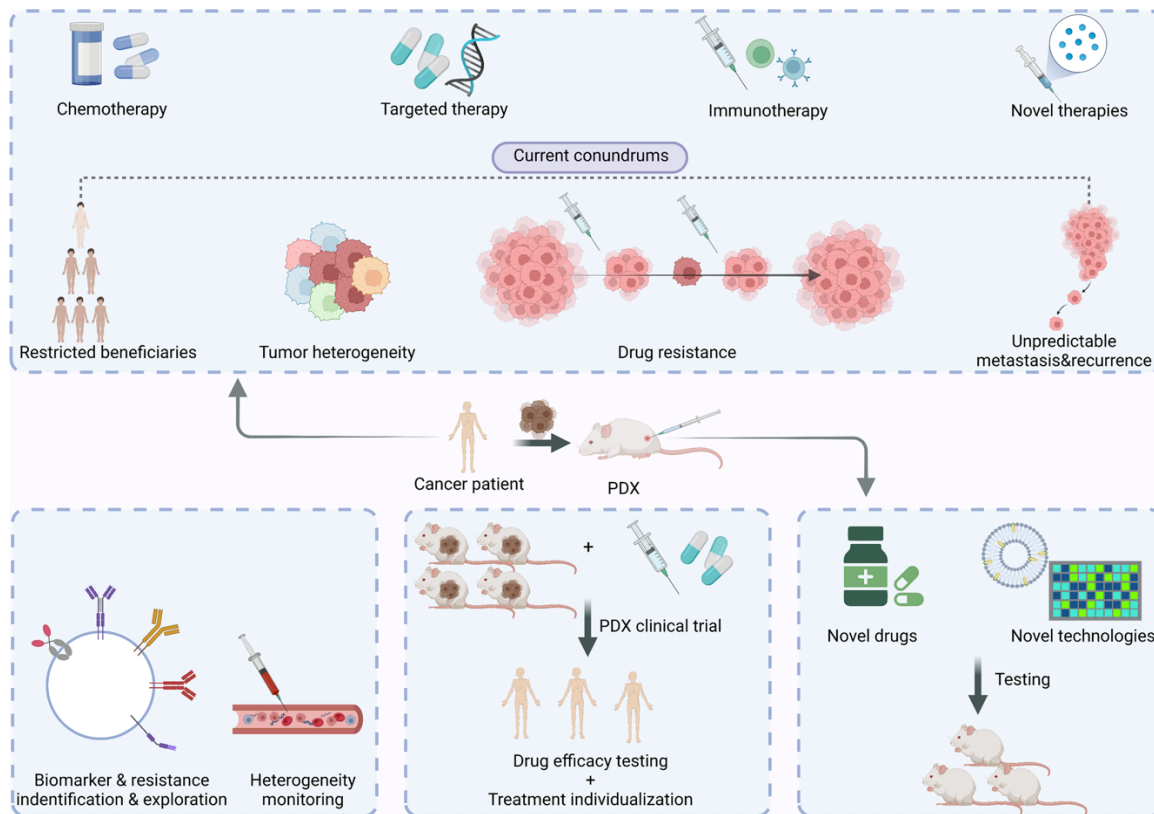


**Figure 7: PDX models for preclinical drug testing is the new era of cancer research**

*PDX models are used to study tumor biology and capture the mutational landscape including driver genes and various genomic alterations observed in the initiation and development of patient tumor. (Figure taken from Liu. et. al., 2023[193])*

PDX models involve the implantation of fresh surgically resected patient tumor tissues into immunocompromised or humanized mice. The conventional establishment of a PDX model involves the subcutaneous transplantation of the intact tissue into the dorsal region of immune deficient mice. Following tumor growth within the mouse model, it is re-transplanted into the next generation of mice, this process being often known as serial transplantation [194]. Apart from the conventional subcutaneous transplantation, orthotopic transplantation is the process of transplantation of tumor material into the same organ of the mouse as the original patient tumor. Orthotopic transplantation is more technically challenging and requires extensively skilled personnel and expensive imaging techniques to monitor responses to preclinical establishment and experiments [194]–[196]. Studies have shown that orthotopically generated models offer advantages over conventionally subcutaneously transplanted models. Such models are observed to be better for tumor metastasis, tumor location and microenvironment can influence therapy response and lastly, orthotopic models are also observed to increase tumor engraftment or take rate [195], [197].

Single-mouse trials entails each mouse models have a tumor originating from a distinct patient and is closely monitored to observe tumor progression or regression during the course of therapy. This approach enables the evaluation of 30 or more tumors of the same type, such as melanoma, potentially yielding response rates that more accurately mirror clinical response rates. Leveraging the simplicity of generating new PDX models, the strategy of using one mouse to represent a tumor significantly expands the capacity to assess numerous tumor lines. This, in turn, may provide a more comprehensive understanding of potential response rates in human patients or facilitate the identification of subsets of tumors within a specific histotype that exhibit heightened or reduced sensitivity to drugs[198].

PDX models have demonstrated their effectiveness in replicating tumor characteristics such as intratumor heterogeneity, the special structure of the tumor and the clinical outcome, making them a more reliable and powerful preclinical model[193], [195], [196]. To assess whether the tumor biology is fully preserved, various techniques can be implemented to compare the initial tumor to the PDX. It has been studied that the histopathological and sub-cellular landscape can be evaluated using electron microscopy, nevertheless, it should be considered that human stroma can be quickly infiltrated by mouse stroma [194], [195], [199]. Therefore, to avoid any mouse contamination in the next-generation sequencing of PDX models, the mouse reads need to be excluded to avoid any false-positive results. This can be performed by aligning the sequencing reads of the mouse genome against the human genome [200].

Studies have shown that the clonal heterogeneity of a PDX model is often maintained while continuously evolving. However, in certain instances, more significant clonal expansion events are observed, including instances where minor clones dominate in the PDX or where clonal populations are lost in the PDX[201]–[205]. The question of whether such ongoing evolution also transpires in human patients remains to be fully researched and understood. A study in sarcoma PDX models indicating parallel evolution in PDX models as in human patients, showed that newly acquired focal amplifications were typically observed in both PDX and human tumors[206]. Another means of assessing the fidelity of PDX models is by correlating the outcomes of preclinical testing in PDX models with actual clinical results. This can be accomplished in two ways: firstly, by comparing preclinical trials in PDX models to concurrent clinical trials, and secondly, by creating PDX models from individual patients and drawing direct comparisons between the treatment outcomes of the patient and the PDX model's response to therapy[205]. However, it's important to note that direct comparisons of preclinical and clinical data can be challenging due to utilization of different response criteria [205]. Successful observations have been made regarding the utilization of PDX models in preclinical drug testing, which have positive clinical response outcomes to *BRAF* inhibitors (vemurafenib) in melanoma[205], [207]. Additionally, these models have demonstrated the potential to overcome resistance to *BRAF* inhibition by combining *BRAF* inhibitors with *MEK* inhibitors, a phenomenon that has been replicated in PDX models [207].

## 1.5 Precision medicine for pediatric tumors

Childhood cancer remains to be the leading cause of death by disease in children aged 1-19. Over the last two decades, however the 5-year relative survival rate has increase from 61.7% to 81.4%, with over 90% in some entities in the first world [208]. While several large-scale national precision oncology programs have been launched to dedicate substantial efforts and produced valuable outcomes, the identification of druggable targets across different pediatric tumor types and subtypes still remains a challenge (Figure 8).

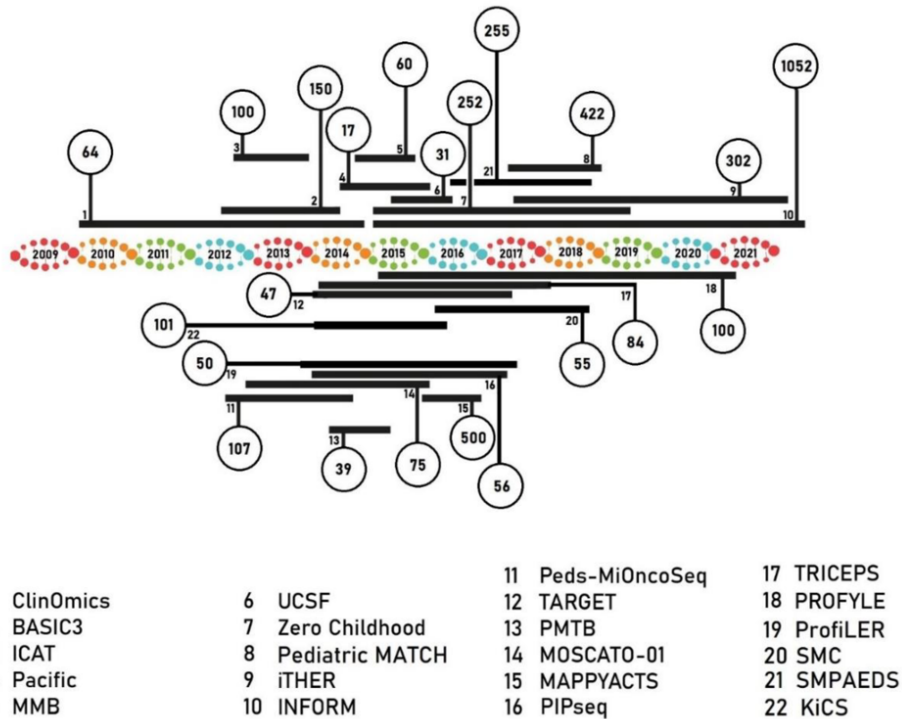


**Figure 8: Established Pediatric precision oncology programs**

Over the last decade various pediatric precision oncology research programs have been established. The overview showing the timeframes of studies and the number of patients included in the programs. (Figure taken from [209] )

To improve the annotation and characterization of PDX models from various tumors, and make this information usable to researchers, the ITCC-P4 consortium (Innovative Therapies for Children with Cancer Pediatric Preclinical Proof-of-concept Platform) supported by the European consortium ‘Innovative Medicines Initiative’ (IMI) has been established. This international consortium between 30 collaborating partners from different European academic institutions and European Federation of Pharmaceutical Industries and Associations (EFPIA), across 10 European countries, enables the establishment of a large PDX cohort across different high-risk pediatric tumors. This consolidation of numerous PDX cohorts and characterizing omics information into a single database, transforms this collaborative resource into a powerful tool for oncologists, clinicians and enables successful pediatric cancer research [210].

## 1.6 AIMS

### 1.6.1 ITCC-P4: Molecular characterization and multi-omic analysis of Patient-Derived Xenograft (PDX) models from high-risk pediatric cancer

Pediatric cancer is a life-threatening disease that often leads to secondary malignancies with many patients having to endure adverse effects and toxicity due to conventional treatments. Over the past two decades, genomic profiling of pediatric solid tumors has enabled tumor classification into well-defined subgroups and has also facilitated the identification of novel genetic alterations and biomarkers for mechanism-of-action based therapy development. The progress of preclinical drug testing to enhance the discovery of effective treatments tailored to the tumor's molecular profile faces two main challenges: (1) a lack of molecular genetic data on relapsed pediatric tumor patients and longitudinal comparisons between primary tumors and matching relapses, limiting our grasp of tumor evolution and treatment resistance, and (2) the absence of suitable, well-characterized patient-derived models and genetically engineered mouse models for several high-risk pediatric cancer types.

The main goals of this study under the ITCC-P4 entailed: (1) collection and establishment of a sustainable platform of >400 fully characterized PDX models from high-risk pediatric cancers. This currently included 251 PDX models as well as their matching human tumors and germline samples (controls available for 161/251 PDX models, 64.1%) (2) Performing a comprehensive multi-omics molecular characterization (DNA methylation profiling; whole-exome and low-coverage whole-genome sequencing, RNA sequencing, and gene expression profiling) of the entire ITCC-P4 PDX cohort and original tumors (3) This project aimed to assess how accurately the models reflect the molecular features of the corresponding patient tumors. (4) This large repertoire of PDX models also included a few established models originating from tumor samples serially collected from the same patients (“serial PDX models”) which represented valid modes to investigate tumor plasticity during disease progression. Overall, the in-depth characterization aims to assist in the selection of PDX models for *in vivo* testing of novel mechanism-of-action based treatments.

Applying a multi-omics approach when characterizing the models in our cohort enables us to define the biology of each pediatric PDX model in a high-throughput and systematic fashion, reflecting either known molecular subtypes or driver alterations. Here we provide insight into the mutational landscape, clonal evolution and molecular patterns of the PDX models thus providing an overview of molecular mechanisms, facilitating the identification and prioritization of oncogenic drivers and potential biomarkers for proof-of-concept *in vivo* drug testing in all PDX models.

The ITCC-P4 PDX data will be made publicly available in the freely accessible data repository (<https://r2.amc.nl/>), allowing further data downstream analysis, visualization and interpretation by clinicians and researchers. Taken together, the ITCC-P4 sustainable

platform represents a validated and powerful tool to investigate the biology of pediatric cancer based on the establishment and characterization of pediatric cancer PDX models ultimately envisaged to contribute to the development of innovative therapeutic options for childhood cancer patients.

### **1.6.2 Target Actionability Review (TAR): a systematic evaluation of replication stress as a therapeutic target for pediatric solid malignancies**

To assist the prioritization of mechanism-of-action-driven drugs for pediatric cancer clinical trials, this Target Actionability systematic literature review strategy was developed, with the aim of summarizing current knowledge to serve as proof-of-concept modules as part of the ITCC-P4 consortium.

In the TAR on Replication stress, our goal was to assess specific targets of the replication stress response (RSR). Replication stress represents a significant contributor to genomic instability and stands as a critical vulnerability in cancer cells. This susceptibility can be exploited for therapeutic purposes identifying and stratifying target proteins responsible for orchestrating the DNA damage response in conjunction with cell cycle regulation.

The TAR methodology focused on matching targeted anti-cancer drugs with distinct cancer subtypes, guided by published preclinical studies. Our objective was to compile a comprehensive, well-structured, evidence based and thoroughly reviewed literature source regarding targeting of replication stress in both intracranial and extracranial solid pediatric malignancies. We also aimed to highlight emerging targets and address gaps in published literature addressing replication stress.

Ultimately, the main aim was to create an extensive pediatric resource that can be accessed on the R2 platform. The target actionability review on replication stress, along with molecular characterized data from the ITCC-P4 PDX project could be used in supporting further preclinical research, designing pre-clinical trials and assist in the development of innovative treatments in pediatric cancer patients.

## 2 MATERIALS AND METHODS

This chapter provides a comprehensive overview of the experimental design, collection of raw data, and analysis methodologies employed in both studies: the ITCC-P4 Omics data analyses and the Target Actionability Review on replication stress. This chapter is crucial as it outlines the systematic approach, methodology, materials used in data collection, analysis, and interpretation. It ensures the reliability and reproducibility of the findings while addressing the study aims of this thesis. Hence facilitating a thorough understanding of the research process.

### 2.1 Materials based on ITCC-P4 Genomic profiling

#### 2.1.1 Human tumor samples

Patient consent was obtained in accordance with the approved protocol from the Ethics Board of the Medical Faculty at the University of Heidelberg. For this ITCC-P4 consortium project, patient tumor and germline samples were included. Fresh tumor samples were biopsied at the time of diagnosis, while patient blood samples served as germline controls, whenever available. Surgically resected fresh-frozen patient tumor material was extracted and stored for PDX transplantation. If available, clinical information including pathological and molecular diagnosis reports, tumor events (such as primary/diagnostic, relapse, metastasis), tumor stage, tumor location, treatment history, basic follow-up information, patient's age at diagnosis, and patient's gender have been collected. The collection of patient tumors was conducted in collaboration with 30 European partnering institutions, representing various tumor entities (Table 1).

INSTITUTION BARCODE	INSTITUTION
s01	Deutsches Krebsforschungszentrum (DKFZ), Germany
s02	Institute for Cancer Research (ICR), United Kingdom
s03	Innovative Therapies for Children with Cancer (ITCC), France
s04	Institute Gustave Roussy (IGR), France
s05	Alleanza Contro il Cancro (ACC), Italy
s06	Zürich University (UZH), Switzerland
s07	Medizinische Universität Wien (MUW), Austria
s08	Fundació Sant Joan de Déu Barcelona (FSJD), Spain

s09	EPO-Berlin-Buch GmbH (EPO), Germany
s10	Academic Medical Center (AMC), Netherlands
s11	XenTech (XT), France
s12	Children's Cancer Research Institute (CCRI), Austria
s13	Institut Curie (IC), France
s14	Charité Berlin (Charite), Germany
s15	Prinses Maxima Center Utrecht (PMC), Netherlands
s16	Eli Lilly and Co (Eli Lilly), United Kingdom
s17	Roche (ROCHE), Switzerland
s18	Pfizer (PFZ), United Kingdom
s19	Bayer AG (BAY), Germany
s20	PharmaMar (PHARMAMAR), Spain
s21	Charles River Discovery Research Services GmbH (CR), Germany
s22	Janssen Pharmaceutica (Janssen), Belgium
s23	Martin-Luther-Universität, Halle-Wittenberg (MLU), Germany
s24	University of Newcastle Upon Tyne (UNEW), United Kingdom
s25	AstraZeneca (AZ), Sweden
s26	Universität Ulm (UULM), Germany
s27	AMGEN (AMGEN), Belgium
s28	Institut de Recherche Servier (Servier), France
s29	Sanofi-Aventis Recherche & Development (Sanofi), France
s30	St. Anna Kinderkrebsforschung GmbH (CCRI), Austria

**Table 1: ITCC-P4 European partnering institutes and their ITCC-P4 barcodes**

### 2.1.2 PDX model establishment

Majority of the ITCC-P4 brain tumor samples were established at the DKFZ, by technicians Norman Mack and Benjamin Schwalm, in the group of Prof. Dr. Marcel Kool (Department of Prof. Dr. med. Stefan Pfister, Hopp Children's Cancer Center, KiTZ Heidelberg). However, all institutions followed the standard protocol for PDX establishment.

Freshly obtained tumor samples were immersed in a cell culture medium (Neurobasal, NeuroCult NS, or RPMI 1640) without FCS or other growth factors. Subsequently, the fresh or FFPE tumors were promptly transplanted into immunodeficient NOD-SCID gamma mice (NSG). The successful establishment of the PDX model was determined by the growth of a tumor in the P2 mice and the ability of a revived serum/ Dimethyl sulfoxide (DMSO) frozen tumor fragment to regenerate the PDX model.

The fresh brain tumor tissues were processed to obtain a single cell suspension either through gentle pipetting or by treating them with accutase (Accumax, eBioscience) and incubating at 37 °C for 15 minutes. The resulting cell suspension was centrifuged at 1200 rpm, the supernatant was carefully removed, and 1ml of cell culture medium was added. The cells were then passed through a cell strainer (Neolab) to obtain a single-cell suspension. Subsequently, the cells were counted and evaluated for viability.  $\sim 2 \times 10^6$  cells were stored for molecular characterization, while an additional  $\sim 1 \times 10^6$  cells were intracranially injected into 2-6 NSG mice. The growth of brain tumors was monitored using MRI (Magnetic Resonance Imaging). Fresh non-brain tumors were dissected into multiple small fragments and transplanted into either the flank or under the intrascapular fat pad of 2-6 NSG mice. The mice were monitored regularly for tumor growth, and the tumors were measured at consistent intervals during their growth. For subsequent passages, the tumors were extracted from euthanized mice and dissected into several small fragments in a sterile cell culture dish. FFPE-transplanted tumors when first implanted into mice are called *P0*. Once the brain tumor reached its maximum volume, further passages (*P1-2*) were initiated. At least two additional mouse-to-mouse passages (*P1*, *P2*) had to be performed before establishment. A PDX model was considered established if the tumor has grown in the *P2* mice and if the stored frozen tumor fragment was able, upon re-injection, to regenerate the PDX model (Figure 9).

Established PDX tumors were isolated and processed for molecular characterization. DNA and RNA were extracted from tissue samples using the automated Maxwell nucleic acid purification system and specific kits for blood or tissue samples. The quantity and quality of DNA were assessed using the Qubit system and high-resolution electrophoresis. Similarly, the quantity and quality of RNA, when available, was determined using the Agilent Bioanalyzer system. A threshold of RNA Integrity Number (RIN) values  $\geq 7$  was set to ensure the integrity of the RNA samples. Information regarding the PDX models was collected and included data on the mouse strain utilized, the transplantation site of the tumor, the passage number, and the growth latency.

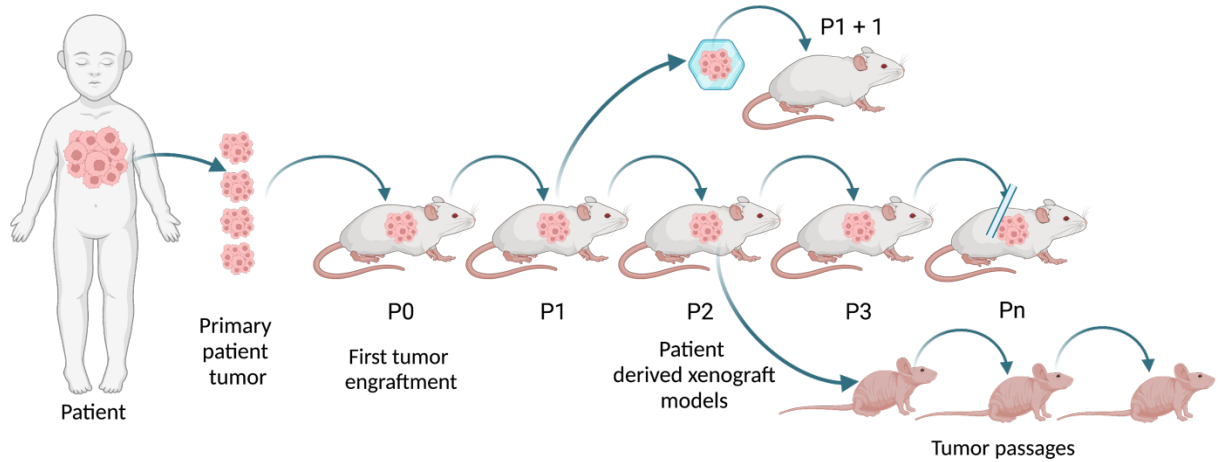


**Figure 9: PDX model establishment process**

Tumor biopsy extracted surgically resected tumor represents the primary tumor. Once engrafted into the first NOD-SCID gamma (NSG) immunodeficient mouse, this represents the P0 mouse model. On reaching maximum volume further passages are initiated (P1-P2) to establish the PDX model.

### 2.1.3 ITCC-P4 Cohort

For this thesis, I focused on the analyses of the first 251 fully molecularly characterized PDX models out of the 400 PDX models being established within the ITCC-P4 consortium project. All PDX models and patient tumor samples, as well as their relative molecular data, has been registered on the R2 portal (<https://r2-itcc-p4.amc.nl/>) with standardized barcodes reflecting essential details: institution ID, entity ID, sample type material ID and data type (Table 2).

ENTITY ID	DESCRIPTION
CK	Clear cell sarcoma of kidney
EP	Ependymoma
ES	Ewing sarcoma
HB	Hepatoblastoma
HG	High grade glioma
HGNET	High-grade neuroepithelial tumor
LL	Large-cell Lymphoma
NS	Malignant nerve sheath tumor

MB	Medulloblastoma
ML	Melanoma
NB	Neuroblastoma
OS	Osteosarcoma
PLEX	Plexus tumor
RB	Retinoblastoma
RT	Rhabdoid Tumor
RS	Rhabdomyosarcoma
S	Sarcoma
NP	Wilms' Tumors-Nephroblastoma

SOURCE ID	DESCRIPTION
T	Tumor
P	PDX

SAMPLE ID	DESCRIPTION
NB	Normal Blood
TP	Tumor Primary
TR	Tumor Relapse
TM	Tumor Metastasis
TT	Tumor progression under current treatment
PP	PDX Primary
PR	PDX Relapse
PM	PDX Metastasis
PT	PDX of tumor progressed under current treatment
PU	PDX model of unknown event

MATERIAL ID	DESCRIPTION
F	Fresh frozen
E	FFPE-embedded tissue

ISOLATE ID	DESCRIPTION
D	DNA
R	RNA
P	Protein

ANALYSIS ID	DESCRIPTION
01	lcWGS
02	hcWES
03	RNA-seq
04	Affymetrix
05	850k

**Table 2: ITCC-P4 standardised barcode system**

*A sample barcoding system was established for entity, model, sample, material, isolate and analysis.*

## 2.2 Methods based on ITCC-P4 Genomic profiling

### 2.2.1 Whole Exome Sequencing and Whole Genome sequencing workflow

PDX models and patient tumor samples sequenced at DKFZ used the Agilent SureSelectXT HS Reagent enrichment kits for Illumina Paired-End Sequencing platform (Illumina NovaSeq 6000 S1). In addition to the DKFZ sequenced data, we received raw NGS data (fastq files), from the partnering institutes, that profiled tumor samples independently. This data included merged low-coverage whole genome sequencing (lcWGS), whole exome sequencing data (WES) and RNA sequencing data. Consequently, for this data the WES and WGS library preparation kits and sequencing platform varied accordingly (Table 3 & Table 4).

INSTITUTION	LIBRARY PREPARATION KIT	WES SEQUENCING PLATFORM
DKFZ	Agilent SureSelectXT HS	Illumina HiSeq 2000
CCIA	TruSeq Nano DNA HT	Illumina HiSeq X Ten
CURIE	Agilent SureSelect Clinical Research Exome V2	Illumina NovaSeq 6000
IGR	Agilent SureSelect Clinical Research Exome V2	Illumina NextSeq 500
ICR	Agilent SureSelect Clinical Research Exome V7	Illumina NovaSeq 6000 S2

**Table 3: WES library prep kits and sequencing platforms used in ITCC-P4**

Various PDX models established at different ITCC-P4 partnering sites used different WES kits.

INSTITUTION	WGS SEQUENCING PLATFORM
DKFZ	Illumina NovaSeq 6000 S1
CCIA	Illumina HiSeq X Ten
CURIE	Illumina NovaSeq 6000
Xentech	Illumina HiSeq 2500

**Table 4: lcWGS sequencing platforms used in the ITCC-P4**

The sequencing reads obtained from the patient tumor, PDX sample, and corresponding germline controls were aligned to a merged reference genome that combined the human reference genome (hs37d5) and the murine reference genome (GRChm38mm10). This alignment process was performed using the BWA alignment tool [211] to capture and identify any reads that might have originated from mouse tissue, thereby detecting potential contamination. The samples were aligned and processed through the in-house DKFZ One Touch Pipeline (OTP) of the DKFZ ODCF. Single-nucleotide variants (SNVs) were identified using our in-house workflow (<https://github.com/DKFZ-ODCF/SNVCallingWorkflow>) (version 2.2.0), which involved the utilization of samtools [212] mpileup and bcftools [213]. For the detection of small insertion/deletions (INDELs) the IndelCallingWorkflow (version 3.1.1) that uses Platypus (<https://github.com/DKFZ-ODCF/IndelCallingWorkflow>) was utilized. The confidence of INDEL variant calls is assessed with the Platypus scoring system. The standard ODCF pipeline for processing structural variants (SVs) involved the utilization of the Sophia workflow (<https://github.com/DKFZ-ODCF/SophiaWorkflow>) (version 2.2.3).

### **2.2.2 "No-control workflow": Analysis of samples without patient-matched germline data**

Among the PDXs in our cohort, 90 out of 251 (35.8%) lacked a corresponding germline control. For these cases, we employed a well-established in-house pipeline developed by Dr. Jeongbin Park from the Division of Theoretical Bioinformatics at the German Cancer Research Center (DKFZ) in Heidelberg, Germany. Specifically, the "No-Control workflow" was utilized to process the PDX and tumor data samples and utilized mpileup for SNV calling, Platypus for indel calling, and Sophia for SV processing. The aligned tumor BAM files were soft linked, and pseudo-control BAM files were generated. To call Single-Nucleotide Variants (SNVs), insertions/deletions (indels), and Structural Variants (SVs), I utilized the DKFZ Roddy framework (<https://github.com/TheRoddyWMS/Roddy>) (version 3.5.8). To filter out germline variants, I excluded variants that had exact matches in dbSNP and 1K genomes databases. For variant interpretation and prioritization in coding and non-coding regions, we utilized the Ensembl Variant Effect Predictor (VEP) [214]. To prioritize and include relevant variants, I utilized gnomAD (version 2.1) [215], a widely used database that provides information on minor allele frequencies (MAF) in various populations. After variant calling and filtering, we integrated gnomAD data into our analysis pipeline. Variants with a maximum population allele frequency above a specified threshold of 0.001 were excluded from further consideration, as they were considered more likely to represent common polymorphisms. This filtering step allowed us to focus on variants that were less prevalent in the general population and, therefore, include variants that showed higher rarity or specific enrichment patterns within our cohort, thus enhancing the identification of potentially pathogenic or functionally significant variants.

### **2.2.3 DNA-Methylation profiling and subgroup classification**

To better characterize the models regarding tumor subgroup diagnosis, DNA-methylation-based array profiling was performed by Dr. Aniello Federico (from the group of Prof. Dr. Marcel Kool, Division of Pediatric Neurooncology (KITZ). Genomic DNA was extracted from PDX and patient tumor samples (fresh frozen materials). The methylation profiling process was carried out at: the DKFZ Genomics and Proteomics Core Facility and Institute Curie, using the Illumina Methylation450K [216] and MethylationEPIC BeadChip arrays [217]. The methylation data preprocessing and downstream analyses were conducted within the R environment (version 4.0.1) utilizing the minfi package (version 1.34). To outline the process briefly, the raw data was normalized, probes that overlapped with the X/Y chromosomes were filtered out, as well as those containing SNPs and not uniquely mapping to the human reference genome (hg19). Finally, probe signal intensities (beta-values) per each analyzed sample. Tumor class annotation was performed using the CNS [218] and sarcoma [170] DNA methylation-based tumor classifiers, using unsupervised clustering analyses implementing the t-distributed stochastic neighbor embedding (t-SNE) method. These classifiers and machine learning techniques allowed us to classify the tumor and PDX models into their respective tumor entities and molecular subgroups, leveraging tumor reference datasets for improved accuracy and classification.

### **2.2.4 Copy number variant (CNV) workflow**

Different CNV tools utilize diverse algorithmic approaches to detect and characterize copy number alterations. CNVs, which refer to gains or losses of genomic DNA segments, play a significant role in tumorigenesis and can provide valuable insights into the genomic landscape of cancer. In order to accurately detect and characterize CNVs, we ran a variety of different analysis tools, to account for their specificity, sensitivity and confidence scores.

#### **2.2.4.1 ichorCNA**

ichorCNA [219], is a tool that uses a probabilistic Hidden Markov Model (HMM) to segment the genome and predict large-scale copy number alterations from ultra-low-pass whole genome and whole exome data. One notable feature of ichorCNA is its ability to handle samples with low tumor purity or contaminated by normal cells. It employs a deconvolution algorithm to estimate the tumor purity and ploidy, which are critical factors for accurate copy number inference. This enables the tool to effectively analyze samples with complex genomic profiles and heterogeneous tumor populations. For samples without controls, a panel of normal was generated using existing controls to reduce noise and improve the accuracy of CNV calling. The output ploidy, tumor purity and copy number alterations were interpreted for further analysis.

### **2.2.4.2 Sequenza**

Sequenza [220] is a computational tool for the analysis of cancer genomic data. It utilizes a probabilistic model that runs on only paired tumor-normal DNA sequencing data to calculate copy-number profiles, estimate tumor cell fraction and tumor ploidy from whole exome and genome data. Input parameters take in the aligned BAM files, human-mouse hybrid genome (hs37d5-GRCm38mm10) and the human reference genome (hs37d5), while using a bin size of 100 bases for WES data. This method also allowed for estimation and comparison of tumor purity of patient tumor and PDX samples. These results were used for comparing tumor cell purity and copy number calls.

### **2.2.4.3 CNVkit**

CNVkit [221] (version 0.9.3), is a tool specifically designed to detect and quantify genomic amplifications and deletions in tumor samples. It utilizes a target capture-based sequencing approach to analyze read depths and calculate copy number profiles across the genome. By comparing the read depth of the tumor sample to a reference normal sample, CNVkit identifies genomic regions with copy number alterations, providing insights into the structural changes in the cancer genome. CNVkit analysis was performed by the INFORM Bioinformatics team (Dr. Christopher Previti), Clinical Bioinformatics, Hopp Children's Cancer Center (KiTZ), using the "in-house" standard pipeline with default parameter settings on whole exome sequencing data of PDX and tumor samples. Only samples with germline controls could be analysed using this tool. I extracted and concatenated the  $\log_2$  ratio values from the processed CNVkit output for each fragment and for all the ITCC-P4 samples; further comparative analysis and variant calling was also performed. The results of these analyses were used for tumor cell purity comparative analysis and to annotate the driver gene copy number alterations reported in the genomic landscape analysis of the PDX models and pediatric tumors.

## **2.2.5 RNA sequencing workflow and gene fusion calling**

The RNA sequencing data was processed using the DKFZ OTP in-house pipeline (version 3.0.0) available at <https://github.com/DKFZ-ODCF/RNAseqWorkflow>, which is based on the established Roddy workflow (<https://github.com/TheRoddyWMS/Roddy>). In summary, the reads from the samples were aligned to the human reference genome (hg37d5) using the STAR aligner [222]. The mapped BAM files were then subjected to FeatureCounts to quantify the gene expression using the GENCODE v19 reference annotation. For the identification of gene fusions, the RNA-sequencing input data was analyzed using Arriba (version) [223]. Gene fusions reported by Arriba with high or medium confidence levels were extracted and considered for further analysis.

## 2.2.6 Driver gene annotation of somatic and germline mutations

To identify and annotate important driver genes for the mutational landscape analysis in our study, we utilized the 2022 World Health Organization (WHO) Classification of Pediatric Tumors [224] and a published review by Jones et al. on pediatric solid cancers[225] as references. These references were used to curate a comprehensive list of known somatic and germline driver mutations. Within the ITCC-P4 PDX and tumor cohort, we performed an analysis to identify significant genomic events, chromosomal alterations, fusion events, and copy number alterations specific to each cancer entity and their relative molecular subgroups. The driver alterations identified from the processed variant calling data for all samples, including those without germline controls, were highlighted. These specific alterations served as the focal point for downstream analysis and interpretation of the mutational landscape within the ITCC-P4 cohort.

## 2.2.7 Tumor mutational burden (TMB) analysis

Tumor mutational burden (TMB) is a measure used to assess the overall number of genetic mutations present in a tumor sample. It quantifies the total number of somatic mutations, including single nucleotide variants (SNVs), small insertions/deletions (indels), and structural variations, within the tumor genome. TMB serves as an important clinical metric that allows predicting response to immunotherapy [226][227]. The estimation of TMB was performed by Dr. Christopher Previti (INFORM Bioinformatics, KITZ) using the standard INFORM pipeline. The TMB was calculated on whole-exome sequencing data only over those coding regions targeted by the respective WES library prep kits using only high-confidence somatic and functional exonic SNVs and INDELS. The TMB values were compiled and used to compare mutational load across cancer subgroups, disease states and model types to assess high burden of genetic alterations.

## 2.2.8 Variant allele frequency (VAF) calculation

To understand the intra-tumor heterogeneity, clonal selection, distinguishing somatic and germline variants and evolution within the PDX samples, the variant allele frequency (VAF) of somatic functional SNVs was calculated. From the aligned and processed somatic functional SNV files, the so-called DP4 values were extracted. This DP4 value provides information about the depth of sequencing coverage for each allele (reference and alternate) in each sample. It is typically used to indicate the number of reads supporting each allele. It contains four subfields that represent the sequencing reads covering a variant. These subfields specifically indicate the coverage of the reference allele by forward reads, the coverage of the reference allele by reverse reads, the coverage of the alternate allele by forward reads, and the coverage of the alternate allele by reverse reads. VAF scores were then calculated using this formula:

$$VAF = \frac{Forward_{non-ref} + Reverse_{non-ref}}{Forward_{ref} + Reverse_{ref} + Forward_{non-ref} + Reverse_{non-ref}}$$

### **2.2.9 Tumor cell fraction (TCF) – ESTIMATE, Sequenza and CNVkit**

Tumor cell fraction refers to the proportion of tumor cells within the overall cell population[228]. In cancer samples, the presence of normal cells can dilute the frequency of somatic mutations, leading to inaccurate VAF scores. To exclude any biases of sample purity affecting analysis, the tumor cell fraction of each PDX and tumor sample were calculated. To obtain a comparative assessment of tumor purity, three different computational tools were utilized on the ITCC-P4 cohort: Sequenza, CNVkit, and ESTIMATE. ESTIMATE [229], a deconvolution tool that leverages RNA sequencing gene expression data (TPM values), was applied to all available RNA sequencing samples. to infer the fraction of infiltrating stromal and immune cells within a sample. However, a subset of 41/251 PDX models lacked matching RNAseq data due absence of sequencing data. ESTIMATE provides three scores: (1) amount of stroma (non-immune) cells in the tumor tissue, (2) the infiltration of immune cells in tumor tissue and (3) the tumor purity. These scores offer valuable insights into the composition of the tumor microenvironment and allow for a more comprehensive evaluation of tumor purity.

### **2.2.10 Variant allele frequency using estimated tumor cell fraction**

Using the CNVkit tumor purity scores, the variant allele frequencies were corrected for all samples to consider the purity of the sample. VAF scores for somatic SNVs were divided by the purity of the tumor or PDX sample respectively and then normalized within each sample to obtain the corrected VAF scores for tumor and PDX models. Normalizing tumor cell fraction-corrected variant allele frequency (VAF) scores is important to account for the differences in tumor purity and accurately compare VAF values across samples.

$$TCF \text{ corrected VAF score} = \frac{VAF \text{ score}}{Tumor \text{ cell fraction}}$$

### **2.2.11 PDX-Tumor correlation: Pearson scores, delta-VAF and VAF-ratio**

To compare and infer and correlate clonal discordance between the variant allele frequencies of tumors and PDX models, we introduced a metric known as delta-VAF. This metric was calculated by subtracting the PDX VAF from the difference in tumor VAF[199]. The identification of PDX-specific variants within a sample played a significant role in investigating crucial subclones. To analyze overlapping or exclusive variants between PDX and tumor, we introduced another metric called "VAFratio." The VAFratio scores were computed by summing the PDX VAF and dividing it by the sum of the tumor VAF for each individual patient sample.

## 2.3 Methods based on the ITCC-P4 Target Actionability Review - Replication Stress

As a result of significant number of pediatric cancer-related fatalities in the past decade, the exploration of therapeutic advancements in childhood cancer has become a highly investigated area. Although classical chemotherapy provides some therapeutic benefits, it often leads to long-term persisting complications among survivors. Therefore, there is an urgent need to identify new targeted therapies.

Replication stress, a prominent contributor to genomic instability in cancer, causes the stalling of replication forks. The inability of DNA damage checkpoints, DNA repair mechanisms, and replication fork restart to effectively respond to this stress can exacerbate the condition and activate cell death pathways, making it an attractive target for novel therapeutic interventions. To bridge the gap between preclinical evidence and clinical application, a literature-driven systematic review methodology was employed to assess the actionability of targets based on published proof-of-concept (PoC) data related to replication stress.

The Target Actionability Review methodology consisted of four major steps (Figure 10), with minor deviations from the originally established appraisal approach by Schubert et al. [230].

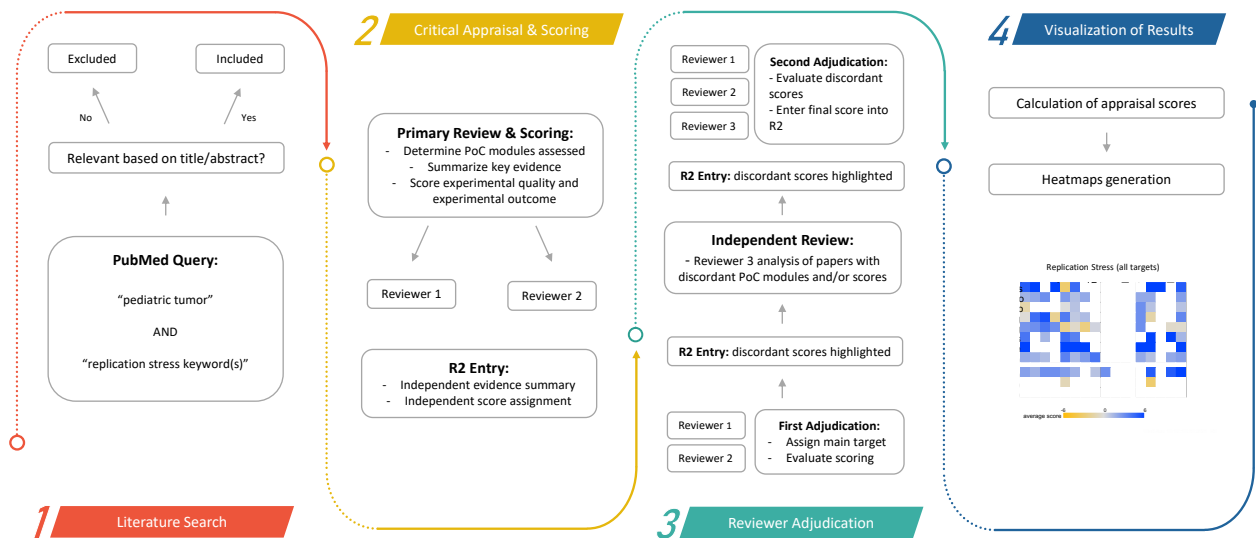


**Figure 10: Overview of Replication Stress TAR methodology**

The overview shows the four main steps modified from the established workflow and implemented in this TAR. (taken from the 2022 published review in the European Journal of Cancer [231])

### 2.3.1 Step 1: Literature search

Literature search across 16 different pediatric solid tumors, using specific and general keywords (Table 5) related to replication stress, was conducted via PubMed using the R package RISmed version2.2. Multiple search query terms were used with the tumor type of interest' ([‘pediatric tumor’ AND ‘replication stress keyword’]). Literature published between 2014 and 2021 (last literature search was performed on date: 27-01-2021) that contained the search term from the query in the title or abstract and had addressed relevant Proof of Concept modules (PoC) (Table 6) was considered. Only publications that fulfilled the above-mentioned criteria qualified to be included for further review.

The final list of PubMed IDs (PMIDs) was uploaded to the TAR portal on R2 for further scoring by two different reviewers and a third independent reviewer as explained below. The interactive R2 platform [[r2.amc.nl](https://hgserver1.amc.nl)] is a data mining and data discovery platform created by Dr. Jan Koster from the Amsterdam Medical Center (AMC, Netherlands) that includes all the resulting visualizations. [[https://hgserver1.amc.nl/cgi-bin/r2/main.cgi?optionZimi2\\_targetmap\\_v1](https://hgserver1.amc.nl/cgi-bin/r2/main.cgi?optionZimi2_targetmap_v1)].

	<i>Replication stress keywords Tumor entities</i>		
<b>General keywords:</b>	replication stress	Neuroblastoma (NBL)	
	genomic instability	Rhabdomyosarcoma (RMS)	
	chromothripsis	Synovial sarcoma (SS)	
	BRCA	Malignant peripheral nerve sheath tumor (MPNST)	
	R-loops	Ewing’s sarcoma (ES)	
	mutational signature	Osteosarcoma (OS)	
	MYC amplification	Atypical teratoid/rhabdoid tumor (AT/RT) & Malignant rhabdoid tumor (MRT)	
	MYCN amplification	Wilms tumors/nephroblastoma (WT)	
	high MYC expression	Hepatoblastoma (HB)	
	high MYCN expression	Inflammatory myofibroblastic tumor (IMT)	
	mitotic catastrophe	Retinoblastoma (RB)	
	reactive oxygen species	Extracranial germ cell tumor (extracranial GCT)	
	synthetic lethal treatment	Low-grade glioma (WHO grades I & II; LGG) High-grade glioma (WHO grades III & IV, incl. glioblastoma; HGG)	
	<b>Specific keywords:</b>	ATM	Ependymoma (EPN)
		ATR	Medulloblastoma (MB)
DNA-PK/DNA-PKcs/PRKDC			
CHK1/CHEK1			
WEE1			
PARP			

**Table 5: Replication stress keywords and cancer entities for PubMed queries**

### 2.3.2 Step 2: Critical review and scoring

Each article was evaluated by two separate reviewers, using the established PoC modules (Table 6) and all relevant data was entered as separate evidence into the R2 TAR platform. Key findings for each publication were summarized individually by reviewers 1 and 2. We excluded studies evaluating micro- or long non-coding RNA, natural compounds, or monotherapy with classical chemotherapy or radiotherapy due to the potential variation in sensitivity of pediatric tumors to these agents. This variation can arise from the distinct molecular pathways and cellular processes involved in pediatric oncogenesis. Additionally, the use of monotherapy with classical chemotherapy or radiotherapy in pediatric cancer may necessitate customized dosing and treatment strategies to achieve optimal efficacy.

Using the established scoring criteria previously defined by Schubert et al. [230], each module for each different tumor type was assessed while assigning quality and outcome scores (Table 7 & 8). Experimental quality scores ranged from +1 to +3, indicating the robustness of the study, while experimental outcome scores ranged from -3 to +3, indicating whether the study results warrant the targeting of a specific protein/pathway for the treatment of a pediatric solid or brain tumor.

<b>Proof of concept module (PoC)</b>	<b>Critical appraisal questions</b>	<b>Information to include in summary of experimental findings</b>
<b>PoC 1: target/pathway activation in pediatric clinical series</b>	<p><b>Is the target pathway active in the tumor of interest?</b></p> <p>Target/pathway evaluation in clinical series: DNA aberrations, (over)expression, methylation changes?</p> <p>Target DNA aberrations: mutation, translocation, amplification, in/del, CNV</p> <p>Percent of samples with aberrant target/pathway in clinical series</p> <p>Correlation to clinical outcome</p> <p>Correlation to other tumor biology</p> <p>Target expression/pathway activity compared to normal tissue, other cancers and/or other reference tissue</p>	<p>Total size of cohort (only consider the number of patient samples, not cell lines)</p> <p>Methodology used</p> <p>Percent of samples expression the target (and associated alterations or mutation) or with activated target pathway</p>
<p><b>Tumor target dependence</b></p> <p><b>PoC 2: in vitro</b></p>	<p><b>Is the tumor of interest dependent on the target/pathway for survival?</b></p> <p><b>In vitro</b></p> <p>Molecular target gene silencing in cells (RNAi, AOs, CRISPR etc.);ectopic expression; preferably <math>\geq 3</math> cell lines</p> <p>Phenotype analysis (apoptosis, cell viability, etc.)</p> <p>Biological effect of molecular silencing or ectopic expression of target</p> <p>Appropriate controls (use of use of multiple silencing tools, rescue experiments, control cell lines, etc.)</p>	<p><b>In vitro/ in vivo</b></p> <p>Model system(s)</p> <p>Methodology used</p> <p>Results of initial experiment (cell viability or tumor growth)</p> <p>Rescue experiment used</p> <p>Validation (effects on apoptosis, proliferation, cell cycle, migration, gene or protein expression, etc.)</p>

<p><b>PoC 3: in vivo</b></p>	<p>Additional functional assays showing target or pathway dependence for mutated/translocated/amplified target genes</p> <p><b>In vivo</b></p> <p>Molecular silencing or overexpression of target gene in xenografts (inducible shRNA or expression vectors)</p> <p>Transgenic models (mice, zebrafish, etc.) for mutated/translocated/amplified target genes or for activated pathways</p>	
<p><b>Sensitivity to compound/drug</b></p> <p><b>PoC 4: in vitro</b></p> <p><b>PoC 5: in vivo</b></p>	<p><b>Does the targeted compound reduce survival of the tumor of interest in preclinical models?</b></p> <p><b>In vitro</b></p> <p>Preferably <math>\geq 4</math> cell lines with target dependence (preferably with <math>\geq 1</math> control cell line without target dependence)</p> <p>Cell viability: IC<sub>50</sub>, GI<sub>50</sub>, LC<sub>50</sub>, dose-response curves</p> <p>Biological efficacy: preferably measured with pharmacodynamic (PD) assays intended for extrapolation to clinical studies</p> <p>Correlation of efficacy with tumor biology</p> <p><b>In vivo</b></p> <p>Xenografts/PDX/GEMM (both with dependency on evaluated target)</p> <p>Preferably measured with predictive biomarker to be used in clinical trial for patient selection</p> <p>Pharmacokinetics (PK; plasma and intra-tumoral)</p> <p>Pharmacodynamics in tumor: (1) target binding, (2) target inhibition, (3) pathway modulation, (4) biological effect</p> <p>PK-PD relationships: preferably use assays intended for extrapolation to clinical studies</p> <p>Response rates and survival measures (use established, measurable tumors)</p> <p>Efficacy-PD-PK relationships</p>	<p><b>In vitro</b></p> <p>Type (establish cell line or patient-derived [i.e., <i>ex vivo</i>] and number of cell lines used [including controls])</p> <p>Drug(s) used and concentration range tested; time point(s) used to assess cell viability</p> <p>Percent of sensitive lines (IC<sub>50</sub> <math>\leq</math> 500 nM of clinically relevant [if known/applicable])</p> <p>Validation (effects on apoptosis, proliferation, cell cycle, migration, gene or protein expression, etc.)</p> <p><b>In vivo</b></p> <p>Model(s) (cell line or patient-derived xenografts, transgenic mice, orthotopic vs. subcutaneous, etc.) and <i>n</i>/arm</p> <p>Dosing schedule used</p> <p>Tumor growth inhibition and/or overall response extrapolation for each experiment</p> <p>Validation (effects on apoptosis, proliferation, cell cycle, migration, gene or protein expression, etc.)</p>
<p><b>PoC 6: predictive biomarkers</b></p>	<p><b>Can biological compound efficacy be determined by a specific marker in preclinical models?</b></p> <p>Evaluation of existing, validated biomarkers in PoC 4 and PoC 5</p> <p>Predictive biomarker (intended for extrapolation to clinical studies and patient selection)</p> <p>Efficacy biomarkers (PD markers)</p>	<p>Biomarker(s) reported</p> <p><i>In vitro/in vivo</i> correlation (include statistical values if available)</p> <p>Patient correlation (include statistical values if available)</p>

<b>PoC 7: resistance</b>	<p><b>Are the mechanisms of resistance understood?</b> (Analyzed in preclinical models, use knowledge from adult studies, added observations in patient samples from trials)</p> <p>Target mutations</p> <p>Upregulation of alternative pathways</p> <p>Increased drug transporters</p> <p>Other mechanisms</p>	<p>Model(s) (<i>in vitro/in vivo</i>)</p> <p>Methodology</p> <p>Resistance reported and drug concentration/validation (if applicable)</p>
<b>PoC 8: combinations</b>	<p><b>Are synergistic combinations with other drugs/compounds established?</b></p> <p>Rational combinations: based on pathway knowledge and/or resistance observations from PoC 7</p> <p>Compound/drug + cytotoxic drug</p> <p>Compound/drug + targeted compound</p>	<p>Model(s) (<i>in vitro/in vivo</i>)</p> <p>Methodology for combination</p> <p>Drug(s) used and concentration range tested; time point(s)</p> <p>Results (combination index [CI]/method of determining combination effect, percent of models showing synergism)</p> <p>Validation (effects on apoptosis, proliferation, cell cycle, migration, gene or protein expression, etc.)</p>
<b>PoC 9: clinical evaluation</b>	<p><b>Can the targeted compound safely be administered to children with cancer? (Phase I)</b></p> <p>Has a formal phase I trial been conducted with a targeted compound in children with cancer?</p> <p>Has a recommended dose been established for single drug use?</p> <p>Has a recommended dose been established for use in combination in standard of care (SOC)?</p> <p>Does the targeted compound show efficacy (clinical or biological) in relapsed/refractory disease (Phase II)</p> <p>Has a formal phase II trial been performed with a targeted compound in children with cancer?</p> <p>In which diseases has efficacy been investigated?</p> <p>In which stage of disease (relapsed/refractor? Treatment-naïve?)</p> <p>Were trials done with single drug or in combination?</p> <p>Has 'biological efficacy' (PD biomarkers) been shown?</p> <p>Does the targeted compound add benefit to the standard-of-care treatment? (Phase III)</p>	<p>Number of patients included in the trial and tumor types considered</p> <p>Study design (phase, type of design [open label, randomized, controlled, other])</p> <p>Toxicity profile</p> <p>Recommended phase II dose (RP2D); if applicable</p> <p>Efficacy observed (ORR, CR, PR, SD or PD); if applicable</p>

**Table 6: Proof of concept (PoC) modules for the TAR**

The PoC modules highlight the nine different modules that were essential to score and review each selected publication on replication stress. This was performed independently by two reviewers.

<b>Proof of Concept (PoC) Module</b>	<b>Description</b>	<b>Scoring and Criteria</b>	
<b>PoC 1: target/pathway activation in pediatric clinical series</b>	Number of pediatric samples	3	n ≥ 20 pediatric patient samples; ≥ 2 different methods OR next-generation sequencing
	Type of analysis	2	20 > n > 10 pediatric patient samples; ≥ 1 reliable method
		1	n ≤ 10 pediatric patient samples; 1 method
<b>PoC 2: tumor target dependence in vitro</b>	Methodology	3	Different methods to alter target expression in ≥ 3 cell lines; phenotypic analysis of knockdown
	Tumor cell viability	2	Single method to alter target expression in < 3 cell lines
	Biological pathway readout	1	Questionable alteration of gene expression
<b>PoC 3: tumor target dependence in vivo</b>	Model(s) used	3	Transgenic mouse model or ≥ 2 different xenografts with appropriate controls and/or different methods of genetic modification <i>in vivo</i> (shRNA/CRISPR)
	Tumor formation/growth	2	≥ 2 different xenografts without appropriate control
	Biological pathway readout	1	1 xenograft model without appropriate control
<b>PoC 4: in vitro sensitivity to compound/drug</b>	Number of cell lines	3	5+ cell lines and ≥ 2 appropriate controls; validation
	Measurement of PD markers	2	2-5 cell lines and ≥ 1 appropriate control; validation
	Phenotypic response	1	1 cell line and/or lack of control and/or validation
<b>PoC 5: in vivo activity of compound/drug</b>	Number and type of model(s)	3	≥ 2 xenograft models or 1 transgenic mouse model with appropriate controls; treatment with clinically relevant dose; validation
	Measurement of PD markers	2	1 xenograft model with appropriate control; treatment with clinically relevant dose; validation
	Phenotypic response	1	1 xenograft model OR use of supra-clinical dose levels; no appropriate control or validation
<b>PoC 6: predictive biomarkers</b>	Confirmation of correlation	3	Correlation molecularly confirmed in ≥ 2 models (eg: silencing, overexpression, etc.); patient selection
	Patient selection	2	Correlation confirmed in 1 model
		1	Correlation not confirmed
<b>PoC 7: resistance</b>	Mechanism of resistance	3	Reported resistance and comprehensive analysis and reversing/overcoming resistance
	Molecular analysis	2	Reported resistance and analysis of molecular changes underlying/due to resistance
	Method to overcome resistance	1	Only reporting resistance
<b>PoC 8: combinations</b>	Concentrations tested	3	> 4 concentrations of each compound are tested and combination index values calculated; combination evaluated <i>in vivo</i>
	<i>In vitro</i> combination index values	2	1-4 concentrations of each compound are tested and combination index values calculated; with or without evaluation of combination <i>in vivo</i>
	<i>In vivo</i> combination	1	1 concentration of each compound tested; no evaluation of combination <i>in vivo</i>

<b>PoC 9: clinical evaluation</b>	Pediatric patient selection Toxicity, Efficacy	1	number of patients; tumor types included in study; study design
-----------------------------------	---	---	---

**Table 7: Experimental quality scoring**

The table highlights the experimental “quality score” for all the PoC modules. The first and second reviewer score each selected publication based on the different description and criteria.

<b>Proof of Concept (PoC) Module</b>	<b>Description</b>	<b>Scoring and Criteria</b>	
<b>PoC 1: target/pathway activation in pediatric clinical series</b>	Prevalence of target/pathway in cohort	3 1 -3	>10% of cohort Between 2% and 10% ≤ 2% of cohort
<b>PoC 2: tumor target dependence in vitro</b>	Level of dependency and phenotypic recapitulation	3 1 -3	Full dependency (> 75% cell death <u>or</u> transformation) Partial dependency (< 75% cell death <u>or</u> altered growth) No dependency
<b>PoC 3: tumor target dependence in vivo</b>	Level of dependency and phenotypic recapitulation	3 1 -3	Full dependency (CR) after knockdown/knockout <u>or</u> transformation in GEMM Partial dependency (< 75% response) No dependency
<b>PoC 4: in vitro sensitivity to compound/drug</b>	IC <sub>50</sub> observed after 72-hour exposure	3 1 -1 -3	IC <sub>50</sub> < 500 nM <u>or</u> ≤ clinically relevant concentration IC <sub>50</sub> = 500- 1000 nM IC <sub>50</sub> > 1500 nM No activity (IC <sub>50</sub> > 10 μM)
<b>PoC 5: in vivo activity of compound/drug</b>	<i>In vivo</i> tumor response	3 1 -1 -3	Response comparable to PR/CR Response comparable to SD Very minor response (between SD and PD, slight TGI) No activity or clear PD; growth comparable to control
<b>PoC 6: predictive biomarkers</b>	Correlation of biomarker status with anti-cancer activity of a targeted drug <i>in vitro/in vivo</i>	3 1 -3	Strong correlation (presence of biomarker results in significantly different drug response) Moderate correlation (presence of biomarker results in different drug response; not significant) No correlation (presence of biomarker does not correlate with drug response)
<b>PoC 7: resistance</b>	Reported resistance with drug exposure	3	Resistance reported at clinically relevant concentrations/dose and identification/description

		1	of mechanism Resistance reported with no mechanism
<b>PoC 8: combinations</b>	Synergy in combination testing at clinically relevant dosages in relevant <i>in vitro</i> and/or <i>in vivo</i> models	3	Strong synergy reported— CI < 0.5
		1	Moderate synergy/additive effect observed— CI 0.5 - 0.9
		-1	Very minor synergy/additive effect observed— CI 0.9 - 1.1
		-3	No combination benefit
<b>PoC 9: clinical evaluation</b>	Phase I	3	Toxicity profile acceptable, RP2D identified and early efficacy observed
		1	DLT observed with still acceptable safety and no efficacy reported
		-3	Toxicity profile not acceptable
		3	Efficacy observed greater than historical ORR, DoR and/or PFS and acceptable toxicity
	Phase II	1	Limited efficacy observed above the historical ORR, DoR and/or PFS and acceptable toxicity
		-3	No efficacy observed and/or unacceptable toxicity
	Phase III	3	Added efficacy over SOC in appropriate pivotal trial with acceptable benefit/risk profile; new drug now part of SOC
		1	Added efficacy over SOC but new agent not part of SOC due to trial design issues and/or benefit/risk assessment
		-3	Insufficient efficacy in pivotal trial

**Table 8: Experimental outcome scoring**

The table highlights the experimental “outcome” score for all the PoC modules. The first and second reviewer score each selected publication based on the different description and criteria.

### **2.3.3 Step 3: Adjudication by reviewer**

Once articles received a score, any discordant scored paper was further assessed and discussed. In the adjudication process, both reviewer 1 and 2 re-evaluated the collected evidence for each article. The main replication stress target was identified, and the assigned quality and outcome scores were reassessed. Each discrepant module or score was briefly discussed by the two reviewers and adjusted if necessary. Articles with further discordant scores were then sent to an independent third reviewer, who then scored the article without knowing the modules or scores given by reviewer 1 and 2. If the score assigned by reviewer 3 was discordant with scores given by the first two reviewers, the article entered a second adjudication phase, where reviewers 1, 2 and 3 evaluated the article and reassessed the discrepant score until a final consensus score was assigned to the article.

### **2.3.4 Step 4: Data visualisation**

The final experimental outcome and quality scores for each article were entered into the R2 TAR platform and a single appraisal score was calculated by multiplying the discussed experimental outcome and the quality scores. The final scores ranged from -9 to +9 creating a gradient indicative of the importance of each study. POC scores across each of the 16 entities were averaged and interactive heatmaps were created to visualize the data were made on the TAR portal of the R2 platform. This allows users to view and read the curated articles, the number of articles, average appraisal score for each module in each malignancy for overall replication stress as well as specific targets included in the study. All the summarised evidence, scores and PubMed links can be found by clicking each individual tile within the heatmap on the R2 portal.

[ [https://hgserver1.amc.nl/cgi-bin/r2/main.cgi?option=imi2\\_targetmap\\_v1](https://hgserver1.amc.nl/cgi-bin/r2/main.cgi?option=imi2_targetmap_v1) ]

This chapter provided a comprehensive overview of the experimental procedures and the analysis performed in both the studies. By providing this overview, we have ensured the reproducibility and reliability of our research. These details of the methodology can serve as a foundation for subsequent analysis and interpretation of the results obtained in both these studies.

## 3 RESULTS

### 3.1 Results based on the molecular characterization and multi-omic analysis of Patient-Derived Xenograft (PDX) models from high-risk pediatric cancer

In this chapter, I focus on the key findings and outcomes of the ITCC-P4 PDX molecular profiling. The resulting manuscript draft will be submitted for peer review this year. Data collection, processing and analysis were a joint effort between me and a postdoctoral researcher Dr. Aniello Federico working in Prof. Dr. Marcel Kool's group at the KiTZ, Heidelberg, Germany. The contributions of the co-authors and collaborators involved are indicated in the *Material and Methods* chapter of this thesis. The results showed that this cohort (n=251 PDX models) was able to fully recapitulate a diverse range of tumor types and molecular lesions important to pediatric cancer research.

#### 3.1.1 ITCC-P4 PDX model cohort generation and characterization

The ITCC-P4 pediatric cohort consists of 401 total PDX models established from 2017-2022. In this study we focused on 251 / 401 (62.5%) PDX models that have been comprehensively characterized during this period (Figure 11). Patient ages in the study cohort range from 1.2 months to 20 years, with a median age of 9.1 years. Fresh patient samples were obtained after surgery, and brain tumors were injected directly into the brain (orthotopically), while non-brain tumors were transplanted into the subcutaneous tissue (either the flank or the fat pad) of immunodeficient mice (NSG). The pipeline of PDX collection, transplantation and establishment is described in the Methods section (Chapter 2.1.2, Figure 9).

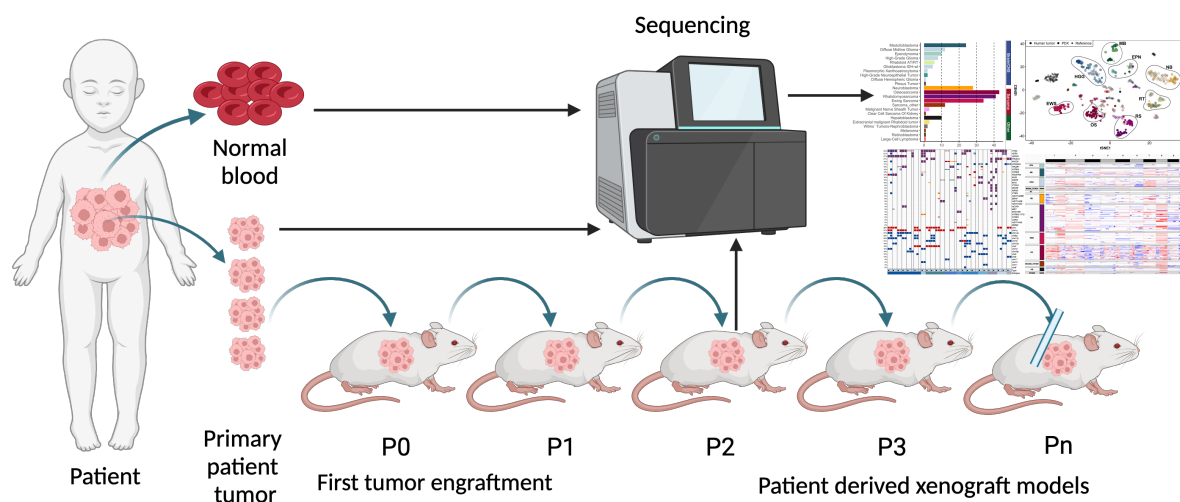


**Figure 11: Schematic illustration of ITCC-P4 PDX model establishment**

Schematic illustration of the establishment and characterization workflow of the ITCC-P4 PDX models. The normal blood from the patient was sequenced along with the primary patient tumor and the established PDX model (P2). Multi-omics profiling was performed on these sample types.

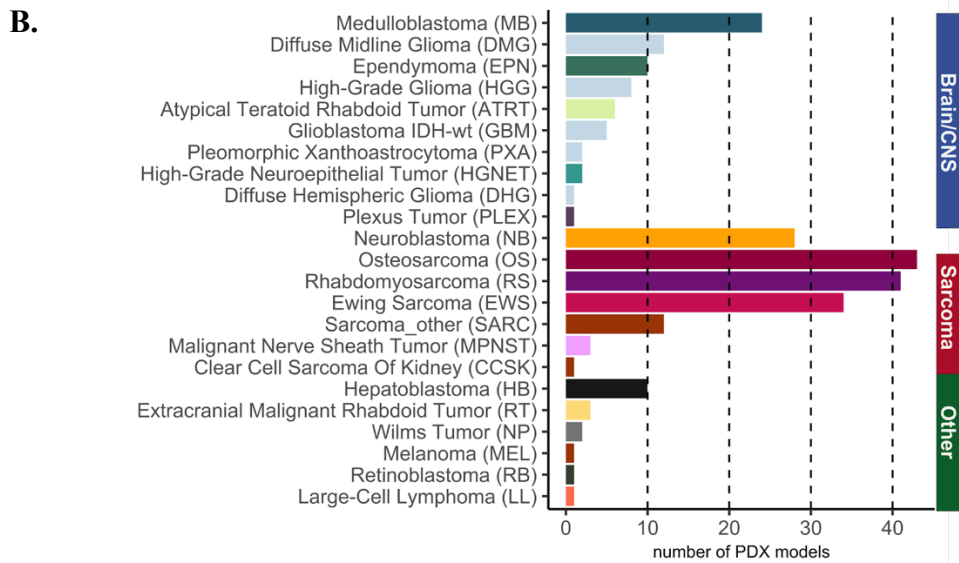
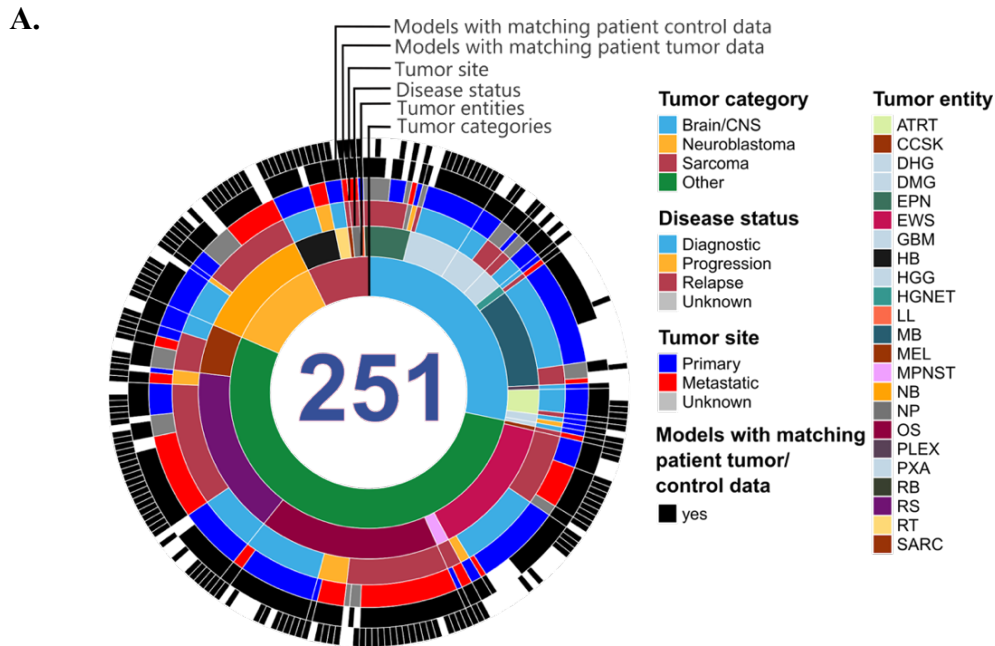


**Figure 12: ITCC-P4 PDX model generation and subgroup classification**

A.) ITCC-P4 PDX cohort overview representing main pediatric solid tumor categories, disease states, tumor site, germline availability and tumor entities. B.) DNA-methylation based subgroup annotation of the ITCC-P4 entities highlighting number of entities tumor subgroups identified across per main tumor category (CNS, Brain, other).

The cohort contained balanced representation of models derived from relapsed tumors (119/251; 47.4%), primary/diagnostic tumors (115/251: 45.41 %) or tumor progression (17/251; 6.8%). These PDXs have been generated from different sites, primary (141/251; 56.5%), metastatic site (76/251; 6.8%) or site undefined/unknown (34/251, 13.5%). Additionally, we established PDX models (36/251) originating from serially collected samples of the same 16 patients referred to as “Serial PDX models”. This sub-cohort is comprised of models derived from matching diagnostic samples and samples generated from one or multiple relapses (n=6); primary and one or multiple metastasis (n=3); a collection of models from multiple recurrences (n=2) or metastatic events (n=1). Patients could be grouped by age ranging from: 5-15 years (79/251; 31.4%), 0-5 years (54/251; 21.5%), greater than 15 years (48/251; 19.1%) and a group with age data unavailable (70/251; 27.8%). Classifying the gender of the patients, we saw a predominance of males (139/251; 55.3%) over females (104/251; 41.4%) (Figure 13A).

The PDX cohort represented a diverse range of pediatric tumor models encompassing both CNS (71/251; 28.3%) and non-CNS (180/251: 71.7%) models (Figure 12B). CNS tumors represented several different entities - high-grade gliomas (HGG; n=28), medulloblastomas (MB; n=24), ependymomas (EPN; n=10), atypical teratoid rhabdoid tumors (ATRT; n=6), high-grade neuroepithelial tumors (HGNET; n=2) and a plexus tumor (PLEX; n=1). It also contains models of malignant extracranial solid tumors comprised of sarcomas (including osteosarcomas (OS; n=43); rhabdomyosarcomas (RMS; n=41); Ewing sarcomas (EWS; n=34); malignant peripheral nerve sheath tumors (MPNST; n=3); small blue round cell tumors with CIC alteration (SBRCT\_CIC; n=5)) and neuroblastomas (NB; n= 28). Additionally, models generated from pediatric solid malignancies such as hepatoblastomas (HB; n=10); Wilms tumors (NP; n=2); retinoblastoma (RB; n=1) and melanoma (ML; n=1)) and liquid tumors, large cell lymphoma (LL; n=1) were included (Figure 12 C & 13A).

The criteria needed to be considered “established” in our cohort was that PDX tumors had to be effectively grown by passing them through an initial human-to-mouse (*P0*) transplantation and subsequently into at least 2 mouse-to-mouse (*P1-P2*) transplantation passages. Established models in some cases exhibited distinct growth pattern when they were assessed for tumor latency and penetrance, indicating variation depending on tumor type.

To have the most comprehensive understanding of the molecular characteristics in these models, tumor fragments obtained from these established PDX models with corresponding healthy patient tissue were gathered whenever available and analyzed. The cohort consisted of PDXs with matching human tumor characterization data (219/251, 87.3%) and number of PDXs with matching germline control data (161/251; 64.1%) This thesis included molecular characterization of PDX models using DNA methylation profiling (234/251; 93.2%), low-coverage whole genome sequencing (lcWGS; n=185/251; 73.7%), high-coverage whole exome sequencing (WES 236/251; 94%), RNA sequencing (RNAseq; 210/251; 83.7%) and Affymetrix gene expression profiling (45/251; 17.9%) (Figure 13B).

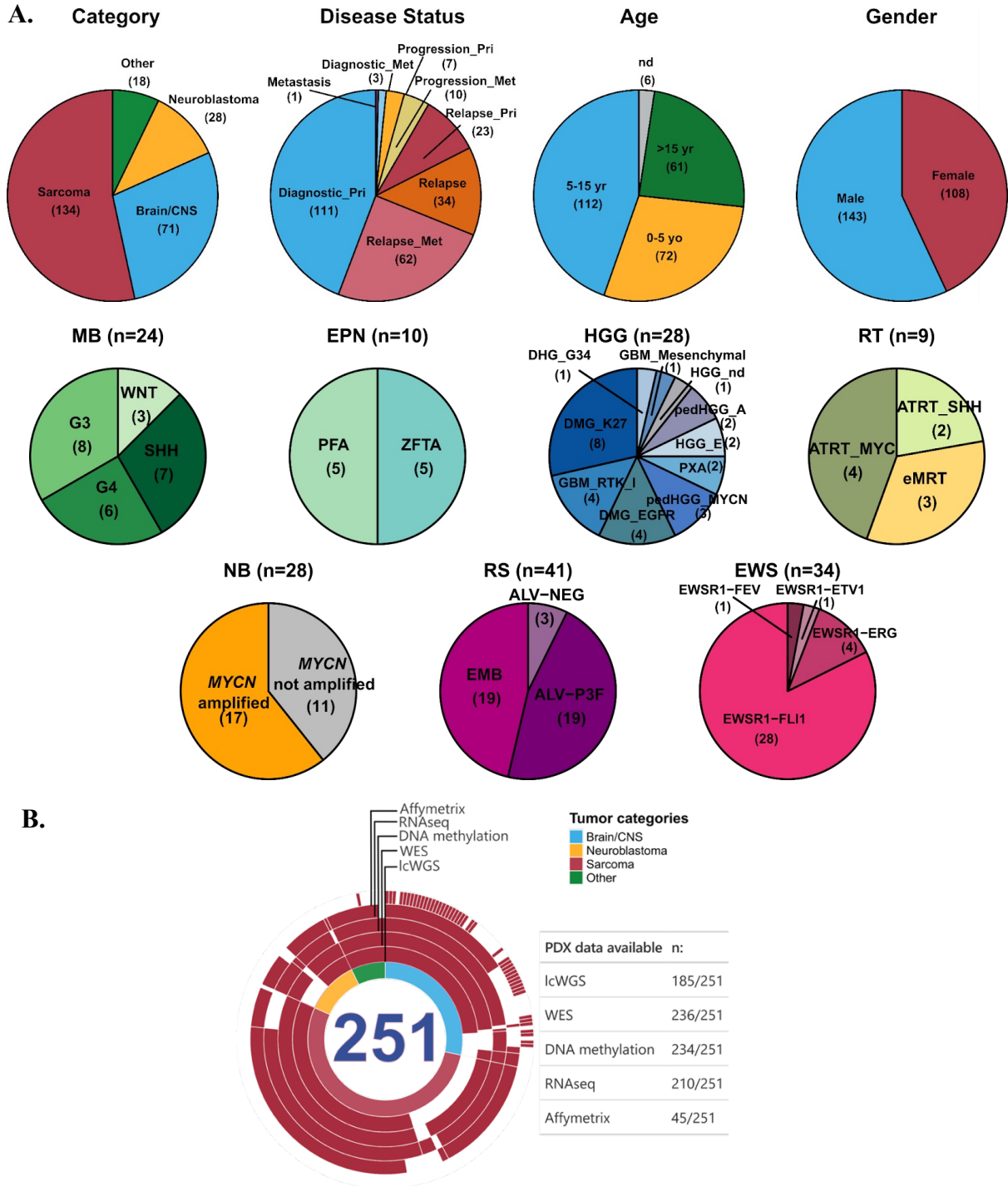


**Figure 13: ITCC-P4 PDX model characterization**

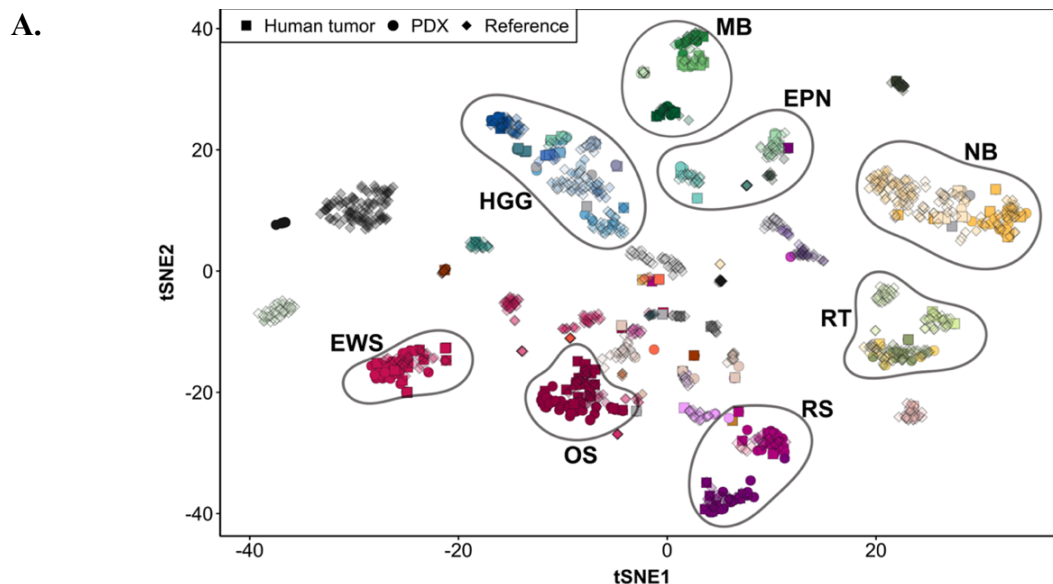
A. Row 1) Clinical characterization of the PDX models based on the main cancer category, disease stage, patient age, and biological sex. (A. Row 2-3) Number of PDX models generated for each tumor and methylation classified subgroup.

B.) Overview of PDX sequencing data collected for the ITCC-P4 cohort including Affymetrix RNAseq, DNA methylation, WES and IcWGS.

### 3.1.2 Molecular subgrouping of pediatric solid tumors based on DNA methylation and transcriptomic analysis

To enable uniform molecular classification of our PDX cohort, we performed DNA based methylation profiling. DNA methylation has emerged as a robust tool for classification of tumor samples, particularly CNS tumors [218] and sarcomas [232], into their respective types and molecular subtypes based on the clustering of their unique methylation patterns.

We assigned a predicted tumor class to each PDX and tumor case using the brain classifier v12.5 for Brain/CNS tumors, neuroblastomas, and retinoblastoma models. For sarcomas, extracranial malignant rhabdoid tumors and melanomas classification using the sarcoma classifier v12.2 (<https://www.moleculareuropathology.org/mnp/>) was performed. Among the tumor categories described, we observed 60/91 models that belonged to the predicted class by the MNP classifier and displayed a calibrated classification score of  $\geq 0.9$  (set as the optimal cut off reference). Additionally, we observed 80/122 PDX methylation samples that were predicted using the sarcoma classifier. Hence, a total of 140/214 (65.7%) PDX methylation datasets resulted in an optimal classification score. To enhance the classification of our ITCC-P4 PDX cohort based on their methylome profiles, we employed the t-distributed stochastic neighbour embedding (t-SNE) approach. This analysis aimed to include tumor cases such as hepatoblastomas, nephroblastoma and large-cell lymphomas, which were not included in the current MNP methylation classifier reference cohort. Additionally, data points with a calibrated score lower than the cut-offs were analyzed to determine their cluster behavior (Figure 14A). To achieve this, we analyzed the ITCC-P4 PDX models and corresponding human tumor DNA methylation data collectively with external methylation datasets. These datasets encompassed the same tumor types within our PDX cohort and additional pediatric tumors (n=1214; references) classified by the World Health Organization (WHO) in our analysis. Using t-SNE visualization, we examined the top 5000 probes with the highest variability in standard deviation.



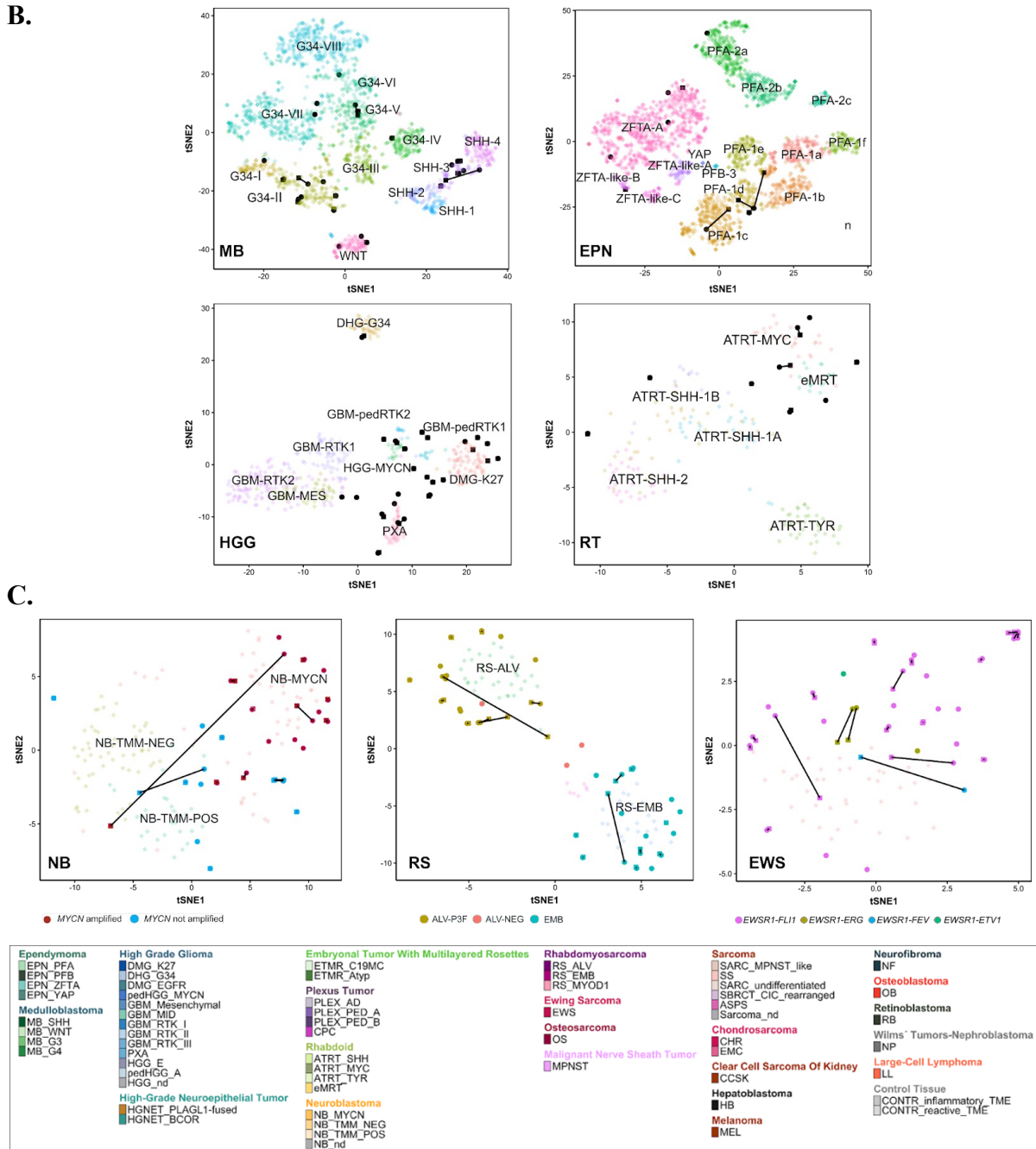


**Figure 14: DNA Methylation analysis**

A.) Global methylation-based t-SNE clustering identified using the brain and sarcoma classifier. Highlights the distinct PDX models, human tumors and the WHO classified references cases.

B.) Brain and CNS tumors mainly MB, EPN, HGG and AT/RT clustering into defining subgroups.

C.) Classification of NB, RS, EWS into their respective subgroups. Sub-clustering analysis confirmed positive overlap of PDX models to their corresponding patient tumor samples.

The results indicated that our ITCC-P4 cohort samples and reference samples overall exhibited similar methylation patterns, forming clusters and sub-clusters that corresponded to known molecular subtypes. Overall, the PDX samples clustered together with the reference samples, accurately reflecting their respective tumor types. Additionally, the primary patient tumors showed close proximity to their corresponding tumor within their specific clusters, further validating the fidelity of the PDX models (Figure 14A). In highly heterogeneous and most abundant tumor types within our cohort, we performed a sub-clustering analysis including the reference tumor cases. This included brain tumors: medulloblastomas, ependymomas, high-grade gliomas and atypical-teratoid-rhabdoid tumors, where the PDX models demonstrated distinct aggregation patterns within stable subclusters effectively defining the respective tumor subtypes for each main tumor entity (Figure 14B-C). For example, the PDX models accurately clustered into all major molecular subgroups of medulloblastoma (Figure 14B); wingless (MB WNT), sonic hedgehog (MB SHH), group 3 (MB G3), and group 4 (MB G4) as described previously [233] [234]. For the ependymomas (EPN), we observed representation of the most aggressive subtypes: EPN-PFA, EPN-ZFTA, however, none of our models co-clustered within the EPN PFB and EPN YAP1 subclusters seen in the reference cohort. High grade glioma (HGG) models exhibited substantial heterogeneity, with observed classification with the DMG H3-K27 altered, DMG EGFR-altered, PXA, glioblastoma, GMB\_MID, DHG\_G34 and HGG\_MYCN subgroups. For the Atypical teratoid/rhabdoid tumors (ATRTs), our analysis reported ATRT-MYC and ATRT-SHH models, but not for the ATRT-TYR subtype.

Within the Neuroblastoma clusters, PDX models and matching tumors characterized by the presence or absence of *MYCN* amplifications tended to form two distinct subclusters (Figure 14B). The rhabdomyosarcoma (RMS) cluster demonstrated clear separation between the alveolar (RMS-ALV) and embryonal (RMS-EMB) subtypes, both of which were well-represented in our PDX cohort (Figure 14B). The Ewing sarcoma models were mainly characterized by the *EWSR1-FLI* fusion and co-clustered with the consensus EWS tumors, while those models presenting alternative *EWSR1* fusions (*EWSR1-FLI*, *EWSR1-FEV*) were scattered throughout (Figure 14B). The methylation-based subtype classification of these models supported the model stratification based on genomic alterations [224]. Although most of the matched tumor samples co-clustered with their respective PDX models, overall, 17 /214 (0.07%) exceptions of divergent samples could be observed within the neuroblastoma, rhabdomyosarcoma, and Ewing sarcoma subclusters (Figure 14C). In the cases of entities such as hepatoblastoma (HB), melanoma (ML) and large cell lymphoma (LL), a distinct separation between PDX and reference samples were observed. This distinct clustering behaviour could potentially be attributed to the presence of samples with unique molecular characteristics, variations in tumor cell purity or the absence of reference cases that fully capture the heterogeneity present within these tumor types. As a result, all the PDX models have been thoroughly annotated and classified based on both, their genomic landscapes and methylome profiles.

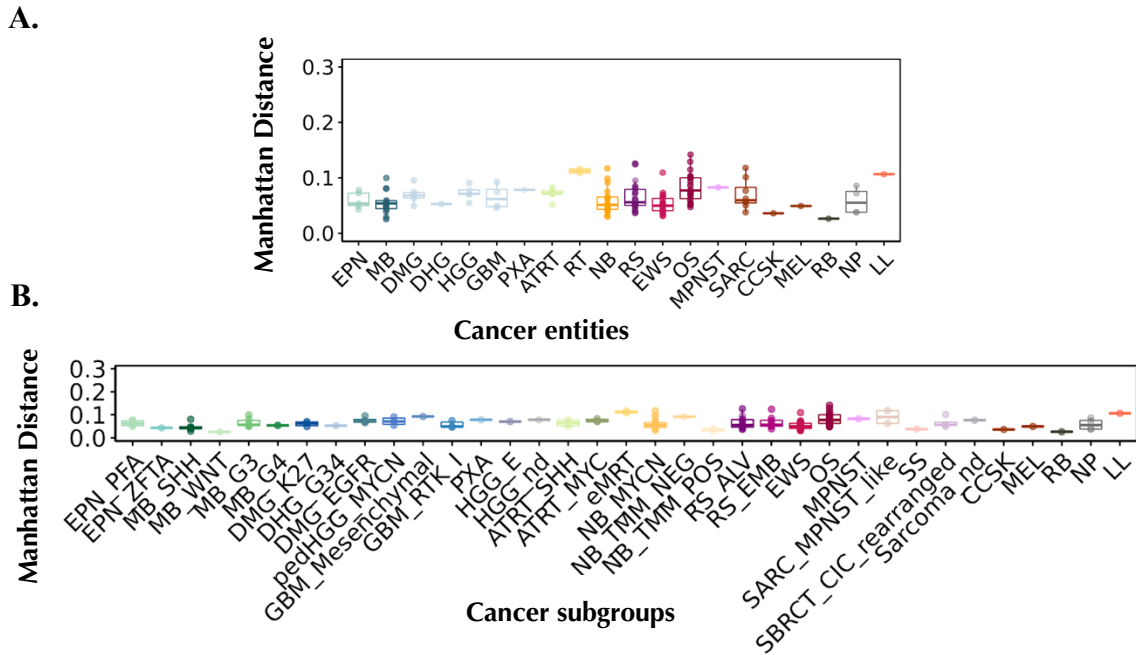


**Figure 15: Epigenomic correlation assessment of each subgroup**

A.) Manhattan distance score between PDX model and reference samples based on methylation profiling demonstrating consistent levels of similarity between the PDX and tumor epigenetic profiles across cancer entities. B.) Manhattan distance scores across the various cancer subgroups. The scores showed high similarity overall for the PDX and corresponding tumor pairs.

To assess the epigenomic correlation between the PDX models and the corresponding patient tumor from which they were derived, the similarity index for these pairs (n=136) was calculated by an industry project collaborator at the oncology department at Bayer (Berlin, Germany) Dr. Justyna Wierzbinska. The Manhattan distance was calculated for each PDX-tumor pair (Figure 15A and 15B), revealing a consistently high level of similarity overall (98% of PDX models having a distance of <0.1 to the corresponding tumor sample). This indicated that the PDX models possess the capability to accurately replicate the epigenetic profiles observed in the human tumors. However, certain entities and molecular subgroups such as RT, NB, ES, OS, sarcoma\_MPNST\_like, exhibited greater variability in the similarity values.

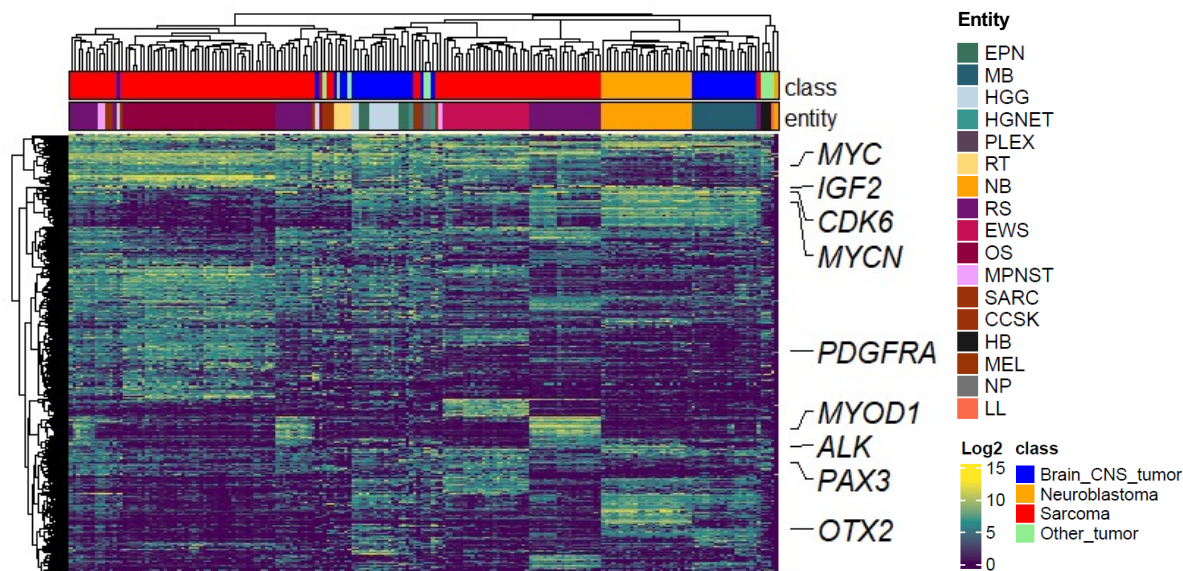


**Figure 16: Analysis of PDX cohort transcriptomic profile**

Unsupervised hierarchical clustering heatmap, based on gene expression profiles derived from the RNA-sequencing data. ITCC-P4 PDX cohort displayed clustering of PDX models (columns) into their respective tumor class and subgroup entities of high-risk pediatric cancers. Samples are colored based on their defined molecular subgroup. The relative intensity of gene expression regulation is depicted in the heatmap. The listed genes, *MYC*, *IGF2*, *CDK6*, *MYCN*, *PDGFRA*, *MYOD1*, *ALK*, *PAX3*, *OTX2* were observed to be upregulated in different subgroup types. (Analysis performed by Dr. Aniello Federico)

Subsequently, the analysis of PDX and tumor transcriptome data was performed, with a specific emphasis on grouping samples according to their similarity in gene expression patterns. By performing unsupervised hierarchical clustering of PDX models based on their gene expression data (utilizing the top 1000 variable genes), we observed a tendency for the models to cluster together based on their respective tumor types. Notable the co-clustering of PDX models was predominantly influenced by the expression levels of tumor biomarkers such as *MYCN*, *ALK* (upregulated in neuroblastoma); *MYOD1*, *FGFR1* (expressed in RS) that are known to be differentially deregulated in pediatric solid tumors (Figure 16). When comparing human tumor samples to PDX tumor samples based on differentially expressed genes we observed a consistent preservation of the tumor-core signature. As expected, PDXs derived from brain/CNS or sarcoma/other tumors indicated a significantly lower expression of gene signatures indicative of the lack of tumor microenvironment (immune and stromal cells). We observed a common set of downregulated genes in both brain and extracranial PDXs (“PDX\_DOWN”), which exhibited enrichment in the tumor samples of our cohort. The enrichment levels were higher in Osteosarcoma (OS) and high-grade glioma (HGG) tumors, while medulloblastoma (MB) tumors showed a lower level of enrichment score. These findings align with previous reports [195], [235] and are consistent with tumor

purity scores calculated using DNA methylation and RNA-sequencing data for both PDX and tumor samples.

Collectively, our findings derived from epigenetic and transcriptomic data indicate that the ITCC-P4 PDX models effectively represent the primary molecular features of pediatric malignant tumors. This includes the accurate representation of well-defined and clinically significant molecular subtypes, with a high degree of similarity observed between PDX models and corresponding human tumors. The molecular disparity observed between tumors and PDXs can be attributed in many cases to variations in cellular composition, primarily resulting from absence of human stromal and immune components in the PDX models.

### **3.1.3 Genomic landscape of pediatric solid tumors**

To identify the most suitable PDX models for preclinical studies, it is crucial to have a comprehensive understanding of the mutation patterns associated with disease relevant oncogenes and tumor suppressor genes. This consideration also remains significant especially when considering the molecular subgroups of the patient tumors. Therefore, we performed a comprehensive genomic analysis of the ITCC-P4 PDX mutational landscape. Models were examined using whole exome (WES) (n=236), low coverage whole genome (WGS) (n=186), RNA sequencing data (RNA) (n=210) and if available, also the matching patient tumor (n=219). As matching germline controls were not available for 90 of the 251 PDX models for sequencing, the comprehensive calling of somatic variants was performed using the ‘No-control workflow’ (Methods chapter, 2.2.2) and the copy number alterations were inferred based on the methylation arrays. Variants with a variant allele frequency of lower than 0.1% in the population were excluded and cancer genes that exhibited recurrent mutations in the specific tumor types based on previous sequencing studies, were highlighted as potential driver genes. To mitigate the risk of false positive mutation calls caused by mouse DNA contamination, we performed sequencing read alignment against a merged human and mouse reference genome. Any reads which mapped to the mouse genome were subsequently excluded from further analysis. To prioritize a set of functional and clinically relevant driver genes per entity and subgroup we referred to an annotated list from the 2022 WHO classification [224] and a previously published precision medicine review [225]. Overall, we investigated the single nucleotide variants (SNVs), small insertions/deletions (indels), structural variations (SV), copy number variations (CNVs) and gene fusion events. The comprehensive report detailing annotated variants for each model is available on our public platform ITCC-P4 data scope in R2 ([r2-itccp4.amc.nl](https://r2-itccp4.amc.nl)).

The total number of somatic mutations, known as the tumor mutational burden (TMB) [236] was measured in the PDX models and the patient tumor samples. We did not observe a significant difference between PDXs and human tumors. However, comparing TMB across disease states, a slight increase in mutations per mega base (Mb) was detected in human distal metastasis compared to the primary tumors, relapse tumors and those tumors under treatment (Figure 17A-B).

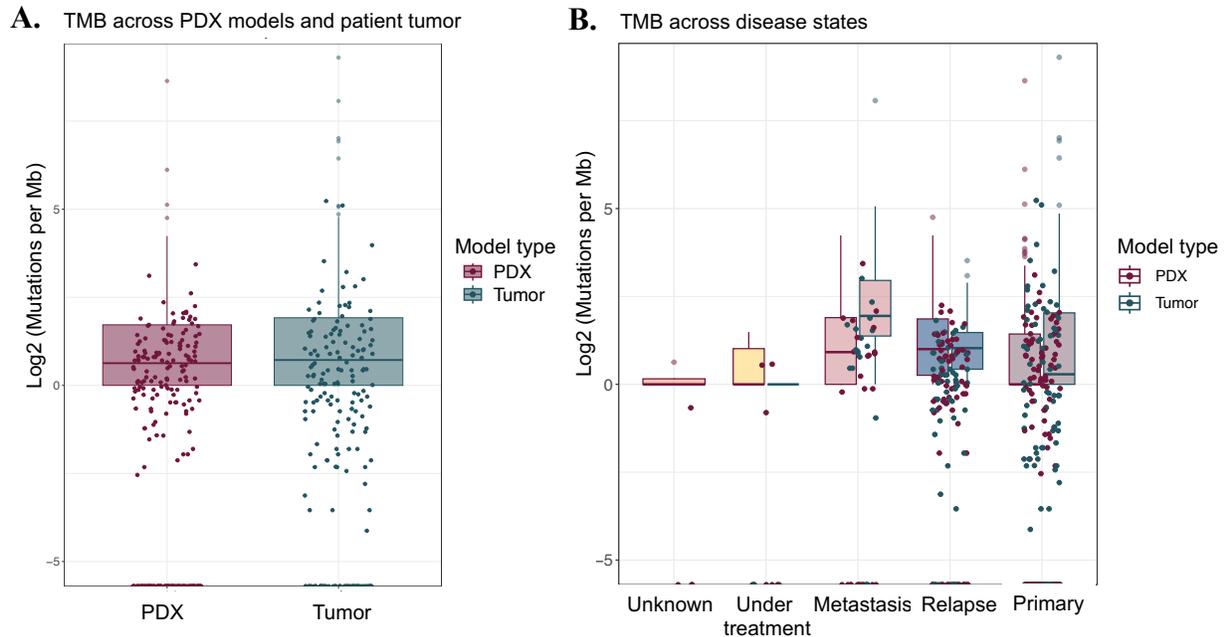


**Figure 17: Tumor mutational burden across PDX and tumor**

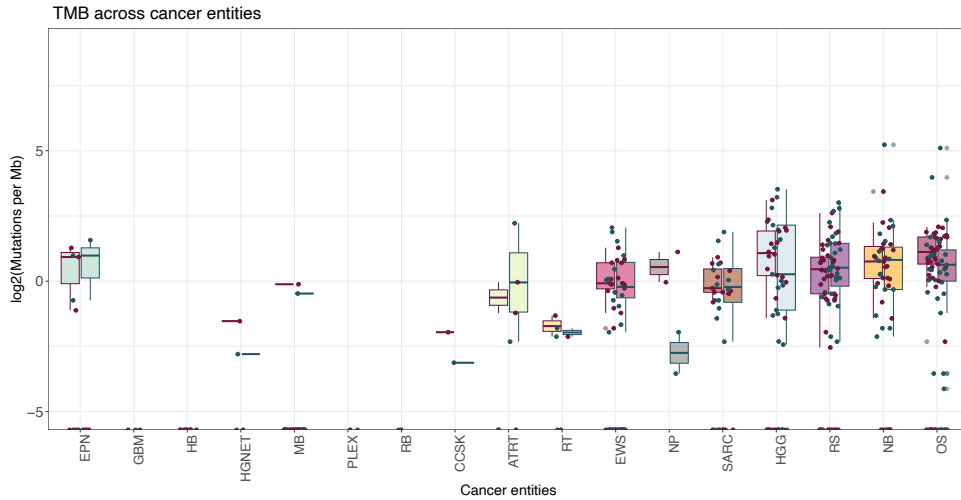
A.) Tumor mutational burden (TMB) across PDX and tumor models showing comparable coding mutations in both the sample types. B.) TMB comparison across disease states showing metastasis tumors having a slightly higher mutation load as compared to primary, relapse or models under treatment.

When comparing the various subgroups, we observed that majority of the cancer entities displayed a comparable tumor mutational burden between PDXs and tumors. However, Osteosarcomas known for their highly unstable genome, displayed a higher difference in the TMB between the tumor and PDX pairs. This was followed by Neuroblastoma, rhabdomyosarcoma and high-grade glioma models (Figure 18A). The neuroblastoma *MYCN* amplified tumors had higher TMB coding mutations per mega base. On further looking into the TMB of different subgroups of the entities, we observed that the high-grade glioma subgroups DMG\_EGFR, DMG\_K27 and pedHGG\_A showed a higher variance in TMB between PDX and tumor (Figure 18B).

To prioritize clinically relevant and functionally targetable variants, I curated a shorter list of entity-specific driver genes, based on their involvement in tumorigenesis from the 2022 WHO classification[224] and a review by Jones et al.[237]. The following observations are based on these results and a full report of the annotated variants for each model is available on our public platform ITCC-P4 data scope in R2.

([https://hgserver3.amc.nl/cgi-bin/r2/main.cgi?dscope=ITCCP4&option=about\\_dscope](https://hgserver3.amc.nl/cgi-bin/r2/main.cgi?dscope=ITCCP4&option=about_dscope))

**A.**



**B.** TMB across cancer entities

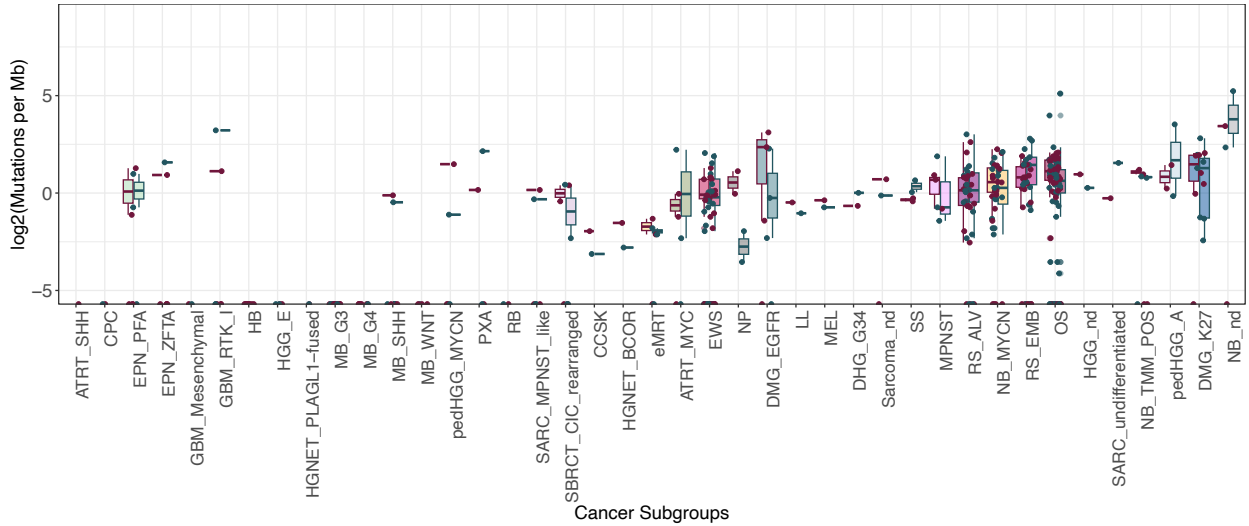


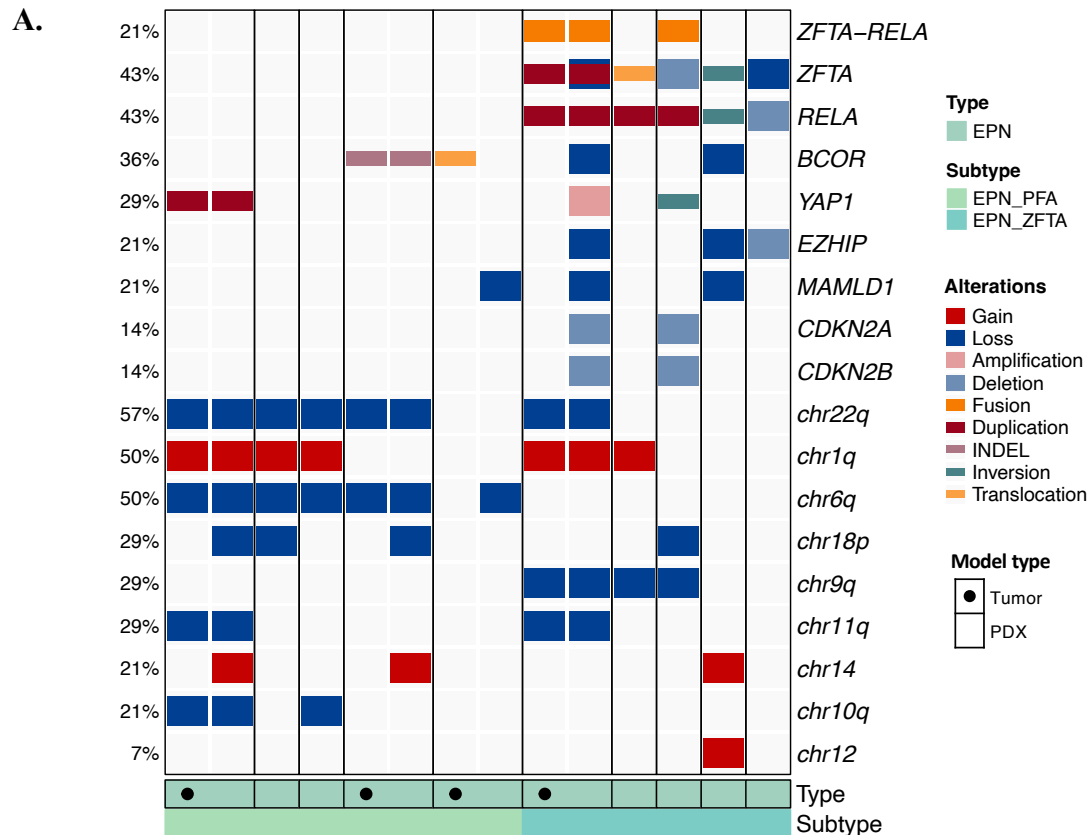
**Figure 18: Tumor mutational burden across cancer types and subtypes**

A.)  $\log_2$  scaled TMB (mutations per megabase) in the Y-axis across the cancer entities (X-axis). Although the TMB was comparable between tumor and their subgroups, the highest mean PDX TMB was identified in neuroblastoma and rhabdomyosarcoma. B.)  $\log_2$  scaled TMB (mutations per megabase) in the Y-axis across the cancer subgroups. The brain tumor subgroups DMG\_K27 and pedHGG\_A showed highest TMB across the subgroups.

## Central nervous system (CNS) tumor and rhabdoid tumor PDX models

The mutational landscape of the PDX model cohort along with the patient tumor samples were analysed and key oncogenic drivers were detected across the different cancer entities. The PDX models derived from pediatric brain and central nervous system malignancies exhibited frequent recurrent mutations that corresponded to their specific tumor type and the predicted molecular subtypes as determined by DNA methylation profiling.

Among the ependymoma (EPN) PDXs (n=10), we observed frequent structural alterations and/or fusion events in the following genes: *RELA* (2/10 models), *C11orf95/ZFTA* (5/10 models)[238], *CXorf67/EZHIP* (3/10 models), *CDKN2A/B* (2/10 models) and *YAP1* (3/10 models). All models with these mutations were classified as supratentorial ependymoma with *ZFTA-RELA* fusions. PDX models *BCOR* indel and focal loss (3/10 models) were detected in addition to models with *MAMLD1* focal loss (3/10 models) in two ependymoma subtypes present in our cohort, the supratentorial *ZFTA-RELA* fused and posterior fossa A (PFA)[239]. Copy number variations analysis revealed several cases with characteristic CNVs associated with high-risk ependymomas such as chromosome 1q gain (5/10 models), chr6p loss (5/10 models, exclusive for PFA ependymomas[240]), chr18p loss (4/10 models) and chr22q loss (4/10 models)[241] (Figure 19A)



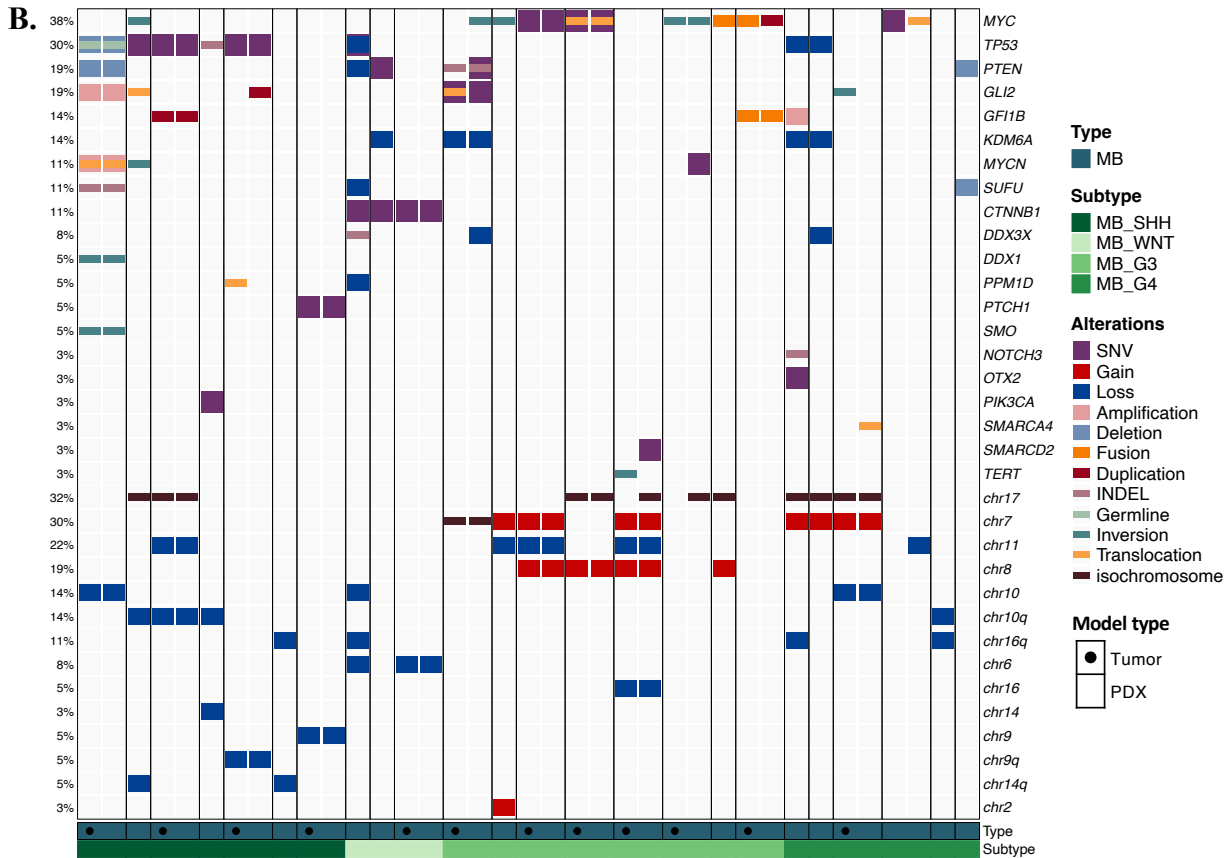


**Figure 19: Mutational landscape of Ependymoma and Medulloblastoma**

A.) Mutational landscape of Ependymomas showed classical ZFTA-RELA fusions, RELA CNV alterations and ZFTA mutations in the EPN\_ZFTA subgroup. Copy number loss in chr22a, 6q and 9q were observed mostly in the EPN\_PFA subgroup and gains in chr1q, chr 12 and chr 14.

B.) Mutational landscape of MB across various subgroups. MB-SHH samples showed somatic TP53 alterations as SNV, indel or copy number losses. One sample displayed a germline TP53 in the PDX and tumor. Two samples showed isochromosome17. The MB-WNT samples all had CTNNB1 SNVs, some samples showed losses in TP53, KDM6A, PPM1D, chr16q, chr6, chr9. MB-G3 samples displayed alterations in MYC, TERT, SMARCD2, isochromosome17, gains in chr 7 and losses in chr11 and chr16. MB-G4 samples displayed alterations in MYC, SUFU, PTEN, TP53, DDX3X. Loss of chr7 and gains of chr 11, chr 10q, chr 16q and chr10 were observed.

The mutational landscape observed in the 24 medulloblastoma (MB) models (Figure 19B) exhibited a high degree of heterogeneity, revealing subgroup specific variants. MYC amplification was predominantly observed in MB group 3 (MB G3) models, with 5 out of 7 MB models carrying this amplification. Conversely, 5 out of 7 MB SHH subgroup models displayed the prototypic TP53 mutations, including one germline TP53 mutation for the sample with available germline control. Other gene variants specific to MB SHH subgroup included GLI2 (3/24 models), PTCH1 (1/24) and SMO (1/24 models). KDM6A loss was only detected in MB group 3/4 which aligns with previous findings[242], [243]. Several recurrent copy number variations associated with medulloblastoma were also

identified, such as isochromosome 17 (9/24 models), chromosome 7 gain (6/24 models) and chr 8 gain (4/24 models) exclusively in MB G3/4 models as well as chromosome 6 loss (2/24 models) in MB WNT cases and losses in chromosome 11 (5/24 models), 10q (5/24 models) and 16q (4/24 models).

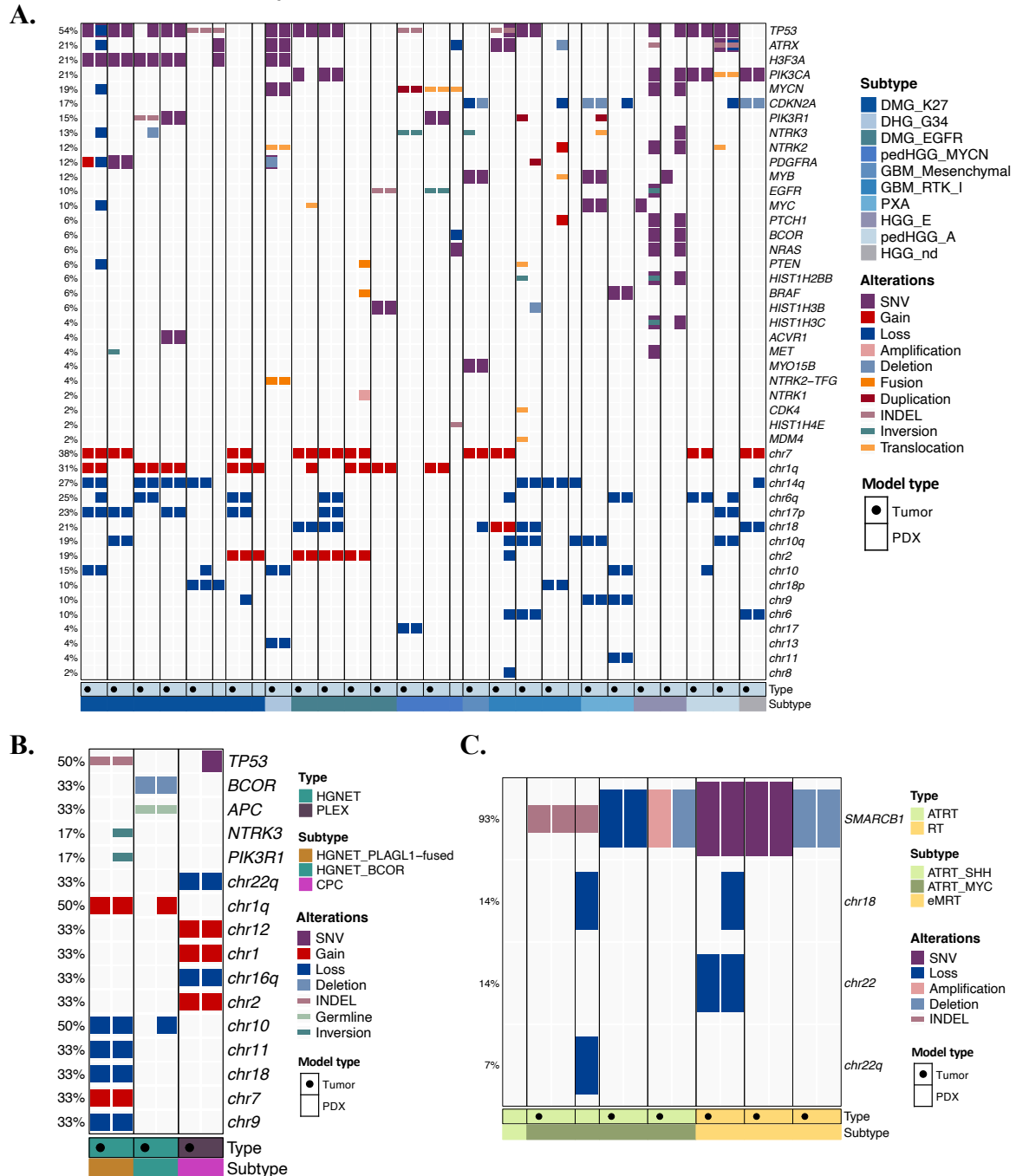


**Figure 20: Mutational landscape of High-grade glioma, HGNET-PLEX and AT/RT**

A.) HGG samples displayed characteristic somatic SNV alterations in *TP53*, *ATRX*, *MYCN*, *PIK3CA*, *MYB*, *CDKN2A*. The most prominent chromosomal gains were *chr7*, *chr 1q* and *chr2*. Losses of *chr 10q*, *chr 6q*, *chr10*, *chr 14q*, *chr 17p*, *chr 6* were observed.

B.) HGNET tumors showed mutations in *TP53*, *APC* and *BCOR*. Along with loss of chr 10, chr 11, chr 18, chr 9 and gain of chr 7. The PLEX sample had a *TP53* mutation in the PDX model and not in the patient tumor and concurrent chromosomal losses in chr 22q, chr 16q and gain of chr 12, chr 1 and chr 2 was observed.

C.) AT/RT subgroups all showed defining *SMARCB1* mutations and loss in chr 16 and chr 22.

In our cohort, pediatric high-grade glioma (HGG) encompassed a heterogeneous assortment of tumors including diffuse midline gliomas (n=10), H3-/IDH- wildtype gliomas (n=8), IDH-wild type glioblastoma (n=5), pleomorphic xanthoastrocytoma (n=2) and G34-mutant hemispheric glioma (n=1). The most frequently mutated gene within the HGG models was *TP53* (16/28), predominantly found in DMG H3 K27-altered models. Additionally, mutations were identified in *ATRX* (8/28 models), *H3F3A* (7/28 models, commonly observed in DMG H3 K27-altered PDX models), *MYC* (7/28 models, exclusive to H3-/IDH-wildtype gliomas) and *CDKN2A* (6/28 models). Recurrent mutations affecting signalling pathway effectors such as *BRAF*, *NRAS*, *PIK3CA*, *PTEN*, *EGFR* and *MYB*, as well as structural variations involving (CNV) level, the majority of DMG models exhibited whole chromosome 7 gain (10/28 models) and chromosome 1q gain (8/28 models), while losses of chromosome 6q (7/28 models) and 10q (7/28 models) were also observed in other glioma subgroups [116], [244], [245] Figure 20A).

The brain tumor cohort included two CNS embryonal tumors known as high-grade neuroepithelial tumors (HGNETs) Based on their DNA methylation classification, one of these tumors (EP0077) was annotated as HGNET with *BCOR* exon 15 internal tandem duplication, which was confirmed by the identification of *BCOR* structural variation. Additionally, an *APC* germline variant was identified in this PDX model and in the matching patient tumor. The second tumor (HG0080) was classified as HGNET *PLAG1*-fused based on methylation data, although no fusion events involving the *PLAG1* gene were observed possibly due to low tumor purity. Instead, PDX HG0080 and matching tumor exhibited structural rearrangements affecting *NTRK3* and *PIK3R1*, along with a *TP53* mutation. The XT0556 PDX model originated from a patient diagnosed with choroid plexus carcinoma (CPC) associated with Li-Fraumeni syndrome. The molecular characterization of this PDX model confirmed its classification as CPC based on the methylation profile analysis and the detection of *TP53* mutation. Typical chromosomal alterations, including chromosome 1 gain and multiple chromosomal imbalances were also observed in this model (Figure 20B).

PDX models derived from CNS atypical teratoid/rhabdoid tumors (AT/RTs, n=6) and extracranial malignant rhabdoid tumors (eMRTs, n=3) showed few genetic alterations, primarily involving the *SMARCB1* gene, SNV alterations in 2/9 models, indel mutations in 2/9 models, along with copy number losses in 2/9 models. Additionally, we also observed chromosome 22q deletions in a subset of cases 2/9, which aligns with the expected genetic profiles of these tumor types (Figure 20C).

## Neuroblastoma PDX models

Neuroblastoma (NB), one of the most common solid tumors in children [246], was well represented in this ITCC-P4 study, featuring a diverse group of PDX models consisting of 28 genetically heterogeneous samples [247]. The majority of the analyzed PDXs (17/28 models) exhibited *MYCN* alterations, most commonly observed as a focal gene amplification. Furthermore, frequent neuroblastoma-associated driver mutations affecting *ALK*, *ATRX*, *CDKN2A/B* and *DDX1* [248][249] were also identified with 11, 10, 9 and 6 out of the 28 models respectively. Notably, *BRAF*, *TP53* and *NF1* mutations were present in certain NB PDXs. The copy number variation analysis revealed a significant number of cytogenic aberrations. Particularly in *MYCN*-amplified NB models, the most prevalent CNVs included chromosome 17q gain (15/28 models), chromosome 1p loss (14/28 models) [250] and chromosome 3p loss (8/28 models). Additionally, CNVs associated with aggressive disease and poor prognosis [166], [167], such as chromosome 1q gain (7/28 models) and 11q gain (9/28 models) were also observed (Figure 21).

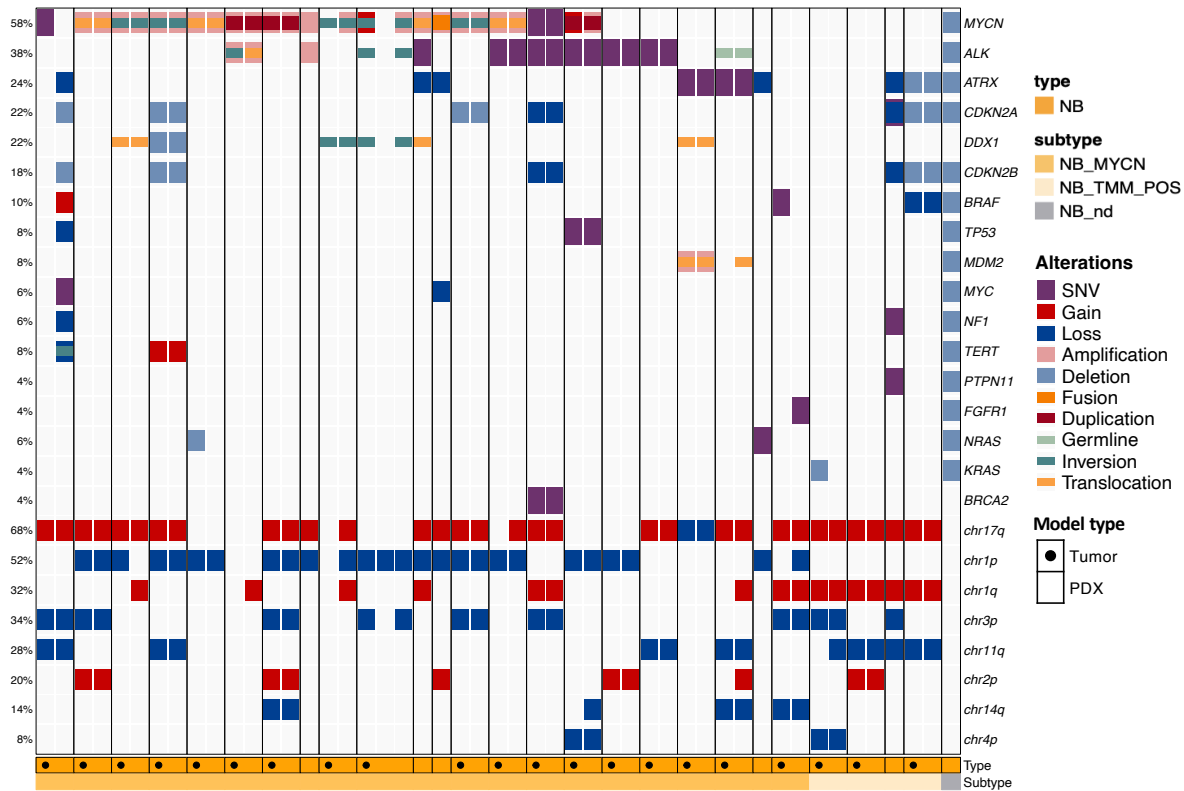


**Figure 21: Mutational landscape of Neuroblastoma**

Neuroblastoma samples represented mainly *MYCN* driven alterations followed by *ALK*, *ATRX* and loss of *CDKN2A*, *CKDN2B* in most samples. Mutations in *BRAF*, *DDX1*, *MYC*, *NF1* *TP53* were also observed. Chromosomal gain of *chr1q* was most predominant followed by gain of *chr7*, *chr 14q* loss, *10q* gains, *chr18* gains.

### STS/Bone sarcoma PDX models

Pediatric sarcomas exhibit a diverse and intricate mutational landscape that varies across different sarcoma types. Our cohort of patient-derived xenograft (PDX) models accurately recapitulates the specific mutations including structural variations and gene fusions that are known to drive tumorigenesis in various sarcoma types and subtypes.

Among the large group of rhabdomyosarcomas (RS) PDX models (n=41), a clear distinction was observed. In cases with available RNA-seq data, 19/41 models exhibited the classical *PAX3-FOXO1* fusion, a key alteration associated with the alveolar subgroup. This subgroup classification was also confirmed by the DNA-methylation classification. 17/41 PDX models harboured mutations in *TP53*, 10/41 models showed a *CDKN2A* deletion and 4/41 showed an *NRAS* mutation, which were more commonly linked to embryonal rhabdomyosarcoma. 5/41 models showed an *MYOD1* fusion and an indel alteration in one model. Our findings also revealed a high recurrence of *BCOR* mutations in 8/41 models, *NCOA2* gain in 9/41 models *CDK4* gain and SV alterations in 10/41 models and *NF1* structural rearrangements (Figure 22). The CNV profiles of these models showed a high prevalence of unbalanced CNVs, with numerous gains and losses affecting entire chromosome arms. Chromosome 8 gain, associated with embryonal rhabdomyosarcoma was detected in 16 models, 14 of which had confirmed embryonal subtype identity based on DNA-methylation classification. Among the most recurrent CNVs, the gain of whole chromosome 2 (17/41 models), chromosome 12 gain (18/41 models) and gain in chromosome 20 (18/41 models), as well as gain of 1q arm (10/41 models) and loss of entire chromosome 16 (8/41 models) was observed but did not show sub-type specific association.

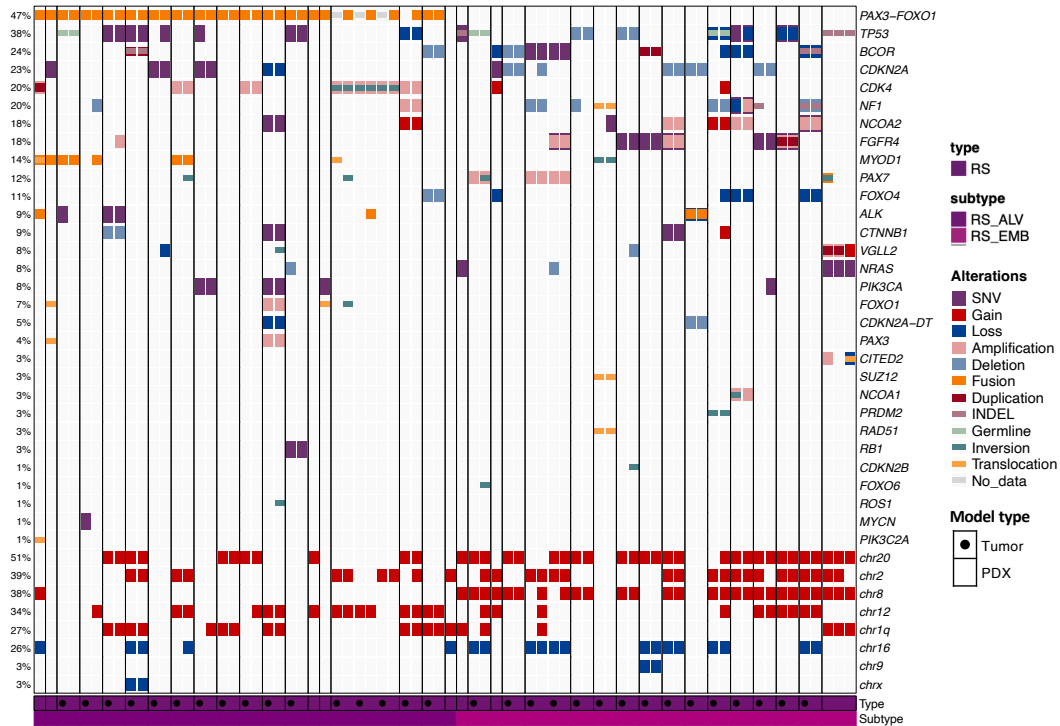


### Figure 22: Mutational landscape of Rhabdomyosarcoma

The Rhabdomyosarcoma samples showed distinct classical alterations based on their subgroups. RMS alveolar subgroup, contained the *PAX3-FOXO1* signature gene fusion, for all the samples that had RNA-sequencing information. For samples that didn't have this RNA-seq performed is marked as "no data". Mutations in *TP53*, *NCOA2*, *CDK4* along with chromosomal gain of chr 20, chr 2 and chr 1q was observed. In the RMS embryonal subgroup, the main drivers were *TP53*, *NCOA2*, *BCOR*, *CDKN2A*, *NF1*, *FGFR4*, *VGLL2*, *MYOD1*, *NRAS* and *NCOA1*. RMS\_EMB also displayed chromosomal gains in chr 20, chr2, chr 8m chr 12 and chr1q and loss in chr16.

Ewing sarcoma (EWS) PDX models (n=34) revealed the characteristic, disease defining fusion of the *EWSR1- and FLI1* genes observed in 67.7% (23 of 34 PDX) of the models. Additionally, rarer fusions involving *EWSR1* with genes such as *ERG* (4/34 models) and *FEV* (1/34 models) were observed. Mutations affecting genes associated with chromatin remodeling and DNA repair, such as *STAG2*, *ETS1*, and *TP53*, have been detected in a subset of EWS models. Consistent with findings in other pediatric tumor types, *CDKN2A* loss was identified in 12 EWS PDXs. Over 60% of the established EWS models exhibited the characteristic gain of the entire chromosome 8, while other known copy number variations (CNVs) associated with EWS, such as gain of chromosome 1q, gain of chromosome 12, and loss of chromosome 16q, were frequently observed within our cohort (Figure 23).

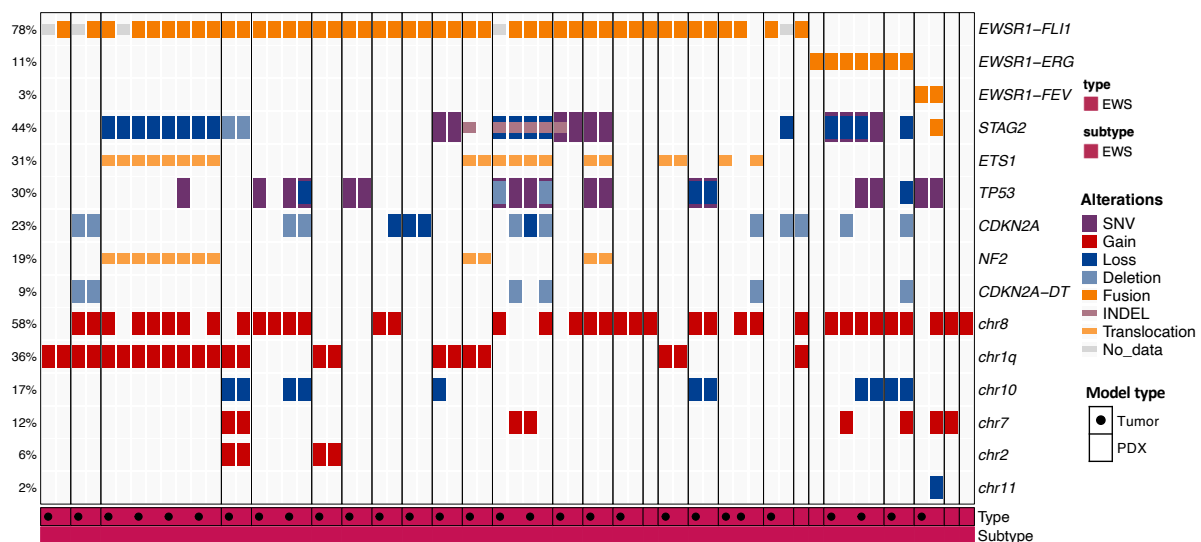


### Figure 23: Mutational landscape of Ewing sarcoma

Ewing sarcoma PDX and tumor models were highly concurrent in their genomic profiles as they showed the classic translocation resulting fusion *EWSR1-FLI1* fusion in 67.7% of the samples. Samples that did not have this fusion either displayed *EWSR1-ERG* or *EWSR1-FEV* fusions. Other commonly occurring alterations were observed in *STAG2*, *TP53*, *CDKN2A*, *NF2*, *ETS1* and gain of chr8, chr 1q, chr 7 and loss of chr 10.

The osteosarcoma (OS) models (n=43) demonstrated a comprehensive representation of the genetic complexity observed in human tumors, specifically characterized by the detection of numerous somatic variants, mainly CNVs, due their highly unstable genomes. Among the analyzed OS PDX subcohort (n=30/43), mutations in the tumor suppressor genes *TP53* and *RB1* were frequently observed, with *TP53* mutations detected in 30/43 models and *RB1* mutations detected in 25/43 models. Additionally, *ATRX* loss (10/43 models), *MYC* gain (11/43 models), *IGF1R* structural variations/copy number variations (11/43 models), *NF1* loss/structural variations (8/43 models), and *CDKN2A* loss/structural variations (10/43 models) were also observed in varying frequencies within the OS PDX models. The copy number variation (CNV) landscape of these models displayed a high degree of complexity, with each case exhibiting a unique pattern of CNV alterations. Notably, the most recurrent aberrations included gain of chromosome 8q and loss of chromosome 10 either full arm or single arm observed in multiple models (19/43 models) (Figure 24).

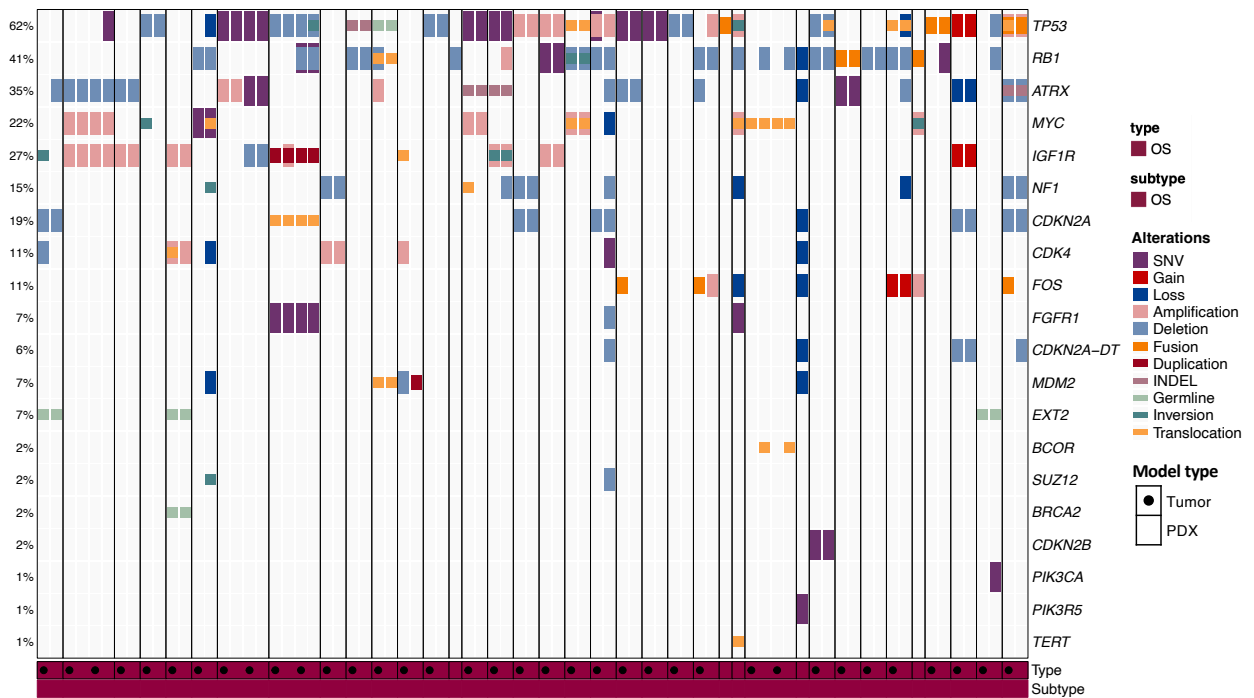


**Figure 24: Mutational landscape of Osteosarcoma**

Osteosarcoma is known for its highly unstable genome. Genomic alterations in *TP53*, *RB1* were commonly seen in majority of the samples, followed by *MYC* gains and *ATRX* losses. Mutations in *IGF1R*, *NF1*, *FGFR1*, *CDKN2A* losses, *FOS* gains and fusions. One sample also had a germline *BRCA2* mutation. Although the copy number profiles showed high chromosomal instability, with loss of chr10 and chrX commonly observed.

Additionally, PDX models were generated that represent rare sarcoma entities, including malignant peripheral nerve sheath tumors (MPNSTs), clear cell sarcoma of the kidney (CCSK), synovial sarcomas (SS), small-blue round-cell tumors (SBRTs), and undifferentiated sarcomas. These models exhibited similar alterations commonly observed in other sarcomas, such as *CKDN2A* loss, *MYC* gain, *NF1* loss, *TP53* mutations, and *BCOR* fusion events. Furthermore, we observed an enrichment of *CIC* rearrangements in SBRT models, while SS cases exhibited mutations affecting *SSX* family member genes. The most recurrent chromosome aberrations in MPNST PDXs included chr7 and chr8 gain, as well as losses in chr9p and 17p (Figure 25).

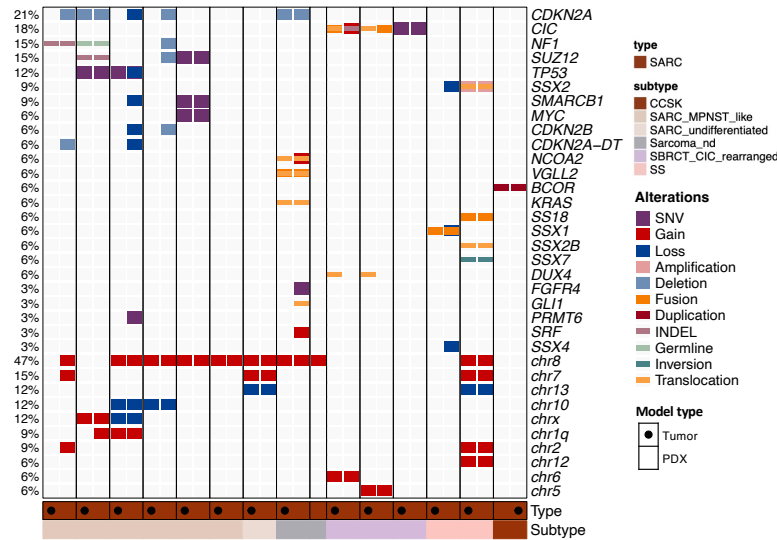


**Figure 25: Mutational landscape of additional SARC tumors**

A smaller group of SARC tumors consisted of malignant peripheral nerve sheath tumor, synovial sarcoma, small-blue round-cell tumors and undifferentiated sarcoma. They harbored mutations in *CDKN2A* losses, *CIC* rearrangements, *NF1* mutations, *SUZ12* and *SSX2* mutations.

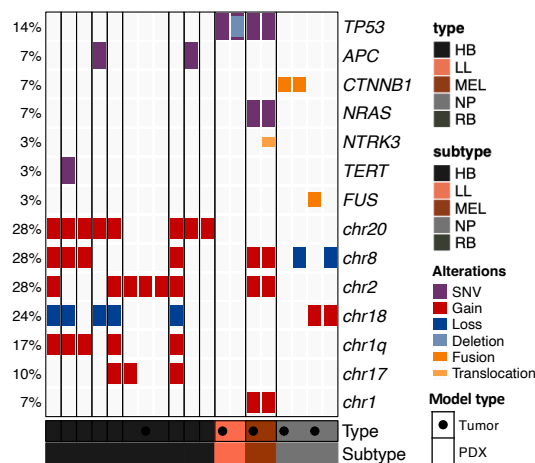


**Figure 26: Mutational landscape of other tumors**

Other tumors including Hepatoblastoma, melanoma, large cell lymphoma displayed *TP53*, *APC*, *CTNNB1*, *NRAS* mutations and gains in *chr20*, *chr2*, *chr18*, *chr1q*, *chr17* and loss in *chr18*.

### ***Other PDX models***

Finally, we also established PDX models encompassing a diverse range of extracranial and rare pediatric tumors. The hepatoblastoma (HB) PDXs (n=10) did not exhibit any recurrent driver gene alterations, but frequently displayed chromosome 1q and whole chromosome 20 gain, as well as chromosome 18 loss. The XT0676 model, derived from a pediatric melanoma (MEL) tumor, harbored *TP53* and *NRAS* mutations and exhibited chromosome 1q gain. Notably, chromosome 1q amplification was also observed in the RB0665 model (retinoblastoma, RB) and two out of three neuroblastoma (NP) PDX models, highlighting its recurrence among our PDX cohort. Additionally, the NP models displayed chromosome 5 and 7 gains in multiple cases. Lastly, the XT0681 model represented a large cell lymphoma (LL) case, characterized by *TP53* mutation, *ALK* fusion, chromosome 17q gain, and chromosome 11q loss (Figure 26).

### **3.1.4 Copy number landscape of ITCC-P4 PDX models**

We utilized the tool Sequenza [220], to investigate the overall copy number landscape of the study cohort (Figure 27), aiming to identify significant chromosomal abnormalities across various cancer entities. Within the ependyoma models, classical alterations were observed, including gains of chromosome 1q and losses of chromosome 22q, chromosome 6q, and chromosome 16q. Medulloblastoma models exhibited varying alterations, with a notable presence of the defining isodicentric chromosome 17q [251], [252]. Additionally, losses in chromosomes 10 and 11 were also observed. High-grade glioma models displayed gains and amplifications in chromosome 7 and 19q, while experiencing losses in chromosome 6q and chromosome 10q [253]. Neuroblastoma models were characterized by gains in 1q, 7, and 17q. Rhabdomyosarcomas frequently demonstrated chromosomal gains in chromosome 2, chromosome 8, and chromosome 12. The majority of Ewing sarcomas exhibited the common translocation resulting in the fusion of *EWSR1* with *FLI1*, while less frequent translocations involved other partner genes such as *FEV*, *ERG* and *ETV1*. Chromosomal instability is a distinctive characteristic of osteosarcoma [182] with multiple gains and losses leading to unstable genomes, this was observed within our models. Notably, there were losses of chromosome 10 and 13, along with defined gains in chromosome 8q and chromosome 17q [180], [183]. Finally, hepatoblastoma models displayed gains in chromosome 2 and chromosome 8, alongside losses in chromosome 4 and 16.

These copy number alterations identified within the ITCC-P4 pediatric cohort can function as prognostic indicators and have the potential to be linked to aggressive tumor behaviour, increased chances of metastasis, or resistance to personalized treatments. Hence enabling PDX model selection for further clinical studies.

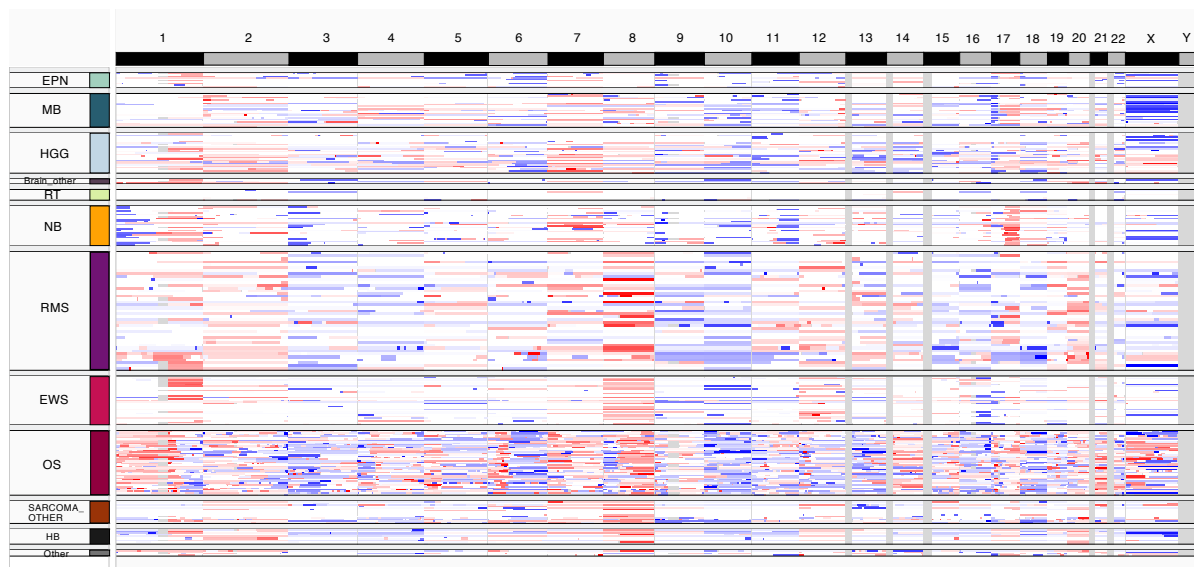


**Figure 27: Copy number landscape of ITCC-P4 PDX cohort (generated on IGV)**

Sequenza and ichorCNA results were both visualised on IGV. This overview of the copy number landscape generated from the Sequenza output, shows the overview of the ITCC-P4 PDX profiles grouped per tumor type. The blue colour defined chromosome losses and red colour signified amplifications. Ependymoma samples showed losses in chr 8, medulloblastoma samples displayed the distinct isodicentric chromosome 17q and amplification in chr 7. High grade glioma PDX showed high amplification of chromosome 7, deletions in chromosome 9, 10. Neuroblastoma samples exhibited recurrent alterations of chr 1p, chr3p and chr11q deletion. Gains in chr1q, chr 2p, chr 7 and chr17q. Rhabdomyosarcoma PDX models displayed gains in chr 2, chr8, chr12 and chr20 and losses in chr 9, chr 10. Ewing sarcoma samples displayed the classical EWSR1-FLI1 fusion causes by translocation of chr 22 and chr 11. Osteosarcoma samples displayed a highly unstable genome with chromothripsis occurring in majority of the samples.

### 3.1.5 PDX model fidelity compared to matching patient tumor

Tumor purity refers to the proportion of cancer cells in a tumor sample compared to non-cancerous cells[254], such as stromal or immune cells within the tumor microenvironment. As tumor purity decreases, there is a reduction in the proportion of reads carrying somatic mutations, resulting in a diminished signal that makes it more challenging to differentiate true somatic mutations from sequencing errors[255]. Therefore, to eliminate false positives a tool called ESTIMATE [229] was run on the available RNA sequencing data.

The ESTIMATE scores, ranging from -6000 to +6000, inversely correlated with tumor purity, where lower scores indicated higher purity[256]. After converting these scores to percentage values for more accurate estimation, we observed that PDX models consistently exhibited higher tumor purity, as expected (Figure 28A). The growth of the PDX tumor in mice leads to the out competition of normal non-cancerous cells, resulting in a higher proportion of cancer cells within the PDX sample. Consequently, the tumor purity is increased compared to the original patient tumor sample. Upon analysing PDX models within their different subgroups, we identified a range of purity percentages, with HGNET, melanomas, MB\_SHH, and Neuroblastoma displaying the highest median purity overall. This indicated lower stromal and immune cell infiltration into the tumor tissue (Figure 28B).

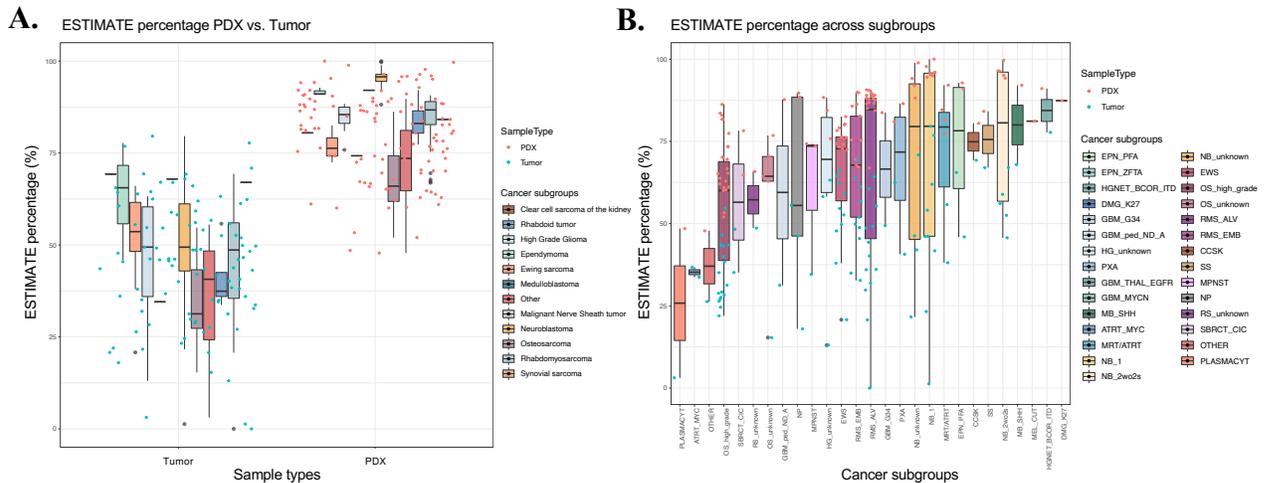


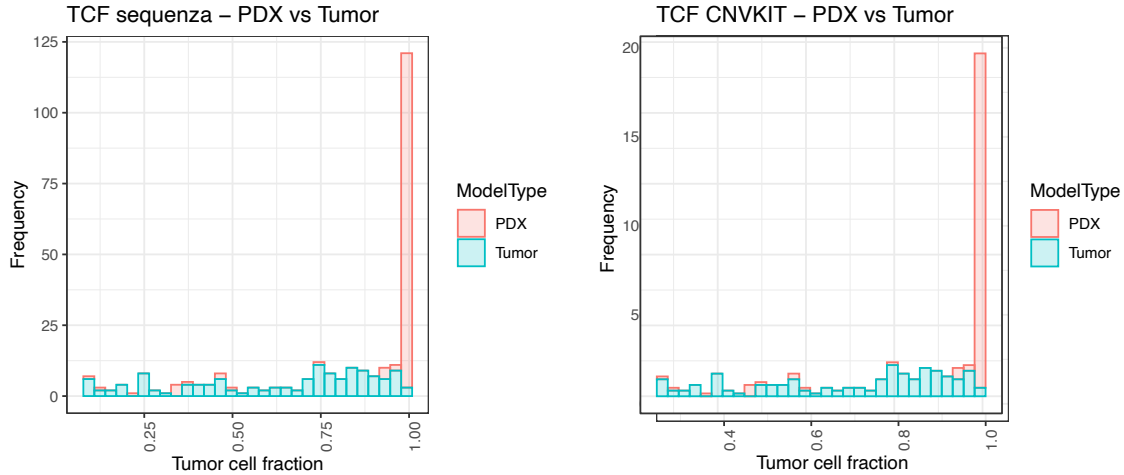
**Figure 28: Tumor cell purity between PDX and tumors**

A.) Tumor cell purity based on ESTIMATE scores applied to available RNAseq data, showed a lower overall ESTIMATE purity score for the PDX models (blue dots) compared to the patient tumor (red dots). This signifies higher tumor purity of the PDX models compared to the original tumor across main entities. B.) Overview of ESTIMATE scores across different cancer subgroups.

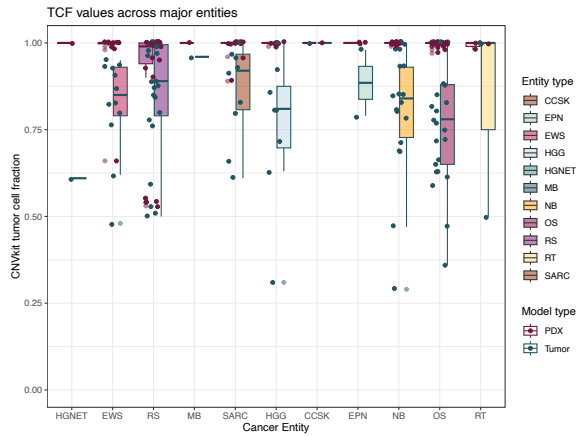
To account for the absence of RNA sequencing data from some samples, the tumor cell fraction (TCF) scores between Sequenza and CNVkit were compared to identify the most accurate tool to quantify TCF across PDX models and patient tumors. On comparing the

results and using 0.4 purity as a threshold, although both tools calculated a TCF of 1 for most PDX models, the Sequenza TCF scores for patient tumors exhibited a lower overall score, with a higher number of samples scoring below 0.4 TCF. In contrast, the CNVkit scores showed higher overall TCF values and less than 15 samples (30%) displaying values below 0.4 TCF. The higher TCF values calculated by CNVkit provided confirmation of its greater accuracy, thereby validating its use to correct variant allele frequency (VAF) scores for tumor purity (Figure 29A).

**A.**



**B.**



**C.**

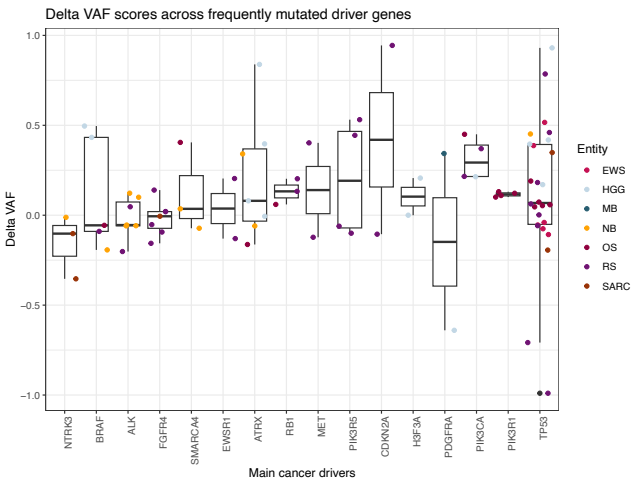


**Figure 29: Tumor cell fraction comparisons**

A.) TCF values generated from Sequenza and CNVkit to assess accuracy of the tool across patient tumor and PDX models. TCF values of the PDX models using both tools were 1, signifying high purity of the PDX models as expected. However, using 0.4 as an arbitrary purity cutoff, the tumor scores from Sequenza had higher number of samples below the cut off compared to CNVkit. Majority of the tumor TCF values from CNVkit were >0.4 and hence used for analysis. B) TCF values CNVkit divided across subgroups showing PDX score (maroon) had a high value of 1, while the tumor scores ranged from 0.25-1. C.) Difference in PDX and tumor TCF corrected VAF

*score was termed as Delta VAF. The main driver and frequently mutated genes per each main entity was identified to identity degree of clonal discordance between PDX and tumor.*

To assess the molecular fidelity of the PDX models compared to the patient tumor samples, we used TCF values to correct the somatic SNV VAF scores for all the samples with controls. The corrected and scaled CNVkit TCF scores were analyzed per subgroup and as expected the PDX TCF values for all the major entities were 1 (Figure 29 B). The difference in the TCF corrected VAF scores of the PDX models from the TCF corrected VAF scores of the patient tumor samples, enabled us to observe various degrees of clonal discordance between the pairs. This change in PDX and tumor VAF “delta-VAF” was used as a metric to identify models with overall higher mutually exclusive somatic SNVs in PDX models compared to patient tumor, across the 16 most frequently mutated driver genes and across different subgroups (Figure 29C).

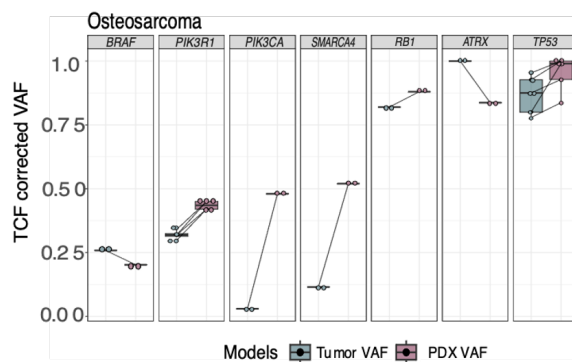
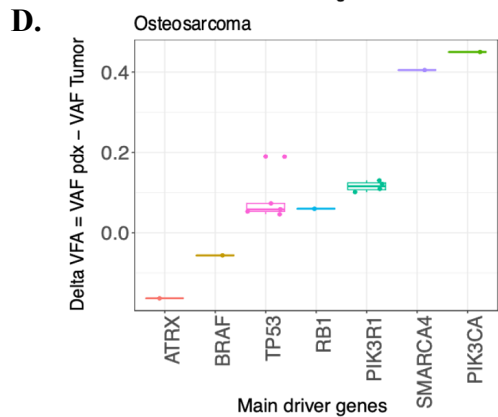
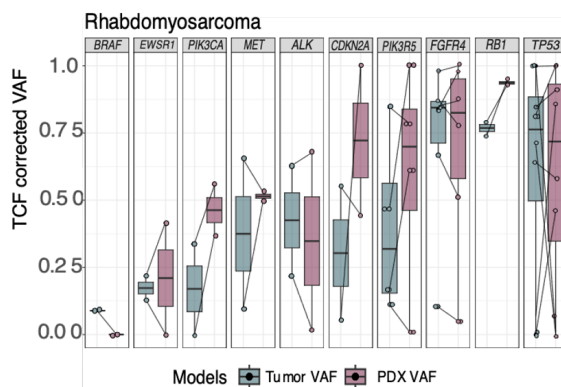
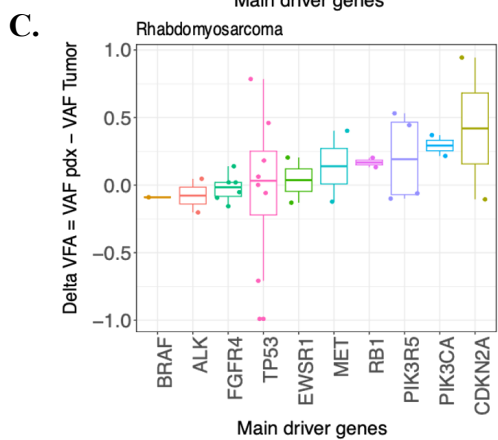
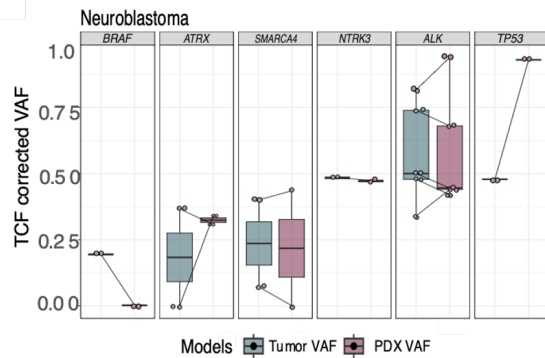
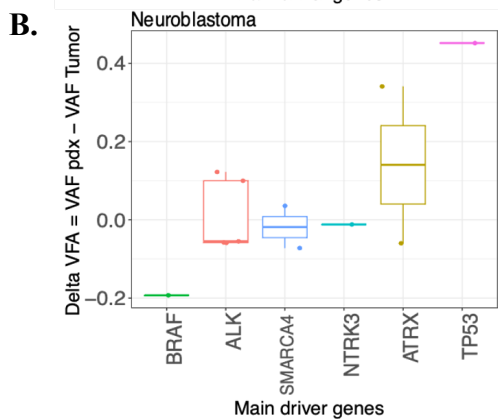
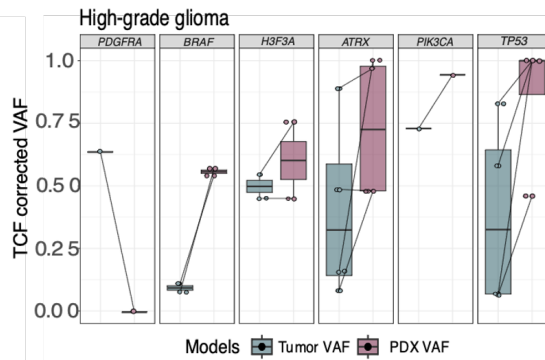
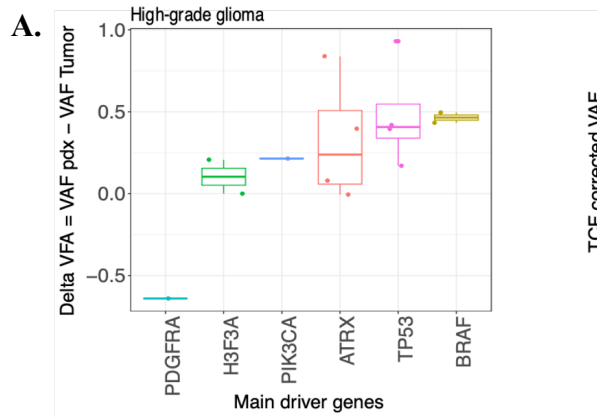


**Figure 30: Change in PDX and tumor variant allele frequency (delta-VAF)**

(left) DeltaVAF scores representing change in the TCF corrected PDX and tumor VAF scores was calculated for the most frequently mutated driver genes across main tumor entity. (right) TCF values for each frequently altered gene against PDX-tumor sample pairs, to identify exclusive somatic mutations in PDX or patient tumors, identifying high concordance or unique SNVs.

A.) High-grade glioma showed frequent somatic alterations *BRAF*, *TP53*, *ATRX*, *PIK3CA*, *H3F3A* and *PDGFRA*. (right) *PDGFRA* was observed exclusively in the Tumor sample of one sample and not in the PDX, while the other genes showed good concordance in PDX and tumors.

B.) Neuroblastoma showed frequent somatic alterations *BRAF*, *ATRX*, *SMARCB1*, *NTRK3*, *ALK* and *TP53*. (right) *BRAF* and *SMARCB1* were observed exclusively in the Tumor sample of one sample and not in the PDX, while the other genes showed good concordance in PDX and tumors.

C.) Rhabdomyosarcoma showed frequent somatic alterations *BRAF*, *EWSR1*, *PIK3CA*, *MET*, *ALK*, *CDKN2A*, *FGFR4*, *RB1* and *TP53*. (right) Mutually exclusive SNVs present in the tumor were observed in *TP53*, *PIK3CA* and *CDKN2A* for some samples, while the other genes showed good concordance in PDX and tumors.

D.) Osteosarcoma showed frequent somatic alterations *BRAF*, *PIKCR1*, *PIK3CA*, *SMARCB4*, *RB1*, *ATRX* and *TP53*. (right) *SMARCA4* and *PIK3CA* showed exclusive mutations in the PDX models while the other variants had good correlation with the tumor samples.

We then specifically focused on somatic SNV mutations found to be most frequently altered in our cohort and reporting any changes in the allele frequencies of these variants between tumor and matched PDX samples. The most frequently mutated driver genes for those entities with a larger sub-cohort size namely high-grade glioma, neuroblastoma, rhabdomyosarcoma, osteosarcoma was analysed. The delta-VAF scores for these variants indicated that, in most cases, shared somatic mutations also presented low changes in PDX/tumor ratios (delta-VAF scores ranging from -0.2 and 0.2). Alternatively, we identified distinct rises in variant allele frequencies within tumors (denoted as negative delta-VAF) or in the xenografts (indicated by positive delta-VAFs). Within the high-grade gliomas, as expected *PDGFRA*, *H3F3A*, *PIK3CA*, *ATRX*, *TP53* and *BRAF* genes were most recurrent[257]. *TP53* and *BRAF* PDX VAFs showed good comparison to their corresponding tumors. Conversely, *PDGFRA* mutation was solely observed within the human tumors, with no presence detected in the PDXs (Figure 30A). Neuroblastoma and Rhabdomyosarcoma showed a high overlap in variants between the PDX and tumors. However, *BRAF* and *SMARCB1* were observed to be exclusively expressed in the tumor models in the NB models (Figure 30B). Exceptions of mutually exclusive detections involving *TP53*, *PIK3CA* and *CDKN2A* in the patient tumor (Figure 30C). Significant changes in mutation frequencies favouring the PDX models were also observed in osteosarcoma models involving *SMARCA4* and *PIK3CA* SNVs (Figure 30D).

To investigate the somatic sub-clonal SNV events between PDX models and patient tumor samples, the TCF corrected variant allele frequency for those samples with germline controls was analysed further. Within the major entity groups, the VAF scores were calculated per sample to identify interesting subclones and to see how well the

PDX correlated with the respective tumor. For the brain tumors (Figure 31), the high-grade glioma models, we observed overlapping SNVs in 5/8 samples signifying good overall correlation between PDX models and tumor. As expected, we observed samples with *TP53*, *ATRX*, *BRAF*, *H3F3A*, *TERT*, *PDGFRA* and *PIK3CA* somatic SNV mutations. In sample HG0230 the shared *PIK3CA* has a VAF score of 0.9 in the PDX while the tumor displays a VAF score of 0.8. Sample HG0349 shows an interesting *TP53* nonsynonymous mutation with a VAF of 1 in the PDX but 0.11 in the tumor sample, the shared frameshift-deletion *ATRX* mutation in the PDX and tumor sample both showed a VAF of 0.5. However, the stop-gain *ATRX* mutation in sample HG0354 although shared between the PDX and tumor, had a VAF of 1 in the PDX model, while only 0.2 in the tumor sample. Hence, this subclonal selection within the PDX model would be an interesting targetable biomarker. HG0355 and HG0356 both showed a shared *BRAF* mutation between both their respective PDX models and tumor. HG0245 seemed to be a highly correlating sample with majority shared SNVs including *MYCN*, *HGF3A*. Shared *TP53* and *ATRX* both displayed high VAF of 1 and 0.9 respectively. However, a nonsynonymous *PDGFRA* with a VAF of 0.6 was seen to be mutually exclusive within the tumor sample and was not selected within the PDX model. HG0533 displayed several exclusive SNVs only within the PDX and only very few shared SNVs including *TP53* and *H3F3A*.

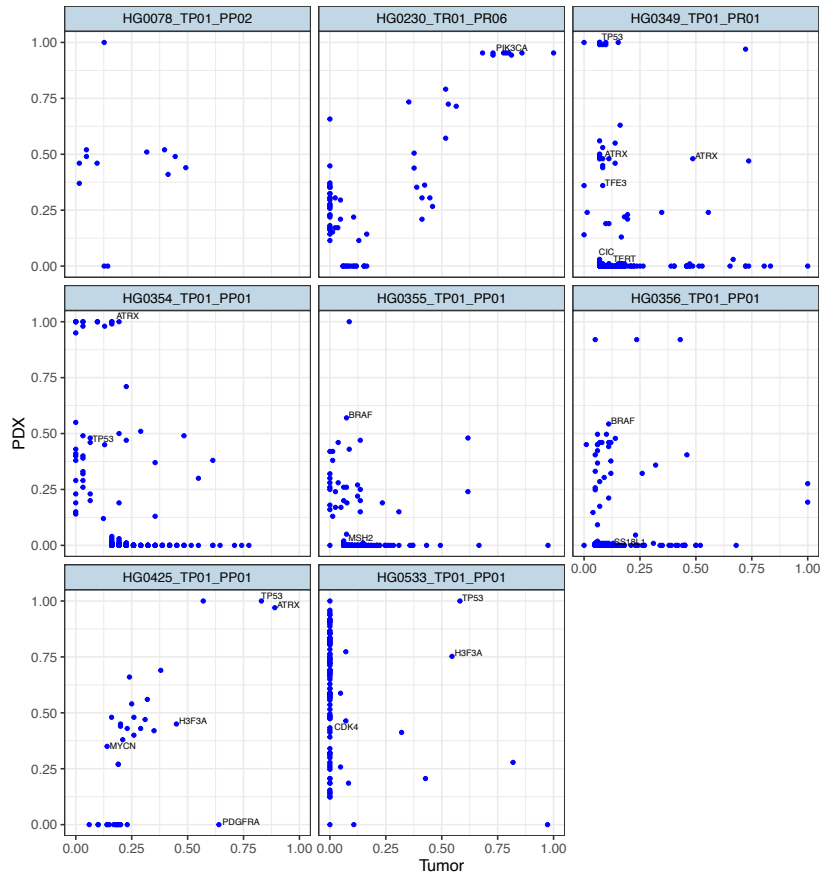


**Figure 31: VAF plot for high-grade glioma samples**

VAF score of PDX (y-axis) and tumor (x-axis) to show significant driver SNVs and identify novel subclones. There was an overall good correlation for the sample with hares SNVs, however some samples HG0349 and HG0345 showed higher TP53 and ATRX VAF scores respectively in the PDX models than tumor. HG0425 showed TP53 and ATRX somatic SNVs shared with a high VAF score in both PDX and tumor samples, however showed a distinct PDGFRA somatic SNV only present in the tumor sample, which seems to be lost in the PDX.

Ewing sarcoma samples showed high somatic correlation. Sample ES0202 was a serial case containing PDX models from primary patient (PP) and relapsed patient (PR) tumor. On comparing the PDX and tumor, we observed a TP53 mutation exclusive to the tumor, in both the primary and relapsed model. Interestingly, the relapsed PDX model showed a TP53 mutation with VAF of 1.0 in the model, while not being present in the primary PDX. This subclone was seemingly selected exclusively within the relapsed patient sample. Sample ES0312 showed a nonsynonymous IGF1R mutation with a VAF of 0.2 only in the tumor sample and not within the PDX model (Figure 32).

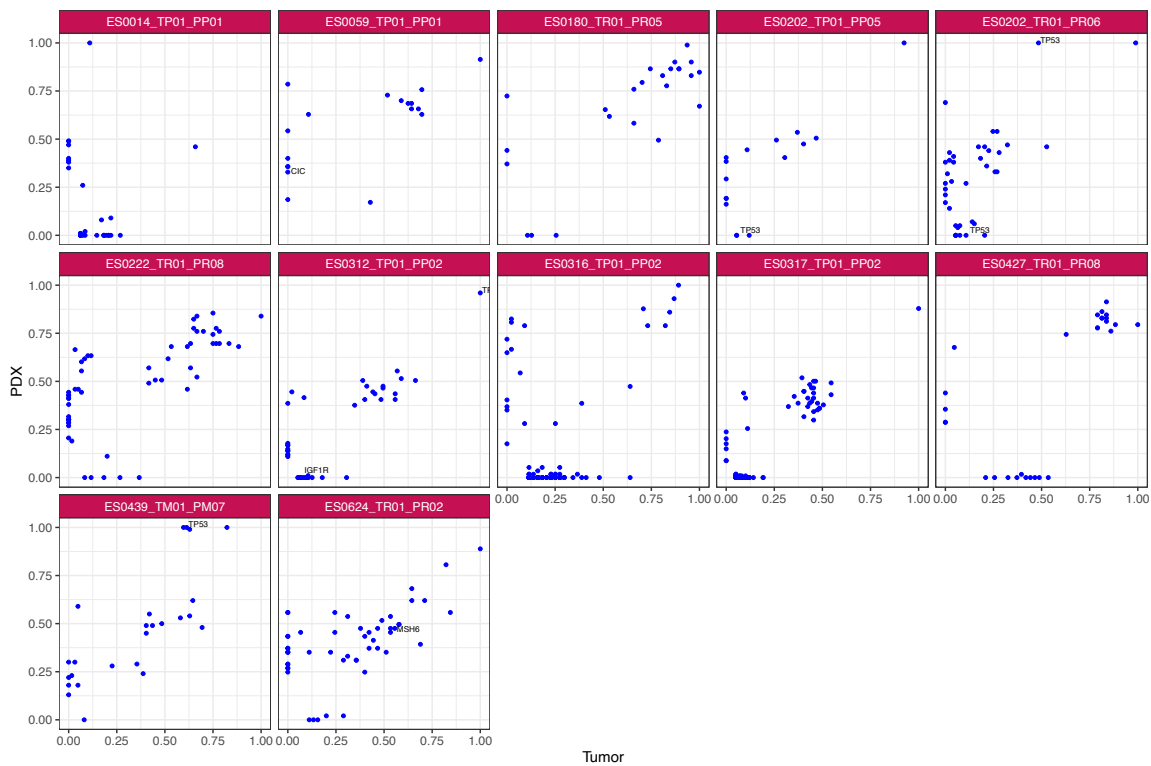


**Figure 32: VAF plot for Ewing sarcoma samples**

Ewing sarcoma samples showed overall highly concordant somatic profile of the PDX and tumor models. However, some cases ES0202 and ES0312 showed mutually exclusive SNVs of TP53 and IGF1R in only the tumor samples respectively. Other shared mutations in TP53 and MSH6 were also observed.

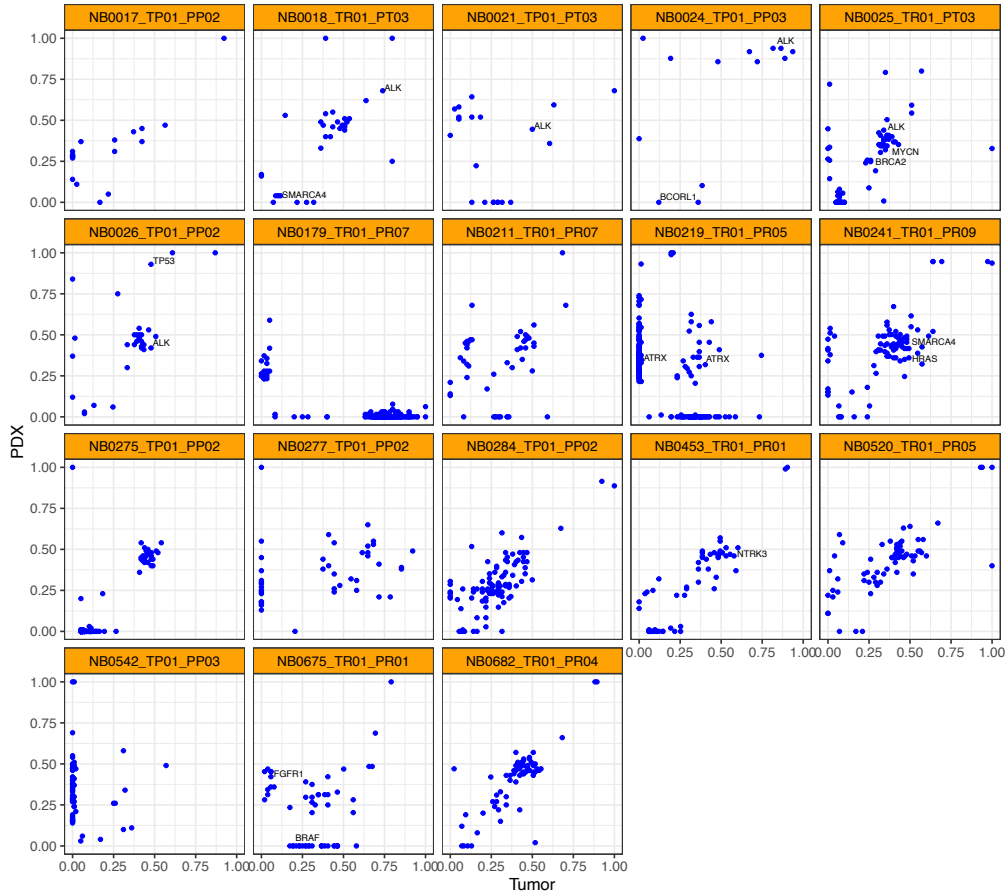


**Figure 33: VAF plot for Neuroblastoma samples**

Neuroblastoma samples had a high overall overlap in PDX and tumor with shared mutations observed in *ALK*, *MYCN*, *BRCA2*, *NTRK3*, *TP53*. Notably there were some interesting cases such as NB0179 that had no shared somatic events, that could be accounted for low sequencing quality. Tumor exclusive mutations could also be observed in NB0675 with *BRAF* SNV and NB0018 having *s* *SMARCA4* in the tumor sample and not present in the PDX.

Overall, the neuroblastoma samples showed high concordance between the PDX models and the patient tumors. With 5/13 models shows shared somatic *ALK* mutations. *MYCN*, *ATRX*, *NTRK3*, *BRAC2* somatic SNVs were also commonly shared alterations. However, one sample NB0275 displayed a nonsynonymous *BRAF* mutation with a VAF score of 0.2 exclusively in the tumor (Figure 33).

Rhabdomyosarcoma samples exhibited a high overall concordance in the somatic SNV profiles between the PDX models and tumor. Frequently recurrent genes that were observed to be shared were *FGFR4* (4/21), *TP53* (3/21), *ALK* (2/21), *CDKN2A* (1/21) and *PIK3CA* (1/21) cases. RS0147, RS0178, RS0401, RS0633 showed tumor exclusive mutations in *ALK*, *MYCN*, *STAG2*, *FGFR4* genes respectively. *TP53* tumor somatic mutations were observed in two patient RS0397 and RS0432. PDX specific *TP53* was seen in sample RS0238 which interestingly displayed extremely few somatic SNVs within the tumor sample (Figure 34).

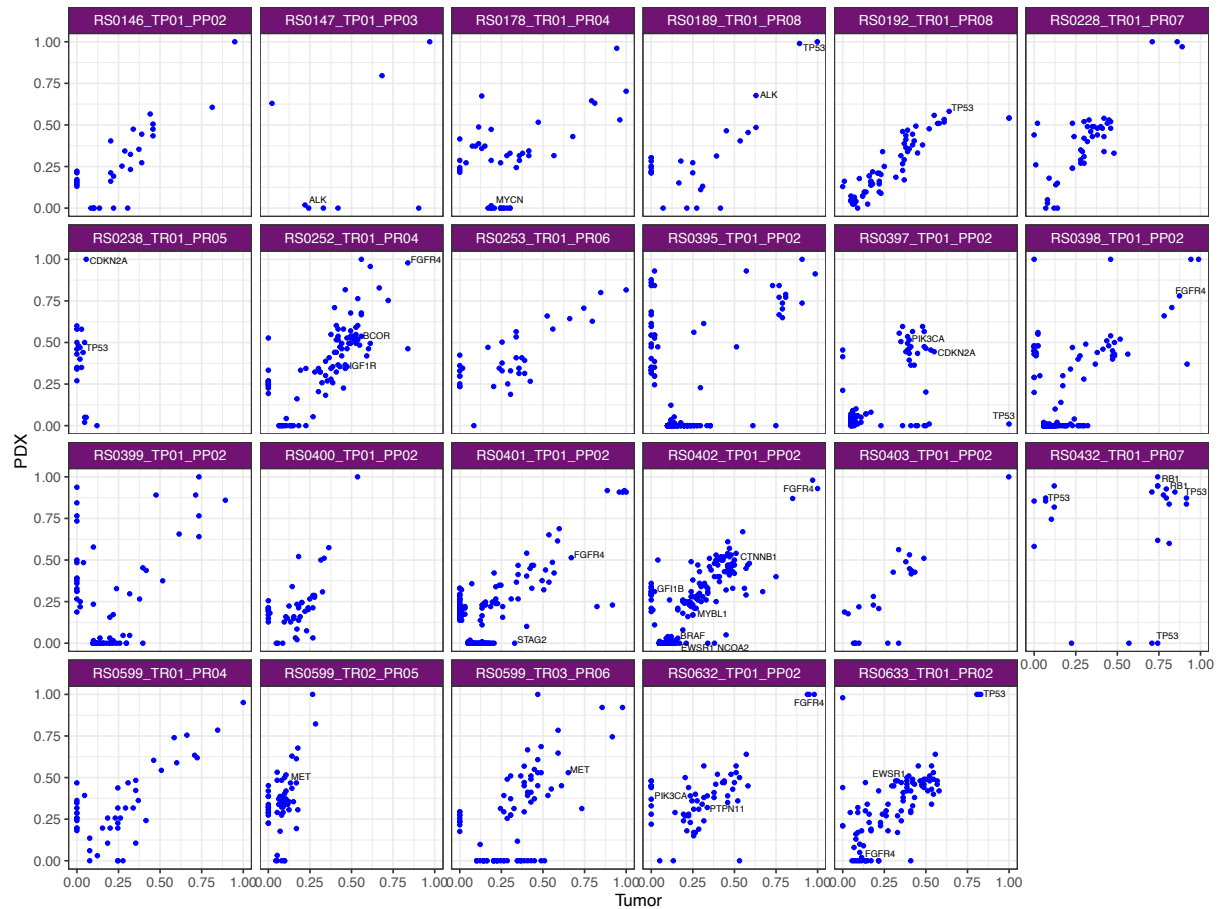


**Figure 34: VAF plot for Rhabdomyosarcoma samples**

Rhabdomyosarcoma samples had frequently recurring somatic SNVs in *FGFR4*, *TP53*, *ALK*, *CDKN2A*, *PIK3CA*. Some models such as RS0147, RS0178, RS0401 and RS0633 displayed tumor exclusive mutations in mutations in *ALK*, *MYCN*, *STAG2*, *FGFR4* genes respectively.

Finally, the Osteosarcoma samples are known to display a highly unstable genome with a higher mutational load[180], [258]. The samples had a high overall shared somatic variant between the PDX and tumor, but 14/26 models were overrepresented in having PDX and tumor mutually exclusive variants. Shared targetable drivers included *TP53*, *ATRX*, *RB1*, *BRAF* and *PIK3R1*. *PTEN* and *PIK3CA* were observed to be exclusively in the PDX models for OS0215 and OS0639 cases respectively. OS0444 showed tumor exclusive nonsynonymous SNVs of *NTRK1*, *PAX3* and *MYOD1* genes (Figure 35).

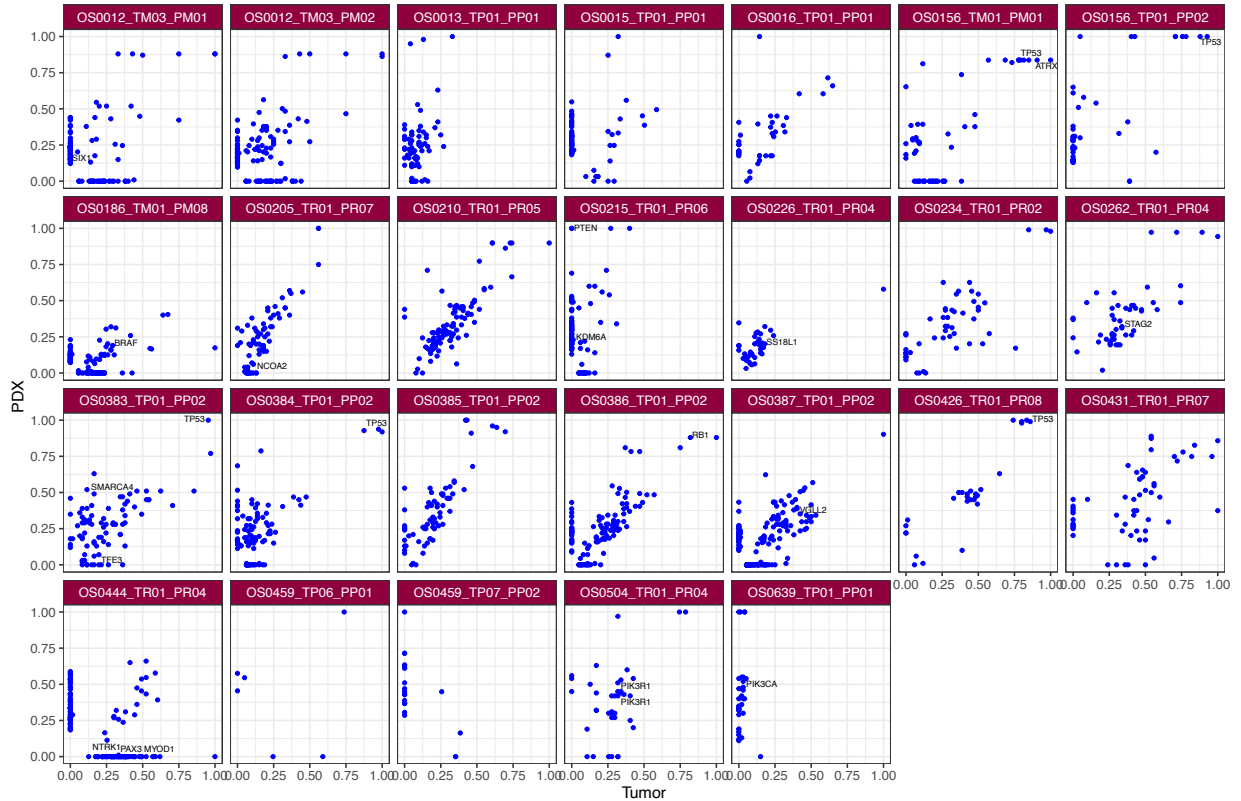


**Figure 35: VAF plot for Osteosarcoma samples**

Osteosarcoma samples were observed to have overall high shared somatic mutations in the PDX and tumor samples, with main driver genes in *TP53*, *ATRX* and *RB1*, usually showing a high VAF score in both PDX and tumor, emphasizing high clonal selection in these genes could be interesting for further investigation.

Within the cohort, majority of the samples fully recapitulated, the mutational repertoire of PDX models, and the key driver alterations that characterized the respective patient tumor. A few cases highlighted below show the range of correlation and divergence on the genomic and CNV level. Neuroblastoma patient NB0025, showed high convergence of SNVs *ALK*, *MYCN* and *BRCA2*, while another rhabdomyosarcoma - case RS0189 - showed a *TP53* and *ALK* mutation with a VAF >0.5 highly concurrent in PDX model and the tumor sample (Figure 36A). Divergent cases such as RS0397 with a *TP53* SNV exclusively present in the tumor and HG0354 showing a PDX exclusive *TP53*, make these cases specifically interesting to further investigate for preclinical drug testing.

On assessing the chromosomal landscape of these cases, NB0025 and RS0189 PDX models showed a strong concordance with their respective tumor types, displaying amplifications in chromosome 1q, loss of chromosome 3p, isochromosome 17 in the neuroblastoma sample. Similarly, amplification of chromosome 1 and loss of chromosome 3, 10 and 17 in the rhabdomyosarcoma model. In contrast, model RS0397 and HG0354 exhibited irregular chromosomal aberrations that were different between the PDX and tumor sample (Figure 36B).

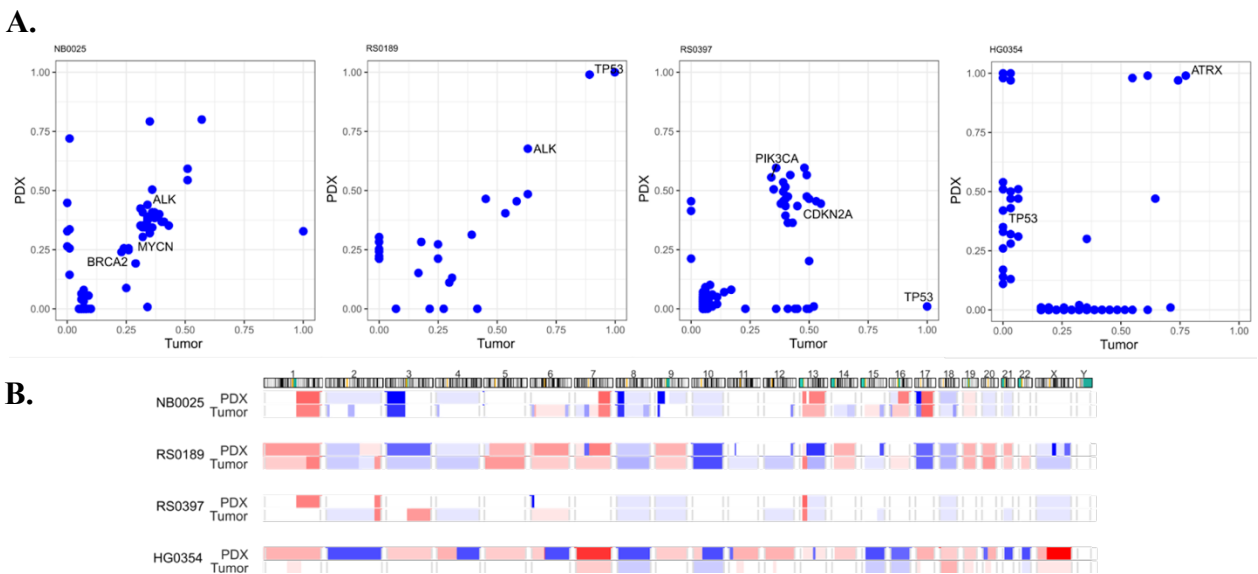


**Figure 36: Chromosomal landscape and VAF plot concordance in PDX tumor pairs**

A.) VAF score of interesting cases with NB0025 displaying shared SNVs in *ALK*, *MYCN*, *BRAF*. RS0189 showing *TP53* shared in PDX and tumor with a high VAF score of 1, while a shared *ALK* mutation VAF >0.5. Divergent cases displaying mutually exclusive *TP53* somatic SNV present in RS0397 only in the Tumor (VAF=1), while this subclone was not selected in the PDX. However, another distinct example is HG0354 having an *ATRX* mutation (PDX VAF=1; Tumor VAF=0.75). B.) This clonal selection and concordance could also be observed on comparison with the chromosomal landscape profiles of cases with high and low concordance in PDX models and patient tumor sample.

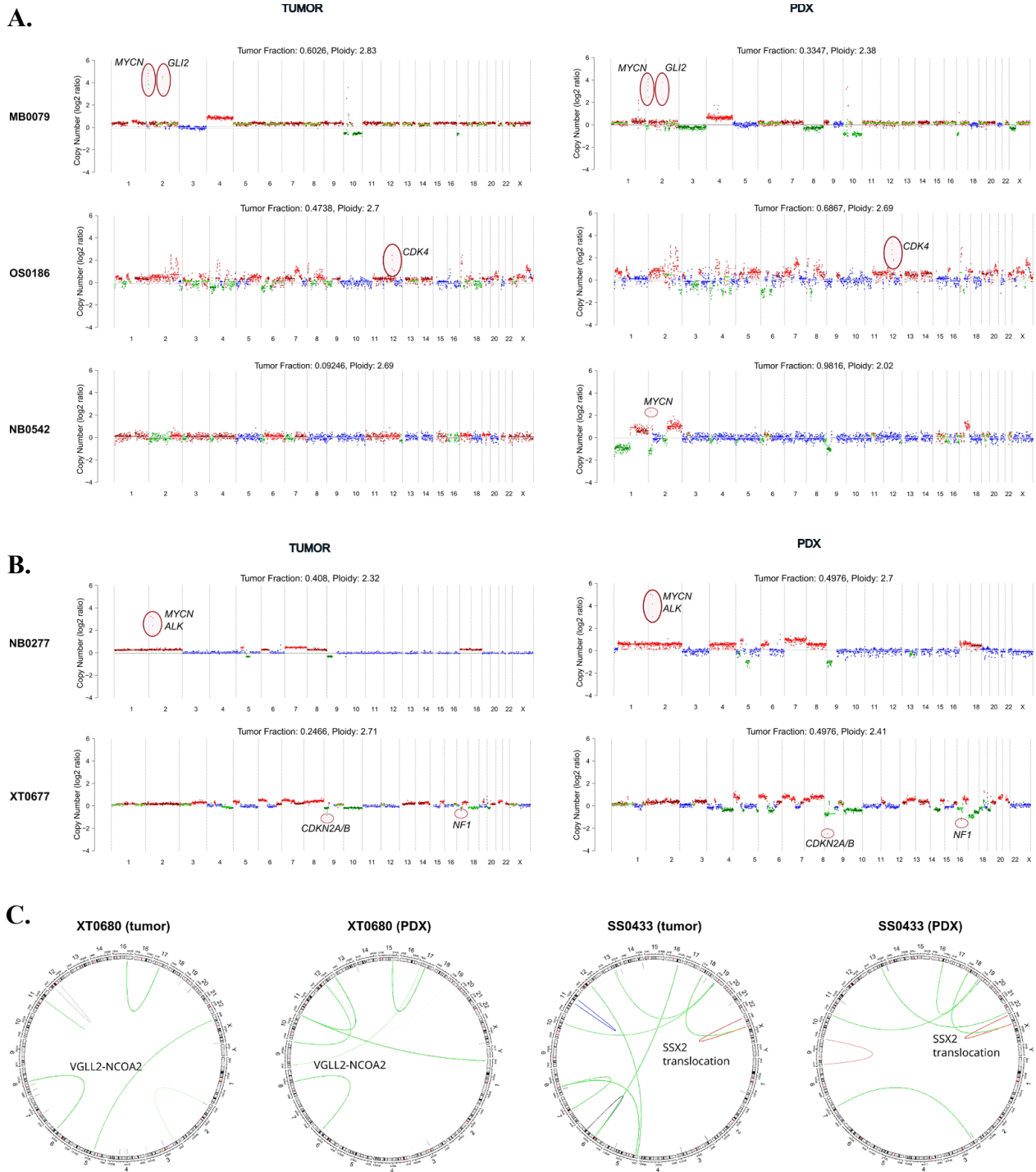


**Figure 37: ichorCNA CNV profiles and Circos plots for SV comparison**

A.) ichorCNA coverage plots to assess concordance and divergence in specific gene alterations. Mb0079 showed overlapping focal amplifications in MYCN and GLI2. OS0186 has focal amplifications in CDK4. However, NB0542 had a focal MYCN amplification only in the tumor and not the PDX. B) High CNV concordance in NB0277 and XT0677. C.) Circos plots depicting structural variant similarities in VGLL2 and SSX2 translocation between PDX and tumor models.

Inspecting the ichorCNA copy number plots for further samples, we observed consistent focal gene amplifications in *MYCN* and *GLI2* on chromosome 2, in medulloblastoma MB0079 PDX and tumor sample. In PDX-tumor pair of the osteosarcoma sample OS0186 a focal *CDK4* amplification on chromosome 12 was observed. Sarcoma sample XT0677, presented *CDNK2A/B* and *NF1* focal loss on chromosome 9 and 17 respectively. Similarly, NB0277 showed a focal amplification of *MYCN* and *ALK* on chromosome 2. On the other hand, a divergent case of neuroblastoma sample NB0542 with a focal *MYCN* amplification on chromosome 2 only in the tumor was observed (Figure 37A-B). To validate the significant variations between tumor and PDX data arising from diverse levels of tumor purity or fractions of malignant cells, we examined their transcriptomic profiles. Differentially expressed genes between human tumors and PDX define the lack of non-malignant/tumor microenvironment compartments in the xenograft models as a major difference. Further, the structural variant profiles were also examined to assess PDX-tumor concordance, SV characterizing sarcoma tumors, such as *VGLL2* rearrangement and *SSX2* translocation, were faithfully detected in the matching PDX models (Figure 37C).

### 3.1.6 Modeling of tumor progression: “Serial” PDX comparisons

Within the ITCC-P4 PDX repository we also had a few models generated from tumor material longitudinally collected from the same patient throughout the course of the disease. All throughout tumor progression and in cases of relapse/recurrence/refractory, cancerous cells can undergo significant molecular changes from the primary patient tumor, leading to possible variations in tumor biology, tumor behaviour and response to treatment. Hence, the necessity of having preclinical PDX models obtained from different time points of cancer development, becomes essential to examine whether they faithfully mirror these transitions. Serial PDX models acquired from the same patient provide insights into the underlying mechanisms that driver tumor progression and support this study by enabling development of targeted therapeutic approaches tailored to specific stages of disease states.

Within the ITCC-P4 cohort, 36 serial PDX models have been generated from 16 patients. The serial cases included pairs of models derived from primary tumors pre- and post-treatment; pairs of primary and recurrent (or multiple recurrent) PDX; PDX model pairs representing progression under treatment and recurrence; several PDX derived from multiple recurrences; and PDXs obtained from multiple metastatic tumors (Figure 38).

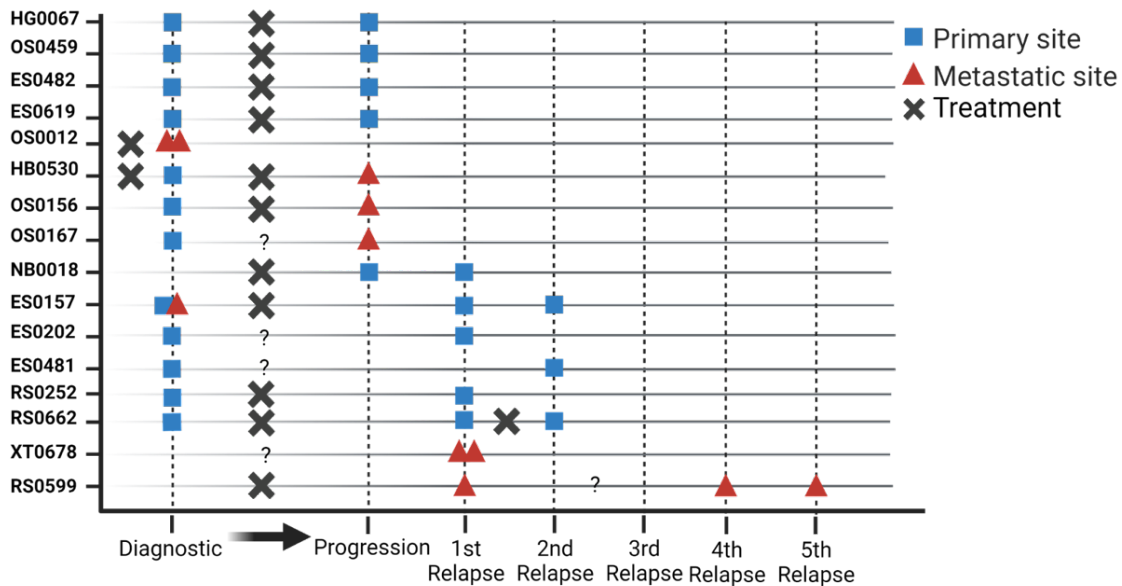


**Figure 38: Serial cases comparisons**

*Serial PDX model cases obtained from different disease states of the patient tumor, highlighting tumor progression from diagnosis to primary and relapse, along with treatment points.*

The multi-omics characterization for these serial cases resulted in the PDX models portraying unique molecular characteristics relative to their tumor specific events. A detailed summary of the key driver gene alterations and chromosomal events can be found in the oncoprints (Figure 19-26). A few interesting cases were observed after

analysing the DNA methylome profiles further, which suggested close overlap of molecular characteristics between the serial PDX models. However, in a few cases such as, ES0202 and OS0156, we could detect strong differences within the PDX models resulting in distinct molecular landscapes (Figure 39).

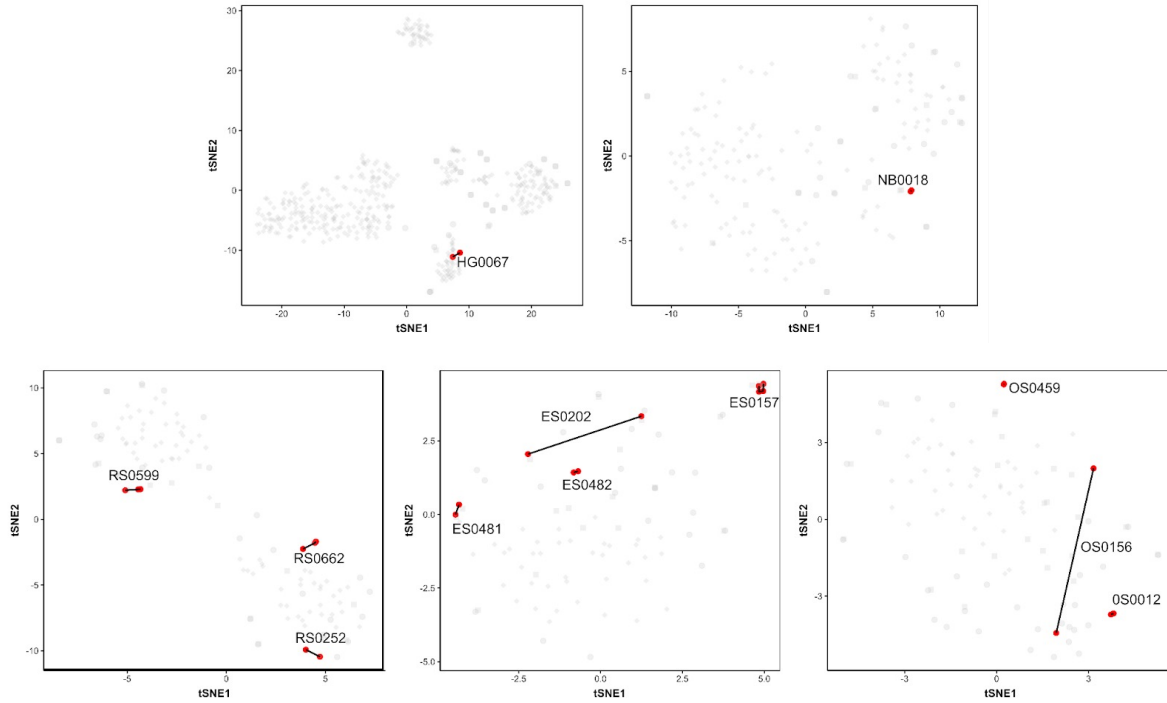


**Figure 39: DNA methylation based tSNE for Serial cases**

*DNA methylation-based t-SNE analysis of serial PDX cases showing distinct differences in progression and disease states. Although most cases had high concordant and clustered together, strikingly ES0202 and OS0156 showed a higher distance between serial cases samples.*

For model ES0202, serial cases were generated from the primary and recurrent tumors of a patient with Ewing sarcoma (Figure 38). The molecular characterization performed on the primary PDX (PP) and recurrent PDX (PR) models along with their respective patient tumor samples (TP and TR) indicated that the two sets of PDX and patient tumor cases displayed distinct somatic mutational landscapes. Specifically, we observed the presence of the *TP53* mutant p53-R175H, frequently detected in various tumor types and actively promotes tumorigenesis and drug resistance[259] present only within the relapse cases of the PDX and tumor models; PR and TR (Figure 40A). Serial case OS0156, generated from a diagnostic primary tumor and metastasis developed following treatment (tumor =TM, PDX = PM) showed the presence of a shared nonsynonymous *TP53* mutation across all the primary and relapse disease states, but an *ATRX* nonsynonymous SNV mutation only present in the metastatic samples PM and TM (Figure 40B).

Although the CNV landscape confirmed the overall PDX models truthfully recapitulating the patient tumor, within the “serial cases” of the same model the profiles did exhibit differences. It was observed that novel relevant CNV alterations were present in models

generated from later disease stages. ES0202\_PR displayed gain of chromosome 6 and loss of chromosome 10, while the model OS0156\_PM clearly shows a loss of chromosome 6q16-23 frequently observed in osteosarcoma (Figure 40C).

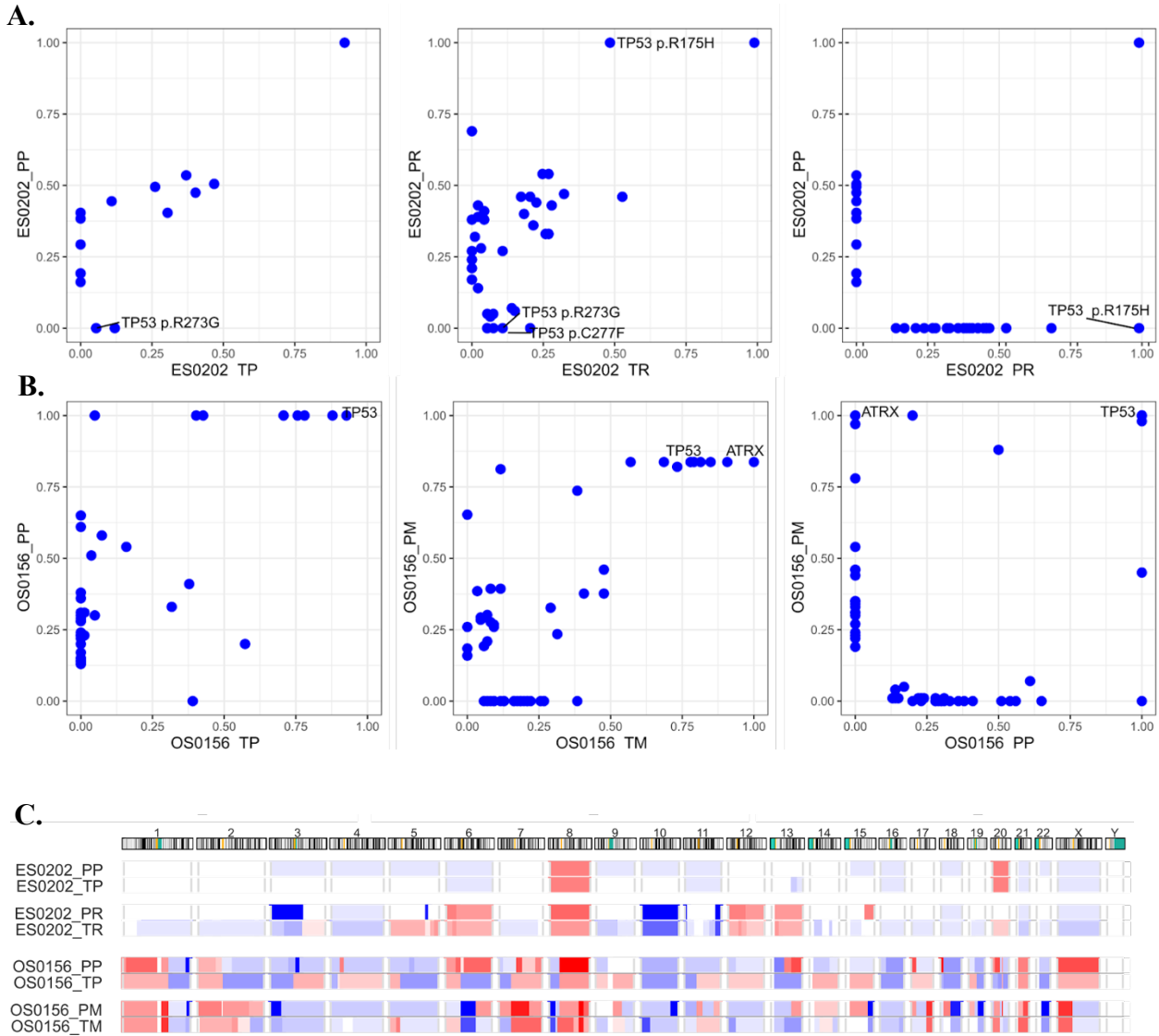


**Figure 40: Serial cases - VAF and copy number profile comparison**

A.) VAF plots of sample ESO202 Primary and relapse models highlighting TP53 mutant p53-R175H presence only in the relapse models of PDX and tumor B.) Sample OS0156 primary and metastatic VAF plots displaying a TP53 with a high variant allele frequency score of 1, present only in the primary PDX model and not in the metastatic PDX model. C.) CNV landscape of the disease states of the two samples, showing overlap, but differences observed in ESO202\_PR displayed gain of chromosome 6 and loss of chromosome 10 and not in the primary PDX. OS0156\_PM clearly shows a loss of chromosome 6q16-23 frequently observed in osteosarcoma.

In addition, *CDKN2A/B* deletion and *FLI1* loss were exclusively detected in ES0202\_PR, (Figure 41 A) while in OS0156\_PP showed a *CCND2* gain which could not be detected in the matching metastatic PDX model (PM) (Figure 41 B). Another pair of serial PDX models generated from the primary tumor RS0252\_PP and the subsequent recurrent model RS0252\_PR, exhibited a *CDKN2A/B* focal deletion and amplification of *MDM2*, represented mutually exclusive aberrations in the early and late tumor events respectively (Figure 41C).

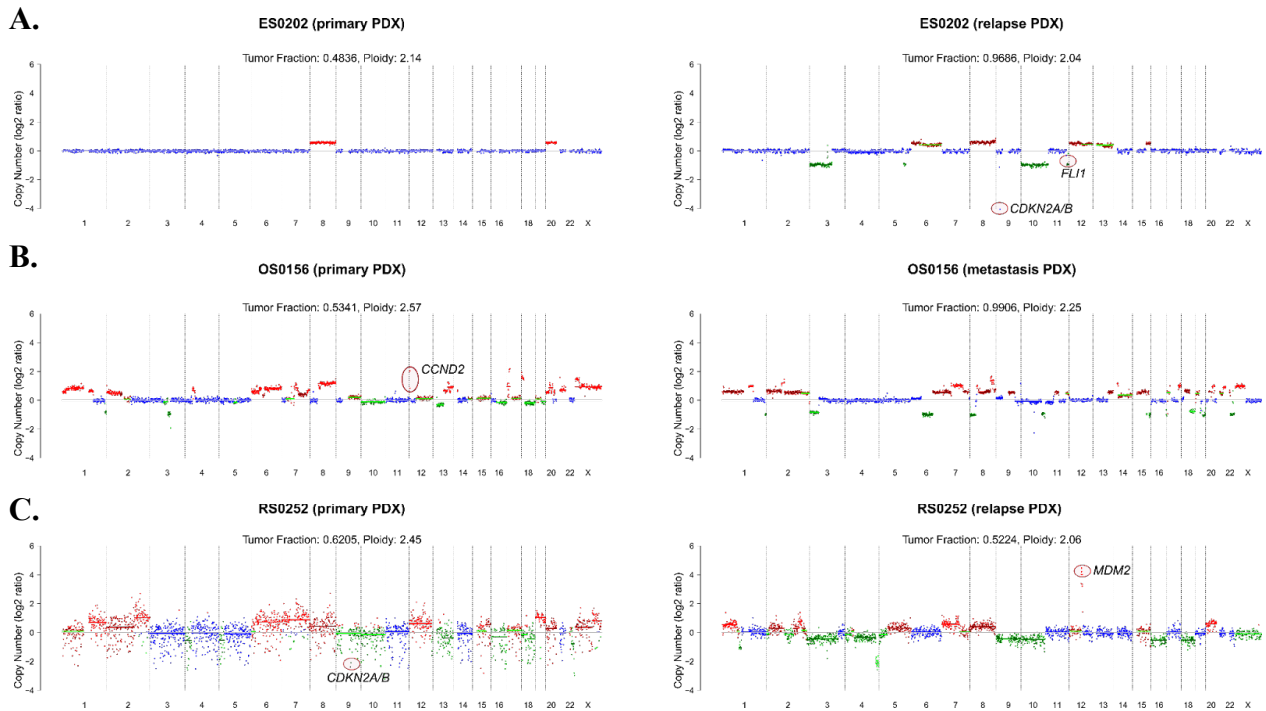


**Figure 41: Coverage plots of Serial cases highlighting driver gene events**

A.) Coverage plots of samples highlighting key driver gene alterations within serial cases PDX. In relapse PDX of sample ES0202, the *FLI1* loss was present and not seen in the primary PDX. B.) OS0156 harboured a *CCND2* gain in the primary PDX and not observed in the metastatic PDX. C.) RS0252 had a distinct *CDKN2A/B* loss in the primary while an *MDM2* focal amplification was observed in the relapse PDX.

Therefore, the establishment of serial PDX models from different stages across the course of cancer progression in pediatric patients highlights a crucial approach for monitoring cancer progression, understanding resistance, assessing drug efficacy according and tailoring disease treatment strategies to the molecular and functional events occurring in such tumors.

Furthermore, the necessity of establishing a centralized repository that consolidates molecularly characterized data from PDX models, patient tumors and their matching germline controls cannot be overstated. Such a resource would play a pivotal role in advancing personalized cancer treatments and facilitating future pre-clinical studies.

### 3.1.7 ITCC-P4 data scope portal: R2 platform

Finally, we worked in close collaboration with Dr. Jan Koster from the Amsterdam Medical Center (AMC, Netherlands) to upload all available patient and PDX molecular data to the public ITCC-P4 datascope portal on the R2 platform ([r2-itccp4.amc.nl](http://r2-itccp4.amc.nl)). This resource is constantly growing with ongoing sequencing data and further characterization, to also include information on genetically engineered mouse models (GEMM) and organoids.

The R2 portal offers an intuitive overview of our multi-omics analysis, allowing users to evaluate potential targets for further treatment. Each sample is comprehensively represented, hence providing a deep understanding of PDX and tumor data. The ITCC-P4 data scope encompasses sample barcoding nomenclature, ITCC-P4 target-actionability reviews, a PDX explorer for data retrieval based on PDX models and enables users to identify samples through collected omics data. The 18 entities are classified into subgroups, accompanied by detailed representations of their mutational landscapes which can be visualized by curated oncprints. Individual sample VAF plots for SNVs and Circos plots for SVs allows investigation of each individual model. Additionally, methylation, gene expression, and CNV analyses can be explored to identify potential druggable targets and alterations. The portal also incorporates information on available drug treatments information for samples, providing details on different treatment arms and facilitating model selection for preclinical studies. This platform is constantly growing and updated with information on newly generated PDX models and results based on the molecular characterization (Figure 42).

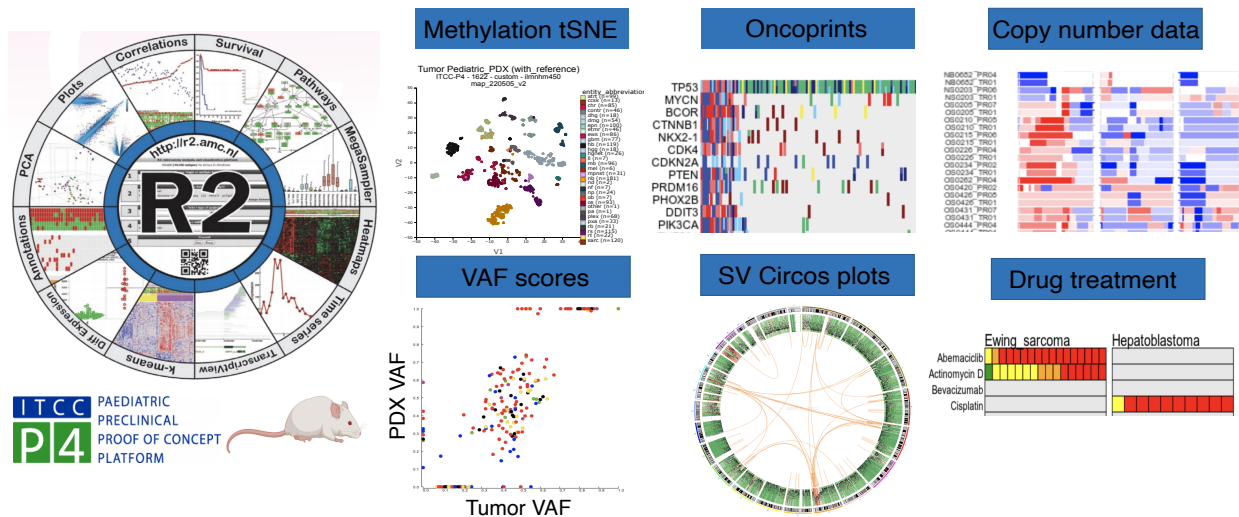


**Figure 42: ITCC-P4 data scope on the R2 platform**

Overview of the ITCC-P4 PDX and tumor data available on the R2 platform, further downstream analysis can be implemented by users to access the PDX molecular data and assess the cohort.

## 3.2 Results from the ITCC-P4 Target Actionability Review (TAR): Replication stress

The following study has been published as “*Keller KM\*, Krausert S\*, Gopisetty A\*, et al. Target Actionability Review: a systematic evaluation of replication stress as a therapeutic target for paediatric solid malignancies, European Journal of Cancer (2022)[231]*”. Dr. Kaylee M. Keller, Dr. Sonja Krausert, and I were the primary reviewers and were equally involved in data collection, analysis, result generation and manuscript drafting. Dr. Dan Luedtke was the independent reviewer. Here, I discuss the main results of the collaborative analysis performed in this study. Some content including figures, tables and text shown in this chapter has been directly adopted and modified from the above-mentioned publication.

### 3.2.1 Systematic evaluation of replication stress literature

In this study, all literature pertaining to targeting replication stress (published between 2014- 2021) across 16 different solid pediatric tumor types was systematically evaluated. Using the curated search queries elaborated in the methods chapter (Chapter 2.3), 708 unique articles were collected. The literature was further selected based on the presence of at least one PoC module in the title or abstract, as a result, 319 articles (45%) entered the critical appraisal stage. At this stage, 174 articles did not fulfil the inclusion criteria and were consecutively removed from the study (largely due to the use of micro or long non-coding RNA, natural compounds, or monotherapy with classical chemotherapy or radiotherapy). Conclusively, 145 articles were scored and summarized into 392 evidence entries within the R2 data portal. The first adjudication process resulted in 68 articles (47%) having at least one discrepancy with the scored PoC modules and/or the assigned scores for experimental quality or outcome. The articles next went onto the independent review process, scored by a third reviewer. 58 discrepancies remained out of the 392 evidence entries (18%). A second adjudication step resulted in re-scoring the 58 publications, involving 37 different drug targets (Figure 43). Ultimately, the final appraisal scores were calculated and interactive heatmaps were generated for replication stress overall and for the 6 main targets focused on in this study.

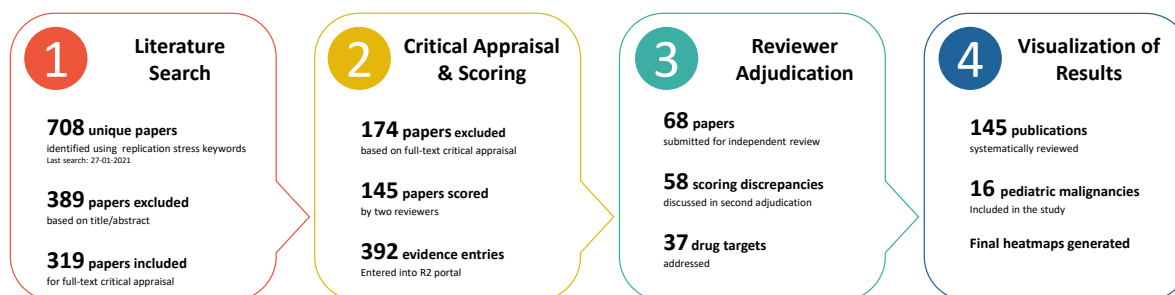
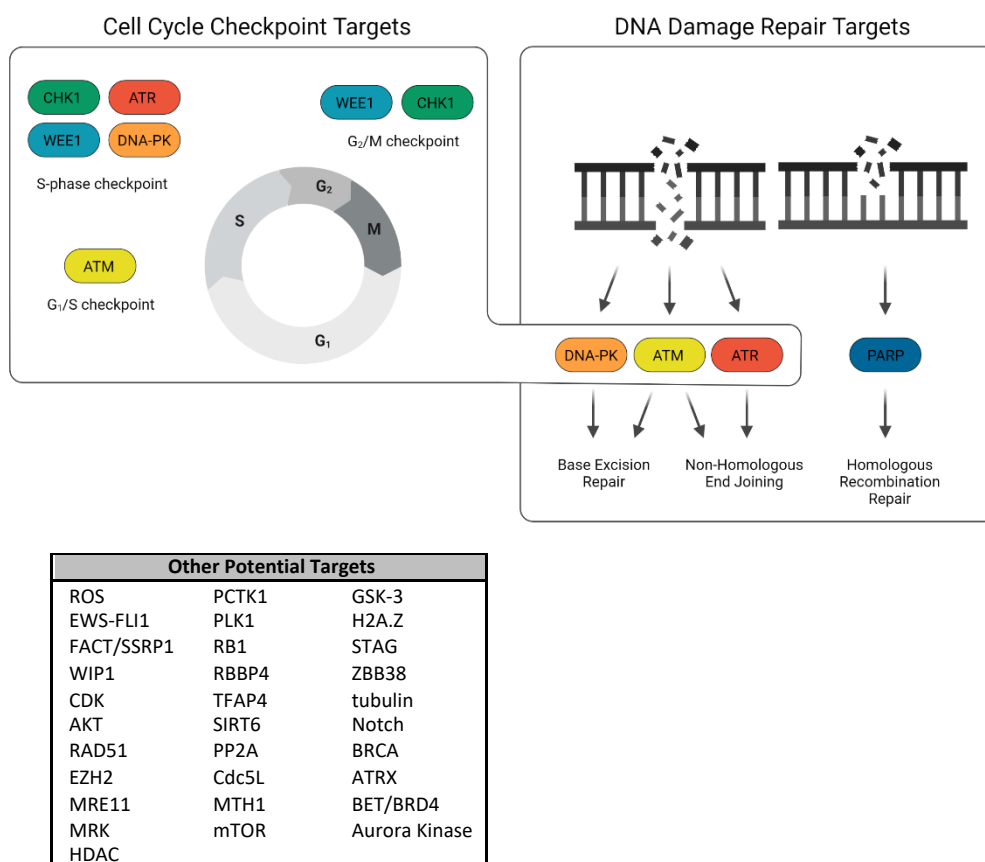


Figure 43: The TAR workflow process

### 3.2.2 Druggable targets of replication stress and biomarker scoring

Previous TAR studies had focused on single targets, for example *MDM2*[260] hence limiting the scope of the literature under review. Conversely, replication stress is an extremely broad process which hence proves challenging to conform to the established TAR methodology. To tackle this, a two-pronged search strategy was implemented by involving both general and specific replication stress related keywords.

The 6 main targets focused on in this TAR are 1.) *ATM*, 2.) *ATR*, 3.) *CHK1*, 4.) *DNA-PK*, 5.) *PARP* and 6.) *WEE1*. These proteins are heavily involved in DNA repair pathways and cell cycle control (Figure 44), two well-known components of replication stress response (RSR).



**Figure 44: Overview of replication stress targets** (taken from Keller et.al 2022)

Overview of replication stress targets involved in cell cycle checkpoint and DNA damage repair. Alternative potential replication stress targets identified using general replication stress keywords.

However, replication stress extends beyond these targets and to obtain literature and identify potential targets outside of DNA repair pathways and cell cycle control, further general keywords were included in the search strategy. Overall, resulting in 31 alternative replication stress targets (Figure 45), which accounted for 127 (32%) of the total evidence entries across all the PoC modules. Although a detailed systematic

evaluation of all these alternative targets was not performed within the scope of this study, this general keyword approach aids in creating an extensive overview of replication stress targets which can be further explored on the R2 TAR platform, which allows users to explore data via interactive heatmaps [[https://hgserver1.amc.nl/cgi-bin/r2/main.cgi?optionZimi2\\_targetmap\\_v1](https://hgserver1.amc.nl/cgi-bin/r2/main.cgi?optionZimi2_targetmap_v1)].

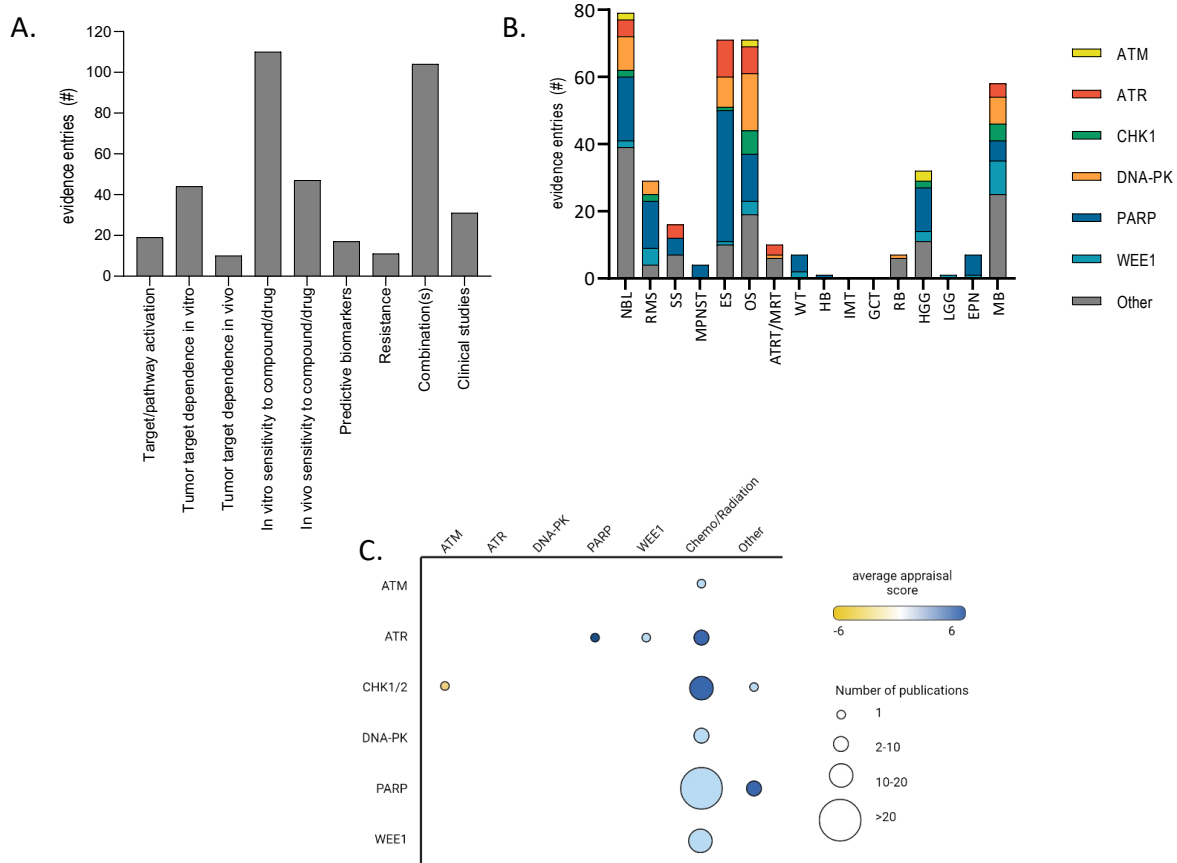


**Figure 45: Evidence and therapeutic combination reported for TAR**

A.) Complete evidence reported for each PoC module reported in the TAR. B.) The total number of evidence entries per paediatric entity distributed across the different targets of interest. C.) Overview of therapeutic combinations reviewed, size of dots represents the number of evidence entries, and the colour depicts the average appraisal score for all publications for the specific combination. PoC, proof-of-concept; TAR, target actionability review. (taken from Keller et.al 2022 [231])

Assessing replication stress for the specific and alternative identified targets, Neuroblastoma (NBL), Ewing sarcoma (ES), Osteosarcoma (OS), Medulloblastoma (MB) were most robustly represented malignancies within our study. These entities also showed the highest number of evidence entries (NBL= 79, ES=71, OS=71 and MB=58), in addition to all PoC modules being addressed in these malignancy types, creating a comprehensive overview for these tumors. Despite all PoC modules being represented in NBL, ES, OS, MB, it is worth highlighting that some modules are represented by only one publication. For example, PoC module 'target/pathway activation' in ES received a

negative overall appraisal score but was represented by one single publication. Overall, these findings are not a negative indication for targeting replication stress in ES (not limited to only this one instance), but highlights the paucity of data, indicative of the necessity for further preclinical research focused within these specific entities. Within this TAR, there was an underrepresentation of data that explores the fundamental biology of targeting replication stress, that is PoC modules of modules 'target/pathway activation', 'predictive biomarkers', 'resistance', across all tumor types, highlighting the direction of future potential studies (Figure 45A).

To enhance the current state of targeting replication stress for pediatric cancer treatment, this TAR study also compiles existing preclinical data available for *ATM*, *ATR*, *CHK1*, *DNA-PK*, *PARP* and *WEE1*. *PARP* was the best represented target off the specific target proteins, accounting for 127 (32%) of the total number of evidence entries and was also the only specific target to include data in all nine PoC modules (in all entities except AT/RT & MRT, IMT, GCT, RB and LGG) (Figure 45B). Given the abundance and robustness of data available for *PARP*, this target is perhaps the most promising, especially considering the data supporting *PARP* inhibitor combinations with classical chemotherapeutic agents (Figure 45C and Figure 45B). Nevertheless, it should not be implied that the remaining specific targets lack potential. Although represented by fewer evidence entries overall, *ATM* (n=7), *ATR* (n=35), *CHK1* (n=50), *DNA-PK* (n=18), *WEE1* (n=29) remain targets of interest (Figure 45B). This TAR study defines the current landscape of research in targeting these proteins in pediatric tumors, with the hope to provide direction to future exploratory research on these targets.

Similar to *PARP*, inhibitors of all other specific targets were also explored in combination with classical chemotherapy. Notably, *CHK1* and *ATR* both received higher average appraisal scores in the 'combinations' module compared to *PARP*, suggesting great potential in these therapeutic approaches (Figure 45C). Additionally, *ATR* and *CHK1* both showed higher overall scores in medulloblastoma (Figure 46C-D). MB scored positively in all addressed modules for *ATR* ('in vitro/in vivo sensitivity to compound', 'resistance' and 'combinations'), although based on one article, nevertheless suggesting that *ATR* might be a particularly interesting target for MB[261]. In addition to *ATR*, MB also demonstrated high scores in all modules evaluated targeting *CHK1* ('target/pathway activation', 'tumor target dependence in vitro', 'in vitro sensitivity to compound' and 'combinations'). Noticeably, *CHK1* showed overall positive scores across all included tumor types (Figure 47). It is pertinent to note that ES, which score negatively in modules 'tumor target dependence in vitro' and 'in vivo sensitivity to compound', contradicted the positive results obtained in module 'in vitro sensitivity to compound' and 'combinations' for the entity ES (Figure 46D). Although, these scores are derived from a limited number of included publications (2-3 publications for each module addressed in ES), additional studies need to be carried out to fairly assess *CHK1* as a target in Ewing sarcoma.

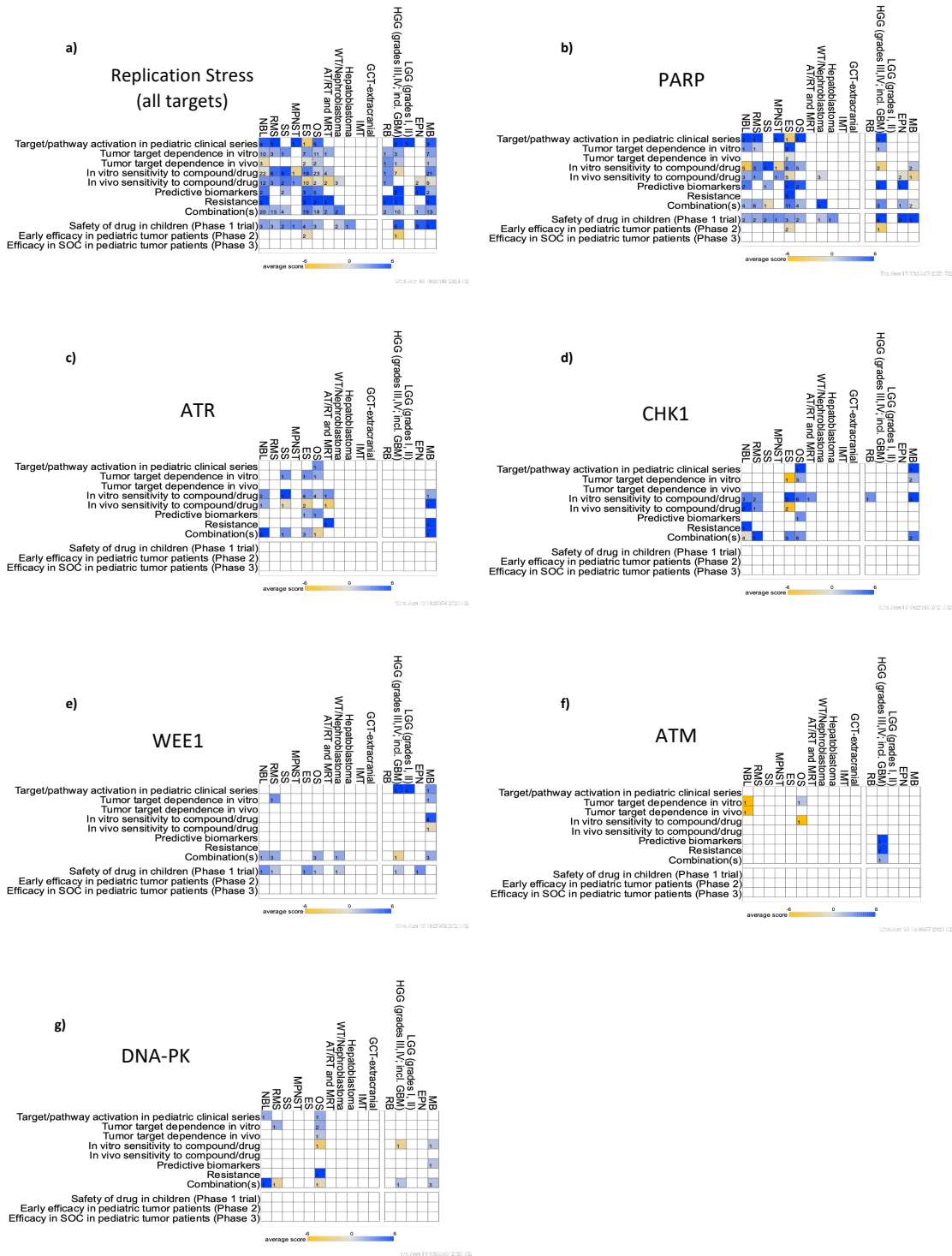


**Figure 46: Summary of TAR appraisal scores**

Overview of TAR appraisal scores (a) overall replication stress, (b) PARP, (c) ATR, (d) CHK1, (e) WEE1, (f) ATM and (g) DNA- PK. Each box represents the averaged appraisal score in which yellow denoting a negative result and blue indicates a positive result. The number within indicates the quantity of evidence entries. The interactive heatmaps can be accessed via the R2 TAR platform [[https:// hgserver1.amc.nl/cgi-bin/r2/main.cgi?optionZimi2\\_targetmap\\_v1](https://hgserver1.amc.nl/cgi-bin/r2/main.cgi?optionZimi2_targetmap_v1)]

Another significant target that showed overall high scores is *WEE1*. Even though the literature surrounding *WEE1* was limited, the target received overall positive scores in all malignancies (Figure 33). The combination therapy involving a *WEE1* inhibitor and chemotherapeutic agents yielded superior responses compared to *WEE1* inhibition by itself. Additionally, a Phase I clinical trial utilizing *WEE1* inhibition in combination with irinotecan scored positively in NBL, HGG, RMS, EPN, ES, OS, and WT [262]. A striking observation was the insufficiency of data across the other PoC modules specifically ‘predictive biomarkers’ and ‘resistance’ (which were not addressed at all) and strongly implied that further research needs to be conducted to explore the full potential of *WEE1* as a target in pediatric tumor entities (Figure 46E).

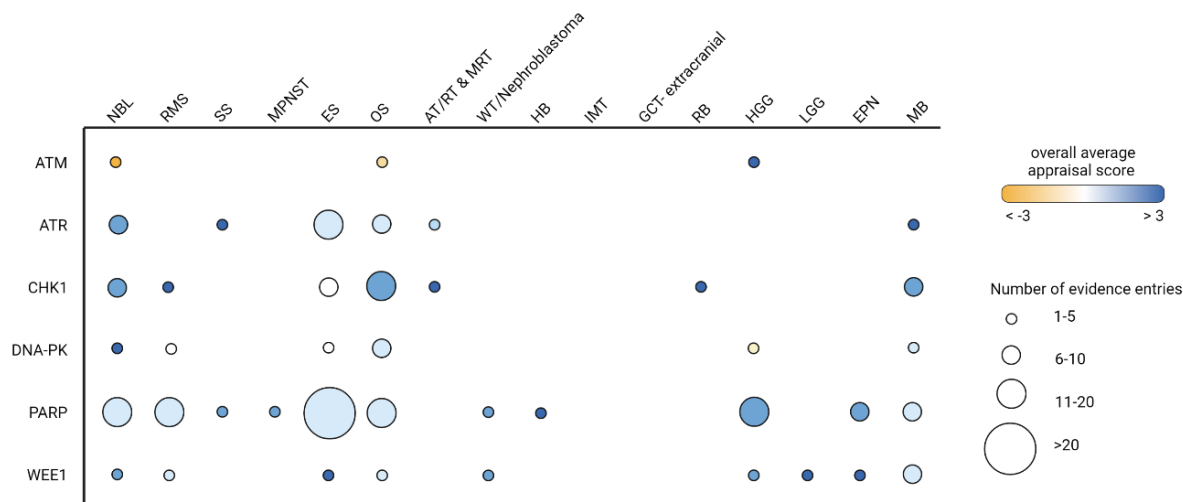


**Figure 47: Overview of specific therapeutic targets**

The colour of the dot reflects the overall average appraisal scores derived from all PoC modules for that target and malignancy, while the size of the dot represents the volume of evidence entries.

*ATM* and *DNA-PK* were the two specific targets that were least encountered in this study and were often represented by only one publication across limited number of PoC modules and tumor types. *ATM* was observed to include only seven evidence entries overall, addressing only a limited number of PoC modules in NBL, OS and HGG (Figure 46F). High-grade glioma was observed to score overall positively for *ATM*, although the data was limited. This suggests the efficacy of targeting *ATM* in HGG and reveals direction of future potential research prospects (Figure 33) [263], [264].

Conversely, *DNA-PK* was more diversely represented as it addressed all preclinical PoC modules except for ‘in vivo tumor target dependence’ across 5 out of the 16 tumor types namely, NBL, RMS, OS, HGG and MB (Figure 46G). Observed results for ‘resistance’ in Osteosarcoma[265] and ‘combinations’ in neuroblastoma[266] were modules that scored highly for *DNA-PK* suggesting that combination therapy with *DNA-PK* inhibitors could be an effective strategy to target certain tumors. However, *DNA-PK* scored neutrally across all modules and tumor types, emphasizing the need to evaluate this target further (Figure 47).

## 4 DISCUSSION

This study elucidates and provides a deeper insight into one of the most complex problems in oncology research and medicine: pediatric cancer. Childhood cancer remains one of the leading causes of disease-related death in the world in patients aged 1-19. There have been remarkable advancements in pediatric cancer treatment over the past decade by better understanding tumor biology and developing personalized treatment strategies, that enabled an increase in cure rates up to 80% on average.

However, there is a massive knowledge gap in core aspects such as tumor cell of origin and mechanisms of tumor immune evasion as compared to what is known about adult cancer. Due to the lack of published molecular and genetic data on pediatric solid tumors from relapsed and metastatic patients, significant efforts not only need to be made to enhance the quality of life for pediatric cancer survivors, who often suffer from enduring effects of treatments like radiotherapy, cytotoxic chemotherapy, and surgical intervention but also to find a cure for the remaining ~20% of children affected by childhood cancer. Therefore, it is crucial to recognize that pediatric cancers diverge significantly from their adult counterparts in terms of foundational mutational mechanisms, cellular origin, mutational burden, driver gene mutations, genetic complexities, predisposing factors, and epidemiological characteristics. These challenges, make it essential to improve clinical studies and trials by developing preclinical models to identify predictive biomarkers and for testing innovative therapeutic interventions, for children suffering from childhood cancer.

This thesis includes two separate studies under the Innovative Therapies for Children with Cancer Pediatric Preclinical Proof-of-concept Platform (ITCC-P4) projects supported by the European consortium 'Innovative Medicines Initiative' (IMI). In the first study, "ITCC-P4: Genomic Profiling and Analyses of Pediatric Patient Tumor and Patient-Derived Xenograft (PDX) Models", I focused primarily on the multi-omics analysis and characterization of PDX models by assessing their mutational landscape, tumor cell content, methylation profiling and copy number profiling to see how well these PDX models recapitulate the original pediatric patient tumor. The second project, "TAR: A systematic evaluation of replication stress as a therapeutic target for pediatric solid malignancies", provides a comprehensive, structured, and critically evaluated overview of literature targeting replication stress in pediatric solid tumors, allowing further development of specific inhibitors for targets in pediatric cancer treatment.

## 4.1 Discussion based on ITCC-P4 genomic profiling

### 4.1.1 PDX models in pediatric cancer

This project aims to establish a robust repository of ~400 PDX models that will serve as a powerful resource for pediatric cancer research. This heterogeneous repository of established PDX models along with accompanying well characterized molecular and clinical data represents one of the few international initiatives developed for pediatric cancer modelling. Collectively, the ITCC-P4 PDX repertoire demonstrates a well-represented variety of 18 different pediatric cancer entities across 43 distinct subgroups and different disease/molecular statuses based on single-mouse trials [224]. Previous studies such as by Stewart et al. (2017) containing 168 pediatric cancer patients and 67 orthotopic PDX models, only assesses 12 cancer types. And another study by Yang et al. (2020) although gathers 324 PDX models, lacks crucial information about the original patient tumor or germline controls [267]. Hence, a key strength of our study is the size of 251 PDX models (still expanding to ~400) but also the availability of patient tumor samples and germline controls for majority of the pediatric solid tumor types.

Compared to previous studies[268]–[271], a defining strength of this study lies not only in the robust genomic alignment between PDX and patient tumor samples (including WES, lcWGS, and RNA-seq data) but also in the thorough integration and examination of DNA-methylation data for these models. Recent studies such as Rokita et al. (2019) characterize 261 PDX models from 37 cancer types [268]. While this study scrutinized the genomics and transcriptomics profiles of PDX models, it lacks the crucial aspect of collecting and analysing DNA-methylation data, for precise tumor sub-classification, which is the distinguishing feature of our study from previously published data.

This multi-omics data integration and analysis allowed for a significantly more detailed representation of the PDX model's molecular status. Besides identifying key targetable driver genes for each entity, the unsupervised clustering of the RNA-sequencing data for the PDX models based on their expression profiles facilitated the precise annotation of frequently recurrent and essential fusion events observed in sarcomas and other pediatric entities[224][168], [272]–[275]. This multi-omics layered analysis approach served as a particularly effective method in defining key oncogenic hits for the 251 analysed PDX models, while the cases where only single omics data was available, resulted in a less comprehensive molecular characterization of PDXs.

Overall, key driver events were enriched within the PDX models, exhibiting tumorigenic alterations that mirrored specific aggressive tumor types. Although there was an array of molecular subtypes within brain tumors in the cohort that were initially catalogued, for the Ependymoma samples, we observed only the most aggressive subgroups: EPN-PFA and EPN-ZFTA that seem to have been engrafted better in the PDX model generation, compared to more benign tumor types[203], [276]. Similar observations were made for other entities within the cohort. This finding is in line with previous studies on sarcomas[277] and breast cancer[278].

We noticed an underrepresentation of rarer and/or least aggressive tumor types and molecular subtypes models, such as low-grade gliomas, embryonal tumors with multilayered rosettes (ETMR), malignant rhabdoid tumors etc. The establishment of tumors from these rarer entity types are significantly challenging as, not only is obtaining adequate numbers of patients with these cases to cover a whole spectrum of childhood cancer diseases but also optimizing PDX establishment protocol for the growth of these tumors needs to be further refined.

Within these aggressive tumor types we also observed the enrichment of specific genetic alterations such as somatic and germline *TP53* mutations in MB G3 PDX [279]–[281] and tumor models with *MYC* amplifications and somatic variants[282]. Gain of chromosome 7 that we observed in six PDX models has also be linked to poor prognosis in various studies[283], [284]. Our finding also aligned with studies in Neuroblastoma with recurrent gains in chromosome 17q and 1q loss[166], [167]. We observed the classic mutations in sarcoma models such as *EWSR1-FLI* fusions[285] were common in this cohort, but interestingly we also observed only two cases with less common *EWSR1-ERG* and *EWSR1-FEV* fusions in our PDX samples.[286], [287]. Germline *TP53* and *STAG2* somatic mutations[288][289], *CDKN2A/B* mutations[290] that have been linked to poor disease prognosis were also frequently observed in the high-grade gliomas and sarcoma models [244], [245], [290]–[292]. Another observation within our cohort is the presence of a hallmark chimeric oncogenic transcription factor *PAX3-FOXO1* fusion of the aggressive alveolar RMS. This fusion was detected in 46% of the Rhabdomyosarcoma PDX models. Various studies show PAX gene fusions, in conjunction with other genetic alterations, play a crucial role as oncogenic drivers in fusion-positive RMS tumors. These fusion transcription factors stimulate the expression of several transcriptional targets that support the process of oncogenic transformation, including *MET*, *ALK1*, *MYCN*, *IGFR1*, and *FGFR4*. It is also noted that, fusion-positive RMS tumors exhibit a much lower overall count of somatic mutations, with few, if any, recurring mutations when compared to fusion-negative RMS samples, which we also observe in our RMS PDX cohort. The expression of *PAX3-FOXO1* has the capacity to induce oncogenic transformation in both cell culture and animal models and hence represents an attractive target for therapeutic strategies[293].

Given these observations it is crucial to match PDX cohorts to their respective patient subgroup population and not directly to clinical cohorts. That is, PDX models retain and recapitulate the characteristics of patient tumors. However, not all tumors within a specific type or diagnosis are the same, as we do observe differences in genetic alterations, molecular and clinical behaviour. Therefore, it's crucial to ensure that the PDX models chosen for a study closely resemble the specific patient subgroups or types of tumors under investigation.

These rare tumors are less frequently encountered in clinical cohorts compared to highly prevalent, aggressive, or common tumor types. As a result, if a PDX cohort consists mainly of highly aggressive tumors, it might not accurately represent the broader spectrum of tumors within the targeted patient population. The lack of availability of more rare tumor types compared to highly aggressive tumors can skew the tumor

subgrouping leading to further biases in clinical settings. Addressing these key factors, would ensure that research findings can more accurately be representative and applicable to clinical scenarios.

#### **4.1.2 PDX models compared to their corresponding patient tumor**

A fundamental strength of this work is that for the first time, we present a massive cohort of fully molecularly characterized pediatric patient tumor PDX models along with the generation, interpretation, and comprehensive comparative analysis to their corresponding patient tumor data. This multi-layered data approach is essential to assess the capacity of the xenograft models to faithfully recapitulate the molecular features of the tumor and disease states from which they were generated. The molecular comparison in matched PDX and tumor pairs overall show high confidence concordance with identified genetic variants, tumor mutational burden, copy number, epigenetic and even the transcriptomic profiles.

In the context of the methylome landscape, we observed high fidelity between PDX models and their matched patient tumors as clustering analysis shows PDX clusters overlapping with patient tumor clusters and the large reference cohort that defines the canonically accepted subtypes. In some rare cases we do see slight shift in the distance between the PDX and their tumors. However, these cases did retain the same subgroup assignment, but often seemed to cluster more similar to the reference samples of the same subgroup than the patient tumor itself.

Tumor microenvironment plays an important role in cancer progression and response to treatment. It consists of various cell types, such as immune cells, fibroblasts, blood vessels etc. This microenvironment is known to be highly dynamic, and its composition can change with time[294], [295]. However, the tumor microenvironment is significantly different from the murine microenvironment, which includes different immune cell populations, stromal cells, and cytokines. Over time, after transplantation into the PDX, the tumor cells may adapt to the mouse microenvironment. This could cause changes in gene-expression, epigenetic modifications and as a result, DNA-methylation patterns of tumor cells in the PDX can shift, making them more similar to the reference samples of the same subgroup. Another factor, affecting the dynamic DNA-methylation process, is tumor cells can undergo continuous demethylation of specific genomic regions. This could also be a possible explanation of the clustering patterns in DNA methylation of the PDX models [296].

On analyzing the genomic data, we also interestingly observed instances where strong clonal outgrowths were identified in the PDX models from their tumor samples and vice-versa. The presence of numerous subclones accounts for the differing rates of response to treatment within a single tumor mass itself due to the highly heterogeneous continuously evolving population of tumor cells. Genetic heterogeneity is an intrinsic factor in cancer and the rapid growth of subclones leads to more aggressive tumors, which contributes to the rapid development of acquired drug resistance[297], [298]. For

instance, a study showed identification of a minor *KRAS*-mutant clone can predict which colorectal cancer patients will eventually become resistant to therapy that targets the epidermal growth factor receptor (*EGFR*) [201], [299].

To understand the potential origin of these disparities, certain aspects need to be considered. Primarily, the difference in the tumor cell fraction, which we and others report to be higher in the PDX models, while human tumors are characterized by infiltration of additional cellular components that arise from the patient's immune system and the stromal microenvironment. Essentially, the native tumor microenvironment is eliminated in the PDX models due to the impaired immune system within the immune-deficient mice that are used for xenograft establishment and multiple passages[204]. For this purpose, we considered the correction of the variant allele frequencies (VAF) detected in sample based on the estimated tumor cell purity as a normalization method for better comparison of all analyses [300]. A further outcome of the TCF disparity between matched PDX tumor pairs is that in some instances oncogenic hits can be "masked" i.e remaining undetectable in highly infiltrated tumor sample data, while these drivers can emerge in the corresponding tumor-cell enriched PDX data[301]–[304]. Furthermore, for somatic mutations that are predominantly enriched in either PDX or tumor samples, we speculate that this is a result of subclonal selection during establishment of the xenograft or might be attributed to the absence of the immune system, permitting a significant growth advantage for a variant in the PDX model[301], [305].

Finally, another major strength of our study is the presence of "serial" PDX models in our cohort, generated from the same patient tumors collected at different stages over the course of the disease. The characterization and comparative analysis on these "serial" cases emphasized the importance of investigating the molecular changes that occur in the same patient across disease progression and or upon exposure to treatment. [295], [306]–[308]. We hence highlight the importance of comprehensive representation and multi-omics analysis of the different disease stages in pediatric cancer. The driver mutational landscape changes from primary to metastatic to relapsed stages of cancer progression. A study from 2017, by Yates et. al. [309], performed sequencing of 299 breast cancer samples from 170 patients. It was observed that the enrichment of driver mutations in relapse/metastasis samples compared with the cohort of primary breast cancers was much higher. These acquired mutations included clinically actionable alterations and mutations inactivating *SWI-SNF* and *JAK2-STAT3* pathways, significant for breast cancer progression.

The higher enrichment in metastatic/relapse cases could be accounted due the genomic instability observed in the primary cancer tumor, may create a favourable environment for the emergence of subpopulations of cancer cells with varying genetic profiles. These clonal subpopulations could include cells with greater resistance to therapy, which could lead to treatment failure and relapse. Cancer cells that disseminate from the primary tumor site may continue to evolve as they encounter different tissue environments, immune responses, and response to therapeutic interventions. This

ongoing evolution can result in the selection of more aggressive or drug-resistant subclones, which could explain the relapse phenomenon observed in some cases[309].

Hence the characterization of different disease stages in pediatric cancer is essential for tailoring treatments, predicting outcomes, advancing research, improving early detection. Our multi-omics study addressing longitudinal cases from the same patient, enhances our comprehension of cancer progression and evolution and also validates PDX model selection for further preclinical pediatric cancer studies.

### **4.1.3 PDX models as a tool for preclinical drug testing**

The data generated for this study aims to serve as a strong foundation for further investigative research in the field of pediatric cancer. Keeping this goal in mind, the ITCC-P4 PDX data scope on the R2 platform was established to allow free access of this published data to the entire scientific community. As this study uncovers the full molecular characterization of 251 profiled PDX models and available matching patient tumors, it is steadily expanding in cohort size to further include ~150 newly established PDX models as well as ongoing establishment of GEMM and PDX-derived organoid lines as additional preclinical models. Thus, making this a comprehensive and unique resource within the field.

The currently generated molecular data contributed to the stratification of PDX models on their clinical and molecular profiles. This PDX repository serves as a resource for the identification of emerging molecular vulnerabilities for pre-clinical drug testing on various PDX models. This proof-of-concept drug testing will eventually be provided as a service in the next stages of the ITCC-P4 sustainability platform. What started off as an international consortium project, has now developed into a non-profit company (gGmbH: company with limited liability) continuing a close collaboration with three contract-research organisations. This platform aims to support the drug testing research for pediatric cancers stemming from the large portfolio of fully characterized and established PDX model cohort.

The ITCC-P4 platform represents a powerful tool for investigative biology and in-depth multi-omics research of pediatric cancer contributing to the development of novel and innovative therapeutic options for pediatric cancer patients.

## 4.2 Discussion based on TAR Replication stress

### 4.2.1 Targeting Replication stress as a therapeutic approach

The Target actionability review (TAR) methodology was developed [260] to match the mechanism-of-action targeting anti-cancer drugs for cancer specific subtypes in preclinical studies. This study implemented the previously established TAR methodology taking it one step further to systematically analyze and evaluate the broader ‘targets’ of replication stress. Since replication stress is such a vast mechanism encompassing multiple targetable proteins, it was essential to narrow down the possible driver genes. In order to enhance the level of specification in this study, we focused on six distinct drug targets. This approach aimed to provide insight into the prioritization of drug targets for further preclinical development.

As expected, this posed unique challenges to the TAR methodology. As summarized previously in the TAR Results chapter (chapter 3.2), each specific target in our study was characterized by assessing varying amounts of published literature and assigning an average appraisal score which also differed based on the particular malignancy under investigation. These factors collectively complicated the determination of which specific targets should take precedence in future studies. Furthermore, delving into a multifaceted subject such as replication stress necessitated a clearly defined and stringent search strategy, which defies the intrinsic complexity of replication stress. These aspects collectively exemplify the unique limitations, in addition to the broader constraints inherent in the overall TAR methodology. For instance, accommodating the unexpected change and occasionally unforeseen patient reactions in clinical trials is unattainable, and due to the rarity of certain tumor types, creating a consistent overview of evidence becomes unfeasible across all entities of tumors.

Regardless of these limitations, replication stress continues to be an attractive avenue for therapeutic approaches in pediatric cancer. The extensive scope of RSR presents a range of innovative therapy options, which we have highlighted in this TAR. We methodically investigated and focused on six specific drug targets, *ATM*, *ATR*, *CHK1*, *DNA-PK*, *PARP* and *WEE1*. Among these six targets, *PARP* emerged as the most extensively researched and promising therapeutic candidate. Beyond comprehensively addressing all the PoC modules and having the highest representation within the literature, *PARP* also achieved positive overall scores across all the 16 investigated tumor entities. Particularly noteworthy are the results derived from the “combinations” module, which highlighted the synergistic potential of *PARP* inhibitors when combined with classical chemotherapeutics. This two-fold approach in targeting replication stress offers the potential of harnessing the efficacy of chemotherapy while mitigating the adverse side effects linked with high-dose treatment. The results of our study, lend support to this notion, for examples in the “phase I clinical studies” module, where *PARP* was combined with chemotherapy (temozolomide and/or irinotecan) or radiotherapy [310]–[314]. Nevertheless, the results from the “phase II clinical studies” module, which stands out, due to the absence of data across all potential targets of replication stress, does not

demonstrate notable clinical effectiveness. Based on limited accessible data, outcomes ranged from a lack of clinical improvement for HGG[310] to maintaining disease stability for ES[314], [315]. This emphasizes the need for additional explorative research.

Additionally, this dual strategy approach targeting replication stress was not only limited to literature focusing on *PARP*. The exploration of the “combinations” module was extended across all other targets included in the study, and most of these studies included targeted inhibitors with conventional chemotherapeutic agents. Considering the role of these proteins in DNA damage repair pathways, it is not unexpected that the majority of cases demonstrated a slight synergistic effect upon combination with chemotherapy and/or radiation. However, particularly noteworthy were the results of *CHK1* inhibition combined with chemotherapy, which consistently exhibited synergistic outcomes across MB, ES, OS, NBL and RMS[316]–[318]. Furthermore, certain studies that investigated the combination treatment involving two RSR-targeted inhibitors, such as pairing *ATR* with *WEE1* [319] or *PARP* [320] inhibitors. Dual targeting, without the reliance on chemotherapy, presents an alluring therapeutic approach for targeting replication stress. This method avoids the use of therapies, known to induce toxicity and the potential long-term health ramifications [321]. Moreover, insights from studies combining *RAF* and *MEK* inhibitors in metastatic melanoma demonstrate the efficacy of targeting multiple proteins within a shared signalling pathway, then offering enhanced therapeutic outcomes in adults. This prompts the question of whether this is also a valid approach in targeting replication stress in pediatric tumors.

In our TAR, we observed two distinct strategies of targeted intervention: 1.) a ‘vertical blockade’, entailing the inhibition of two proteins within the same signalling axis and 2.) a ‘lateral blockade’, involving the inhibition of two proteins engaged in different signalling pathways within the RSR. While these two strategies were sparsely observed within the study, noteworthy instances emerged: the ‘lateral blockade’ approach involving *ATR* and *PARP* inhibitors in NBL[320] and the ‘vertical blockade’ strategy with *ATR* and *WEE1* inhibitors in ES[319], both displayed synergistic effects. Given the success of the ‘vertical blockade’ strategies in adult malignancies, it is conceivable that adopting a similar approach to target replication stress could potentially offer better therapeutic efficacy with fewer side effects in pediatric malignancies, in comparison to combination strategies involving chemotherapeutics and radiation. However, generating more preclinical research spanning all targets and pediatric tumor types is necessary to ascertain superior targets and strategy.

Enhancing treatment effectiveness relies not only on well-designed combination strategies, but also on robust preclinical investigations. With deeper understanding of the biological mechanisms governing a treatment approach, the selection of models or patients possessing the appropriate molecular background is improved, thus ensuring fair evaluation of the therapy. A prominent observation throughout our study was the evident scarcity of literature dedicated to unravelling the biological foundations of targeting replication stress for therapeutic purposes. ‘Predictive biomarkers’ and ‘resistance’ emerged as modules with notably limited representation, accounting for less than 10% of all evidence entries across all targets and tumor types. Furthermore, the

absence of reported tumor subtypes, and the omission of certain tumor types altogether, such as Inflammatory myofibroblastic tumor (IMT) and extracranial germ cell tumors (GCT), has been significant. While these gaps can to an extent be attributed to research prioritization and the availability of preclinical models, a more comprehensive representation across tumor (sub)types could yield valuable insights into treatment stratification and warrants attention in future studies. For example, the presence of the *EWS-FLI1* fusion gene (identified in approximately 85% of ES patients) has been associated with deficient DNA repair mechanisms, inefficient DNA transcription, and an overall increase in replication stress [322], [323]. In the scope of targeting replication stress, this could be a significant fusion event to consider for further studies.

Understanding the mechanisms of action of treatment therapies and the effects of diverse tumor types and subtypes might have on their functioning is pivotal for designing effective and successful clinical trials. The limited availability of literature exploring these aspects in our targeted actionability review (TAR) highlights a potential knowledge gap that needs to be addressed further.

### 4.3 Limitations

Despite the successful characterization of the n=251 ITCC-P4 PDX models and the extensive multi-omics analysis explored in the first study in this thesis, enabling the creation of a comprehensive resource for further personalized pediatric cancer research, some key challenges need to be tackled in the studies to come. The PDX model establishment is a technically intricate protocol that relies on high levels of expertise and a specific protocol for each tumor entity, hence there needs to be better technology that can automate and assist in the model generation. Considerable efforts also still need to be developed to improve systematic generation of under-represented tumor types and subgroups, enabling the collection of not only the most aggressive tumor subtypes that can resist the tumor microenvironment, but also rare and less aggressive subtypes of pediatric cancer. We also see a deficit of liquid models in this study, which should be included in successive studies, to have a comparative overview of different clinical models.

Finally, since this is a massive collaborative effort with several partner institutions, there is a lack of germline control samples from a significant number of patients, hence the establishment of a standardized protocol with collection of all required metadata information for optimized analysis is highly essential to avoid biases and overrepresentation. As this platform is constantly growing with inclusion of several PDX, GEMM and organoid models, with advancement in NGS tools and analysis, the inclusion of additional ChipSeq, ATACseq, DNA and RNA single-cell sequencing would be vital to get the most comprehensive overview of PDX models. These methods can further address gene regulation and epigenetic modifications and would be useful to

unveils cellular diversity, identifies rare cell types, and elucidates dynamic changes in gene expression during development, disease progression, or in response to treatments in PDX models compared to the patient tumor. In summary, this marks the first study established under the umbrella of the ITCC-P4 PDX model characterization and profiling, of it is imperative to optimize subsequent studies to expand and enhance this valuable resource for the future.

My second study highlighted the Target Actionability Review (TAR) methodology as a part of the ITCC-P4 sustainable platform. Although we successfully evaluated and created a structured overview of recently published literature (from 2015-2020), related to targeting replication stress, there are a few challenges that need to be addressed. *ATM*, *ATR*, *CHK1*, *DNA-PK*, *PARP* and *WEE1* were the top proteins for targeting replication stress. However, we see different amounts of published literature for each target, creating biases towards more well-known targets such as *PARP*. This makes it difficult to prioritize targets for future clinical studies. We also noticed a bias created by the aggressiveness of some tumor types, which was associated with more studies and data being published on them. The TAR methodology was created for single target identification but needs to be further refined for boarder topics such as replication stress to enable promising research with the hope of helping the development of safe and effective therapeutics for children with cancer.

## 4.4 Future directions

This study provides a comprehensive foundation for PDX model selection, with a strong focus on PDX model vs patient tumor comparison for future research focusing on pediatric cancer trials. There is an imperative need to establish an extensively curated resource of molecular data on pediatric tumors from relapsed and metastatic patients and their germline controls, from a wide range of tumor types and subtypes. We observe some PDX models showing multiple enriched targetable driver genes which are of further interest. A follow up analysis to co-relate co-occurring genomic events within tumor subgroups would be an opportunity for personalized anti-cancer therapy, as well as the expanding field of precision oncology.

As this study works in collaboration with 30 different partnering European academic and clinical institutions and pharmaceutical companies, it provides a unique setting for preclinical testing of novel molecularly targeted compounds. This study functions as the precursor to multiple drug treatment pipelines for phase-I clinical trials, for the identification of predictive biomarkers to allow for accurate matching of targets and drugs.

Models that have targetable alterations in these biomarkers will undergo thorough drug testing within faithful disease models that mimic pharmacokinetics and pharmacodynamics. One such example would be evaluation of drug penetration into the brain. The drug testing process will also encompass a minimum of three commonly used reference drugs across all models, serving as a basis for comparisons. This drug testing and chemotherapy arms on pre-selected PDX models has already begun for a few tumor types, such as single drug treatments of Copanlisib, Lorlatinib and Idasanutlin for neuroblastoma [324], [325]; Methotrexate, Cisplatin, for osteosarcoma [326], but also combination treatment options such as liposomal Doxorubicin and Cyclophosphamide for Ewing sarcomas[327]. This resource enables clinical stratification and expedites the development of improved drug prioritization for diverse pediatric tumor types. Establishing this platform through a collaboration between public and private partnership creates a cooperative framework that could potentially be expanded to various cancer entities and patient groups in the future.

The inclusion of the target actionability review within the ITCC-P4 framework allows for a systematically curated overview approach that facilitates further drug prioritization besides the data driven analysis conducted in the genomic profiling study. This study narrows down published literature and potential targets such as *ATM*, *ATR*, *CHK1*, *DNA-PK*, *PARP* and *WEE1*, focused on targeting replication stress. It also highlights the importance of exploring emerging targets further (for example: *WEE1* and *CHK1*) and the potential of using novel combination strategies for future studies. This combined resource would serve to greatly advance further understanding of pediatric solid tumor biology and lays a foundation for computational analysis for larger cohorts.

## 5 BIBLIOGRAPHY

- [1] H. Sung *et al.*, “Global Cancer Statistics 2020: GLOBOCAN Estimates of Incidence and Mortality Worldwide for 36 Cancers in 185 Countries.,” *CA Cancer J Clin*, vol. 71, no. 3, pp. 209–249, May 2021, doi: 10.3322/caac.21660.
- [2] R. L. Siegel, K. D. Miller, H. E. Fuchs, and A. Jemal, “Cancer statistics, 2022,” *CA Cancer J Clin*, vol. 72, no. 1, pp. 7–33, Jan. 2022, doi: 10.3322/caac.21708.
- [3] R. L. Siegel, K. D. Miller, N. S. Wagle, and A. Jemal, “Cancer statistics, 2023,” *CA Cancer J Clin*, vol. 73, no. 1, pp. 17–48, Jan. 2023, doi: 10.3322/caac.21763.
- [4] D. Hanahan and R. A. Weinberg, “The Hallmarks of Cancer,” *Cell*, vol. 100, no. 1, pp. 57–70, Jan. 2000, doi: 10.1016/S0092-8674(00)81683-9.
- [5] D. Hanahan and R. A. Weinberg, “Hallmarks of Cancer: The Next Generation,” *Cell*, vol. 144, no. 5, pp. 646–674, Mar. 2011, doi: 10.1016/j.cell.2011.02.013.
- [6] D. Hanahan, “Hallmarks of Cancer: New Dimensions,” *Cancer Discov*, vol. 12, no. 1, pp. 31–46, Jan. 2022, doi: 10.1158/2159-8290.CD-21-1059.
- [7] B. D. Preston, T. M. Albertson, and A. J. Herr, “DNA replication fidelity and cancer,” *Semin Cancer Biol*, vol. 20, no. 5, pp. 281–293, Oct. 2010, doi: 10.1016/j.semcancer.2010.10.009.
- [8] B. Miles and P. Tadi, *Genetics, Somatic Mutation*. 2023.
- [9] F. H. Crick, “Codon--anticodon pairing: the wobble hypothesis.,” *J Mol Biol*, vol. 19, no. 2, pp. 548–555, Aug. 1966, doi: 10.1016/s0022-2836(66)80022-0.
- [10] W. Meyerson, J. Leisman, F. C. P. Navarro, and M. Gerstein, “Origins and characterization of variants shared between databases of somatic and germline human mutations,” *BMC Bioinformatics*, vol. 21, no. 1, p. 227, Dec. 2020, doi: 10.1186/s12859-020-3508-8.
- [11] M. Pudjihartono, J. K. Perry, C. Print, J. M. O’Sullivan, and W. Schierding, “Interpretation of the role of germline and somatic non-coding mutations in cancer: expression and chromatin conformation informed analysis,” *Clin Epigenetics*, vol. 14, no. 1, p. 120, Dec. 2022, doi: 10.1186/s13148-022-01342-3.
- [12] W. R. Bodily *et al.*, “Effects of germline and somatic events in candidate BRCA-like genes on breast-tumor signatures.,” *PLoS One*, vol. 15, no. 9, p. e0239197, 2020, doi: 10.1371/journal.pone.0239197.
- [13] Z. Li, H. Wang, Z. Zhang, X. Meng, D. Liu, and Y. Tang, “Germline and somatic mutation profile in Cancer patients revealed by a medium-sized pan-Cancer panel,” *Genomics*, vol. 113, no. 4, pp. 1930–1939, Jul. 2021, doi: 10.1016/j.ygeno.2021.04.029.
- [14] F. Dubois, N. Sidiropoulos, J. Weischenfeldt, and R. Beroukhim, “Structural variations in cancer and the 3D genome.,” *Nat Rev Cancer*, vol. 22, no. 9, pp. 533–546, Sep. 2022, doi: 10.1038/s41568-022-00488-9.
- [15] G. A. Logsdon, M. R. Vollger, and E. E. Eichler, “Long-read human genome sequencing and its applications.,” *Nat Rev Genet*, vol. 21, no. 10, pp. 597–614, Oct. 2020, doi: 10.1038/s41576-020-0236-x.
- [16] C. Mérot, R. A. Oomen, A. Tigano, and M. Wellenreuther, “A Roadmap for Understanding the Evolutionary Significance of Structural Genomic Variation,” *Trends Ecol Evol*, vol. 35, no. 7, pp. 561–572, Jul. 2020, doi: 10.1016/j.tree.2020.03.002.
- [17] P. H. Sudmant *et al.*, “An integrated map of structural variation in 2,504 human genomes.,” *Nature*, vol. 526, no. 7571, pp. 75–81, Oct. 2015, doi: 10.1038/nature15394.

- [18] P. H. Sudmant *et al.*, “Diversity of human copy number variation and multicopy genes,” *Science*, vol. 330, no. 6004, pp. 641–6, Oct. 2010, doi: 10.1126/science.1197005.
- [19] L. E. Macconail and L. A. Garraway, “Clinical implications of the cancer genome,” *J Clin Oncol*, vol. 28, no. 35, pp. 5219–28, Dec. 2010, doi: 10.1200/JCO.2009.27.4944.
- [20] I. A. E. M. van Belzen, A. Schönhuth, P. Kemmeren, and J. Y. Hehir-Kwa, “Structural variant detection in cancer genomes: computational challenges and perspectives for precision oncology,” *NPJ Precis Oncol*, vol. 5, no. 1, p. 15, Mar. 2021, doi: 10.1038/s41698-021-00155-6.
- [21] K. Yi and Y. S. Ju, “Patterns and mechanisms of structural variations in human cancer,” *Exp Mol Med*, vol. 50, no. 8, pp. 1–11, Aug. 2018, doi: 10.1038/s12276-018-0112-3.
- [22] A. Shlien and D. Malkin, “Copy number variations and cancer,” *Genome Med*, vol. 1, no. 6, p. 62, Jun. 2009, doi: 10.1186/gm62.
- [23] K. Taniue and N. Akimitsu, “Fusion Genes and RNAs in Cancer Development,” *Noncoding RNA*, vol. 7, no. 1, Feb. 2021, doi: 10.3390/ncrna7010010.
- [24] J. ZHENG, “Oncogenic chromosomal translocations and human cancer (Review),” *Oncol Rep*, vol. 30, no. 5, pp. 2011–2019, Nov. 2013, doi: 10.3892/or.2013.2677.
- [25] P. C. NOWELL and D. A. HUNGERFORD, “Chromosome studies on normal and leukemic human leukocytes,” *J Natl Cancer Inst*, vol. 25, pp. 85–109, Jul. 1960.
- [26] B. C. Parker and W. Zhang, “Fusion genes in solid tumors: an emerging target for cancer diagnosis and treatment,” *Chin J Cancer*, vol. 32, no. 11, pp. 594–603, Nov. 2013, doi: 10.5732/cjc.013.10178.
- [27] F. Mertens, B. Johansson, T. Fioretos, and F. Mitelman, “The emerging complexity of gene fusions in cancer,” *Nat Rev Cancer*, vol. 15, no. 6, pp. 371–81, Jun. 2015, doi: 10.1038/nrc3947.
- [28] D. Ostroverkhova, T. M. Przytycka, and A. R. Panchenko, “Cancer driver mutations: predictions and reality,” *Trends Mol Med*, vol. 29, no. 7, pp. 554–566, Jul. 2023, doi: 10.1016/j.molmed.2023.03.007.
- [29] J. R. Pon and M. A. Marra, “Driver and Passenger Mutations in Cancer,” *Annual Review of Pathology: Mechanisms of Disease*, vol. 10, no. 1, pp. 25–50, Jan. 2015, doi: 10.1146/annurev-pathol-012414-040312.
- [30] M. V. and E. E. Glennis Logsdon, “‘Review: How Long-Read Sequencing Is Revealing Unseen Genomic Variation’ -HUMAN GENETICS RESEARCH (<https://www.pacb.com/human-genetics-research/review-how-long-read-sequencing-is-revealing-unseen-genomic-variation/>),” HUMAN GENETICS RESEARCH.
- [31] M. Macheret and T. D. Halazonetis, “DNA replication stress as a hallmark of cancer,” *Annu Rev Pathol*, vol. 10, pp. 425–48, 2015, doi: 10.1146/annurev-pathol-012414-040424.
- [32] S. Ortega, M. Malumbres, and M. Barbacid, “Cyclin D-dependent kinases, INK4 inhibitors and cancer,” *Biochim Biophys Acta*, vol. 1602, no. 1, pp. 73–87, Mar. 2002, doi: 10.1016/s0304-419x(02)00037-9.
- [33] A. Bric *et al.*, “Functional Identification of Tumor-Suppressor Genes through an In Vivo RNA Interference Screen in a Mouse Lymphoma Model,” *Cancer Cell*, vol. 16, no. 4, pp. 324–335, Oct. 2009, doi: 10.1016/j.ccr.2009.08.015.
- [34] L. H. Hartwell and M. B. Kastan, “Cell Cycle Control and Cancer,” *Science (1979)*, vol. 266, no. 5192, pp. 1821–1828, Dec. 1994, doi: 10.1126/science.7997877.
- [35] E. Y. H. P. Lee and W. J. Muller, “Oncogenes and tumor suppressor genes,” *Cold Spring Harb Perspect Biol*, vol. 2, no. 10, p. a003236, Oct. 2010, doi: 10.1101/cshperspect.a003236.

- [36] W. C. Hahn and R. A. Weinberg, "Rules for making human tumor cells.," *N Engl J Med*, vol. 347, no. 20, pp. 1593–603, Nov. 2002, doi: 10.1056/NEJMra021902.
- [37] B. P. Kopnin, "Targets of oncogenes and tumor suppressors: key for understanding basic mechanisms of carcinogenesis.," *Biochemistry (Mosc)*, vol. 65, no. 1, pp. 2–27, Jan. 2000.
- [38] Y. Li, Y. Zhang, X. Li, S. Yi, and J. Xu, "Gain-of-Function Mutations: An Emerging Advantage for Cancer Biology.," *Trends Biochem Sci*, vol. 44, no. 8, pp. 659–674, Aug. 2019, doi: 10.1016/j.tibs.2019.03.009.
- [39] C. G. Broustas and H. B. Lieberman, "DNA damage response genes and the development of cancer metastasis.," *Radiat Res*, vol. 181, no. 2, pp. 111–30, Feb. 2014, doi: 10.1667/RR13515.1.
- [40] C. R. Boland, "Roles of the DNA mismatch repair genes in colorectal tumorigenesis.," *Int J Cancer*, vol. 69, no. 1, pp. 47–9, Feb. 1996, doi: 10.1002/(SICI)1097-0215(19960220)69:1<47::AID-IJC11>3.0.CO;2-H.
- [41] L. H. Thompson, "Properties and applications of human DNA repair genes.," *Mutat Res*, vol. 247, no. 2, pp. 213–9, Apr. 1991, doi: 10.1016/0027-5107(91)90017-i.
- [42] A. Ronen and B. W. Glickman, "Human DNA repair genes.," *Environ Mol Mutagen*, vol. 37, no. 3, pp. 241–83, 2001, doi: 10.1002/em.1033.
- [43] K. Cong and S. B. Cantor, "Exploiting replication gaps for cancer therapy.," *Mol Cell*, vol. 82, no. 13, pp. 2363–2369, Jul. 2022, doi: 10.1016/j.molcel.2022.04.023.
- [44] T. Ubhi and G. W. Brown, "Exploiting DNA Replication Stress for Cancer Treatment.," *Cancer Res*, vol. 79, no. 8, pp. 1730–1739, Apr. 2019, doi: 10.1158/0008-5472.CAN-18-3631.
- [45] R. L. Schilsky, "Personalized medicine in oncology: the future is now.," *Nat Rev Drug Discov*, vol. 9, no. 5, pp. 363–366, May 2010, doi: 10.1038/nrd3181.
- [46] J. Zugazagoitia, C. Guedes, S. Ponce, I. Ferrer, S. Molina-Pinelo, and L. Paz-Ares, "Current Challenges in Cancer Treatment.," *Clin Ther*, vol. 38, no. 7, pp. 1551–66, Jul. 2016, doi: 10.1016/j.clinthera.2016.03.026.
- [47] D. T. Debela *et al.*, "New approaches and procedures for cancer treatment: Current perspectives.," *SAGE Open Med*, vol. 9, p. 20503121211034370, 2021, doi: 10.1177/20503121211034366.
- [48] L. Falzone, S. Salomone, and M. Libra, "Evolution of Cancer Pharmacological Treatments at the Turn of the Third Millennium.," *Front Pharmacol*, vol. 9, Nov. 2018, doi: 10.3389/fphar.2018.01300.
- [49] P. Sharma, V. Jhawar, P. Mathur, and R. Dutt, "Innovation in cancer therapeutics and regulatory perspectives.," *Medical Oncology*, vol. 39, no. 5, p. 76, May 2022, doi: 10.1007/s12032-022-01677-0.
- [50] Z. Agur, M. Elishmereni, U. Foryś, and Y. Kogan, "Accelerating the Development of Personalized Cancer Immunotherapy by Integrating Molecular Patients' Profiles with Dynamic Mathematical Models.," *Clin Pharmacol Ther*, vol. 108, no. 3, pp. 515–527, Sep. 2020, doi: 10.1002/cpt.1942.
- [51] M. Kalia, "Personalized oncology: recent advances and future challenges.," *Metabolism*, vol. 62 Suppl 1, pp. S11-4, Jan. 2013, doi: 10.1016/j.metabol.2012.08.016.
- [52] E. R. Malone, M. Oliva, P. J. B. Sabatini, T. L. Stockley, and L. L. Siu, "Molecular profiling for precision cancer therapies.," *Genome Med*, vol. 12, no. 1, p. 8, Dec. 2020, doi: 10.1186/s13073-019-0703-1.

- [53] B. E. Slatko, A. F. Gardner, and F. M. Ausubel, "Overview of Next-Generation Sequencing Technologies.," *Curr Protoc Mol Biol*, vol. 122, no. 1, p. e59, Apr. 2018, doi: 10.1002/cpmb.59.
- [54] E. R. Mardis, "A decade's perspective on DNA sequencing technology.," *Nature*, vol. 470, no. 7333, pp. 198–203, Feb. 2011, doi: 10.1038/nature09796.
- [55] E. E. Schadt, S. Turner, and A. Kasarskis, "A window into third-generation sequencing.," *Hum Mol Genet*, vol. 19, no. R2, pp. R227–40, Oct. 2010, doi: 10.1093/hmg/ddq416.
- [56] M. J. Bamshad *et al.*, "Exome sequencing as a tool for Mendelian disease gene discovery.," *Nat Rev Genet*, vol. 12, no. 11, pp. 745–55, Sep. 2011, doi: 10.1038/nrg3031.
- [57] M. J. Clark *et al.*, "Performance comparison of exome DNA sequencing technologies.," *Nat Biotechnol*, vol. 29, no. 10, pp. 908–14, Sep. 2011, doi: 10.1038/nbt.1975.
- [58] E. Y. Zhao, M. Jones, and S. J. M. Jones, "Whole-Genome Sequencing in Cancer.," *Cold Spring Harb Perspect Med*, vol. 9, no. 3, Mar. 2019, doi: 10.1101/cshperspect.a034579.
- [59] L. Sabour, M. Sabour, and S. Ghorbian, "Clinical Applications of Next-Generation Sequencing in Cancer Diagnosis.," *Pathol Oncol Res*, vol. 23, no. 2, pp. 225–234, Apr. 2017, doi: 10.1007/s12253-016-0124-z.
- [60] C. S. Pareek, R. Smoczynski, and A. Tretyn, "Sequencing technologies and genome sequencing.," *J Appl Genet*, vol. 52, no. 4, pp. 413–35, Nov. 2011, doi: 10.1007/s13353-011-0057-x.
- [61] L. D. Moore, T. Le, and G. Fan, "DNA Methylation and Its Basic Function," *Neuropsychopharmacology*, vol. 38, no. 1, pp. 23–38, Jan. 2013, doi: 10.1038/npp.2012.112.
- [62] A. Schumacher, "Microarray-based DNA methylation profiling: technology and applications," *Nucleic Acids Res*, vol. 34, no. 2, pp. 528–542, Jan. 2006, doi: 10.1093/nar/gkj461.
- [63] B. van Steensel and S. Henikoff, "Epigenomic profiling using microarrays.," *Biotechniques*, vol. 35, no. 2, pp. 346–50, 352–4, 356–7, Aug. 2003, doi: 10.2144/03352rv01.
- [64] A. Schumacher, "Microarray-based DNA methylation profiling: technology and applications," *Nucleic Acids Res*, vol. 34, no. 2, pp. 528–542, Jan. 2006, doi: 10.1093/nar/gkj461.
- [65] K. Galbraith and M. Snuderl, "DNA methylation as a diagnostic tool.," *Acta Neuropathol Commun*, vol. 10, no. 1, p. 71, May 2022, doi: 10.1186/s40478-022-01371-2.
- [66] C. Virtanen and J. Woodgett, "Clinical Uses of Microarrays in Cancer Research," 2008, pp. 87–113. doi: 10.1007/978-1-60327-148-6\_6.
- [67] B. van Steensel and S. Henikoff, "Epigenomic profiling using microarrays," *Biotechniques*, vol. 35, no. 2, pp. 346–357, Aug. 2003, doi: 10.2144/03352rv01.
- [68] Y. J. Heo, C. Hwa, G.-H. Lee, J.-M. Park, and J.-Y. An, "Integrative Multi-Omics Approaches in Cancer Research: From Biological Networks to Clinical Subtypes," *Mol Cells*, vol. 44, no. 7, pp. 433–443, Jul. 2021, doi: 10.14348/molcells.2021.0042.
- [69] M. Olivier, R. Asmis, G. A. Hawkins, T. D. Howard, and L. A. Cox, "The Need for Multi-Omics Biomarker Signatures in Precision Medicine," *Int J Mol Sci*, vol. 20, no. 19, p. 4781, Sep. 2019, doi: 10.3390/ijms20194781.
- [70] D. Chakravarty and D. B. Solit, "Clinical cancer genomic profiling," *Nat Rev Genet*, vol. 22, no. 8, pp. 483–501, Aug. 2021, doi: 10.1038/s41576-021-00338-8.

- [71] Y. Xiao, M. Bi, H. Guo, and M. Li, "Multi-omics approaches for biomarker discovery in early ovarian cancer diagnosis," *EBioMedicine*, vol. 79, p. 104001, May 2022, doi: 10.1016/j.ebiom.2022.104001.
- [72] M. Olivier, R. Asmis, G. A. Hawkins, T. D. Howard, and L. A. Cox, "The Need for Multi-Omics Biomarker Signatures in Precision Medicine.," *Int J Mol Sci*, vol. 20, no. 19, Sep. 2019, doi: 10.3390/ijms20194781.
- [73] Max Roser and Hannah Ritchie, "'Cancer'. Published online at OurWorldInData.org. Retrieved from: 'https://ourworldindata.org/cancer' ."
- [74] L. M. Force *et al.*, "The global burden of childhood and adolescent cancer in 2017: an analysis of the Global Burden of Disease Study 2017," *Lancet Oncol*, vol. 20, no. 9, pp. 1211–1225, Sep. 2019, doi: 10.1016/S1470-2045(19)30339-0.
- [75] K. D. Miller *et al.*, "Cancer treatment and survivorship statistics, 2022.," *CA Cancer J Clin*, vol. 72, no. 5, pp. 409–436, Sep. 2022, doi: 10.3322/caac.21731.
- [76] K. D. Miller *et al.*, "Cancer treatment and survivorship statistics, 2016.," *CA Cancer J Clin*, vol. 66, no. 4, pp. 271–89, Jul. 2016, doi: 10.3322/caac.21349.
- [77] "European Commission - ECIS - European Cancer Information System," <https://ecis.jrc.ec.europa.eu/>.
- [78] Z. J. Ward, J. M. Yeh, N. Bhakta, A. L. Frazier, and R. Atun, "Estimating the total incidence of global childhood cancer: a simulation-based analysis," *Lancet Oncol*, vol. 20, no. 4, pp. 483–493, Apr. 2019, doi: 10.1016/S1470-2045(18)30909-4.
- [79] E. Ward, C. DeSantis, A. Robbins, B. Kohler, and A. Jemal, "Childhood and adolescent cancer statistics, 2014," *CA Cancer J Clin*, vol. 64, no. 2, pp. 83–103, Mar. 2014, doi: 10.3322/caac.21219.
- [80] L. M. Kopp, P. Gupta, L. Pelayo-Katsanis, B. Wittman, and E. Katsanis, "Late effects in adult survivors of pediatric cancer: a guide for the primary care physician.," *Am J Med*, vol. 125, no. 7, pp. 636–41, Jul. 2012, doi: 10.1016/j.amjmed.2012.01.013.
- [81] P. E. Bidstrup *et al.*, "Effects on Pediatric Cancer Survivors: The FAMily-Oriented Support (FAMOS) Randomized Controlled Trial.," *J Pediatr Psychol*, vol. 48, no. 1, pp. 29–38, Jan. 2023, doi: 10.1093/jpepsy/jsac062.
- [82] I. Schuitema, T. Alexander, M. M. Hudson, K. R. Krull, and K. Edelstein, "Aging in Adult Survivors of Childhood Cancer: Implications for Future Care," *Journal of Clinical Oncology*, vol. 39, no. 16, pp. 1741–1751, Jun. 2021, doi: 10.1200/JCO.20.02534.
- [83] D. T. W. Jones *et al.*, "Molecular characteristics and therapeutic vulnerabilities across paediatric solid tumours," *Nat Rev Cancer*, vol. 19, no. 8, pp. 420–438, Aug. 2019, doi: 10.1038/s41568-019-0169-x.
- [84] S. N. Gröbner *et al.*, "The landscape of genomic alterations across childhood cancers," *Nature*, vol. 555, no. 7696, pp. 321–327, Mar. 2018, doi: 10.1038/nature25480.
- [85] C. Kandoth *et al.*, "Mutational landscape and significance across 12 major cancer types.," *Nature*, vol. 502, no. 7471, pp. 333–339, Oct. 2013, doi: 10.1038/nature12634.
- [86] G. M. Brodeur, K. E. Nichols, S. E. Plon, J. D. Schiffman, and D. Malkin, "Pediatric Cancer Predisposition and Surveillance: An Overview, and a Tribute to Alfred G. Knudson Jr.," *Clin Cancer Res*, vol. 23, no. 11, pp. e1–e5, Jun. 2017, doi: 10.1158/1078-0432.CCR-17-0702.
- [87] K. Huang *et al.*, "Pathogenic Germline Variants in 10,389 Adult Cancers," *Cell*, vol. 173, no. 2, pp. 355-370.e14, Apr. 2018, doi: 10.1016/j.cell.2018.03.039.
- [88] J. Zhang *et al.*, "Germline Mutations in Predisposition Genes in Pediatric Cancer," *New England Journal of Medicine*, vol. 373, no. 24, pp. 2336–2346, Dec. 2015, doi: 10.1056/NEJMoa1508054.

- [89] F. Saletta, L. Dalla Pozza, and J. A. Byrne, "Genetic causes of cancer predisposition in children and adolescents.," *Transl Pediatr*, vol. 4, no. 2, pp. 67–75, Apr. 2015, doi: 10.3978/j.issn.2224-4336.2015.04.08.
- [90] S. Pakakasama and G. E. Tomlinson, "Genetic predisposition and screening in pediatric cancer.," *Pediatr Clin North Am*, vol. 49, no. 6, pp. 1393–413, Dec. 2002, doi: 10.1016/s0031-3955(02)00095-0.
- [91] S. A. Frank, "Genetic predisposition to cancer - insights from population genetics.," *Nat Rev Genet*, vol. 5, no. 10, pp. 764–72, Oct. 2004, doi: 10.1038/nrg1450.
- [92] P. Kattner *et al.*, "Compare and contrast: pediatric cancer versus adult malignancies," *Cancer and Metastasis Reviews*, vol. 38, no. 4, pp. 673–682, Dec. 2019, doi: 10.1007/s10555-019-09836-y.
- [93] M. C. de Jong, W. A. Kors, P. de Graaf, J. A. Castelijns, T. Kivelä, and A. C. Moll, "Trilateral retinoblastoma: a systematic review and meta-analysis," *Lancet Oncol*, vol. 15, no. 10, pp. 1157–1167, Sep. 2014, doi: 10.1016/S1470-2045(14)70336-5.
- [94] M. Kool *et al.*, "Genome sequencing of SHH medulloblastoma predicts genotype-related response to smoothed inhibition.," *Cancer Cell*, vol. 25, no. 3, pp. 393–405, Mar. 2014, doi: 10.1016/j.ccr.2014.02.004.
- [95] S. Subramanian and T. Ahmad, *Childhood Brain Tumors*. 2023.
- [96] A. Gajjar, D. C. Bowers, M. A. Karajannis, S. Leary, H. Witt, and N. G. Gottardo, "Pediatric Brain Tumors: Innovative Genomic Information Is Transforming the Diagnostic and Clinical Landscape.," *J Clin Oncol*, vol. 33, no. 27, pp. 2986–98, Sep. 2015, doi: 10.1200/JCO.2014.59.9217.
- [97] Q. T. Ostrom *et al.*, "CBTRUS Statistical Report: Primary Brain and Other Central Nervous System Tumors Diagnosed in the United States in 2012-2016.," *Neuro Oncol*, vol. 21, no. Suppl 5, pp. v1–v100, Nov. 2019, doi: 10.1093/neuonc/noz150.
- [98] D. N. Louis *et al.*, "The 2021 WHO Classification of Tumors of the Central Nervous System: a summary.," *Neuro Oncol*, vol. 23, no. 8, pp. 1231–1251, Aug. 2021, doi: 10.1093/neuonc/noab106.
- [99] M. Antonelli and P. L. Poliani, "Adult type diffuse gliomas in the new 2021 WHO Classification.," *Pathologica*, vol. 114, no. 6, pp. 397–409, Dec. 2022, doi: 10.32074/1591-951X-823.
- [100] B. T. Whitfield and J. T. Huse, "Classification of adult-type diffuse gliomas: Impact of the World Health Organization 2021 update.," *Brain Pathol*, vol. 32, no. 4, p. e13062, Jul. 2022, doi: 10.1111/bpa.13062.
- [101] D. Sturm, S. M. Pfister, and D. T. W. Jones, "Pediatric Gliomas: Current Concepts on Diagnosis, Biology, and Clinical Management," *Journal of Clinical Oncology*, vol. 35, no. 21, pp. 2370–2377, Jul. 2017, doi: 10.1200/JCO.2017.73.0242.
- [102] T. Milde, F. J. Rodriguez, J. S. Barnholtz-Sloan, N. Patil, C. G. Eberhart, and D. H. Gutmann, "Reimagining pilocytic astrocytomas in the context of pediatric low-grade gliomas.," *Neuro Oncol*, vol. 23, no. 10, pp. 1634–1646, Oct. 2021, doi: 10.1093/neuonc/noab138.
- [103] A. R. Quiroz Tejada *et al.*, "Gangliogliomas in the pediatric population.," *Childs Nerv Syst*, vol. 37, no. 3, pp. 831–837, Mar. 2021, doi: 10.1007/s00381-020-04900-3.
- [104] C. A. López-Pérez, X. Franco-Mojica, R. Villanueva-Gaona, A. Díaz-Alba, M. A. Rodríguez-Flórida, and V. G. Navarro, "Adult diffuse midline gliomas H3 K27-altered: review of a redefined entity.," *J Neurooncol*, vol. 158, no. 3, pp. 369–378, Jul. 2022, doi: 10.1007/s11060-022-04024-5.

- [105] J. D. Schulte *et al.*, “Clinical, radiologic, and genetic characteristics of histone H3 K27M-mutant diffuse midline gliomas in adults,” *Neurooncol Adv*, vol. 2, no. 1, Jan. 2020, doi: 10.1093/NOAJNL/VDA4142.
- [106] C. Antin *et al.*, “EZHIP is a specific diagnostic biomarker for posterior fossa ependymomas, group PFA and diffuse midline gliomas H3-WT with EZHIP overexpression,” *Acta Neuropathol Commun*, vol. 8, no. 1, p. 183, Dec. 2020, doi: 10.1186/s40478-020-01056-8.
- [107] I. J. Findlay *et al.*, “Pharmaco-proteogenomic profiling of pediatric diffuse midline glioma to inform future treatment strategies,” *Oncogene*, vol. 41, no. 4, pp. 461–475, Jan. 2022, doi: 10.1038/s41388-021-02102-y.
- [108] C. Park *et al.*, “Clinical and Genomic Characteristics of Adult Diffuse Midline Glioma,” *Cancer Res Treat*, vol. 53, no. 2, pp. 389–398, Apr. 2021, doi: 10.4143/crt.2020.694.
- [109] D. A. Solomon *et al.*, “Diffuse Midline Gliomas with Histone H3-K27M Mutation: A Series of 47 Cases Assessing the Spectrum of Morphologic Variation and Associated Genetic Alterations,” *Brain Pathology*, vol. 26, no. 5, pp. 569–580, Sep. 2016, doi: 10.1111/bpa.12336.
- [110] I. J. Findlay *et al.*, “Pharmaco-proteogenomic profiling of pediatric diffuse midline glioma to inform future treatment strategies,” *Oncogene*, vol. 41, no. 4, pp. 461–475, Jan. 2022, doi: 10.1038/s41388-021-02102-y.
- [111] S. Bender *et al.*, “Reduced H3K27me3 and DNA Hypomethylation Are Major Drivers of Gene Expression in K27M Mutant Pediatric High-Grade Gliomas,” *Cancer Cell*, vol. 24, no. 5, pp. 660–672, Nov. 2013, doi: 10.1016/j.ccr.2013.10.006.
- [112] U. Schüller *et al.*, “Mutations within FGFR1 are associated with superior outcome in a series of 83 diffuse midline gliomas with H3F3A K27M mutations,” *Acta Neuropathol*, vol. 141, no. 2, pp. 323–325, Feb. 2021, doi: 10.1007/s00401-020-02259-y.
- [113] J. Schwartzentruber *et al.*, “Driver mutations in histone H3.3 and chromatin remodelling genes in paediatric glioblastoma,” *Nature*, vol. 482, no. 7384, pp. 226–231, Feb. 2012, doi: 10.1038/nature10833.
- [114] C. Marlow, J. A. Cuoco, A. R. Hoggarth, M. S. Stump, L. S. Apfel, and C. M. Rogers, “Pediatric diffuse hemispheric glioma H3 G34-mutant with gains of the BRAF locus: An illustrative case,” *Rare Tumors*, vol. 15, p. 20363613231168704, 2023, doi: 10.1177/20363613231168704.
- [115] A. Lasocki, G. Abdalla, G. Chow, and S. C. Thust, “Imaging features associated with H3 K27-altered and H3 G34-mutant gliomas: a narrative systematic review,” *Cancer Imaging*, vol. 22, no. 1, p. 63, Nov. 2022, doi: 10.1186/s40644-022-00500-3.
- [116] K. Bender *et al.*, “Diffuse paediatric-type high-grade glioma, H3-wildtype and IDH-wildtype: case series of a new entity,” *Brain Tumor Pathol*, Aug. 2023, doi: 10.1007/s10014-023-00468-3.
- [117] S. M. Pfister *et al.*, “A Summary of the Inaugural WHO Classification of Pediatric Tumors: Transitioning from the Optical into the Molecular Era,” *Cancer Discov*, vol. 12, no. 2, pp. 331–355, Feb. 2022, doi: 10.1158/2159-8290.CD-21-1094.
- [118] W. Hu, L. Yuan, and J. Zeng, “HGG-01. INFANT-TYPE HEMISPHERIC GLIOMA: NEW MOLECULAR ALTERATIONS AND PRECISION-MEDICINE TREATMENT,” *Neuro Oncol*, vol. 25, no. Supplement\_1, pp. i38–i38, Jun. 2023, doi: 10.1093/neuonc/noad073.150.
- [119] M. R. Garcia, L. Bell, C. Miller, and D. Segal, “A Case of Infant-Type Hemispheric Glioma with *NTRK1* Fusion,” *Child Neurol Open*, vol. 9, p. 2329048X2211469, Jan. 2022, doi: 10.1177/2329048X221146982.

- [120] N. Gene-Olaciregui *et al.*, “Clinical and Molecular Evolution of an *ALK* -Driven Infant-Type Hemispheric Glioma Treated Sequentially With Second- and Third-Generation Anaplastic Lymphoma Kinase Inhibitors,” *JCO Precis Oncol*, no. 7, Mar. 2023, doi: 10.1200/PO.22.00547.
- [121] A. Jenseit, A. Camgöz, S. M. Pfister, and M. Kool, “EZHIP: a new piece of the puzzle towards understanding pediatric posterior fossa ependymoma,” *Acta Neuropathol*, vol. 143, no. 1, pp. 1–13, Jan. 2022, doi: 10.1007/s00401-021-02382-4.
- [122] K. W. Pajtler *et al.*, “Molecular Classification of Ependymal Tumors across All CNS Compartments, Histopathological Grades, and Age Groups,” *Cancer Cell*, vol. 27, no. 5, pp. 728–743, May 2015, doi: 10.1016/j.ccell.2015.04.002.
- [123] C. Kresbach, S. Neyazi, and U. Schüller, “Updates in the classification of ependymal neoplasms: The 2021 WHO Classification and beyond,” *Brain Pathology*, vol. 32, no. 4, Jul. 2022, doi: 10.1111/bpa.13068.
- [124] F. Andreiuolo *et al.*, “Childhood supratentorial ependymomas with *YAP1-MAMLD1* fusion: an entity with characteristic clinical, radiological, cytogenetic and histopathological features,” *Brain Pathology*, vol. 29, no. 2, pp. 205–216, Mar. 2019, doi: 10.1111/bpa.12659.
- [125] L. V. Baroni *et al.*, “Ultra high-risk PFA ependymoma is characterized by loss of chromosome 6q,” *Neuro Oncol*, vol. 23, no. 8, pp. 1360–1370, Aug. 2021, doi: 10.1093/neuonc/noab034.
- [126] V. Hovestadt, O. Ayrault, F. J. Swartling, G. W. Robinson, S. M. Pfister, and P. A. Northcott, “Medulloblastomics revisited: biological and clinical insights from thousands of patients,” *Nat Rev Cancer*, vol. 20, no. 1, pp. 42–56, Jan. 2020, doi: 10.1038/s41568-019-0223-8.
- [127] F. M. G. Cavalli *et al.*, “Intertumoral Heterogeneity within Medulloblastoma Subgroups,” *Cancer Cell*, vol. 31, no. 6, pp. 737–754.e6, Jun. 2017, doi: 10.1016/j.ccell.2017.05.005.
- [128] M. D. Taylor *et al.*, “Molecular subgroups of medulloblastoma: the current consensus,” *Acta Neuropathol*, vol. 123, no. 4, pp. 465–472, Apr. 2012, doi: 10.1007/s00401-011-0922-z.
- [129] R. Kumar, A. P. Y. Liu, and P. A. Northcott, “Medulloblastoma genomics in the modern molecular era,” *Brain Pathology*, vol. 30, no. 3, pp. 679–690, May 2020, doi: 10.1111/bpa.12804.
- [130] A. Surun *et al.*, “Medulloblastomas associated with an APC germline pathogenic variant share the good prognosis of CTNNB1-mutated medulloblastomas,” *Neuro Oncol*, vol. 22, no. 1, pp. 128–138, Jan. 2020, doi: 10.1093/neuonc/noz154.
- [131] L. A. Donehower *et al.*, “Integrated Analysis of TP53 Gene and Pathway Alterations in The Cancer Genome Atlas,” *Cell Rep*, vol. 28, no. 5, pp. 1370–1384.e5, Jul. 2019, doi: 10.1016/j.celrep.2019.07.001.
- [132] M. Kool *et al.*, “Integrated Genomics Identifies Five Medulloblastoma Subtypes with Distinct Genetic Profiles, Pathway Signatures and Clinicopathological Features,” *PLoS One*, vol. 3, no. 8, p. e3088, Aug. 2008, doi: 10.1371/journal.pone.0003088.
- [133] P. A. Northcott *et al.*, “The whole-genome landscape of medulloblastoma subtypes,” *Nature*, vol. 547, no. 7663, pp. 311–317, Jul. 2017, doi: 10.1038/nature22973.
- [134] T. G. Oliver *et al.*, “Transcriptional profiling of the Sonic hedgehog response: A critical role for N-myc in proliferation of neuronal precursors,” *Proceedings of the National Academy of Sciences*, vol. 100, no. 12, pp. 7331–7336, Jun. 2003, doi: 10.1073/pnas.0832317100.

- [135] M. Duman-Scheel, L. Weng, S. Xin, and W. Du, "Hedgehog regulates cell growth and proliferation by inducing Cyclin D and Cyclin E," *Nature*, vol. 417, no. 6886, pp. 299–304, May 2002, doi: 10.1038/417299a.
- [136] N. Zhukova *et al.*, "Subgroup-Specific Prognostic Implications of *TP53* Mutation in Medulloblastoma," *Journal of Clinical Oncology*, vol. 31, no. 23, pp. 2927–2935, Aug. 2013, doi: 10.1200/JCO.2012.48.5052.
- [137] M. Kool *et al.*, "Genome Sequencing of SHH Medulloblastoma Predicts Genotype-Related Response to Smoothed Inhibition," *Cancer Cell*, vol. 25, no. 3, pp. 393–405, Mar. 2014, doi: 10.1016/j.ccr.2014.02.004.
- [138] C. Metcalfe *et al.*, "PTEN Loss Mitigates the Response of Medulloblastoma to Hedgehog Pathway Inhibition," *Cancer Res*, vol. 73, no. 23, pp. 7034–7042, Dec. 2013, doi: 10.1158/0008-5472.CAN-13-1222.
- [139] D. J. H. Shih *et al.*, "Cytogenetic Prognostication Within Medulloblastoma Subgroups," *Journal of Clinical Oncology*, vol. 32, no. 9, pp. 886–896, Mar. 2014, doi: 10.1200/JCO.2013.50.9539.
- [140] M. Mynarek *et al.*, "Nonmetastatic Medulloblastoma of Early Childhood: Results From the Prospective Clinical Trial HIT-2000 and An Extended Validation Cohort," *Journal of Clinical Oncology*, vol. 38, no. 18, pp. 2028–2040, Jun. 2020, doi: 10.1200/JCO.19.03057.
- [141] U. Schüller *et al.*, "Acquisition of Granule Neuron Precursor Identity Is a Critical Determinant of Progenitor Cell Competence to Form Shh-Induced Medulloblastoma," *Cancer Cell*, vol. 14, no. 2, pp. 123–134, Aug. 2008, doi: 10.1016/j.ccr.2008.07.005.
- [142] C. Y. Lin *et al.*, "Active medulloblastoma enhancers reveal subgroup-specific cellular origins," *Nature*, vol. 530, no. 7588, pp. 57–62, Feb. 2016, doi: 10.1038/nature16546.
- [143] S. Pfister *et al.*, "Outcome Prediction in Pediatric Medulloblastoma Based on DNA Copy-Number Aberrations of Chromosomes 6q and 17q and the *MYC* and *MYCN* Loci," *Journal of Clinical Oncology*, vol. 27, no. 10, pp. 1627–1636, Apr. 2009, doi: 10.1200/JCO.2008.17.9432.
- [144] Y. Pei *et al.*, "An Animal Model of MYC-Driven Medulloblastoma," *Cancer Cell*, vol. 21, no. 2, pp. 155–167, Feb. 2012, doi: 10.1016/j.ccr.2011.12.021.
- [145] D. Kawauchi *et al.*, "A Mouse Model of the Most Aggressive Subgroup of Human Medulloblastoma," *Cancer Cell*, vol. 21, no. 2, pp. 168–180, Feb. 2012, doi: 10.1016/j.ccr.2011.12.023.
- [146] D. T. W. Jones *et al.*, "Dissecting the genomic complexity underlying medulloblastoma," *Nature*, vol. 488, no. 7409, pp. 100–105, Aug. 2012, doi: 10.1038/nature11284.
- [147] P. A. Northcott *et al.*, "Subgroup-specific structural variation across 1,000 medulloblastoma genomes," *Nature*, vol. 488, no. 7409, pp. 49–56, Aug. 2012, doi: 10.1038/nature11327.
- [148] V. Ramaswamy *et al.*, "Recurrence patterns across medulloblastoma subgroups: an integrated clinical and molecular analysis," *Lancet Oncol*, vol. 14, no. 12, pp. 1200–1207, Nov. 2013, doi: 10.1016/S1470-2045(13)70449-2.
- [149] R. Huether *et al.*, "The landscape of somatic mutations in epigenetic regulators across 1,000 paediatric cancer genomes," *Nat Commun*, vol. 5, no. 1, p. 3630, Apr. 2014, doi: 10.1038/ncomms4630.
- [150] S. M. Waszak *et al.*, "Spectrum and prevalence of genetic predisposition in medulloblastoma: a retrospective genetic study and prospective validation in a clinical trial cohort," *Lancet Oncol*, vol. 19, no. 6, pp. 785–798, Jun. 2018, doi: 10.1016/S1470-2045(18)30242-0.

- [151] M. J. Smith *et al.*, “Germline Mutations in *SUFU* Cause Gorlin Syndrome–Associated Childhood Medulloblastoma and Redefine the Risk Associated With *PTCH1* Mutations,” *Journal of Clinical Oncology*, vol. 32, no. 36, pp. 4155–4161, Dec. 2014, doi: 10.1200/JCO.2014.58.2569.
- [152] H. Lindsay, R. F. Jubran, L. Wang, B. R. Kipp, and W. A. May, “Simultaneous Colonic Adenocarcinoma and Medulloblastoma in a 12-Year-Old with Biallelic Deletions in *PMS2*,” *J Pediatr*, vol. 163, no. 2, pp. 601–603, Aug. 2013, doi: 10.1016/j.jpeds.2013.03.007.
- [153] A. Korshunov *et al.*, “*LIN28A* immunoreactivity is a potent diagnostic marker of embryonal tumor with multilayered rosettes (ETMR),” *Acta Neuropathol*, vol. 124, no. 6, pp. 875–881, Dec. 2012, doi: 10.1007/s00401-012-1068-3.
- [154] S. Lambo, K. von Hoff, A. Korshunov, S. M. Pfister, and M. Kool, “ETMR: a tumor entity in its infancy,” *Acta Neuropathol*, vol. 140, no. 3, pp. 249–266, Sep. 2020, doi: 10.1007/s00401-020-02182-2.
- [155] K. von Hoff *et al.*, “Therapeutic implications of improved molecular diagnostics for rare CNS embryonal tumor entities: results of an international, retrospective study,” *Neuro Oncol*, vol. 23, no. 9, pp. 1597–1611, Sep. 2021, doi: 10.1093/neuonc/noab136.
- [156] C. L. Nesvick, A. A. Nageswara Rao, A. Raghunathan, J. A. Biegel, and D. J. Daniels, “Case-based review: atypical teratoid/rhabdoid tumor,” *Neurooncol Pract*, vol. 6, no. 3, pp. 163–178, May 2019, doi: 10.1093/nop/npy037.
- [157] L. Blümel *et al.*, “Primary cilia contribute to the aggressiveness of atypical teratoid/rhabdoid tumors,” *Cell Death Dis*, vol. 13, no. 9, p. 806, Sep. 2022, doi: 10.1038/s41419-022-05243-4.
- [158] J. A. Biegel, J. Y. Zhou, L. B. Rorke, C. Stenstrom, L. M. Wainwright, and B. Fogelgren, “Germ-line and acquired mutations of *INI1* in atypical teratoid and rhabdoid tumors.,” *Cancer Res*, vol. 59, no. 1, pp. 74–9, Jan. 1999.
- [159] P. D. Johann *et al.*, “Recurrent atypical teratoid/rhabdoid tumors (AT/RT) reveal discrete features of progression on histology, epigenetics, copy number profiling, and transcriptomics,” *Acta Neuropathol*, vol. 146, no. 3, pp. 527–541, Sep. 2023, doi: 10.1007/s00401-023-02608-7.
- [160] R. Wang *et al.*, “CNS tumor with *BCOR* internal tandem duplication: Clinicopathologic, molecular characteristics and prognosis factors,” *Pathol Res Pract*, vol. 236, p. 153995, Aug. 2022, doi: 10.1016/j.prp.2022.153995.
- [161] K. K. Matthay *et al.*, “Neuroblastoma,” *Nat Rev Dis Primers*, vol. 2, no. 1, p. 16078, Nov. 2016, doi: 10.1038/nrdp.2016.78.
- [162] B. Qiu and K. K. Matthay, “Advancing therapy for neuroblastoma”, doi: 10.1038/s41571-022-00643-z.
- [163] S. W. Brady *et al.*, “Pan-neuroblastoma analysis reveals age-and signature-associated driver alterations”, doi: 10.1038/s41467-020-18987-4.
- [164] A. Bellini *et al.*, “Frequency and Prognostic Impact of *ALK* Amplifications and Mutations in the European Neuroblastoma Study Group (SIOPEN) High-Risk Neuroblastoma Trial (HR-NBL1),” *Journal of Clinical Oncology*, vol. 39, no. 30, pp. 3377–3390, Oct. 2021, doi: 10.1200/JCO.21.00086.
- [165] P. Depuydt *et al.*, “Genomic Amplifications and Distal 6q Loss: Novel Markers for Poor Survival in High-risk Neuroblastoma Patients,” *JNCI: Journal of the National Cancer Institute*, vol. 110, no. 10, pp. 1084–1093, Oct. 2018, doi: 10.1093/jnci/djy022.
- [166] J. Guan, B. Hallberg, and R. H. Palmer, “Chromosome Imbalances in Neuroblastoma—Recent Molecular Insight into Chromosome 1p-deletion, 2p-gain, and 11q-deletion

- Identifies New Friends and Foes for the Future," *Cancers (Basel)*, vol. 13, no. 23, Dec. 2021, doi: 10.3390/CANCERS13235897.
- [167] N. Bown *et al.*, "Gain of Chromosome Arm 17q and Adverse Outcome in Patients with Neuroblastoma," <https://doi.org/10.1056/NEJM199906243402504>, vol. 340, no. 25, pp. 1954–1961, Jun. 1999, doi: 10.1056/NEJM199906243402504.
- [168] T. G. Grünewald *et al.*, "Sarcoma treatment in the era of molecular medicine," *EMBO Mol Med*, vol. 12, no. 11, Nov. 2020, doi: 10.15252/EMMM.201911131.
- [169] M. Sbaraglia, E. Bellan, and A. P. Dei Tos, "The 2020 WHO Classification of Soft Tissue Tumours: news and perspectives," *Pathologica*, vol. 113, no. 2, pp. 70–84, Nov. 2020, doi: 10.32074/1591-951X-213.
- [170] C. Koelsche *et al.*, "Sarcoma classification by DNA methylation profiling," *Nat Commun*, vol. 12, no. 1, Dec. 2021, doi: 10.1038/S41467-020-20603-4.
- [171] B. A. Martin-Giacalone, P. A. Weinstein, S. E. Plon, and P. J. Lupo, "Pediatric Rhabdomyosarcoma: Epidemiology and Genetic Susceptibility," *J Clin Med*, vol. 10, no. 9, p. 2028, May 2021, doi: 10.3390/jcm10092028.
- [172] M. Sbaraglia, E. Bellan, and A. P. Dei Tos, "The 2020 WHO Classification of Soft Tissue Tumours: news and perspectives," *Pathologica*, vol. 113, no. 2, pp. 70–84, Nov. 2020, doi: 10.32074/1591-951X-213.
- [173] D. M. Parham and F. G. Barr, "Classification of Rhabdomyosarcoma and Its Molecular Basis," *Adv Anat Pathol*, vol. 20, no. 6, pp. 387–397, Nov. 2013, doi: 10.1097/PAP.0b013e3182a92d0d.
- [174] R. Imle, F. K. F. Kommos, and A. Banito, "Preclinical In Vivo Modeling of Pediatric Sarcoma—Promises and Limitations," *J Clin Med*, vol. 10, no. 8, p. 1578, Apr. 2021, doi: 10.3390/jcm10081578.
- [175] F. G. Barr, N. Galili, J. Holick, J. A. Biegel, G. Rovera, and B. S. Emanuel, "Rearrangement of the PAX3 paired box gene in the paediatric solid tumour alveolar rhabdomyosarcoma," *Nat Genet*, vol. 3, no. 2, pp. 113–117, Feb. 1993, doi: 10.1038/ng0293-113.
- [176] D. S. Shulman *et al.*, "An international working group consensus report for the prioritization of molecular biomarkers for Ewing sarcoma," *NPJ Precis Oncol*, vol. 6, no. 1, p. 65, Sep. 2022, doi: 10.1038/s41698-022-00307-2.
- [177] T. G. P. Grünewald *et al.*, "Ewing sarcoma," *Nat Rev Dis Primers*, vol. 4, no. 1, p. 5, Jul. 2018, doi: 10.1038/s41572-018-0003-x.
- [178] Y. Tsuda *et al.*, "Ewing sarcoma with *FEV* gene rearrangements is a rare subset with predilection for extraskeletal locations and aggressive behavior," *Genes Chromosomes Cancer*, vol. 59, no. 5, pp. 286–294, May 2020, doi: 10.1002/gcc.22828.
- [179] K. Rickel, F. Fang, and J. Tao, "Molecular genetics of osteosarcoma," *Bone*, vol. 102, pp. 69–79, Sep. 2017, doi: 10.1016/j.bone.2016.10.017.
- [180] M. Kovac *et al.*, "The early evolutionary landscape of osteosarcoma provides clues for targeted treatment strategies," *Journal of Pathology*, vol. 254, no. 5, pp. 556–566, Aug. 2021, doi: 10.1002/PATH.5699.
- [181] C.-C. Wu *et al.*, "Immuno-genomic landscape of osteosarcoma," *Nat Commun*, vol. 11, no. 1, p. 1008, Feb. 2020, doi: 10.1038/s41467-020-14646-w.
- [182] J. J. Morrow and C. Khanna, "Osteosarcoma Genetics and Epigenetics: Emerging Biology and Candidate Therapies".
- [183] T. Van Harn *et al.*, "Loss of Rb proteins causes genomic instability in the absence of mitogenic signaling", doi: 10.1101/gad.580710.

- [184] Z. Xing *et al.*, “Analysis of mutations in primary and metastatic synovial sarcoma,” *Oncotarget*, vol. 9, no. 96, pp. 36878–36888, Dec. 2018, doi: 10.18632/oncotarget.26416.
- [185] M. Haldar, J. D. Hancock, C. M. Coffin, S. L. Lessnick, and M. R. Capecchi, “A Conditional Mouse Model of Synovial Sarcoma: Insights into a Myogenic Origin,” *Cancer Cell*, vol. 11, no. 4, pp. 375–388, Apr. 2007, doi: 10.1016/j.ccr.2007.01.016.
- [186] A. Banito *et al.*, “The SS18-SSX Oncoprotein Hijacks KDM2B-PRC1.1 to Drive Synovial Sarcoma,” *Cancer Cell*, vol. 33, no. 3, pp. 527–541.e8, Mar. 2018, doi: 10.1016/j.ccell.2018.01.018.
- [187] M. Sekiguchi *et al.*, “Integrated multiomics analysis of hepatoblastoma unravels its heterogeneity and provides novel druggable targets,” *NPJ Precis Oncol*, vol. 4, no. 1, p. 20, Jul. 2020, doi: 10.1038/s41698-020-0125-y.
- [188] F. Saiyed, E. Hamilton, and M. Austin, “Pediatric melanoma: incidence, treatment, and prognosis,” *Pediatric Health Med Ther*, vol. Volume 8, pp. 39–45, Apr. 2017, doi: 10.2147/PHMT.S115534.
- [189] S. Conroy, J. McIntyre, I. Choonara, and T. Stephenson, “Drug trials in children: problems and the way forward,” *Br J Clin Pharmacol*, vol. 49, no. 2, pp. 93–7, Feb. 2000, doi: 10.1046/j.1365-2125.2000.00125.x.
- [190] M. E. Zettler, “The RACE for children act at one year: progress in pediatric development of molecularly targeted oncology drugs,” *Expert Rev Anticancer Ther*, vol. 22, no. 3, pp. 317–321, Mar. 2022, doi: 10.1080/14737140.2022.2032664.
- [191] T. J. Hwang, L. Orenstein, S. G. DuBois, K. A. Janeway, and F. T. Bourgeois, “Pediatric Trials for Cancer Therapies With Targets Potentially Relevant to Pediatric Cancers,” *JNCI: Journal of the National Cancer Institute*, vol. 112, no. 3, pp. 224–228, Mar. 2020, doi: 10.1093/jnci/djz207.
- [192] J. Rygaard and C. O. Poulsen, “HETEROTRANSPLANTATION OF A HUMAN MALIGNANT TUMOUR TO ‘NUDE’ MICE,” *Acta Pathologica Microbiologica Scandinavica*, vol. 77, no. 4, pp. 758–760, Aug. 2009, doi: 10.1111/j.1699-0463.1969.tb04520.x.
- [193] Y. Liu, W. Wu, C. Cai, H. Zhang, H. Shen, and Y. Han, “Patient-derived xenograft models in cancer therapy: technologies and applications,” *Signal Transduct Target Ther*, vol. 8, no. 1, p. 160, Apr. 2023, doi: 10.1038/s41392-023-01419-2.
- [194] C.-P. Day, G. Merlino, and T. Van Dyke, “Preclinical Mouse Cancer Models: A Maze of Opportunities and Challenges,” *Cell*, vol. 163, no. 1, pp. 39–53, Sep. 2015, doi: 10.1016/j.cell.2015.08.068.
- [195] J. J. Tentler *et al.*, “Patient-derived tumour xenografts as models for oncology drug development,” *Nat Rev Clin Oncol*, vol. 9, no. 6, pp. 338–350, Jun. 2012, doi: 10.1038/nrclinonc.2012.61.
- [196] K. O. McNerney and D. T. Teachey, “Xenograft models for pediatric cancer therapies,” *Fac Rev*, vol. 10, Feb. 2021, doi: 10.12703/r/10-11.
- [197] J. Mattern, M. Bak, E. W. Hahn, and M. Volm, “Human tumor xenografts as model for drug testing,” *CANCER AND METASTASIS REVIEW*, vol. 7, no. 3, pp. 263–284, Nov. 1988, doi: 10.1007/BF00047755.
- [198] B. Murphy *et al.*, “Evaluation of Alternative In Vivo Drug Screening Methodology: A Single Mouse Analysis,” *Cancer Res*, vol. 76, no. 19, pp. 5798–5809, Oct. 2016, doi: 10.1158/0008-5472.CAN-16-0122.
- [199] N. Kawashima *et al.*, “Comparison of clonal architecture between primary and immunodeficient mouse-engrafted acute myeloid leukemia cells,” *Nature*

- Communications* 2022 13:1, vol. 13, no. 1, pp. 1–11, Mar. 2022, doi: 10.1038/s41467-022-29304-6.
- [200] K.-Y. Tso, S. D. Lee, K.-W. Lo, and K. Y. Yip, “Are special read alignment strategies necessary and cost-effective when handling sequencing reads from patient-derived tumor xenografts?,” *BMC Genomics*, vol. 15, no. 1, p. 1172, Dec. 2014, doi: 10.1186/1471-2164-15-1172.
- [201] J. W. Cassidy, C. Caldas, and A. Bruna, “Maintaining Tumor Heterogeneity in Patient-Derived Tumor Xenografts.,” *Cancer Res*, vol. 75, no. 15, pp. 2963–8, Aug. 2015, doi: 10.1158/0008-5472.CAN-15-0727.
- [202] S. M. Pfister, M. Kool, and J. M. Olson, “A biobank of patient-derived pediatric brain tumor models,” *Nat Med*, doi: 10.1038/s41591-018-0207-3.
- [203] H. Gao *et al.*, “High-throughput screening using patient-derived tumor xenografts to predict clinical trial drug response,” *Nat Med*, vol. 21, no. 11, pp. 1318–1325, Nov. 2015, doi: 10.1038/NM.3954.
- [204] G. J. Yoshida, “Applications of patient-derived tumor xenograft models and tumor organoids.,” *J Hematol Oncol*, vol. 13, no. 1, p. 4, Jan. 2020, doi: 10.1186/s13045-019-0829-z.
- [205] M. Hidalgo *et al.*, “Patient-Derived Xenograft Models: An Emerging Platform for Translational Cancer Research,” *Cancer Discov*, vol. 4, no. 9, pp. 998–1013, Sep. 2014, doi: 10.1158/2159-8290.CD-14-0001.
- [206] S. H. Kresse, L. A. Meza-Zepeda, I. Machado, A. Llombart-Bosch, and O. Myklebost, “Preclinical xenograft models of human sarcoma show nonrandom loss of aberrations,” *Cancer*, vol. 118, no. 2, pp. 558–570, Jan. 2012, doi: 10.1002/cncr.26276.
- [207] J. A. Sosman *et al.*, “Survival in BRAF V600–Mutant Advanced Melanoma Treated with Vemurafenib,” *New England Journal of Medicine*, vol. 366, no. 8, pp. 707–714, Feb. 2012, doi: 10.1056/NEJMoa1112302.
- [208] C. H. Pui, A. J. Gajjar, J. R. Kane, I. A. Qaddoumi, and A. S. Pappo, “Challenging issues in pediatric oncology,” *Nat Rev Clin Oncol*, vol. 8, no. 9, pp. 540–549, Sep. 2011, doi: 10.1038/NRCLINONC.2011.95.
- [209] K. P. S. Langenberg, E. J. Looze, and J. J. Molenaar, “The Landscape of Pediatric Precision Oncology: Program Design, Actionable Alterations, and Clinical Trial Development,” *Cancers (Basel)*, vol. 13, no. 17, p. 4324, Aug. 2021, doi: 10.3390/cancers13174324.
- [210] Stefan M Pfister *et al.*, “ITCC P4 - Paediatric Preclinical Proof Of Concept Platform.”
- [211] H. Li and R. Durbin, “Fast and accurate short read alignment with Burrows-Wheeler transform.,” *Bioinformatics*, vol. 25, no. 14, pp. 1754–60, Jul. 2009, doi: 10.1093/bioinformatics/btp324.
- [212] H. Li *et al.*, “The Sequence Alignment/Map format and SAMtools.,” *Bioinformatics*, vol. 25, no. 16, pp. 2078–9, Aug. 2009, doi: 10.1093/bioinformatics/btp352.
- [213] H. Li, “A statistical framework for SNP calling, mutation discovery, association mapping and population genetical parameter estimation from sequencing data.,” *Bioinformatics*, vol. 27, no. 21, pp. 2987–93, Nov. 2011, doi: 10.1093/bioinformatics/btr509.
- [214] W. McLaren *et al.*, “The Ensembl Variant Effect Predictor,” *Genome Biol*, vol. 17, no. 1, pp. 1–14, Jun. 2016, doi: 10.1186/S13059-016-0974-4/TABLES/8.
- [215] S. Chen *et al.*, “A genome-wide mutational constraint map quantified from variation in 76,156 human genomes”, doi: 10.1101/2022.03.20.485034.
- [216] S. Dedeurwaerder, M. Defrance, M. Bizet, E. Calonne, G. Bontempi, and F. Fuks, “A comprehensive overview of Infinium HumanMethylation450 data processing,” *Brief Bioinform*, vol. 15, no. 6, pp. 929–941, Nov. 2014, doi: 10.1093/bib/bbt054.

- [217] R. Pidsley *et al.*, “Critical evaluation of the Illumina MethylationEPIC BeadChip microarray for whole-genome DNA methylation profiling,” *Genome Biol*, vol. 17, no. 1, p. 208, Dec. 2016, doi: 10.1186/s13059-016-1066-1.
- [218] D. Capper *et al.*, “DNA methylation-based classification of central nervous system tumours,” *Nature*, vol. 555, no. 7697, pp. 469–474, Mar. 2018, doi: 10.1038/NATURE26000.
- [219] V. A. Adalsteinsson *et al.*, “Scalable whole-exome sequencing of cell-free DNA reveals high concordance with metastatic tumors,” *Nature Communications* 2017 8:1, vol. 8, no. 1, pp. 1–13, Nov. 2017, doi: 10.1038/s41467-017-00965-y.
- [220] F. Favero *et al.*, “Sequenza: Allele-specific copy number and mutation profiles from tumor sequencing data,” *Annals of Oncology*, vol. 26, no. 1, pp. 64–70, Jan. 2015, doi: 10.1093/ANNONC/MDU479.
- [221] E. Talevich, A. H. Shain, T. Botton, and B. C. Bastian, “CNVkit: Genome-Wide Copy Number Detection and Visualization from Targeted DNA Sequencing,” *PLoS Comput Biol*, vol. 12, no. 4, p. e1004873, Apr. 2016, doi: 10.1371/journal.pcbi.1004873.
- [222] A. Dobin *et al.*, “STAR: ultrafast universal RNA-seq aligner,” *Bioinformatics*, vol. 29, no. 1, pp. 15–21, Jan. 2013, doi: 10.1093/bioinformatics/bts635.
- [223] S. Uhrig *et al.*, “Accurate and efficient detection of gene fusions from RNA sequencing data,” *Genome Res*, vol. 31, no. 3, pp. 448–460, Mar. 2021, doi: 10.1101/gr.257246.119.
- [224] S. M. Pfister *et al.*, “A Summary of the Inaugural WHO Classification of Pediatric Tumors: Transitioning from the Optical into the Molecular Era,” *Cancer Discov*, vol. 12, no. 2, pp. 331–355, Feb. 2022, doi: 10.1158/2159-8290.CD-21-1094/674743/P/A-SUMMARY-OF-THE-INAUGURAL-WHO-CLASSIFICATION-OF.
- [225] M. Blattner-Johnson, D. T. W. Jones, and E. Pfaff, “Precision medicine in pediatric solid cancers,” *Semin Cancer Biol*, vol. 84, pp. 214–227, Sep. 2022, doi: 10.1016/j.semcancer.2021.06.008.
- [226] L. Marcus *et al.*, “FDA Approval Summary: Pembrolizumab for the Treatment of Tumor Mutational Burden-High Solid Tumors”, doi: 10.1158/1078-0432.CCR-21-0327.
- [227] D. M. Merino *et al.*, “Establishing guidelines to harmonize tumor mutational burden (TMB): in silico assessment of variation in TMB quantification across diagnostic platforms: phase I of the Friends of Cancer Research TMB Harmonization Project,” *J Immunother Cancer*, vol. 8, no. 1, Mar. 2020, doi: 10.1136/jitc-2019-000147.
- [228] S. L. Carter *et al.*, “Absolute quantification of somatic DnA alterations in human cancer,” *Nat Biotechnol*, vol. 30, 2012, doi: 10.1038/nbt.2203.
- [229] K. Yoshihara *et al.*, “Inferring tumour purity and stromal and immune cell admixture from expression data,” *Nat Commun*, vol. 4, p. 2612, 2013, doi: 10.1038/ncomms3612.
- [230] N. A. Schubert *et al.*, “Systematic target actionability reviews of preclinical proof-of-concept papers to match targeted drugs to paediatric cancers,” *Eur J Cancer*, vol. 130, pp. 168–181, May 2020, doi: 10.1016/j.ejca.2020.01.027.
- [231] K. M. Keller *et al.*, “Target Actionability Review: a systematic evaluation of replication stress as a therapeutic target for paediatric solid malignancies,” *Eur J Cancer*, vol. 162, pp. 107–117, Feb. 2022, doi: 10.1016/J.EJCA.2021.11.030.
- [232] C. Koelsche *et al.*, “Sarcoma classification by DNA methylation profiling,” *Nat Commun*, vol. 12, no. 1, p. 498, Jan. 2021, doi: 10.1038/s41467-020-20603-4.
- [233] M. Kool *et al.*, “Molecular subgroups of medulloblastoma: an international meta-analysis of transcriptome, genetic aberrations, and clinical data of WNT, SHH, Group 3, and

- Group 4 medulloblastomas," *Acta Neuropathol*, vol. 123, pp. 473–484, 2012, doi: 10.1007/s00401-012-0958-8.
- [234] T. Sharma *et al.*, "Second-generation molecular subgrouping of medulloblastoma: an international meta-analysis of Group 3 and Group 4 subtypes," *Acta Neuropathol*, vol. 138, pp. 309–326, 2020, doi: 10.1007/s00401-019-02020-0.
- [235] S. Okada, K. Vaeteewoottacharn, and R. Kariya, "Application of Highly Immunocompromised Mice for the Establishment of Patient-Derived Xenograft (PDX) Models," *Cells*, vol. 8, no. 8, Aug. 2019, doi: 10.3390/CELLS8080889.
- [236] B. B. Campbell *et al.*, "Comprehensive Analysis of Hypermutation in Human Cancer," *Cell*, vol. 171, no. 5, pp. 1042–1056.e10, Nov. 2017, doi: 10.1016/J.CELL.2017.09.048.
- [237] D. T. W. Jones *et al.*, "Molecular characteristics and therapeutic vulnerabilities across paediatric solid tumours," *Nature Reviews Cancer*, vol. 19, no. 8. Nature Publishing Group, pp. 420–438, Aug. 01, 2019. doi: 10.1038/s41568-019-0169-x.
- [238] M. Parker *et al.*, "C11orf95-RELA fusions drive oncogenic NF- $\kappa$ B signalling in ependymoma," *Nature*, 2014, doi: 10.1038/nature13109.
- [239] T. C. Archer and S. L. Pomeroy, "Cancer Cell Previews Posterior Fossa Ependymomas: A Tale of Two Subtypes", doi: 10.1016/j.ccr.2011.08.003.
- [240] M. Carter *et al.*, "Genetic abnormalities detected in ependymomas by comparative genomic hybridisation," *Br J Cancer*, vol. 86, pp. 929–939, 2002, doi: 10.1038/sj/bjc/6600180.
- [241] R. A. Johnson *et al.*, "LETTERS Cross-species genomics matches driver mutations and cell compartments to model ependymoma," 2010, doi: 10.1038/nature09173.
- [242] P. A. Northcott *et al.*, "Medulloblastomics: the end of the beginning," 2012, doi: 10.1038/nrc3410.
- [243] M. D. Taylor *et al.*, "Molecular subgroups of medulloblastoma: the current consensus," *Acta Neuropathol*, vol. 123, no. 4, pp. 465–472, Apr. 2012, doi: 10.1007/S00401-011-0922-Z.
- [244] J. DeSisto *et al.*, "Comprehensive molecular characterization of pediatric radiation-induced high-grade glioma," *Nat Commun*, vol. 12, no. 1, Dec. 2021, doi: 10.1038/S41467-021-25709-X.
- [245] F. P. B. Dubois *et al.*, "Structural variants shape driver combinations and outcomes in pediatric high-grade glioma," *Nat Cancer*, vol. 3, no. 8, pp. 994–1011, Aug. 2022, doi: 10.1038/S43018-022-00403-Z.
- [246] T. J. Pugh *et al.*, "The genetic landscape of high-risk neuroblastoma," *Nature Publishing Group*, vol. 45, no. 8, 2013, doi: 10.1038/ng.2529.
- [247] J. J. Molenaar *et al.*, "Sequencing of neuroblastoma identifies chromothripsis and defects in neuritogenesis genes," 2012, doi: 10.1038/nature10910.
- [248] Y. P. Mossé *et al.*, "Identification of ALK as a major familial neuroblastoma predisposition gene", doi: 10.1038/nature07261.
- [249] J. J. Molenaar *et al.*, "Sequencing of neuroblastoma identifies chromothripsis and defects in neuritogenesis genes," *Nature*, vol. 483, 2012, doi: 10.1038/nature10910.
- [250] S. J. Diskin *et al.*, "Copy number variation at 1q21.1 associated with neuroblastoma," 2009, doi: 10.1038/nature08035.
- [251] K. Schroeder, S. Gururangan, G. Pediatric, C. Services, P. R. Tisch, and B. Tumor, "Pharmacogenomics and Personalized Medicine Dovepress Molecular variants and mutations in medulloblastoma," *Pharmgenomics Pers Med*, pp. 7–43, 2014, doi: 10.2147/PGPM.S38698.

- [252] M. G. McCabe *et al.*, “Novel Mechanisms of Gene Disruption at the Medulloblastoma Isodicentric 17p11 Breakpoint,” *Genes Chromosomes Cancer*, vol. 48, pp. 121–131, 2009, doi: 10.1002/20625.
- [253] G. H. Gielen *et al.*, “Genetic Analysis of Diffuse High-Grade Astrocytomas in Infancy Defines a Novel Molecular Entity,” 2014, doi: 10.1111/bpa.12210.
- [254] J. Yang *et al.*, “An Integrated Analysis of Tumor Purity of Common Central Nervous System Tumors in Children Based on Machine Learning Methods.,” *Front Genet*, vol. 12, p. 707802, 2021, doi: 10.3389/fgene.2021.707802.
- [255] B. J. Raphael, J. R. Dobson, L. Oesper, and F. Vandin, “Identifying driver mutations in sequenced cancer genomes: Computational approaches to enable precision medicine,” *Genome Med*, vol. 6, no. 1, pp. 1–17, Jan. 2014, doi: 10.1186/GM524/FIGURES/4.
- [256] M. Cmero *et al.*, “Inferring structural variant cancer cell fraction,” p. 78, 2601, doi: 10.1038/s41467-020-14351-8.
- [257] A. M. Buccoliero *et al.*, “Pediatric High Grade Glioma Classification Criteria and Molecular Features of a Case Series.,” *Genes (Basel)*, vol. 13, no. 4, Mar. 2022, doi: 10.3390/genes13040624.
- [258] C. Schott, A. T. Shah, and E. A. Sweet-Cordero, “Genomic Complexity of Osteosarcoma and Its Implication for Preclinical and Clinical Targeted Therapies,” 2020, pp. 1–19. doi: 10.1007/978-3-030-43085-6\_1.
- [259] Y.-T. Chiang, Y.-C. Chien, Y.-H. Lin, H.-H. Wu, D.-F. Lee, and Y.-L. Yu, “The Function of the Mutant p53-R175H in Cancer.,” *Cancers (Basel)*, vol. 13, no. 16, Aug. 2021, doi: 10.3390/cancers13164088.
- [260] N. A. Schubert *et al.*, “Systematic target actionability reviews of preclinical proof-of-concept papers to match targeted drugs to paediatric cancers”, doi: 10.1016/j.ejca.2020.01.027.
- [261] A. G. Henssen *et al.*, “Therapeutic targeting of PGBD5-induced DNA repair dependency in pediatric solid tumors,” *Sci Transl Med*, vol. 9, no. 414, Nov. 2017, doi: 10.1126/SCITRANSLMED.AAM9078.
- [262] K. A. Cole *et al.*, “Phase I Clinical Trial of the Wee1 Inhibitor Adavosertib (AZD1775) with Irinotecan in Children with Relapsed Solid Tumors: A COG Phase I Consortium Report (ADV1312),” *Clin Cancer Res*, vol. 26, no. 6, pp. 1213–1219, Mar. 2020, doi: 10.1158/1078-0432.CCR-19-3470.
- [263] K. Deland *et al.*, “Tumor genotype dictates radiosensitization after Atm deletion in primary brainstem glioma models,” *J Clin Invest*, vol. 131, no. 1, Jan. 2021, doi: 10.1172/JCI142158.
- [264] S. Agnihotri *et al.*, “ATM regulates 3-methylpurine-DNA glycosylase and promotes therapeutic resistance to alkylating agents,” *Cancer Discov*, vol. 4, no. 10, pp. 1198–1213, Oct. 2014, doi: 10.1158/2159-8290.CD-14-0157.
- [265] J. Tian, X. Li, M. Si, T. Liu, and J. Li, “CD271+ Osteosarcoma Cells Display Stem-Like Properties,” *PLoS One*, vol. 9, no. 6, p. e98549, Jun. 2014, doi: 10.1371/JOURNAL.PONE.0098549.
- [266] M. E. M. Dolman *et al.*, “DNA-Dependent Protein Kinase As Molecular Target for Radiosensitization of Neuroblastoma Cells,” *PLoS One*, vol. 10, no. 12, Dec. 2015, doi: 10.1371/JOURNAL.PONE.0145744.
- [267] J. Yang *et al.*, “PCAT: an integrated portal for genomic and preclinical testing data of pediatric cancer patient-derived xenograft models,” *Nucleic Acids Res*, vol. 49, no. D1, pp. D1321–D1327, Jan. 2021, doi: 10.1093/nar/gkaa698.

- [268] J. L. Rokita *et al.*, “Genomic Profiling of Childhood Tumor Patient-Derived Xenograft Models to Enable Rational Clinical Trial Design,” *Cell Rep*, vol. 29, no. 6, pp. 1675–1689.e9, Nov. 2019, doi: 10.1016/j.celrep.2019.09.071.
- [269] E. Stewart *et al.*, “Orthotopic patient-derived xenografts of paediatric solid tumours,” *Nature*, vol. 549, no. 7670, pp. 96–100, Sep. 2017, doi: 10.1038/nature23647.
- [270] A. C. Uzozie *et al.*, “PDX models reflect the proteome landscape of pediatric acute lymphoblastic leukemia but divert in select pathways,” *J Exp Clin Cancer Res*, vol. 40, no. 1, p. 96, Mar. 2021, doi: 10.1186/s13046-021-01835-8.
- [271] P. Richter-Pechańska *et al.*, “PDX models recapitulate the genetic and epigenetic landscape of pediatric T-cell leukemia,” *EMBO Mol Med*, vol. 10, no. 12, p. e9443, Dec. 2018, doi: 10.15252/EMMM.201809443.
- [272] M. Roosen, Z. Odé, J. Bunt, and M. Kool, “The oncogenic fusion landscape in pediatric CNS neoplasms,” *Acta Neuropathol*, vol. 143, no. 4, p. 427, Apr. 2022, doi: 10.1007/S00401-022-02405-8.
- [273] S. LaHaye *et al.*, “Discovery of clinically relevant fusions in pediatric cancer,” *BMC Genomics*, vol. 22, no. 1, Dec. 2021, doi: 10.1186/S12864-021-08094-Z.
- [274] Y. Bouchoucha *et al.*, “Intra- and extra-cranial BCOR-ITD tumours are separate entities within the BCOR-rearranged family,” *J Pathol Clin Res*, vol. 8, no. 3, p. 217, May 2022, doi: 10.1002/CJP2.255.
- [275] M. M. L. Knott, T. L. B. Hölting, S. Ohmura, T. Kirchner, F. Cidre-Aranaz, and T. G. P. Grunewald, “Targeting the undruggable: exploiting neomorphic features of fusion oncoproteins in childhood sarcomas for innovative therapies,” *Cancer Metastasis Rev*, vol. 38, no. 4, p. 625, Dec. 2019, doi: 10.1007/S10555-019-09839-9.
- [276] Y. S. Derose *et al.*, “Tumor grafts derived from women with breast cancer authentically reflect tumor pathology, growth, metastasis and disease outcomes,” *Nat Med*, vol. 17, no. 11, pp. 1514–1520, Nov. 2011, doi: 10.1038/NM.2454.
- [277] H. Castillo-Ecija *et al.*, “Prognostic value of patient-derived xenograft engraftment in pediatric sarcomas,” *J Pathol Clin Res*, vol. 7, no. 4, p. 338, Jul. 2021, doi: 10.1002/CJP2.210.
- [278] M. Kogiso *et al.*, “Xenotransplantation of pediatric low grade gliomas confirms the enrichment of BRAF V600E mutation and preservation of CDKN2A deletion in a novel orthotopic xenograft mouse model of progressive pleomorphic xanthoastrocytoma,” *Oncotarget*, vol. 8, no. 50, pp. 87455–87471, 2017, doi: 10.18632/ONCOTARGET.20713.
- [279] N. Zhukova *et al.*, “Subgroup-specific prognostic implications of TP53 mutation in medulloblastoma,” *J Clin Oncol*, vol. 31, no. 23, pp. 2927–2935, Aug. 2013, doi: 10.1200/JCO.2012.48.5052.
- [280] U. Tabori *et al.*, “Universal poor survival in children with medulloblastoma harboring somatic TP53 mutations,” *J Clin Oncol*, vol. 28, no. 8, pp. 1345–1350, Mar. 2010, doi: 10.1200/JCO.2009.23.5952.
- [281] A. S. Kolodziejczak *et al.*, “Clinical outcome of pediatric medulloblastoma patients with Li-Fraumeni syndrome,” *Neuro Oncol*, Jun. 2023, doi: 10.1093/NEUONC/NOAD114.
- [282] S. L. Ryan *et al.*, “MYC family amplification and clinical risk-factors interact to predict an extremely poor prognosis in childhood medulloblastoma,” *Acta Neuropathol*, vol. 123, no. 4, pp. 501–513, Apr. 2012, doi: 10.1007/S00401-011-0923-Y.
- [283] J. Goddard *et al.*, “Molecular characterisation defines clinically-actionable heterogeneity within Group 4 medulloblastoma and improves disease risk-stratification,” *Acta*

- Neuropathol*, vol. 145, no. 5, pp. 651–666, May 2023, doi: 10.1007/s00401-023-02566-0.
- [284] A. Pezzolo *et al.*, “Loss of 10q26.1-q26.3 in association with 7q34-q36.3 gain or 17q24.3-q25.3 gain predict poor outcome in pediatric medulloblastoma,” *Cancer Lett*, vol. 308, no. 2, pp. 215–24, Sep. 2011, doi: 10.1016/j.canlet.2011.05.006.
- [285] T. G. P. Grünewald *et al.*, “Ewing sarcoma,” *Nat Rev Dis Primers*, vol. 4, no. 1, Dec. 2018, doi: 10.1038/S41572-018-0003-X.
- [286] Y. S. Zou *et al.*, “Complex/cryptic EWSR1::FLI1/ERG Gene Fusions and 1q Jumping Translocation in Pediatric Ewing Sarcomas,” *Genes (Basel)*, vol. 14, no. 6, p. 1139, May 2023, doi: 10.3390/GENES14061139.
- [287] M. Milione *et al.*, “Ewing sarcoma of the small bowel: a study of seven cases, including one with the uncommonly reported EWSR1-FEV translocation,” *Histopathology*, vol. 64, no. 7, pp. 1014–1026, 2014, doi: 10.1111/HIS.12350.
- [288] F. Tirede *et al.*, “Genomic landscape of Ewing sarcoma defines an aggressive subtype with co-association of STAG2 and TP53 mutations,” *Cancer Discov*, vol. 4, no. 11, pp. 1342–1353, Nov. 2014, doi: 10.1158/2159-8290.CD-14-0622.
- [289] N. Gonin-Laurent *et al.*, “RB1 and TP53 pathways in radiation-induced sarcomas,” *Oncogene*, vol. 26, no. 41, pp. 6106–6112, Sep. 2007, doi: 10.1038/SJ.ONC.1210404.
- [290] N. Q. Bui *et al.*, “A clinico-genomic analysis of soft tissue sarcoma patients reveals CDKN2A deletion as a biomarker for poor prognosis,” *Clin Sarcoma Res*, vol. 9, no. 1, Dec. 2019, doi: 10.1186/S13569-019-0122-5.
- [291] P. Śledzińska, M. G. Bebyn, J. Furtak, J. Kowalewski, and M. A. Lewandowska, “Prognostic and Predictive Biomarkers in Gliomas,” *Int J Mol Sci*, vol. 22, no. 19, Oct. 2021, doi: 10.3390/IJMS221910373.
- [292] K. E. Chaney *et al.*, “Cdkn2a Loss in a Model of Neurofibroma Demonstrates Stepwise Tumor Progression to Atypical Neurofibroma and MPNST,” *Cancer Res*, vol. 80, no. 21, pp. 4720–4730, Nov. 2020, doi: 10.1158/0008-5472.CAN-19-1429.
- [293] T. H. Nguyen and F. G. Barr, “Therapeutic Approaches Targeting PAX3-FOXO1 and Its Regulatory and Transcriptional Pathways in Rhabdomyosarcoma,” *Molecules*, vol. 23, no. 11, p. 2798, Oct. 2018, doi: 10.3390/molecules23112798.
- [294] L. Bejarano, M. J. C. Jordão, and J. A. Joyce, “Therapeutic Targeting of the Tumor Microenvironment,” *Cancer Discov*, vol. 11, no. 4, pp. 933–959, Apr. 2021, doi: 10.1158/2159-8290.CD-20-1808.
- [295] Q. Wang *et al.*, “Role of tumor microenvironment in cancer progression and therapeutic strategy,” *Cancer Med*, vol. 12, no. 10, pp. 11149–11165, May 2023, doi: 10.1002/cam4.5698.
- [296] V. Hovestadt *et al.*, “Robust molecular subgrouping and copy-number profiling of medulloblastoma from small amounts of archival tumour material using high-density DNA methylation arrays,” *Acta Neuropathol*, vol. 3, pp. 913–916, 2013, doi: 10.1007/s00401-013-1126-5.
- [297] M. W. Schmitt, L. A. Loeb, and J. J. Salk, “The influence of subclonal resistance mutations on targeted cancer therapy,” *Nat Rev Clin Oncol*, vol. 13, no. 6, pp. 335–347, Jun. 2016, doi: 10.1038/nrclinonc.2015.175.
- [298] S. W. Brady *et al.*, “Combating subclonal evolution of resistant cancer phenotypes,” *Nat Commun*, vol. 8, no. 1, p. 1231, Nov. 2017, doi: 10.1038/s41467-017-01174-3.
- [299] L. A. Diaz *et al.*, “The molecular evolution of acquired resistance to targeted EGFR blockade in colorectal cancers,” *Nature*, vol. 486, no. 7404, pp. 537–40, Jun. 2012, doi: 10.1038/nature11219.

- [300] B. Pereira *et al.*, "Cell-free DNA captures tumor heterogeneity and driver alterations in rapid autopsies with pre-treated metastatic cancer.," *Nat Commun*, vol. 12, no. 1, p. 3199, May 2021, doi: 10.1038/s41467-021-23394-4.
- [301] J. Kendall *et al.*, "Oncogenic cooperation and coamplification of developmental transcription factor genes in lung cancer," *Proc Natl Acad Sci U S A*, vol. 104, no. 42, p. 16663, Oct. 2007, doi: 10.1073/PNAS.0708286104.
- [302] J. Iranzo, G. Gruenhagen, J. Calle-Espinosa, and E. V Koonin, "Pervasive conditional selection of driver mutations and modular epistasis networks in cancer.," *Cell Rep*, vol. 40, no. 8, p. 111272, Aug. 2022, doi: 10.1016/j.celrep.2022.111272.
- [303] L. Salichos, W. Meyerson, J. Warrell, and M. Gerstein, "Estimating growth patterns and driver effects in tumor evolution from individual samples.," *Nat Commun*, vol. 11, no. 1, p. 732, Feb. 2020, doi: 10.1038/s41467-020-14407-9.
- [304] O. L. Veeranki *et al.*, "A novel patient-derived orthotopic xenograft model of esophageal adenocarcinoma provides a platform for translational discoveries.," *Dis Model Mech*, vol. 12, no. 12, Dec. 2019, doi: 10.1242/dmm.041004.
- [305] R. A. Vaubel *et al.*, "Genomic and Phenotypic Characterization of a Broad Panel of Patient-Derived Xenografts Reflects the Diversity of Glioblastoma.," *Clin Cancer Res*, vol. 26, no. 5, pp. 1094–1104, Mar. 2020, doi: 10.1158/1078-0432.CCR-19-0909.
- [306] D.-N. He *et al.*, "Multi-omics analysis reveals a molecular landscape of the early recurrence and early metastasis in pan-cancer.," *Front Genet*, vol. 14, p. 1061364, 2023, doi: 10.3389/fgene.2023.1061364.
- [307] F. Pettini, A. Visibelli, V. Cicaloni, D. Iovinelli, and O. Spiga, "Multi-Omics Model Applied to Cancer Genetics," *Int J Mol Sci*, vol. 22, no. 11, May 2021, doi: 10.3390/ijms22115751.
- [308] Y. J. Shen *et al.*, "Progression signature underlies clonal evolution and dissemination of multiple myeloma.," *Blood*, vol. 137, no. 17, pp. 2360–2372, Apr. 2021, doi: 10.1182/blood.2020005885.
- [309] L. R. Yates *et al.*, "Genomic Evolution of Breast Cancer Metastasis and Relapse," *Cancer Cell*, vol. 32, no. 2, pp. 169–184.e7, Aug. 2017, doi: 10.1016/j.ccell.2017.07.005.
- [310] P. A. Baxter *et al.*, "A phase I/II study of veliparib (ABT-888) with radiation and temozolomide in newly diagnosed diffuse pontine glioma: a Pediatric Brain Tumor Consortium study," *Neuro Oncol*, vol. 22, no. 6, pp. 875–885, Jun. 2020, doi: 10.1093/neuonc/noaa016.
- [311] J. M. Su *et al.*, "A phase I trial of veliparib (ABT-888) and temozolomide in children with recurrent CNS tumors: a Pediatric Brain Tumor Consortium report," *Neuro Oncol*, vol. 16, no. 12, pp. 1661–1668, Dec. 2014, doi: 10.1093/neuonc/nou103.
- [312] R. Chugh *et al.*, "SARC025 arms 1 and 2: A phase 1 study of the poly(ADP-ribose) polymerase inhibitor niraparib with temozolomide or irinotecan in patients with advanced Ewing sarcoma," *Cancer*, vol. 127, no. 8, pp. 1301–1310, Apr. 2021, doi: 10.1002/cncr.33349.
- [313] S. M. Federico *et al.*, "A phase I trial of talazoparib and irinotecan with and without temozolomide in children and young adults with recurrent or refractory solid malignancies," *Eur J Cancer*, vol. 137, pp. 204–213, Sep. 2020, doi: 10.1016/j.ejca.2020.06.014.
- [314] E. S. Schafer *et al.*, "Phase 1/2 trial of talazoparib in combination with temozolomide in children and adolescents with refractory/recurrent solid tumors including Ewing sarcoma: A Children's Oncology Group Phase 1 Consortium study (ADV1411)," *Pediatr Blood Cancer*, vol. 67, no. 2, Feb. 2020, doi: 10.1002/pbc.28073.

- [315] E. Choy *et al.*, “Phase II study of olaparib in patients with refractory Ewing sarcoma following failure of standard chemotherapy,” *BMC Cancer*, vol. 14, no. 1, p. 813, Dec. 2014, doi: 10.1186/1471-2407-14-813.
- [316] E. Prince *et al.*, “MB-22 \* CHECKPOINT KINASE 1 EXPRESSION IS AN ADVERSE PROGNOSTIC MARKER AND THERAPEUTIC TARGET IN MYC-DRIVEN MEDULLOBLASTOMA,” *Neuro Oncol*, vol. 17, no. suppl 3, pp. iii24–iii24, Jun. 2015, doi: 10.1093/neuonc/nov061.98.
- [317] K. L. Goss, S. L. Koppenhafer, K. M. Harmoney, W. W. Terry, and D. J. Gordon, “Inhibition of CHK1 sensitizes Ewing sarcoma cells to the ribonucleotide reductase inhibitor gemcitabine,” *Oncotarget*, vol. 8, no. 50, pp. 87016–87032, Oct. 2017, doi: 10.18632/oncotarget.18776.
- [318] C. D. Lowery *et al.*, “Broad Spectrum Activity of the Checkpoint Kinase 1 Inhibitor Prexasertib as a Single Agent or Chemopotentiator Across a Range of Preclinical Pediatric Tumor Models,” *Clinical Cancer Research*, vol. 25, no. 7, pp. 2278–2289, Apr. 2019, doi: 10.1158/1078-0432.CCR-18-2728.
- [319] S. L. Koppenhafer, K. L. Goss, W. W. Terry, and D. J. Gordon, “Inhibition of the ATR–CHK1 Pathway in Ewing Sarcoma Cells Causes DNA Damage and Apoptosis via the CDK2-Mediated Degradation of RRM2,” *Molecular Cancer Research*, vol. 18, no. 1, pp. 91–104, Jan. 2020, doi: 10.1158/1541-7786.MCR-19-0585.
- [320] H. E. D. Southgate, L. Chen, D. A. Tweddle, and N. J. Curtin, “ATR Inhibition Potentiates PARP Inhibitor Cytotoxicity in High Risk Neuroblastoma Cell Lines by Multiple Mechanisms,” *Cancers (Basel)*, vol. 12, no. 5, p. 1095, Apr. 2020, doi: 10.3390/cancers12051095.
- [321] L. M. Kopp, P. Gupta, L. Pelayo-Katsanis, B. Wittman, and E. Katsanis, “Late Effects in Adult Survivors of Pediatric Cancer: A Guide for the Primary Care Physician,” *Am J Med*, vol. 125, no. 7, pp. 636–641, Jul. 2012, doi: 10.1016/j.amjmed.2012.01.013.
- [322] O. Delattre *et al.*, “The Ewing Family of Tumors -- A Subgroup of Small-Round-Cell Tumors Defined by Specific Chimeric Transcripts,” *New England Journal of Medicine*, vol. 331, no. 5, pp. 294–299, Aug. 1994, doi: 10.1056/NEJM199408043310503.
- [323] X. A. Su *et al.*, “*RAD21* is a driver of chromosome 8 gain in Ewing sarcoma to mitigate replication stress,” *Genes Dev*, vol. 35, no. 7–8, pp. 556–572, Apr. 2021, doi: 10.1101/gad.345454.120.
- [324] K. C. Goldsmith *et al.*, “Lorlatinib with or without chemotherapy in ALK-driven refractory/relapsed neuroblastoma: phase 1 trial results,” *Nat Med*, vol. 29, no. 5, pp. 1092–1102, May 2023, doi: 10.1038/s41591-023-02297-5.
- [325] P. N. Morcos *et al.*, “Model-informed approach to support pediatric dosing for the pan-PI3K inhibitor copanlisib in children and adolescents with relapsed/refractory solid tumors,” *Clin Transl Sci*, vol. 16, no. 7, pp. 1197–1209, Jul. 2023, doi: 10.1111/cts.13523.
- [326] M. E. M. da Costa *et al.*, “Longitudinal characterization of primary osteosarcoma and derived subcutaneous and orthotopic relapsed patient-derived xenograft models,” *Front Oncol*, vol. 13, Jun. 2023, doi: 10.3389/fonc.2023.1166063.
- [327] S. K. Zöllner *et al.*, “Ewing Sarcoma—Diagnosis, Treatment, Clinical Challenges and Future Perspectives,” *J Clin Med*, vol. 10, no. 8, p. 1685, Apr. 2021, doi: 10.3390/jcm10081685.